THE UNIVERSITY *of* EDINBURGH

Visual experience dependent control of NMDAR subunit composition and neuronal gene expression: A critical role for the GluN2A C-terminal Domain

Kirsty Haddow, MSci

A thesis submitted for the degree of Doctor of Philosophy
at the University of Edinburgh

August 2023

College of Medicine and Veterinary Medicine
University of Edinburgh

Supervisors
Prof. Giles E. Hardingham
Prof. Peter Kind

THE UNIVERSITY *of* EDINBURGH

Declaration

I hereby declare that the majority of the following work is my own, with the contributions of others indicated where appropriate. This work has not been submitted for any other degree or professional qualification.

Kirsty Haddow

24/08/2023

Acknowledgements

I thank my supervisors, Giles Hardingham and Peter Kind, for all of their support, expertise and guidance throughout the course of my PhD work.

I am also grateful to the members of the Hardingham lab, who's advice and support have been fundamental in driving my PhD forward. I would particularly like to thank Dr Jamie McQueen for teaching me the skills required for this project, as well as her help in developing and optimising the dark rearing protocol used for this work.

Abstract

The N-methyl-D-aspartate (NMDAR) NMDA receptor is a Ca^{2+} -permeant glutamate receptor which plays key roles in health and disease. Canonical NMDARs are heterotetramers that contain two GluN2 subunits, of which GluN2A and GluN2B are predominant in the forebrain. Moreover, the relative contribution of GluN2A vs. GluN2B is controlled both developmentally and in an activity-dependent manner. The GluN2 subtype influences the biophysical properties of the receptor through differences in their N-terminal extracellular domain and transmembrane regions, but they also have large cytoplasmic Carboxyl (C)-terminal domains (CTDs) which have diverged substantially during evolution. While the CTD identity does not influence NMDAR subunit specific channel properties, it determines the nature of CTD-associated signalling molecules and has been implicated in mediating the control of subunit composition (2A vs. 2B) at the synapse. However, the role of CTD identity in mediating activity-dependent changes in NMDAR subunit composition remains unclear.

First, I investigate the role of sensory experience to changes in the NMDAR GluN2A:GluN2B composition by using two different dark rearing protocols: 1) Mice were dark reared from birth to assess the contribution of sensory experience to the developmental increase in the ratio of 2A to 2B; 2) Mice raised in standard light conditions were taken during the third postnatal week and placed in the dark for 7-days with or without subsequent re-exposure to light to interrogate subunit specific regulation in response to changes in the level of synaptic activity. Here I show that, while dark rearing from birth has little effect on NMDAR subunit composition, 7 days of dark rearing produces a marked decrease in the ratio of 2A to 2B, which is reversed upon re-exposure to light. Crucially, I demonstrate that changes in the ratio are driven by changes in the level of synaptic GluN2A, and not GluN2B. This suggests that GluN2A is dynamically regulated by activity, and points to a GluN2A dependent mechanism of insertion/removal from the synapse.

Historically, much of the research into the differential function of GluN2 CTDs has been conducted *in vitro* by over-expressing mutant subunits, but more recently, the generation of knock-in (KI) mouse models have allowed CTD function to be probed *in vivo* and in ex vivo systems without heterologous expression of GluN2 mutants. Taking advantage of a KI mouse model with the GluN2A CTD (CTD^{2A}) swapped for that of GluN2B (CTD^{2B}) ($GluN2A^{2B(CTR)/2B(CTR)}$), I next investigate the role of the CTD^{2A} in experience-dependent changes in the level of synaptic GluN2A. I demonstrate that the CTD^{2A} is required for activity-dependent synaptic expression of GluN2A. Furthermore, I find that the transcriptomic response to changes in sensory experience is blunted in the absence of the CTD^{2A}.

Collectively, this work establishes an important role for CTD^{2A} in driving activity-dependent changes to both NMDAR subunit composition and gene transcription.

Lay summary

NMDA receptors (NMDARs) are one of the critical receptors in the brain that mediate neuronal excitation and the transmission of signals. NMDARs are made up of four protein subunits, two GluN1 subunits and two GluN2(A-D) subunits, with GluN2A and GluN2B being the most common in the forebrain. The ratio of GluN2A-containing NMDARs to GluN2B-containing NMDARs can change as the brain develops and in response to activity. This change in subunit composition is thought to be one of the key mechanisms by which the brain maintains a functional level of activity in response to changes in sensory input. However, the mechanisms that underpin how subunit composition changes in response to activity are not well understood. GluN2A and GluN2B both have a long tail like region, known as the carboxyl (C)-terminal domain (CTD). CTDs interact with an array of proteins and signalling pathways, therefore it has been suggested that they may play a crucial role in controlling NMDAR subunit composition in response to activity.

To address this gap in the knowledge, I looked at how changing sensory experience in the visual cortex affects the ratio of GluN2A to GluN2B. I found that depriving mice of visual experience decreases the ratio of GluN2A to GluN2B and that this effect can be reversed by restoring visual experience. Importantly, in both cases the changes in the ratio were caused by changes in the level of GluN2A, not GluN2B. This suggests that changes in the ratio require activity-dependent regulation of GluN2A. GluN2A in turn requires its own mechanism for sensing when to increase and decrease. To test whether the GluN2A CTD is required for this mechanism, I use a genetically modified mouse model with the CTD region of GluN2A swapped for that of GluN2B. Visually depriving these genetically modified mice revealed no change in the level of GluN2A, suggesting that the GluN2A CTD is essential for altering the level of GluN2A in response to visual experience and deprivation. Additionally I found that genetic markers of activity were more weakly controlled in mice with no GluN2A CTD. Taken together, this points to an important role for the GluN2A CTD in the neuronal changes that occur in response to changing levels of activity within the visual cortex.

Table of Contents

Abbreviations

NMDA	N-methyl-D-aspartate NMDAR
NMDAR	NMDA receptor
AMPA	α-amino-3-hydroxy-5-methyl-4-isoxazolepropionic acid
AMPAR	AMPA receptor
LTD	Long-term depression
LTP	Long-term potentiation
CaMKII	Ca2+/calmodulin-dependent protein kinase II
CREB	c-AMP response element binding protein
VC	Visual cortex
V1	Primary visual cortex
CTD	cytoplasmic (C)-terminal domain
WT	wild-type
CTD^{2A}	GluN2A CTD
CTD^{2B}	GluN2B CTD
MAGUK	membrane-associated guanylate kinase
$GluN2A^{2B(CTR)/2B(CTR)}$	GluN2A-2B-C-terminal swap
$GluN2B^{(2A(CTR)/2A(CTR)}$	GluN2B-2A-C-terminal swap
PSD	Postsynaptic density

Chapter 1
Introduction

1.1 A brief history of the NMDA receptor

The NMDAR is a ligand gated ion channel that is gated by the principal excitatory neurotransmitter glutamate. They are expressed across the central nervous system (CNS) and serve an important role in numerous physiological processes (Paoletti et al, 2013; Wyllie et al, 2013). However, while now established as one of the key excitatory receptors in the CNS, the path to identifying the NMDAR and its role in mediating synaptic events is one that involved decades of careful research. The journey that set out to identify the key mediators of excitatory neurotransmission in the CNS lead to the identification and characterisation of the subtypes of excitatory amino acid receptors that are widely recognised today.

1.1.1 Acidic amino acids as neurotransmitters within the CNS

In the first half of the 20th century it was understood that synaptic transmission was most likely chemically evoked, leading to a spate of research that was devoted to identifying the chemical involved (Lodge, 2009). Due to their identification as neurotransmitters within the peripheral nervous system, acetylcholine and monoamine were investigated as potential mediators of synaptic excitation within the CNS, however, both failed to elicit the rapid excitation observed at CNS neurons following afferent stimulation (Curtis, 1963). As such, attention moved to other potential chemical candidates.

The acidic amino acids L-glutamate and L-aspartate initially garnered interest due to their high concentration within the brain (Berl and Waelsch, 1958). Additionally, it has also been observed that application of these acidic amino acids to the surface of the cerebral cortex induced convulsions (Hayashi et al., 1952) and spreading depression (van Harreveld, 1959; Purpura et al., 1959). Further investigations using the technique of microelectrophoresis established that extracellular application of both L-glutamate and L-aspartate to cat spinal neurons produced an increase in both depolarisation and action potential firing comparable to the action of synaptic events (Curtis et al., 1959; Curtis et al., 1960). However, while these findings were promising, there were doubts as to whether these amino acids met the requirements for classification as a neurotransmitter. A cumulative effort by several research groups

over the following years was required to address these doubts and establish neurotransmitter status for these molecules (reviewed by Lodge, 2009).

1.1.2 Identifying subtypes of glutamate receptors

Two pieces of evidence prompted researchers to consider the possibility of diversity amongst glutamate receptors. Firstly, the discovery of strychnine and bicuculline as selective antagonists for the inhibitory neurotransmitters glycine and GABA respectively showed a level of diversity of inhibitory synapses implying that similar diversity may exist for excitatory synapses (Curtis and Johnston, 1974). Secondly, the discovery that L-glutamate and L-aspartate showed differential distribution within the CNS and differential potencies in different neuronal populations suggested different roles for these neurotransmitters (Graham et al, 1967; Johnston, 1968; Duggan and Johnston, 1970).

The synthesis and testing of a large number of acidic amino acids further established the concept of "aspartate-preferring" vs "glutamate-preferring" receptors. Two of the key synthetic compounds that were used during this time were N-methyl-d(isoform)-aspartate (NMDA) and kainate, both of which were important for establishing the nomenclature that we use today (Curtis and Watkins, 1963; Shinozaki and Konishi,1970). Based on the results of these studies, NMDA and kainite were tentatively regarded as the synthetic ligands of "aspartate-preferring" and "glutamate-preferring" receptors respectively. However, NMDA and Kainate were not the only key exogenous ligands discovered during this time as another excitatory amino acid, quisqualate, was also identified (Shinozaki and Shibuya, 1974). The identification of these three EAAs lay the groundwork for further investigation and refinement of distinct glutamate receptor subtypes.

1.1.3 Selective antagonists of excitatory receptors

Throughout the 1970s, the discovery of weak glutamate antagonists reinforced the case for glutamate receptor subtypes. The antagonists discovered during this time were glutamic acid diethyl ester (GDEE), D–α–amindipate (DαAA), and 1-hydroxy-3-aminopyrrolidone (HA-966). Initial characterisation of these antagonist demonstrated that GDEE and DαAA/HA-966 showed some degree of selectivity between glutamate

and aspartate respectively, and that this selectivity was greater when using their structural analogues (Haledman and Mclennan, 1972; Biscoe et al., 1977). This pharmacological divide was further addressed by Davies and Watkins (1979) using GDEE and DαAA to investigate their effect on excitatory agonist action within the cat spinal cord. Like the previous studies, they demonstrated that NMDA was sensitive to DαAA while L-glutamate, kainate and quisqualate were DαAA-insensitive. At this early stage, there was compelling evidence for at least two subtypes of excitatory receptors, "NMDA" and "non-NMDA" receptors. Additional evidence for this "NMDA" and "non-NMDA" receptor subdivision came from the observation that responses to NMDA could be selectively blocked by the divalent cation magnesium (Mg^{2+})(Evans et al., 1977). However, evidence for a third subtype of receptor came from the observations of Mclennan and Lodge (1979). This study found that while quisqualate and L-glutamate mediated responses were reduced by GDEE, excitatory responses mediated by kainite remained unaltered. From here a picture was beginning to emerge of three receptor subtypes: NMDA, quisqualate and kainate. Independent observations in the years that followed further confirmed the existence of three receptor subtypes (Davies and Watkins, 1981, Davies and Watkins, 1985). The nomenclature for the three subtypes has largely remained unchanged with the exception of quisqualate. Following the discovery of the potent excitatory action of aamino-3-hydroxy-5-methylisoxazolepropionic acid (AMPA) and its sensitivity to GDEE (Krogsgaard-Larsen et al., 1980) and the later finding that quisqualate acts at metabotropic glutamate receptors (Sladeczek et al., 1985; Nicoletti et al., 1986), AMPA superseded quisqualate in the nomenclature.

1.1.4 New beginnings – dedicated NMDAR research

Early studies using NMDA and DαAA had helped to identify this crucial subtype of excitatory receptor paving the way for further investigations into its role in synaptic events. The development of highly selective NMDAR antagonists such as D-2-amino-5-phosphonopentanoate (AP-5) aided researchers to further characterise this receptor. For a long time, the prevailing assumption was that the endogenous agonist of NMDAR was L-aspartate. However, the observation that L-glutamate displaced AP-5 more potently than other potential agonists, namely L-aspartate, L-homocysteate and quinolinate, forced a rethink of this previous assumption and led to the adoption of L-

glutamate as the neurotransmitter at NMDARs (Olverman et al., 1984). Later AP-5 would also be used to show the role of NMDARs in synaptic plasticity and learning (Collingridge et al., 1983; Morris, 1989). Taken together, the work conducted throughout the 1970s and 1980s helped to identify the NMDAR as an excitatory glutamatergic receptor with crucial roles in mediating synaptic events within the CNS.

1.1.5 Cloning of the NMDA subunits

Throughout the 1990s cloning of the NMDAR subunits provided more detail as to the structure and function of the NMDAR. The first subunit to be cloned was GluN1, or NR1 as it was referred to at the time (Moriyoshi et al., 1991). This was followed shortly after by the identification of the GluN2 subunits (or NR2). Cloning of different GluN2 subunits occured in rats (Monyer et al, 1992; Monyer and Seeburg, 1993) and mice (Meguro et al, 1992; Kutsuwada et al, 1994; Ikeda et al, 1992) around the same time leading to the establishment of a family of four GluN2 subunits, named GluN2A-2D (Ishii et al, 1993). Cloning studies also helped to shed new light on co-agonist binding that had previously been observed in native NMDARs. This came with the observation that glycine binds to the GluN1 subunit, whereas the site of glutamate binding is on the GluN2 subunit. Taken together, these studies provided insight into the diversity of NMDAR subunits and how different subunits convey distinct properties to the receptor, such as ligand binding specificity and ion channel gating kinetics.

In the years that followed, X-ray crystallography and cryo-electron techniques have provided high-resolution structural insights into the organization of NMDA receptor subunits and their assembly into functional tetrameric complexes. While initially, there was some debate as to whether GluN1 and GluN2 subunits were arranged in an adjacent “1/1/2/2” (Balasuriya et al, 2013) or an alternating “1/2/1/2.” (Riou et al, 2012) configuration, more recent evidence from x-ray crystal analysis of the NMDAR favours the latter (Lee et al 2014).

1.1.6 NMDAR structure and binding

NMDARs are heterotetramers consisting of two obligate GluN1 subunits and two GluN2 subunits (GluN2A-D). These subunits contain modulatory domains that

influence receptor function. In particular, NMDAR subunits comprise an amino terminal domain (ATD) that contains binding sites for subtype specific allosteric modulators such as Zn^{2+} and H^{+}. A ligand binding domain (LBD) where the binding of agonists and antagonists regulates channel opening. A transmembrane domain (TMD) that forms the channel pore that allows the passage of ions when Mg^{2+} is not bound. A cytoplasmic (C)-terminal domain (CTD) which binds postsynaptic proteins and mediate intracellular signalling pathways (**Fig 1.1**).

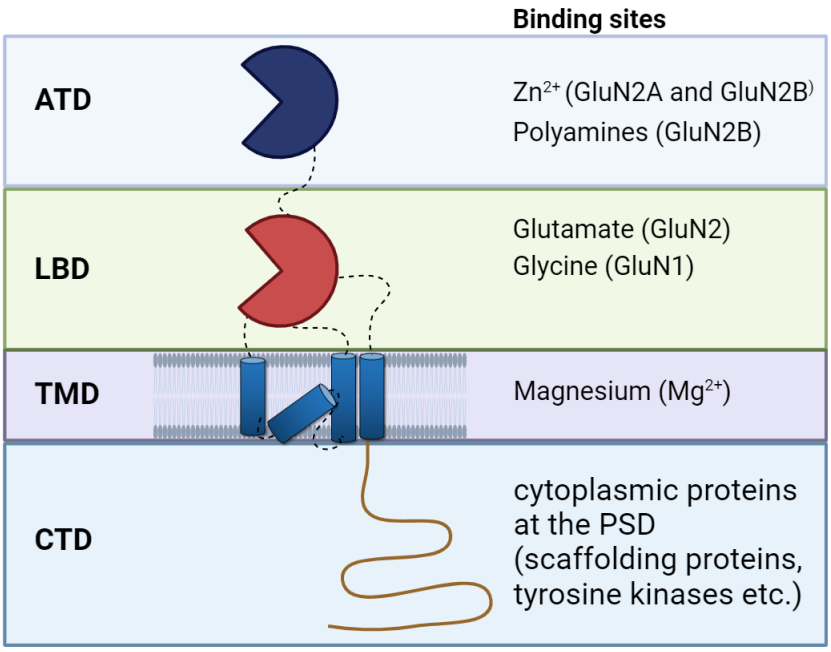

Figure 1.1 – Diagram of NMDAR subunit structure.

1.1.7 Activation of NMDARs

The NMDAR requires binding of Glycine/D-serine at the GluN1 subunit and Glutamate at the GluN2 subunit in order to allows the flow of Ca^{2+}, K^{+} and Na^{+}, of these permeant ion Ca^{2+} is integral to the intracellular signalling cascades which govern synaptic modification and the consequential changes to synaptic strength and plasticity. In addition, NMDARs are also highly voltage dependent owing to the presence of extracellular Mg^{2+} that enters and binds tightly to the NMDAR pore at negative membrane potential preventing ion permeation. The Mg^{2+} block can only be

alleviated a depolarization of sufficient amplitude and duration. Therefore, NMDARs are said to act as coincidence detectors as they require both presynaptic glutamate release and a sufficiently strong postsynaptic depolarisation to permit ion flow (Seeburg et al., 1995)(**Fig 1.2**).

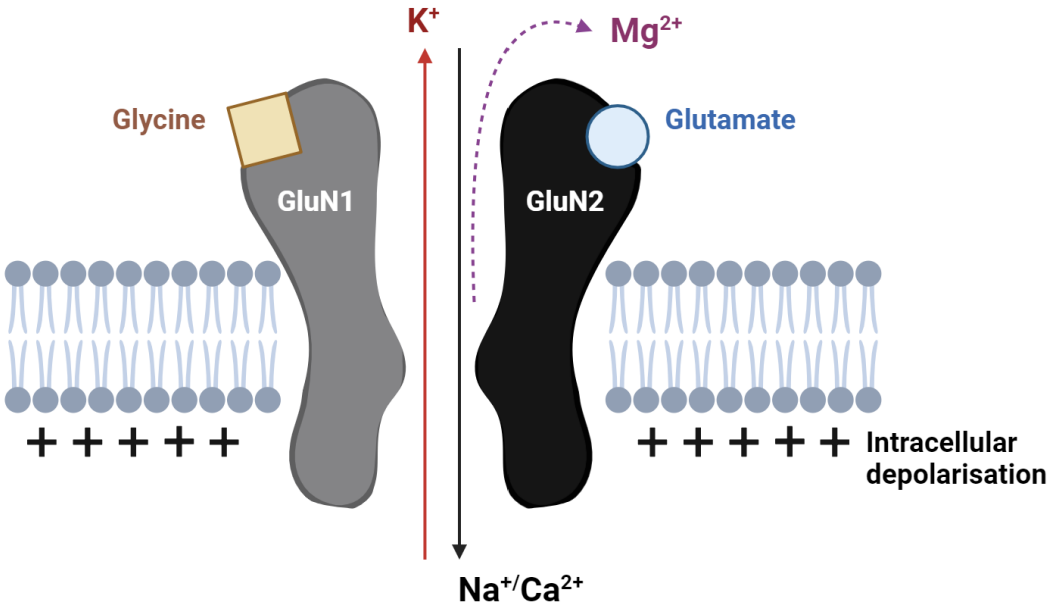

Figure 1.2 - Schematic showing how the NMDAR operates as a co-incidence detector.

Presynaptic release of glutamate is required for glutamate binding to the GluN2 subunit. Glycine/D-serine must also be bound to the GluN1 subunit to mediate a conformational change that results in the NMDAR channel opening. Additionally, sufficient intracellular depolarisation is required to alleviate the Mg^{2+} block of the channel pore. Therefore both presynaptic glutamate release and postsynaptic depolarisation are required to permit the flow of cations.

It should also be noted that NMDARs are expressed on non-neuronal glia (Müller et al, 1993; Conti et al, 1996; Wang et al, 1996) and endothelial cells (Krizbai et al, 1998; Andras et al, 2007). Moreover, these NMDAs diverge from their neuronal counterparts in both their subunit composition and channel properties (Krizbai et al, 1998; Sharp et al, 2003). In general, astrocytes and oligodendrocytes possess NMDARs that exhibit a lower permeability to Ca^{2+} - and a weak Mg^{2+} block even at negative membrane potentials. These differences in glial NMDARs are due to their expression of

triheteromeric receptors incorporating GluN2C, GluN2D or GluN3 subunits (Karadottir et al, 2005; Lalo et al, 2006; Burzomato et al, 2010; Palygin, Lalo and Pankratov, 2011). Interestingly, dihetromeric GluN1/GluN3 NMDARs have been observed in some non-neuronal cells (Pina-Crespo et al, 2010). This atypical configuration results in NMDARs that are both resistant to Mg^{2+} blockade and capable of generating currents following binding of glycine alone (Chatterton et al, 2002). However, the functional relevance of these atypical receptors is not well understood.

1.2 GluN2 Subunits determine NMDAR Biophysical properties.

The four NMDAR GluN2 subunits influence single-channel conductance, Mg^{2+} sensitivity, and Ca^{2+} permeability in different ways. Therefore the NMDAR GluN2 composition is important for determining the permeability and gating properties of the receptor. Considering their biophysical profile, GluN2A and GluN2B have similar properties as do GluN2C and GluN2D. Specifically, GluN2A and GluN2B containing NMDARs generate high conductance channel openings relative to GluN2C/GluN2D containing NMDARs which generate lower conductance channel openings. In addition, GluN2A/GluN2B containing NMDARs have a higher sensitivity to Mg^{2+} blockade and a higher permeability to Ca^{2+} when compared to GluN2C and GluN2D (Kuner and Schoepfer, 1996; Schneggenburger, 1996). GluN2 subunit identity also influences channel open probability, agonist sensitivity and deactivation kinetics. GluN1/2A NMDARs have a high opening probability; however, they possess a relatively low affinity for both glutamate and glycine. In contrast GluN1/2C and GluN1/2D NMDARs have a lower opening probability but stronger agonist affinity. Of the diheteromeric NMDARs GluN1/2A possesses the fastest deactivation kinetics followed by GluN1/2B, GluN1/2C and finally Glun1/2D, which exhibits the longest deactivation time (Vicini et al, 1998) (**Fig 1.3**)

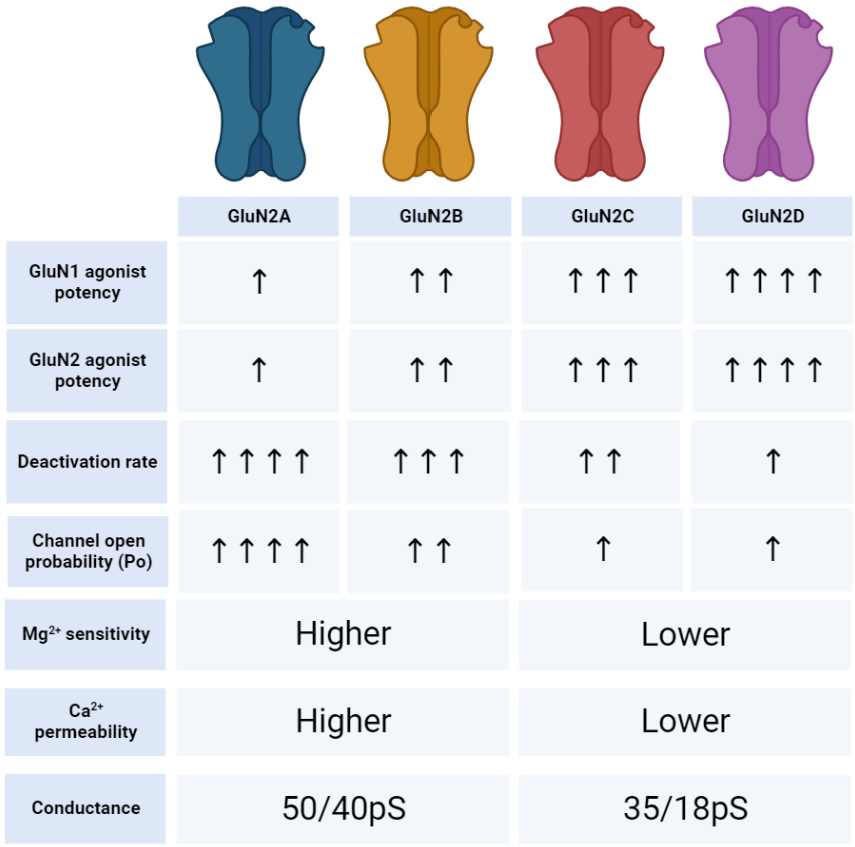

Figure 1.3 – Influence of NMDAR GluN2 subunit identity on biophysical properties (adapted from Wyllie et al,2013)

1.2.1 Regional and temporal expression of GluN2 subunits

Expression of GluN2 subunits is regionally localised amongst excitatory neuronal populations, with GluN2A and GluN2B being predominant in the forebrain, GluN2C expressed in the cerebellum and GluN2D in the midbrain (Paoletti et al, 2013; Wyllie et al, 2013). Furthermore, GluN2A and GluN2B subunits have distinct temporal patterns of expression. For example, compared to GluN2A, GluN2B expression begins earlier in the embryonic brain and maintains high levels of expression during early postnatal development before becoming mainly restricted to the forebrain (Monyer et al, 1994). After the first two postnatal weeks GluN2A steadily increases, becoming

abundant throughout the entire adult CNS. This developmental shift in subunit expression allows for greater GluN2A representation and creates a population of both diheteromeric $GluN1_2$-$GluN2A_2$ and $GluN1_2$-$GluN2B_2$ NMDARs as well as triheteromeric $GluN1_2$-GluN2A-GluN2B NMDARs (Paoletti et al, 2013; Wyllie et al, 2013). As GluN2A and GluN2B are the most abundant subunits within the adult forebrain, they are the most widely studied.

1.2.2 GluN2A and GluN2B subunits have different pharmacological properties.

It has been shown experimentally that GluN2A and GluN2B possess different affinities for endogenous protons, polyamines, and Zn^{2+}. For instance, protons and extracellular polyamines selectively inhibit and enhance GluN2B containing NMDARs respectively whereas Zn^{2+} acts as a selective antagonist of the GluN2A subunit when applied at nanomolecular concentrations (Banke et al, 2005; Mony et al, 2011; Paoletti et al, 1997). Pharmacological agents can also be used to discriminate between NMDAR GluN2 subunits, for instance the drugs ifenprodil and spermine selectively inhibit and potentiate GluN2B containing NMDARs respectively. In addition, the sulphonamide derivative TCN 201 acts as a potent antagonist of GluN2A containing NMDARs (Edman et al, 2012). As these compounds are selective for their respective subunits, their ability to either decrease or potentiate synaptic currents serves as an indication of the levels of either GluN2A or GluN2B containing NMDARs, therefore, these pharmacological compounds act as an important tool for assessing changes to NMDAR subunit composition during development and in response to activity.

1.2.3 Triheteromeric GluN2A/GluN2B NMDARs

In the past much focus has been placed on the study of diheteromeric GluN2A and GluN2B NMDARs where both GluN2 subunits are the same. However, in the last decade research has started to highlight a prominent role for triheteromeric $GluN1_2$-GluN2A-GluN2B NMDARS. For instance, it has been demonstrated that $GluN1_2$-

GluN2A-GluN2B NMDARs are the major population of NMDARs in both acute hippocampal slice and hippocampal culture (Rauner and Köhr, 2011; Tovar, McGinley and Westbrook, 2013). Furthermore, as new techniques have allowed $GluN1_2$-GluN2A-GluN2B to be studied in more detail, it has been found that they uniquely influence both the biophysical and pharmacological sensitivity of NMDARs. Specifically, they display intermediate levels of agonist sensitivity, open probability, deactivation kinetics and sensitivity to antagonists and allosteric modulation (Rauner and Köhr, 2011; Tovar, McGinley and Westbrook, 2013; Hansen et al, 2014; Stroebel et al, 2018). Interestingly, in many cases the profile more closely matches that of GluN2A, thus suggesting a dominant effect of GluN2A in determining NMDAR function (**Fig 1.4**).

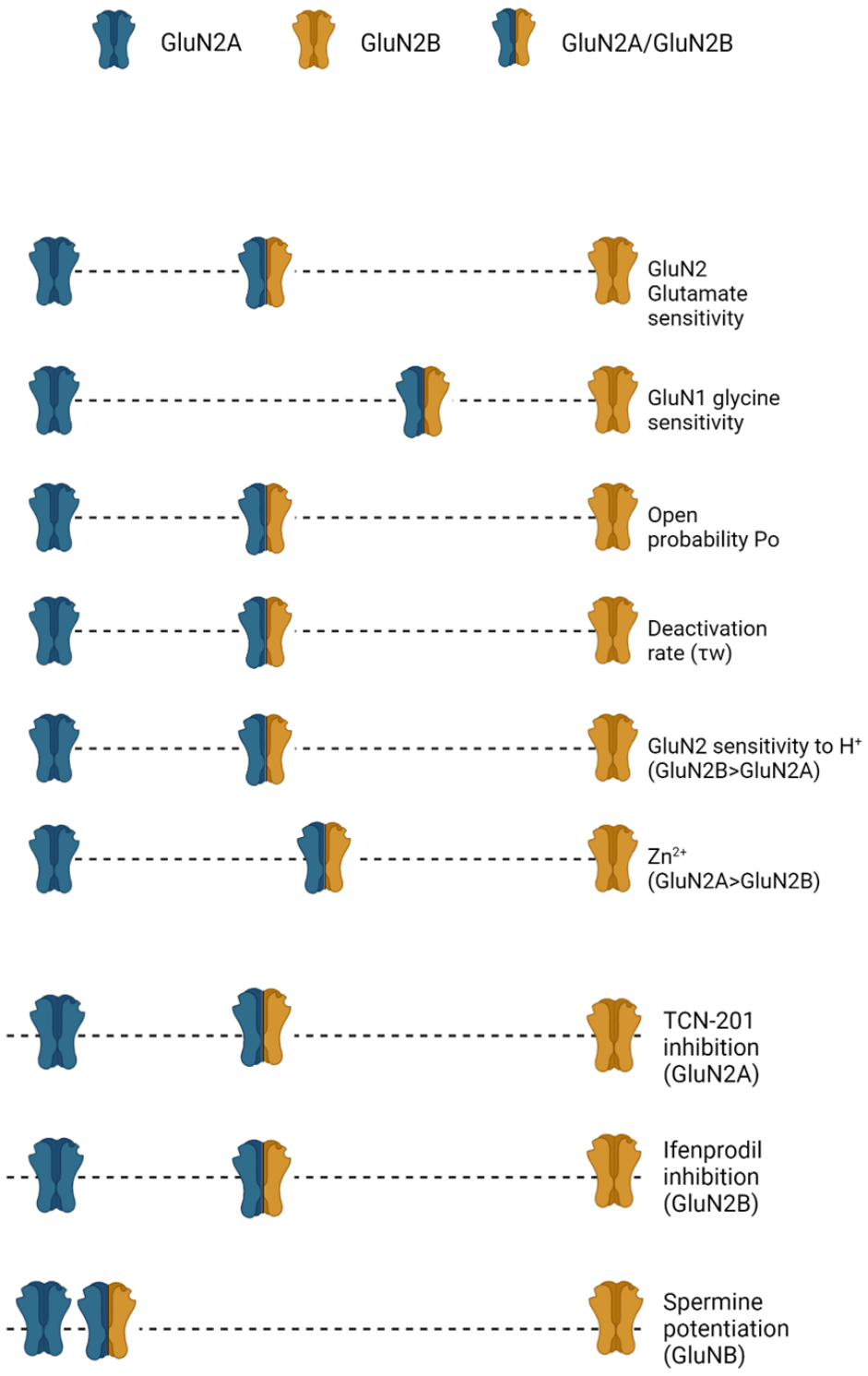

Figure 1.3 – Distinct biophysical and pharmacological characteristics of triheteromeric 2A/2B NMDARs.

Displays whether 2A/2B triheteromeric receptor profile is more closely matched to GluN2A or GluN2B diheteromeric receptors. (Based on refs Rauner and Köhr, 2011; Tovar, McGinley and Westbrook, 2013; Hansen et al, 2014; Stroebel et al, 2018)

1.3 Synaptic plasticity

NMDARs are key integrators of synaptic input, producing an intracellular response relative to the input frequency. Activation of NMDARs by glutamate leads to an influx of Ca^{2+} into neurons that mediates intracellular signalling cascades and changes to gene transcription that either serve to weaken or strengthen synapses dependent upon the strength of synaptic inputs. The polarity of this modification is dependent upon the level of Ca^{2+} admitted via the postsynaptic NMDARs, with modest increases in Ca^{2+} favouring long-term synaptic depression (LTD) and larger increases in Ca^{2+} favouring long-term synaptic potentiation (LTP) (Bear and Malenka, 1994; Yang, Tang and Zucker, 1999; Lüscher and Malenka, 2012) (**Fig 1.5**). During LTP, the entry of Ca^{2+} through NMDARs activates CaMKII which interacts with the actin cytoskeleton to mediate spine enlargement (Bosch et al., 2014, Herring and Nicoll, 2016, Patterson and Yasuda, 2011). Accumulation of AMPARs at the synapse is also observed following LTP (Hayashi et al, 2000). The increased synaptic expression of AMPARs is thought to be mediated by both an activity driven exocytosis of receptors and lateral diffusion of AMPARs from extrasynaptic sites (Borgdorff and Choquet, 2002; Park et al, 2004; Passafaro, Piëch and Sheng, 2001; Patterson et al, 2010). CamKII and PKA also contribute to the retention of AMPARs at the synapse by both directly phosphorylating AMPAR subunits and by facilitating protein-protein interactions that serve to stabilise AMPARs (Roche et al, 1996; Lee et al, 2000; Opazo et al, 2010; Opazo, Sainlos and Choquet, 2012). On the other hand, LTD is associated with dephosphorylation of AMPARs leading to a reduction in the extrasynaptic pool of AMPARs and targeting to lysosomal degradation (He et al, 2009). Therefore, the induction of LTP or LTD can be viewed as dependent on Ca^{2+} - mediated kinase activity, with increased phosphorylation favouring LTP and decreased phosphorylation favouring LTD.

While the most widely accepted role for NMDARs in mediating synaptic plasticity involves the influx of Ca^{2+}, it must also be noted that there has been some evidence to suggest that NMDARs can function independently of ion flux in a purely metabotropic fashion to induce LTD and shrinkage of dendritic spines (Nabavi et al, 2013; Kessels et al, 2013; Stein et al, 2015). This conclusion was reached based on the observation

that open channel blockers failed to prevent LTD. however, separate studies have since demonstrated that channel blockers do in fact block LTD (Babiec et al, 2014) and that Ca^{2+} flux is required for LTD induction (Volianskis et al, 2015; Sanderson et al, 2016). Altogether, the role of non-conventional metabotropic NMDAR signalling is a topic that is still subject to much debate.

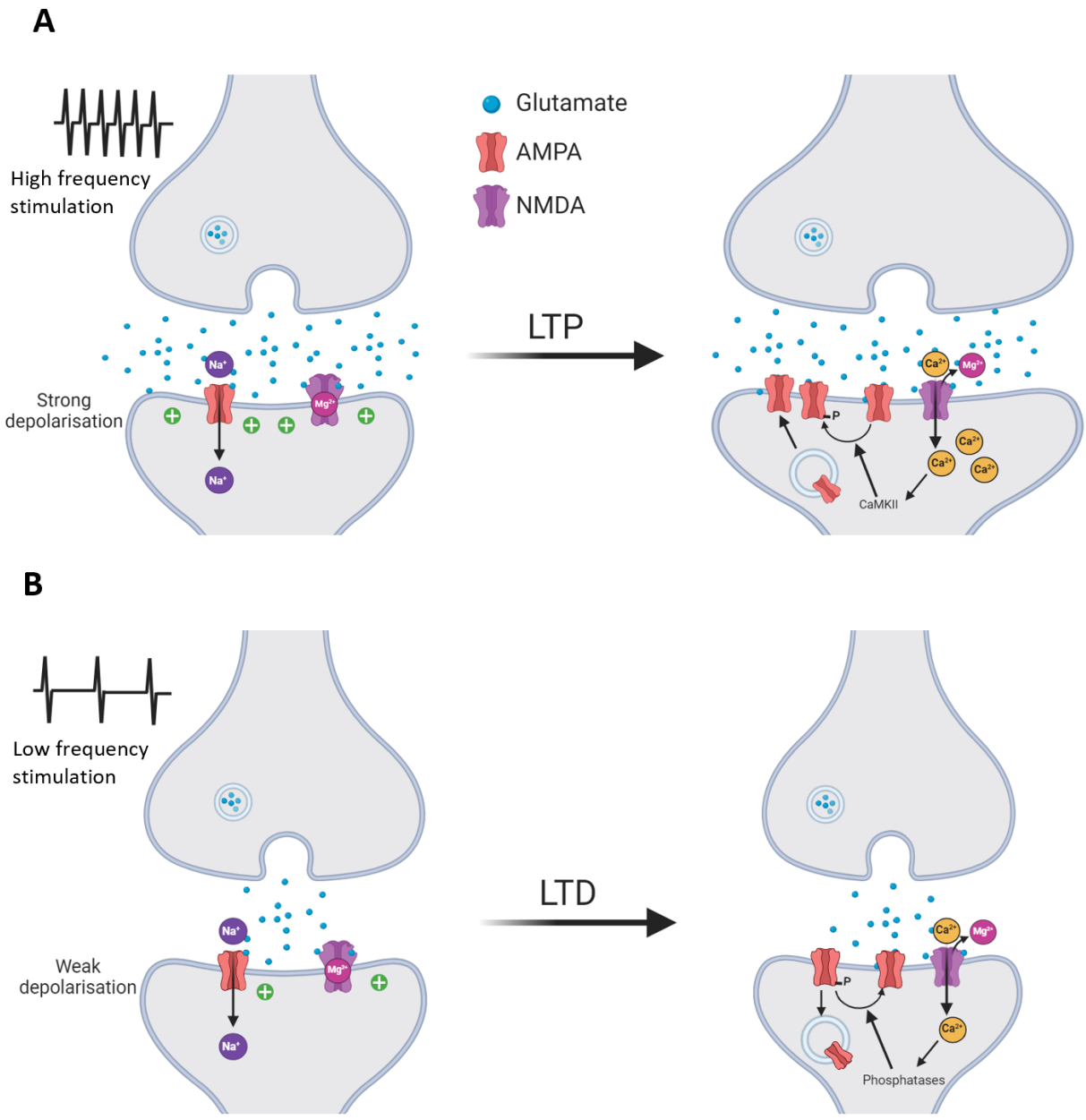

Figure 1.5 – Diagram shows how intracellular Ca^{2+} concentration determines LTP vs LTD.

A) High frequency stimulation leads to a large increase in intracellular calcium concentration and selective activation of protein kinases to induce LTP. **B)** Low-frequency stimulation causes a moderate

increase in intracellular calcium concentration leading to selective activation of phosphatases and induction of LTD.

1.3.1 Role of GluN2A/2B subunits in synaptic plasticity.

Some controversy has surrounded the role of GluN2A and GluN2B in mediating synaptic plasticity. Initial work in this area suggested separate roles for GluN2A and GluN2B in mediating LTP and LTD respectively (Liu et al, 2004; Massey et al, 2004). However, these results were called into question based on the suggestion that non-specific concentrations of GluN2A antagonist NVPAAM077 had been used in these studies. Indeed, subsequent studies found that the concentration of NVPAAM077 used in the original studies was sufficient to antagonise GluN2B (Weitlauf et al, 2005; Frizelle, Chen and Wyllie, 2006). Furthermore, the research that followed these original studies largely refuted the idea that GluN2A and GluN2B play distinct roles in mediating LTP and LTD (Berberich et al, 2005; Weitlauf et al, 2005; Zhao et al, 2005). As such it is currently accepted that the induction of LTD/LTP is not dependent on GluN2A or GluN2B subtype.

1.3.2 NMDAR mediated gene expression and synaptic plasticity.

NMDAR-dependent Ca^{2+} influx plays a critical role in signal transduction by initiating intracellular signalling cascades that propagate the signal to the nucleus leading to the activation of transcription factors and their subsequent binding to regulatory elements of activity-regulated genes (Xia et al, 1996; Hardingham and Bading, 2003). Amongst these activity-regulated genes are the immediate early genes (IEGs). These genes are characterised by their rapid and transient activation in response to a wide range of stimuli. The gene products of many of these IEGs act as transcription factors, therefore they act as a quick primary response that mediate slower, long-lasting changes in the expression of other genes (Wisden et al, 1990). As such, transcription within a critical time-window following stimulation is essential for changes to protein synthesis and synapse structure leading for longer lasting changes to neuronal function (Nguyen,

Abel and Kandel,1994; Arnold et al, 2005). Indeed, IEGs such as cFos, Egr1 (also known as zif268 or krox-24) and Arc have all been associated with neurons undergoing synaptic plasticity (Cole et al, 1989; Plath et al, 2006).

The transcription of many of these genes is controlled by the transcription factor cAMP-response-element-binding-protein (CREB). CREB-mediated transcription requires the phosphorylation of CREB at Ser133 (Gonzales and Montminty, 1989). Synaptic NMDAR-mediated Ca^{2+} influx mediates CREB phosphorylation through two signalling pathways (Hardingham et al, 2001a): the Ras-ERK1/2 pathway and the Ca^{2+}-calmodulin (CaM) kinase IV (CaMKIV) pathway (**Fig 1.6**). As CamKIV itself is Ca^{2+}dependent, Ca^{2+} influx activates CaMKIV which then in turn mediates the rapid phosphorylation of CREB. In contrast, in the Ras-ERK1/2 pathway, Ca^{2+}-dependent activation occurs further upstream leading to a slower downstream activation that persists long after the initial stimulus (Bading and Greenberg, 1991; Finkbeiner and Greenberg, 1996; Hardingham et al, 2001b; Wu, Deisseroth and Tsien, 2001). Therefore, while the CaMKIV pathway mediates the phosphorylation of CREB within seconds of Ca^{2+} flux, the ERK1/2 pathway is required to prolong CREB phosphorylation long after the activity has ceased (Hardingham et al, 2001a; Wu, Deisseroth and Tsien, 2001; Impey et al, 2002).

Phosphorylation of CREB at Ser-133 recruits the transcriptional co-activator CREB binding protein (CBP)(Chrivia et al, 1993). However, in order for transcription to be fully activated, CBP activity is first enhanced through CamKIV-mediated phosphorylation of CBD at Ser-301 (Chrivia et al, 1993; Hardingham et al, 2001a; Hu et al, 1999; Impey et al, 2002). This final step is dependent on an elevation in nuclear Ca^{2+} in order to activate CamKIV (Hardingham et al, 1997; Chawla et al, 1998).

Of note, Ca^{2+}-mediated activation of the mitogen-activated protein kinase (MAPK) pathway can also regulate transcription via the transcription factors serum-response factor (SRF) and Myocyte enhancer factor 2 (MEF2). In this case, transcriptional regulation is largely achieved via post-translational modification of transcriptional co-regulators (Lyons and West, 2011).

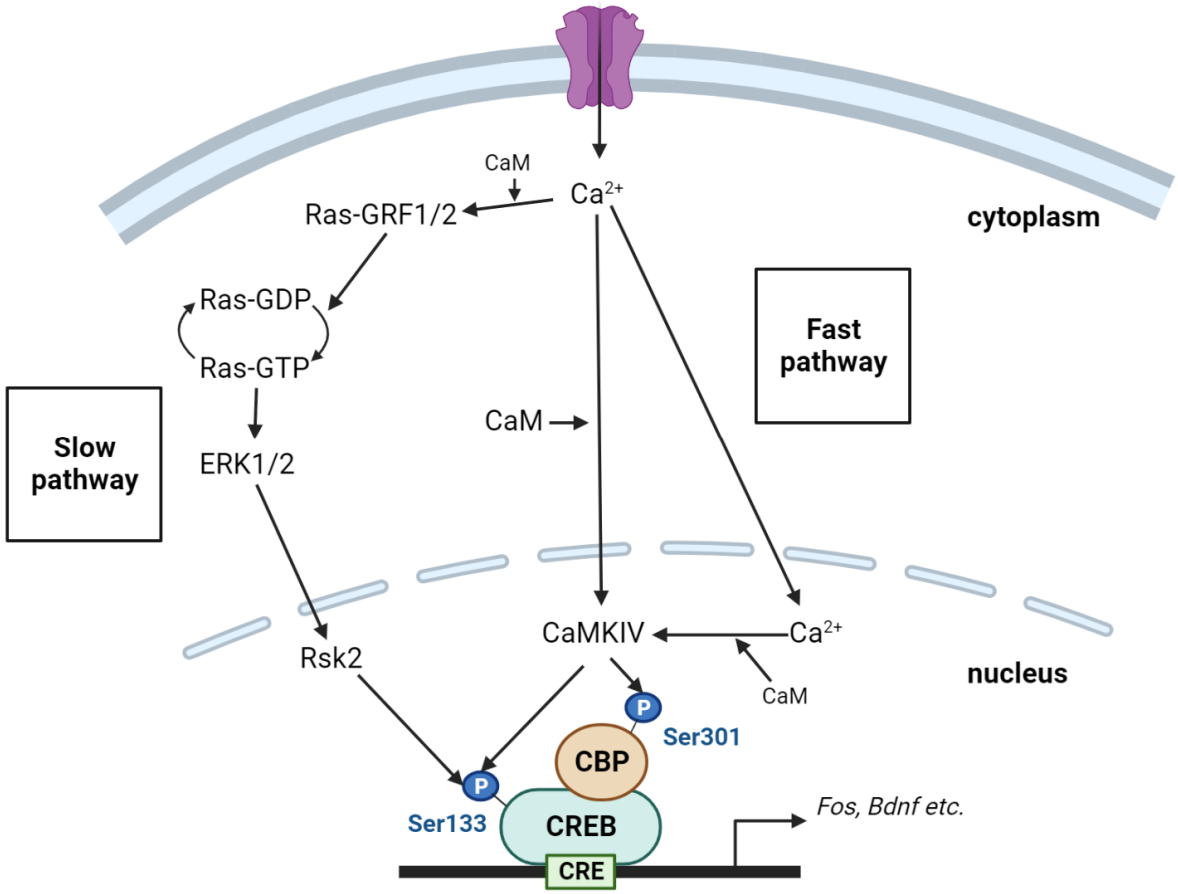

Figure 1.6 – Schematic for the activation of CREB-mediated transcription.

The fast pathway is mediated by synaptic activation and $Ca2^{+}$ influx leading to activation of CaMKIV and rapid phosphorylation of CREB at Ser133 and CPB at Ser301.

The slow pathway is mediated by Ca^{2+} influx and activation of upstream Ras-GRF. Ras-GRF mediates the activation of Ras which in turn activates ERK1/2 and eventually leads to CREB phosphorylation. (Adapted from Hardingham and Bading, 2003)

1.4 Homeostatic plasticity.

The ability to maintain a homeostatic balance is crucial for many organ systems with the brain being no exception. Considering the vast quantity of information that is processed by the brain daily, there must be some mechanism by which activity is kept within a functional range in order to prevent hyperactivity and to ensure the appropriate processing of relevant information. Similarly, in cases where there is low input, this mechanism must be able to ensure that some activity is preserved in order to prevent outright silencing of the network.

Hebbian plasticity states that when one cell consistently participates in firing of another cell, the connection between the two strengthens. However, while Hebbian plasticity forms the groundwork for our understanding of synaptic plasticity, it does not account for the added complexity of a dynamically changing environment in which the level of activity may fluctuate. For instance, Hebbian plasticity sets no restrictions on synaptic strengthening and as a result strong synapses would be allowed to grow unchecked. As such, there must be some restriction that prevents this scenario (Cooper and Bear, 2012). Indeed, this flaw in Hebbian plasticity led to the discovery of non-Hebbian forms of plasticity that serve to maintain homeostatic balance.

1.4.1 Synaptic scaling

In trying to resolve the stability issue of Hebbian plasticity, early theoretical work proposed a system in which neurons are capable of sensing how active they are and adjusting their synaptic weight appropriately in response to both increases and decreases in activity to maintain activity at a set-point (Miller, 1996; Sullivan and de Sa, 2006)(**Fig 1.7**). This concept was very appealing as it would provide stability to neuronal networks in the face of Hebbian based changes in synaptic strength. Indeed, evidence for such a mechanism was identified in neocortical neurons and termed synaptic scaling due to the observation that all synapses on a given neuron globally up-scaled to keep neuronal firing stable in the face of chronic silencing by the voltage-gated sodium channel blocker tetrodotoxin (TTX) (Turrigiano et al., 1998). Similarly,

elevating neuronal activity by using the GABAA antagonist bicuculine was observed to promote a down-scaling of synaptic strength. Unlike LTP and LTD, which occur rapidly (within minutes to hours), synaptic scaling operates over longer timescale (days) (Turrigiano, 2008). As such, this slow time course allows neurons to integrate changes in activity levels over time and adjust synaptic strength accordingly.

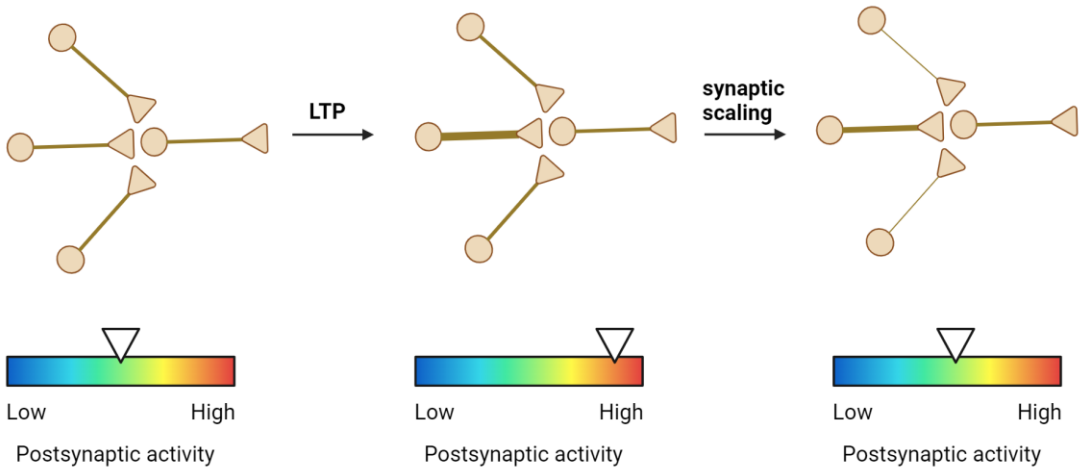

Figure 1.7 – Schematic overview of synaptic scaling.

When LTP of one input leads to an increase in postsynaptic activity, synaptic scaling act to reduce the weighst of all synapses until the firing activity returns to a set-point level.

The mechanisms that underpin synaptic scaling largely converge on the regulation of AMPARs, in both their synaptic abundance and composition. For instance, the phosphorylation status of the Ser845 site of AMPAR subunit GluA1 has been implicated in the control of AMPAR levels at synaptic sites in response to both increases and decreases in the level of activity (Diering, Gustina and Huganir, 2014). Similarly, a compositional switch in the incorporation of Ca^{2+} permeable GluA1 and Ca^{2+} impermeable GluA2 has also been observed to contribute to the mechanisms of synaptic scaling (Sutton et al, 2006; Soares et al, 2013) . In general, chronic reductions in activity appears to favour insertion of Ca^{2+} permeable AMPARs. In addition, subunit specific interactions with postsynaptic scaffolding proteins have also been observed to contribute to both the accumulation and removal of AMPARs (Xia et al, 1999; Matsuda, Mikawa and Hirai, 1999; Osten et al, 2000; Fiuza et al, 2017). As

such, these interactions are thought to contribute to the appropriate control of AMPAR levels required for synaptic scaling.

Aside from AMPAR driven mechanisms, there is also evidence to suggest that NMDAR-mediated Ca^{2+} signalling contributes to synaptic scaling. For instance, mice expressing mutant NMDARs with reduced Ca^{2+} permeability exhibit impaired synaptic scaling of AMPA currents (Pawlak et al., 2005). In addition, changes in CaMKIV signalling have also been implicated in the induction of synaptic scaling. The combined evidence that TTX reduces the level of phosphorylated CaMKIV and that phospho-null CaMKIV mutants mimic the increase in mEPSC amplitude observed in TTX treated mice presents a compelling case for the role of CaMKIV signalling (Ibata, Sun and Turrigiano, 2008). In agreement with a role for CaMKIV as a transcriptional regulation, blocking transcription with actinomycin D prevented AMPAR accumulation following 4 hr of TTX (Ibata, Sun and Turrigiano, 2008). Taken together this suggests a series of events whereby a decrease in postsynaptic firing leads to a drop in intracellular Ca^{2+} and a reduction in CaMKIV activity resulting in transcriptional changes that promote synaptic scaling.

1.4.2 BCM theory

In 1979, Cooper, Liberman and Oja proposed a theory that addresses this issue by introducing a threshold for synaptic modification, referred to as the modification threshold (θm). This theory was termed CLO theory (Cooper, Liberman and Oja, 1979). In CLO theory, the θm acts as a crossover point between LTD/LTP. Simply, activity that fails to surpass the threshold promotes the induction of LTD. This begins to put the pieces together, but it is still a relatively inflexible model that doesn't account for dynamic changes to levels of activity. Therefore, it possesses the same limitations as the original Hebbian plasticity model in that strong connections will always surpass the threshold and grow without bound and weaker connection will always fall short and wither away.

In 1982, Bienenstock, Cooper and Munro sought to address this issue. This led to the birth of BCM theory (so named after its authors). Based on the observation that networks with high cortical activity have a higher LTP threshold in comparison to inactive networks, which have a relatively lower LTP threshold, BCM theory proposed that the θm is dynamic and "slides" as a function of the history of postsynaptic activity (Bienenstock, Cooper and Munro, 1982; reviewed by Bear, 1996) (**Fig 1.8**).

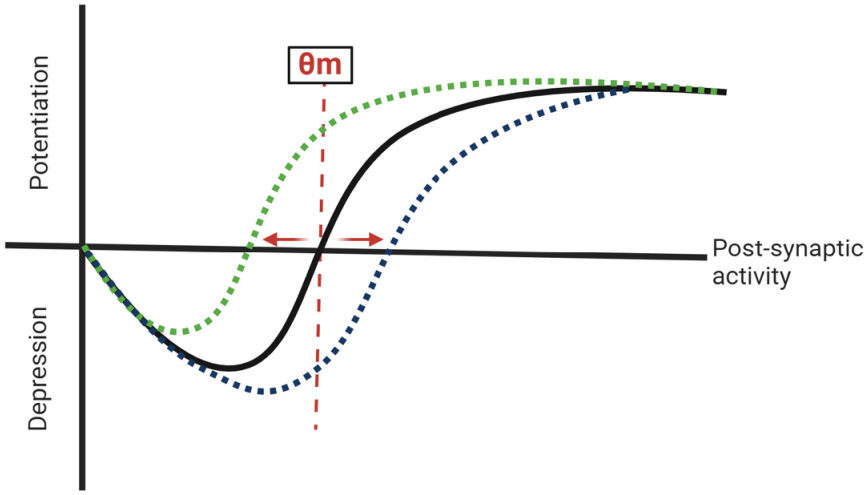

<u>Figure 1.8</u> – Shows the proposed model by which the level of post-synaptic activity shifts the modification threshold in favour of either potentiation or depression.

Increased levels of post-synaptic activity shift the modification threshold in favour of depression, in contrast lower levels of post-synaptic activity favour potentiation.

1.4.2.1 Primary visual cortex – a model system for investigating metaplasticity.

The Primary visual cortex (V1), also known as the striate cortex or area 17, has long served as region of interest in the study of experience dependent plasticity due to the ease at which visual input can be manipulated. The architecture of mouse V1 consists of six main cell layers. However, from a neuroanatomical point of view, there are nine distinct layers of neurons that make up V1. To maintain this six-layer convention, three distinct sublayers of neurons were combined into layer 4 (4A, 4B, 4C). Layer 1, which is located just underneath the pia mater is nearly aneuronal, and mainly consists of axons and dendrites projecting from other cell layers (O'Kusky and Colonnier, 1982). Excitatory pyramidal cells (PC), characterised by the presence of a thick apical dendrite that branches towards more superficial layers and multiple basal dendrites, are distributed across most layers of V1. Spiny stellate cells are another type of excitatory neuron located within the mammalian V1 and are morphologically characterised by spine-covered dendrites that radiate out from the cell body. However, recent evidence suggests that while spiny stellate cells are abundant within L4 of the rodent primary somatosensory cortex (Simons and Woolsey, 1984; Callaway and Borrell, 2011; Scala et al., 2019), they are surprisingly absent in V1 (Scala et al., 2019). Like PC, inhibitory GABAergic interneurons (INs) are also found in most cortical layers of V1. Inhibitory interneurons can broadly be classified into three major subtypes based on the presence of distinct molecular markers: parvalbumin (PV+), somatostatin (SOM+), and vasoactive intestinal peptide expressing (VIP+) (Gonchar et al., 2007). PC and inhibitory INs make up 80-85% and 15-20% of the cell population respectively (Feldman and Peter, 1978). In general, most excitatory synapses form at dendritic spines of PC, while excitatory input onto inhibitory INS typically targets the dendritic shaft. In contrast, INs have a wider range of targets on PCs. Depending on IN subtype, inhibitory synapses may form selectively onto the soma, distal dendrites, or axonal initial segment of a target PC (Kawaguchi and Kubota 1997; Bock et al. 2011; Jiang et al. 2015). As such, different subtypes of interneurons can exert different forms of inhibition that differentially influence the process of dendritic integration as well as the probability and timing of neuronal spiking (Kawaguchi and Kubota 1997; Pouille 2001; Di Cristo et al. 2004; Higley and Contreras 2006; Bock et al. 2011; Atallah et al. 2012; Jiang et al. 2015).

The major pathways of V1 serve to transfer visual information from the retina to the cortex for processing and refinement of visual features such as the visual boundary, direction of motion and orientation. This starts with the transmission of visual information from the retina through the lateral geniculate nucleus (LGN) of the thalamus to V1. Visual information from the left and right eye is segregated in the dorsal LGN (dLGN), and this segregation is maintained in the feedforward afferent inputs to V1 layer 4. This division of input from both eyes results in columns of neurons that are selectively stimulated by one eye over the other, known as ocular dominance columns. Of note, the majority of inputs received by layer 4 come from the contralateral eye (~95%)(Antonini, Fagiolini and Stryker. 1999). Layer 4 PCs transfer visual information to other neurons in layer 4 as well as to layers 2/3 (Bock et al. 2011) Layers 2/3 receive inputs from both L4 neurons that respond to the left eye as well as from L4 neurons that respond to the right eye leading to binocular convergence of information from both eyes (Hubel and Wiesel, 1972). In addition to feedforward inputs from layer 4, layer 2/3 neurons are also subject to extensive recurrent excitatory and inhibitory connections from other layer 2/3 neurons. These lateral excitatory and inhibitory connections play a crucial role in the integration of visual features such as visual boundary and movement (Yang et al, 2013; Cruz-Martin et al, 2014; Roth et al, 2015). Layers 1 and 5 receive afferents from other cortical and subcortical regions and so serve as the main target for top-down feedback from other cortical areas (Tsiola et al, 2003; Hattox and Nelson, 2007; Clascá et al, 2012; Cruz-Martin et al, 2014; Ji et al, 2015;). Layer 6 neurons regulate visually induced cortical activity by projecting to the thalamus and superficial cortical layers of V1 to provide feedback (Olsen et al, 2012; Bortone et al, 2014). As well signalling between laminar layers in V1, information is also relayed to higher visual cortical areas beyond V1 (e.g., V2, V3, V4) forming a hierarchical processing pathway (Lund et al, 1975; Shipp and Zeki, 1989). These higher order areas are involved in more complex visual processing tasks, such as object recognition, motion perception, and spatial awareness (Orban, 2008).

In V1 of cats and monkeys, it has been demonstrated that NMDARs exhibit a heterogenous laminar distribution. In general, NMDARs are found throughout layers 2/3, 4, 5 and 6, but are most prominent in layers 2/3 (Rosier et al, 1993). Interestingly,

studies have shown that selectively blocking or genetically deleting NMDARs in laminar layers 4 and 2/3 leads to impaired visual experience-dependent homeostatic plasticity (Rodriguez et al, 2019; Fong et al, 2020). The role of NMDARs in homeostatic plasticity within V1 will be explored in later sections.

1.4.2.2 BCM theory in action – How theoretical modelling explains experimental observations in V1.

The work of Hubel and Weisel in the 1960s helped to establish one of the classic examples of experience-dependent cortical plasticity, that being ocular dominance plasticity (ODP). In ODP, deprivation of patterned visual input leads to a rapid depression of responses from visual cortical neurons to the deprived eye followed by an increase in responses to the open eye. The initial loss of connections between the visual cortex (VC) and deprived eye could be seen as a "withering" of these connections due to lack of input. However, the observation by Weisel and Hubel, (1965) that monocular deprivation produces more pronounced effects than that of binocular deprivation challenges this view. At first glance the more robust reduction in response observed in monocular deprivation versus binocular deprivation could be interpreted as the result of binocular competition in which strong inputs from the non-deprived eye outcompete the weaker inputs of the deprived eye for a conserved resource and/or generate a signal that promotes the withdrawal of weaker inputs (Oja,1982; Blais,Shouval and Cooper, 1999). However, this view of binocular competition cannot explain the observations made by reverse suture, a process by which the deprived eye is opened, and the previously non-deprived eye is sutured shut. This procedure creates an interesting situation in which the stronger connections are not receiving input and the pathway that is receiving input is weak. This creates an environment of low activity, where neither pathway is stronger than the other and as such competitive mechanisms would reasonably be reduced. Despite this, the connections of the newly deprived eye depress rapidly at a rate comparable to that seen with the initial monocular deprivation, with inputs from the previously deprived eye growing in strength in the days following re-opening (Cooper and Bear, 2012).

A key postulate of BCM theory is that the loss of response and connectivity of inputs from the deprived eye is actively driven by residual activity from the deprived eye. That is to say, when inputs consistently fail to produce strong, correlated postsynaptic activity (postsynaptic activity <θm) then there is a depression of responses. One key way of testing this assumption was to look at the differences between obscuring vision (monocular deprivation or blurring image on retina) and retinal inactivation with TTX. In agreement with BCM theory, the effects of monocular deprivation (where weak, residual activity remains) were shown to cause a much greater depression in responses than retinal inactivation (Rittenhouse et al, 1999; Frenkel and Bear, 2004; Coleman et al, 2010). Furthermore, intraocular injection of TTX was shown to block the changes observed in monocular deprivation, supporting the assumption that the reduction of response is driven by the remaining weak, uncorrelated input from the deprived eye itself. Therefore, noisy uncorrelated input is more detrimental than silencing the pathway outright (Frenkel and Bear, 2004). However, interestingly, while it could reasonably be assumed that retinal inactivation would in turn lead to a silencing of thalamocortical afferents, it was in fact found that TTX does not reduce the firing rate in LGN but does cause an increase in highly correlated neuronal firing, which likely offers some protection (Linden et al, 2009). As such, this reframes the way in which TTX studies should be viewed.

Another key finding in establishing the validity of BCM theory, was the discovery of homosynaptic LTD. While now it is widely accepted that low frequency stimulation drives synaptic weakening, 30 years ago there was much debate as to the existence or even importance of LTD. This changed with the development of the low-frequency stimulation protocol by Dudek and Bear, 1992. This work not only advanced the field of LTD research but also satisfied the assumption put forward by BCM theory that subthreshold activity leads to weakening of synapses.

Now with all the pieces in place we see that BCM theory neatly explains the observations made in both monocular deprivation and reverse suture experiments (**Fig 1.9**). Firstly, residual inputs from the closed eye drive weakening of synaptic connections from the deprived eye through homosynaptic LTD. The resulting depression of inputs from the deprived eye leads to a reduction in cortical activity that,

over the course of a few days, adjusts the θm in favour of promoting LTP. As a result, there is a delayed potentiation of ipsilateral inputs from the non-deprived eye. In the case of reverse suture, responses to the newly deprived eye are rapidly depressed as a result of noisy, uncorrelated inputs (as we see with the initial monocular deprivation). The gradual increase in the strength of response from the newly opened eye is the result of the low activity environment created by the absence of strong pathways, which sets the θm low enough that inputs along the weak, previously deprived pathway are potentiated.

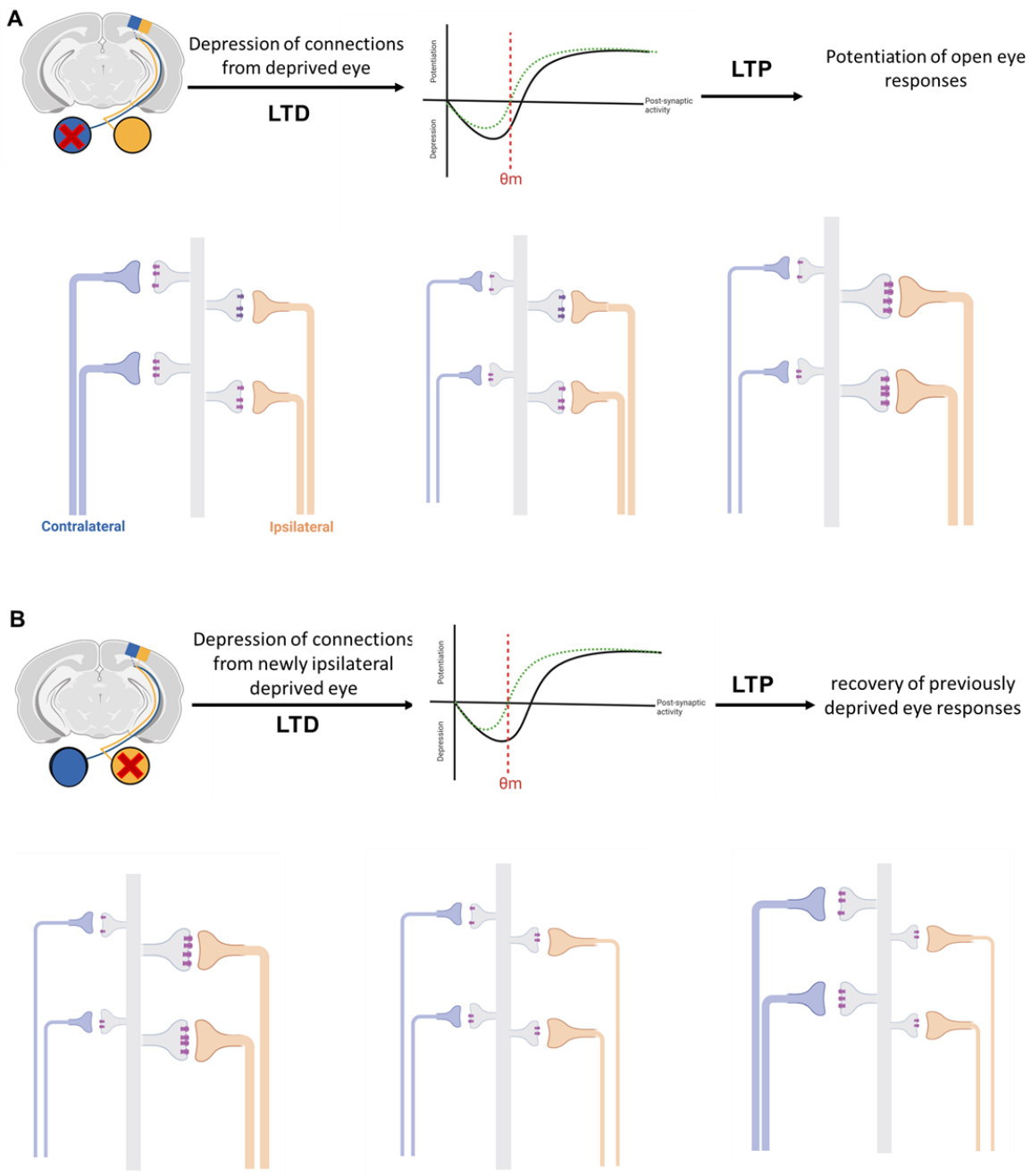

<u>Figure 1.9</u> – Diagrammatic representation of how BCM theory explains observations in monocular deprivation studies.

Contralateral eye (blue) and ipsilateral eye (orange). **A)** In monocular deprivation, weak residual inputs from the deprived contralateral eye drives LTD of synaptic connections from the deprived eye. This leads to a drop in cortical activity that lowers the θm. The lower θm facilitates potentiation of inputs from the open ipsilateral eye. **B)** In reverse suture, closure of previously open ipsilateral eye leads to depression of ipsilateral synaptic connections. The lack of input along the strong pathway and weak connection of the pathway receiving input leads to a significant drop in cortical activity, which shifts

the θm in favour of LTP. The leftward shift of the threshold facilitates recovery of the previously week pathway and potentiation of newly opened eye response.

1.4.2.3 NMDAR is required for sliding θm.

Once it was established that BCM theory could be used to explain the observations made in both monocular deprivation and dark rearing studies, the focus turned to identifying the molecular mechanisms underpinning the sliding θm. However, it wasn't long before a potential candidate emerged. There was already evidence within the literature to suggest that the NMDAR was required for changes to ocular dominance plasticity in the V1 of kittens during monocular deprivation and reverse suture. Specifically, the use of NMDA receptor blocker D,L-2-amino-5-phosphonovaleric acid (APV) was found to block the effects of monocular deprivation on the kitten striate cortex and prevent recovery following re-opening of the deprived eye (Kleinschmidt, Bear and Singer, 1987; Gu, Bear and singer, 1989). Similarly, it was found that partially blocking NMDARs (~50%) with APV prevented the frequency-dependent LTP induction shift in dark-reared rats (Philpot, Espinosa and Bear, 2003). Once it became clear that NMDA activity was required to set the θm in response to changes in activity, the question then became how do NMDARs adjust the threshold?

1.4.2.4 NMDAR composition as a molecular mechanism for sliding synaptic θm

.

As mentioned previously different GluN2 subunits have unique influences on the biophysical properties of the NMDAR. GluN2A containing NMDARs possess faster deactivation kinetics in relation to GluN2B containing NMDARs, and as such the difference in deactivation time between GluN2A and GluN2B containing NMDARS allows synaptic inputs to be integrated differently. Therefore, it has been suggested that the composition of NMDARs may be vital in setting the modification threshold (**Fig 1.10**)

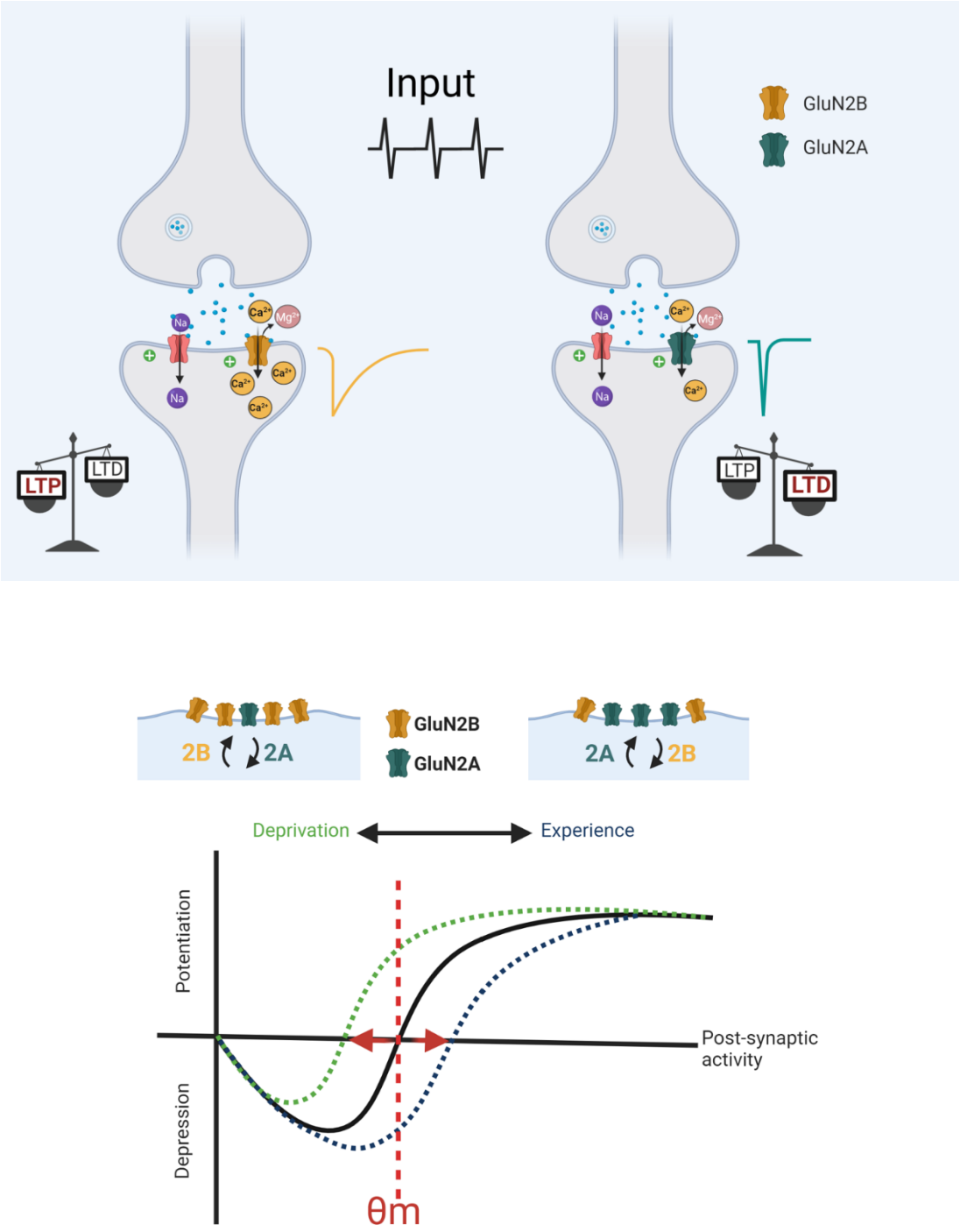

Figure 1.10 – Schematic demonstrating how experience-dependent subunit switch may shift the modification threshold in favour of either LTD or LTP.

During sensory deprivation there is an increase in the proportion of GluN2B containing NMDARs at the membrane and a decrease in GluN2A containing NMDARs, this shifts the modification threshold in favour of LTP. The opposite effect is observed during sensory experience, here there is an increase in GluN2A containing NMDARs and a decrease in GluN2B which shifts the modification threshold in favour of LTD.

1.4.2.5 Evidence for activity-dependent changes in NMDAR subunit composition.

It has been demonstrated that the GluN2A:GluN2B ratio can be bidirectionally modified within V1, with visual experience promoting an increase in the ratio and visual deprivation lowering the ratio. This suggests that activity-dependant subunit composition changes may be one of the key molecular mechanisms by which the modification threshold dynamically shifts in favour of LTP or LTD (Quinlan et al, 1999a; Philpot et al, 2001) (**table 1.1**).

Table 1.1 – Summary of experimental findings for the effect of activity on the GluN2A:GluN2B ratio

System	***Induction method***	***GluN2A:2B ratio***	***Reference***
in vitro	Tetrodotoxin (TTX)	↓	Chen and Bear, 2007
in vitro	MK801	↓	Philpot, Espinosa and Bear, 2003
in vitro	APV	↓	Philpot, Espinosa and Bear, 2003
in vivo	Sensory deprivation-dark rearing	↓	Quinlan et al, 1999a; Quinlan et al, 1999b; Chen and Bear, 2007
in vivo	Light exposure	↑	McQueen, unpublished observation Quinlan et al, 1999a

One possible explanation for these observations is that an activity-dependent effect on subunit turnover controls ratio. For instance, there is some indication that the rapid increase in synaptic GluN2A that occurs upon re-exposing dark reared rats to light for 2Hrs is dependent on the synthesis of new GluN2A subunits (Quinlan et al, 1999a). Therefore, activity might regulate the GluN2A:GluN2B ratio, in part, by influencing synthesis/degradation of subunits. However, an activity-dependent influence over subunit insertion and recycling must also be considered.

Naturally, the GluN2A:2B ratio can be altered by either modifying the levels of GluN2A, GluN2B or both; yet there is still a lack of consensus as to which of these is the key determinant in activity-dependent ratio changes. For example, many of the dark rearing studies carried out in rats indicate that the control of GluN2A is the key factor in changes to the GluN2A:GluN2B ratio (Quinlan et al,1999a; Quinlan et al, 1999b). On the other hand, one study conducted in mice suggests that the effects of dark rearing on the GluN2A:GluN2B ratio occur in two distinct temporal phases 1) Disinhibition of GluN2B protein translation and 2) A decrease in the level of synaptic GluN2A (Chen and Bear, 2007). Moreover, in cortical neurons treated with either TTX or bicuculline, it has been observed that the GluN2A subunits accumulate at the PSD of active synapses, whereas GluN2B is more abundant at inactive synapses (Ehlers, 2003). However, the proposal that activity-dependent control of the ratio is mediated by changes to both subunits has recently been questioned. This will be discussed in more detail in later sections.

1.4.2.6 Alterations in GluN2A and GluN2B at single synapses

It should be noted that there is also evidence to suggest that the GluN2A:GluN2B ratio can be altered at single synapses without affecting neighbouring synapses. This single synapse metaplasticity has been observed at synapses in which the presynaptic terminal has been inactivated. Compared to their active neighbours, silenced synapses were found to accumulate GluN2B and possessed a lower threshold for potentiation (Lee, Yasuda and Ehlers, 2010). This somewhat contradicts the BCM model whereby the modification threshold is the same for all synapses and is set by integrated postsynaptic activity.

1.4 GluN2 C-Terminal Domains

The consequences of NMDAR activation do not rely solely on the influx of ions, but also involve interactions between the NMDAR and several signalling molecules and complexes (Collins and Grant, 2007). The binding sites for these signalling/scaffolding proteins are found within the ~600 amino acid sequence that makes up the GluN2A and GluN2B CTD (CTD^{2A} and CTD^{2B}) (Ryan et al, 2008). While GluN2 subunits are well conserved in the N-terminal and transmembrane regions, their CTDs have diverged much more, allowing CTD identity to differentially influence the recruitment of signalling complexes and downstream signalling, trafficking, and the functional diversity of NMDAR signalling (Ryan et al, 2013). However, there are still outstanding questions as to how CTD identity influences key processes such as activity-dependent changes to NMDAR composition, outcome to excitotoxic insult and its role in chronic neurodegenerative states, as well as its contribution to neurodevelopmental disorders.

A vital tool for evaluating the role of the CTD^{2A} and CTD^{2B} has been provided by the generation of novel knock-in mouse models. Specifically, by deleting and replacing the CTD encoding exon with its paralog it has been possible to generate knock-in mice which possess the GluN2A subunit coupled with the GluN2B CTD and vice versa, referred to as $GluN2A^{2B(CTR)/2B(CTR)}$ and $GluN2B^{2A(CTR)/2A(CTR)}$ respectively. In these mice all GluN2A and GluN2B expressing NMDARs will possess the same CTD, this allows the role of specific CTDs to be evaluated from the biochemical to the behavioural level (Ryan et al 2013).

1.4.1 The role of GluN2 CTD in synaptic plasticity

The subunit composition of an NMDAR can influence plasticity through the biophysical characteristics conveyed by the constituent GluN2 subunits (e.g. Ca^{2+} permeability, Mg^{2+} affinity, open probability etc.). Deletion of GluN2A and GluN2B CTDs alters channel conductance and gating properties of NMDARs, however, simply swapping the CTDs of GluN2A and GluN2B does not alter biophysical properties

(Maki et al, 2012; Punnakkal, Jendritza and Köhr, 2012). Therefore, while intact CTDs are required for normal NMDAR function, distinct CTD sequences are not required to mediate subunit specific biophysical properties.

The influence of CTD identity on synaptic plasticity is less understood, however, it is clear that intact CTDs are also required for normal synaptic plasticity. For instance, it has previously been shown that GluN2A C-terminally truncated mice ($NR2A^{\Delta C/\Delta C}$) exhibit impaired LTP in the presence of GluN2B antagonist (Sprengel et al, 1998; Köhr et al, 2003). In addition, $NR2A^{\Delta C/\Delta C}$ mice exhibit decreased basal levels of ERK2 activity and protein kinase A (PKA) mediated phosphorylation at the GluA1 AMPA receptor subunits (Moody et al, 2011). Similarly, homozygous $GluN2A^{\Delta C/\Delta C}$ and heterozygous $GluN2B^{\Delta C}$ deletion mice exhibit impaired potentiation in response to theta burst stimulation (TBS) induced LTP (Ryan et al, 2013). However, there is also evidence to suggest that CTD identity is important for influencing the quality of plasticity induced by different types of stimulation. For instance, $GluN2B^{2A(CTR)/2A(CTR)}$ exhibit enhanced potentiation in response to TBS, but impaired LTP in response to theta pulse stimulation (Ryan et al, 2013). Therefore, diversification of the GluN2B CTD from the GluN2A CTD provides selectivity for different patterns of neuronal activity thereby influencing the ability to mediate different forms of LTP (Ryan et al, 2013).

1.4.2 Differential protein binding at NMDAR Subunit specific CTDs

The CTDs of GluN2 subunits are known to associate with a wide range of proteins at the postsynaptic density (PSD). Members of the membrane-associated guanylate kinase (MAGUK) family of scaffolding proteins have previously been shown to associate with NMDAR subunit CTDs via binding of the PSD95, Dlg, and ZO-1 Homology (PDZ) domain (Sheng and Pak, 2000; Garner, Nash and Huganir, 2000; Scannevin and Huganir, 2000; Sheng and Kim, 2002). PSD95 in turn interacts with a host of other scaffolding proteins as well as intracellular signalling molecules. This acts to create a complex framework of proteins linking NMDARs to downstream effectors (Sheng and Kim, 2002). Some of the proteins included in the NMDA-CTD-

PSD95 signalling complex are summarised in **figure 1.11** with several being elaborated on in later sections where necessary.

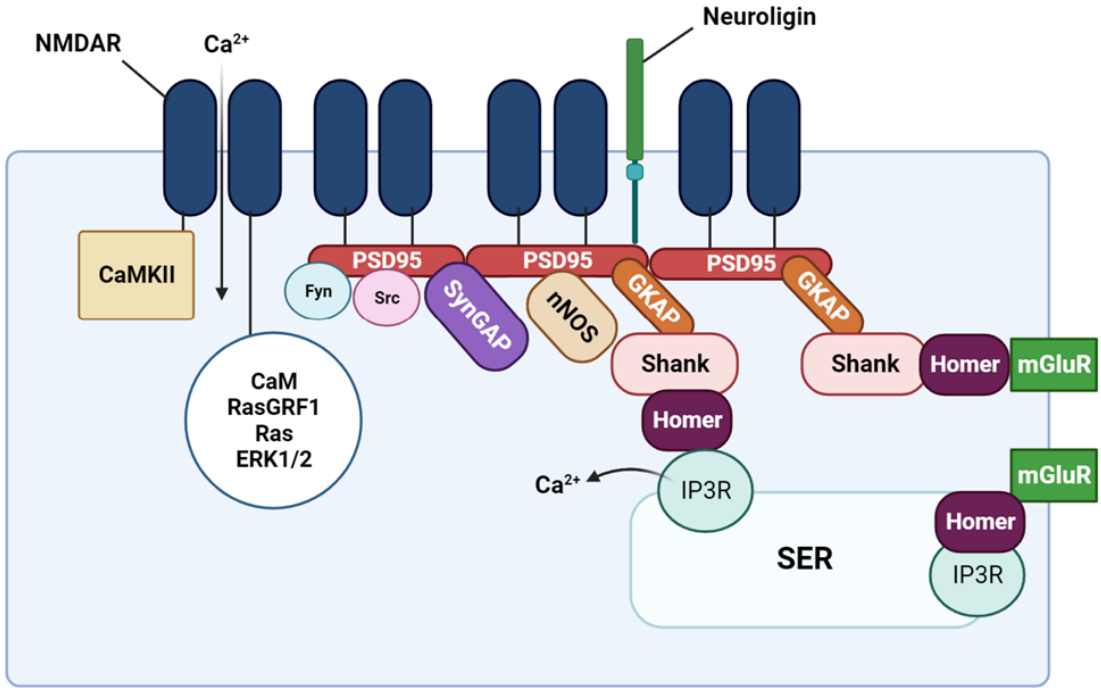

Figure 1.11 – Schematic of some of the NMDAR GluN2 CTD associated protein complexes
GluN2 CTDs associate with MAGUK scaffolding proteins that couple NMDARs to downstream signalling pathways.

The divergent evolution of the subunit CTDs suggest the possibility for differential recruitment of protein complexes and unique protein composition of said complexes between different subunits. In fact, it has been demonstrated that NMDARs are selectively partitioned into 0.8MDa complexes and 1.5MDa supercomplexes. Formation of these NMDAR-supercomplexes requires the presence of the CTD^{2B} and the MAGUK family members PSD95 and PSD93. Crucially, the CTD^{2A} is unable to mediate supercomplex assembly (Frank et al, 2016; Frank et al, 2017). The NMDAR-MAGUK supercomplex family is large owing to their ability to form different combinations of up to 50 different proteins (although the supercomplexes themselves will contain only a fraction of these proteins), including Kir channels, scaffolding

proteins adhesion proteins and signalling enzymes (Frank et al, 2016; Frank et al, 2017). As such, different protein assemblies may differentially influence a wide range of biological functions. In the context of development, the 1.5MDa NMDAR-supercomplexes begin to increase from the second postnatal week onward (Frank et al, 2016). This may suggest a role for NMDAR supercomplex assembly in key developmental processes such as synaptogenesis and synapse maturation.

1.4.3 Influence of GluN2 CTD on subunit trafficking dynamics

The trafficking of NMDARs is tightly regulated both during development and in response to activity (Groc et al, 2007; Otano and Ehlers, 2005). Phosphorylation is one of the key mechanisms for NMDAR trafficking to and from the plasma membrane. Changes to the surface expression of NMDAR can occur over periods of hours (Quinlan et al, 1999a) or more rapidly within the time frame of minutes (Lan et al, 2001), therefore there must be distinct phosphorylation events that mediate both slow and rapid insertion of NMDAR. MAGUK proteins have been observed to preferentially associate with CTD^{2B} over CTD^{2A} (Ryan et al, 2013; Martel et al, 2012), in addition this preferential binding is thought to be vital for GluN2B retention at the plasma membrane, but less important for GluN2A localization at post synaptic sites (Townsend et al, 2003). Furthermore, differential protein interaction between CTD^{2A} and CTD^{2B} could provide an explanation for the increased mobility of GluN2B containing NMDARs relative to $GluN^{2A}$ containing NMDARs. Specifically, CTD^{2B}-specific phosphorylation events have been shown to disrupt $CTD^{2B/}$MAGUK interactions, which may explain the observation that GluN2B NMDARs more readily move in and out of synaptic sites (Groc et al, 2006; Sanz-Clemente et al, 2010; Sanz-Clemente et al, 2013). Additionally, GluN2A and GluN2B subunits have different rates of endocytosis (Lavezzari et al, 2004). Robust internalization of GluN2B is mediated by the interaction of the YEKL endocytic motif located on the CTD with adaptor protein complex 2 (AP-2) (Roche et al, 2001). In comparison, GluN2A exhibits slower internalization mediated by interaction at a dileucine motif on its CTD (Lavezzari et al, 2004).

1.5 The role of the 2A/2B CTD in developmental and activity-dependent changes in NMDAR subunit composition

In rodents, the forebrain NMDAR subunit composition undergoes a developmental shift over postnatal weeks 2-5. During this time, the population of NMDARs shift from predominantly GluN2B-containing to incorporating a greater contribution of GluN2A in the form of $GluN_1$-$GluN2A_2$ diheteromeric receptors and $GluN1_2$-$GluN2A_1$-$GluN2B_1$ triheteromeric receptors (Wyllie et al, 2013). Based on the prevailing theory that GluN2A replaces GluN2B as the most abundant subunit (Monyer et al, 1992; Sanz-Clemente, Nicoll and Roche, 2013), the NMDAR compositional change is often referred to as a "switch". This suggests that GluN2A incorporation comes at the expense of GluN2B.

One model for exchanging GluN2B for GluN2A proposes a series of phosphorylation events at a site on the CTD^{2B} (Sanz-Clemente et al, 2013; Sanz-Clemente et al, 2010). NMDAR activity mediates activation of CaMKIIα leading to the formation of a trimolecular complex consisting of GluN2B/CaMKIIα/Casein Kinase 2 (CK2). This association of CK2 with GluN2B leads to phosphorylation of serine-1480 (S1480) on the CTD^{2B}. Phosphorylation of S1480 leads to disrupted association MAGUK proteins at the CTD^{2B} PDZ ligand and a subsequent reduction in phosphorylation at Y1472 within the YEKL endocytic motif, due to the fact that MAGUKs ordinarily recruit the Y1472 kinase Fyn. These events are suggested to lead to lateral diffusion of GluN2B to extrasynaptic sites via a non-PDZ interaction with SAP102 before they are internalised by AP-2 mediated endocytosis, which recognises YEKL when Y1472 is unphosphorylated (Chen et al, 2012; Sanz-Clemente et al, 2013; Sanz-Clemente et al, 2010) (**Fig 1.12**). However, this model was based on experiments involving ectopic overexpression of mutant subunits, potentially altering the relative stoichiometry of CTD^{2B} and CaMKIIα or other signalling components that may affect the results. Subsequently, a KI mouse model with a non-functional CaMKIIα binding site was generated that had normal synaptic levels of GluN2A in the adult hippocampus suggesting that mutating the CaMKIIα binding site may at most delay the developmental subunit shift (Halt et al, 2012). Moreover, an independently made second KI mouse with a non-functional CaMKIIα binding site ($GluN2B^{\Delta CaMKII}$)

showed that the CaMKIIα site was not required for normal developmental increases in GluN2A:GluN2B ratio (McKay et al, 2018). The same study also utilised a KI mouse model with the CTD of GluN2A replaced by that of GluN2B ($GluN2A^{2B(CTR)2B(CTR)}$) (Ryan et al, 2013) and found that changes to the NMDAR composition in the cortex and hippocampus during development was normal and so do not require GluN2A and GluN2B to have distinct CTDs (McKay et al, 2018).

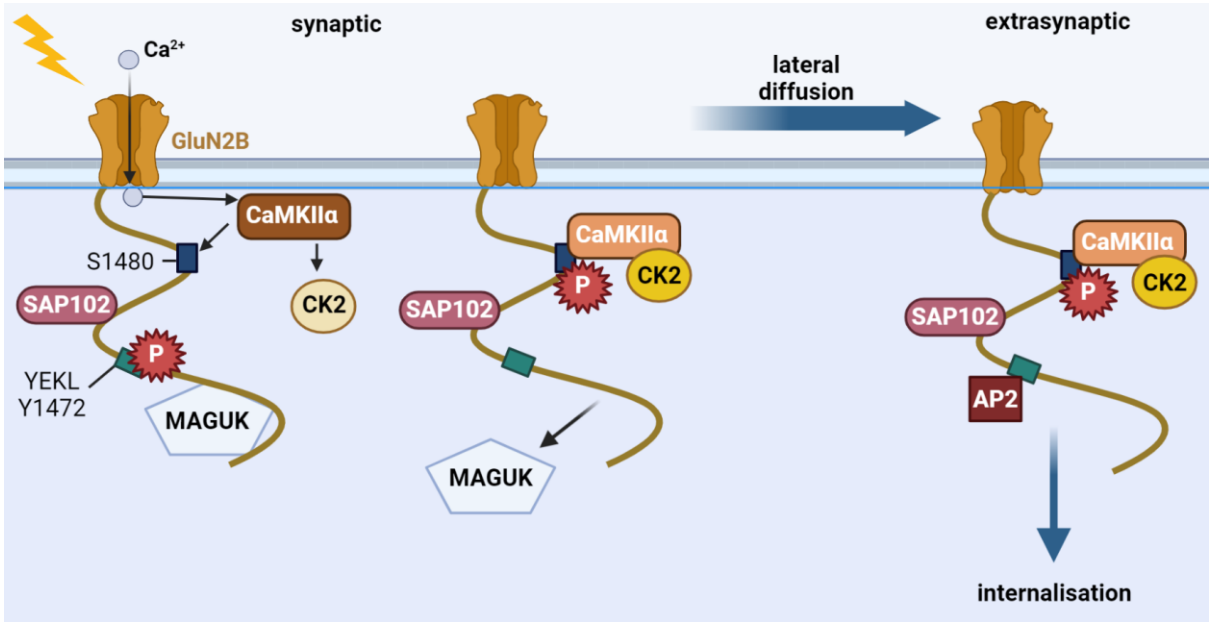

Figure 1.12 – Diagrammatic representation of the CTD^{2B}/CaMKII/CK2 phosphorylation cascade.

Interestingly, while the above study shows that the CTD of GluN2A can be swapped for that of GluN2B with no impairment of GluN2A surface expression, recent studies suggest that in the context of the CTD^{2A}, certain residues may be functionally important for surface expression of GluN2A. Work by Mota Vieira et al, 2020 and Yong et al, 2021 aimed to functionally characterise the epilepsy- associated variant GluN2A-S1459G and identified S1459 as a CaMKIIα phosphorylation site controlled in a developmental and activity-dependent manner whose mutation impaired interactions with SNX27 and PSD95 as well as GluN2A surface expression when ectopically expressed in cultured neurons. Generation and characterisation of a

GluN2A-S1459G KI mouse would further strengthen the case for this phosphorylation event being functionally important for developmental and activity-dependent surface expression of GluN2A.

Overall, there are two elements to the developmental shift in NMDAR subunit composition: an intrinsic developmental programme and an experience-dependent component. The studies which propose the involvement of NMDAR activity mediated CTD phosphorylation events are based predominantly *in vitro* using heterologous expression of mutant receptors, and as such would benefit from *in vivo* studies involving KI mice. The *in vivo* models used thus far have argued against a critical role for the CaMKIIα site of CTD^{2B} and subsequent phosphorylation changes proposed by *in vitro* models. If it is the case that phosphorylation events are not crucial, what are the molecular mechanisms that underpin this change? It is an under-appreciated fact that even in the adult mouse the forebrain contains far more GluN2B than GluN2A (Frank et al, 2016). The dramatic increase in GluN2A during development, alongside flat or falling levels of GluN2B can at first glance appear like a subunit "switch". However, by exploiting KI mice with reciprocal exchange of GluN2 CTDs it was demonstrated that GluN2B levels are around 5-times greater than GluN2A (Frank et al, 2016). This means that increased GluN2A insertion is likely to be the main driver of GluN2A:GluN2B ratio changes since removal of GluN2B on its own would have little effect on the ratio unless very large reductions in GluN2B were involved. Indeed, the GluN2A:GluN2B ratio has been shown to change developmentally with little or no change to GluN2B levels (McKay et al, 2018). This argues against CTD^{2B}-dependent removal of GluN2B being biologically important. The reason why this modest level of GluN2A (even in the adult) has such a strong effect on NMDAR currents (as evidenced by sensitivity to GluN2A antagonists or reduced sensitivity to GluN2B antagonists (Edman et al, 2012; McKay et al, 2012) is that $GluN1_2$-$GluN2A_2$ diheteromeric NMDARs have a higher open probability than $GluN1_2$-$GluN2B_2$ diheteromeric NMDARs and, moreover, $GluN1_2$-GluN2A-GluN2B triheteromeric NMDARs more closely resemble $GluN1_2$-$GluN2A_2$ NMDARS than $GluN1_2$-$GluN2B_2$ NMDARs with regard to their biophysical properties (Stroebel et al, 2018).

If removal of GluN2B plays a limited role in the developmental change of GluN2A:GluN2B ratio and insertion of GluN2A is more important, then what of the role of CTD^{2A}? Since the developmental GluN2A:GluN2B ratio shift occurs normally in $GluN2A^{2B(CTR)/2B(CTR)}$ mice where both GluN2B and GluN2A have the same CTD (CTD^{2B}) (McKay et al, 2018) then CTD^{2A}-dependent events cannot be critical for GluN2A surface delivery. Since GluN2A expression at the mRNA and protein level increases at the same developmental stage as the GluN2A:GluN2B ratio increases, it could be that this is the only change required, coupled with normal turnover of synaptic proteins.

Experience/activity dependent changes in GluN2A:GluN2B ratio represent a different situation, studied in most depth in V1. Studies conducted in rats have demonstrated that dark rearing either from birth or during the critical period reduces the levels of GluN2A at the synapse, resulting in a reduction in the ratio of GluN2A to GluN2B (GluN2A:GluN2B ratio) (Quinlan et al, 1999a; Quinlan et al, 1999b). Interestingly, dark reared rats exhibit a rapid increase in GluN2A following 2 hr re-exposure to light, suggesting that NMDAR subunit composition, and as such the GluN2A:GluN2B ratio, can be bidirectionally modified by activity (Quinlan et al, 1999a; Quinlan et al, 1999b). If sensory deprivation (e.g. dark rearing) causes the GluN2A:GluN2B ratio to fall, and rise again upon re-exposure to light, then these dynamic changes arguably do require a mechanism for recognising GluN2A-containing NMDARs in instances where they are lost/gained on a timescale incompatible with receptor turnover and changes in GluN2A gene expression (GluN2A transcription can be controlled by synaptic activity to influence slower-acting changes (Hoffmann et al, 2000). Investigations into such 'recognition' mechanisms will require further analysis of current KI mouse models as well as new ones, potentially with more targeted mutations in CTD^{2A}.

1.6 Experimental hypotheses and aims

In this introduction I have outlined how unique GluN2 CTD sequences influence signalling, protein interactions and synaptic plasticity. Despite this, there are still many gaps in the knowledge when considering the role of CTDs in sensory driven changes to NMDAR subunit composition and signalling. The work that has been done thus far predominately relies on *in vitro* overexpression models which, while potentially providing some mechanistic insight, don't fully reflect the conditions *in vivo*. The generation of reciprocal KI mice provides the opportunity to interrogate the role of specific CTD sequences in response to well characterised *in vivo* deprivation paradigms. As such, this thesis sets out to use these available tools to test the main hypothesis that CTD^{2A} specific events are required for changes in NMDAR subunit composition at the synapse in response to sensory stimulation/deprivation. To Achieve this, the thesis sets out to address the following primary aims:

- To investigate the effect of different dark rearing paradigms on activity-dependent changes in the GluN2A:GluN2B ratio, and whether changes in GluN2A:GluN2B ratio are mediated by changes in GluN2A, GluN2B, or both subunits.
- To establish weather activity-dependent change in NMDAR subunit composition are attenuated in the absence of CTD^{2A}.
- To investigate whether sensory-experience dependent changes in the transcriptome are reduced in the absence of CTD^{2A}, and what the functional consequences of these gene expression changes may be.

1.7 Thesis summary

In **Chapter 3**, I investigate the contribution of activity in promoting the developmental increase in the GluN2A:GluN2B ratio. Here I question whether the lack of visual input leads to an attenuation of the developmental increase. To address this question, I dark rear mice from birth and collect PSD fractions from the V1 of mice over the first four postnatal weeks. Based on similar studies conducted in rats, I hypothesise that dark rearing will delay the normal increase in GluN2A. However, in **section 3.1** I report no significant effect of dark rearing on the developmental increase of GluN2A. A surprising finding that I attempt to address in the subsequent discussion. In addition, I also attempt to tackle the misconception that the developmental ratio shift represents a subunit "switch". I observe that GluN2B levels remain constant over the first four weeks of postnatal life. Based on this, I make the argument that the developmental shift of the subunit ratio is primarily driven by increasing levels of GluN2A and not, as has been previously suggested, declining levels of GluN2B. This is an argument that was put forward previously for changes in the whole cortex; these finding show that the same applies within the VC. I next investigate sensory-dependent changes to the GluN2A:GluN2B ratio during the critical period. I hypothesise that subunit ratio changes will be driven by changes to both synaptic GluN2A and GluN2B expression. To test this hypothesis, I dark rear WT mice for 7 days during the critical period (P21-28) either with or without subsequent re-exposure to light for 24Hr. In line with previous dark rearing studies, I observe a significant decrease in the expression of synaptic GluN2A following 7-day dark rearing and a significant rebound following 24Hr re-exposure to light. Surprisingly, I also observe a smaller, yet significant, decrease in GluN2B following 7-day dark rearing, but no rebound upon light re-exposure. In spite of the moderate decrease to GluN2B, I observed that 7-day dark rearing lowers the GluN2A:GluN2B ratio. Based on this observation, I argue that the regulation of GluN2A is the driving factor in sensory experience-dependent control of the subunit ratio. In the chapter 3 discussion I present an explanation for the counterintuitive decrease in GluN2B observed following 7-dark rearing.

While the GluN2A$^{2B(CTR)/2B(CTR)}$ mice have been utilised previously to interrogate the role of CTDs in the developmental shift in the GluN2A:GluN2B ratio, they have not

yet been used to investigate sensory experience-dependent shifts in the ratio. Based on the observation that GluN2A drives the sensory-experience dependent subunit ratio shift, a natural next step was to interrogate the requirement for the CTD^{2A} in this process. Therefore, this is the focus of **chapter 4**. As these experiments utilise visual deprivation as the principal method for altering subunit composition, it was important to first establish the relative expression of GluN2A and GluN2B subunits within the V1 of the $GluN2A^{2B(CTR)/2B(CTR)}$ mouse. In **Chapter 4**, I establish that the level of GluN2A and GluN2B at V1 synapses is comparable between both genotypes, thus excluding genotype expression difference as a confounding factor in the activity-dependent genotype expression differences later observed in **Chapter 4**. In **section 4.2** I further characterise the relative synaptic expression of GluN2A and GluN2B subunits in the V1. As the GluN2A:GluN2B ratio can shift due to changes in the level of either subunit, it was important to establish the relative abundance of each subunit. In agreement with previous observations, I find that GluN2B is more abundant than GluN2A at synapses in V1**.** I next attempt to establish the role of CTD^{2A} in activity-dependent changes to NMDAR subunit composition. To address this, I dark rear $GluN2A^{2B(CTR)/2B(CTR)}$ mice using the 7-day dark rearing protocol described in **chapter 3**. I hypothesise that, if CTD^{2A} is required for the activity-dependent removal of GluN2A then $GluN2A^{2B(CTR)/2B(CTR)}$ will exhibit reduced sensory experience dependent changes to the GluN2A:GluN2B ratio. Indeed, in **section 4.5**, I demonstrate that in the absence of CTD^{2A}, changes to both subunit composition and postsynaptic protein composition fail to occur. Considering the robust decrease in a few other postsynaptic proteins, I then ask if the results obtained are truly representative of a shift in postsynaptic protein composition, or whether they are a consequence of synapse loss in response to dark rearing. To answer this, I examine the expression of the postsynaptic marker synaptophysin in presynaptic fractions taken from the same mice. Here I find similar levels of synaptophysin across all light conditions, suggesting that the observations made are in fact the result of changes to composition to the post synapse and not synapse loss.

In the final chapter, I use bulk RNA-seq to interrogate transcriptomic differences between WT and $GluN2A^{2B(CTR)/2B(CTR)}$ both under normal light conditions and in response the changes in activity. To achieve this, I dark reared mice a described

previously, with or without subsequent re-exposure to light for 12Hr. Based upon previous observations that GluN2A$^{2B(CTR)/2B(CTR)}$ exhibit less robust changes in IEG expression following dark rearing, I hypothesise that GluN2A$^{2B(CTR)/2B(CTR)}$ mice will show fewer transcriptionally mediated changes in response to dark rearing. In agreement with this, I observe a less robust regulation of genes in response to both dark and 12Hr re-exposure in GluN2A$^{2B(CTR)/2B(CTR)}$ mice when compared to WT. To investigate whether differences in expression were indicative of heightened or reduced activity within the GluN2A$^{2B(CTR)/2B(CTR)}$ V1, I next investigate those genes that are differentially expressed between genotypes under each light condition. Here I find that genes that are lower in both light conditions yet higher in the dark are enriched for genes that are induced by activity. Similarly, genes that are higher in both light conditions and lower in the dark for GluN2A$^{2B(CTR)/2B(CTR)}$ are enriched for genes that are repressed by activity. Taken together, I propose that in the absence of the CTD^{2A}, mice exhibit a reduced dynamic range in response to activity. **Chapter 5** concludes with a discussion surrounding the possible mechanisms by which the CTD^{2A} may contribute to maintaining this dynamic range.

Chapter 2

Materials and Methods

Chapter 2 - Materials and Methods

2.1 Animals

All animal experiments conformed to national and institutional guidelines including the Animals [Scientific Procedures Act] 1986 (UK), and the Council Directive 2010/63EU of the European Parliament and had full Home Office ethical approval. All animals were maintained in pathogen-free and temperature-controlled conditions. Control animals were raised on a 12:12 light:dark cycle while dark reared animals were raised as outlined in **section 2.3**. Food and water were available ad libitum. Animals were group housed in conventional cages and were provided with environmental enrichment. Both male and female mice were used for all experiments. Animals had not been subject to previous procedures. All animal breeding, maintenance, and experimental procedures were performed under project licence PP2262369.

2.1.1 Generation of GluN2A$^{2B(CTR)/2B(CTR)}$ mouse

The GluN2A$^{2B(CTR)/2B(CTR)}$ line was generated by the Komiyama lab (The University of Edinburgh) Briefly, the exonic sequence encoding the CTD of GluN2B was swapped into the reciprocal genomic loci of GluN2A. The cytoplasmic domains of both the GluN2A and GluN2B subunit are encoded by the terminal exon of their respective genes and share an identical initial amino acid sequence thereby facilitation the formation of a functional chimeric protein. To achieve this, a small fragment of intronic GluN2A DNA was annealed to the GluN2B C-terminal exon and inserted into a target vector using a Redα, Redβ, and Redγ recombineering system. The targeting vector was then used to target the GluN2A loci n 129/OlaHsd mouse embryonic stem (ES) cells. ES cells were screened via long-range PCR to identify successfully target colonies. Targeted clones were injected into a blastocyst and allowed to develop in a foster mother. The resulting F1 progeny were then backcrossed onto C57BL/6J mice to establish a working colony. Full details of the generation of this line and the primers used can be found in Ryan et al, 2013.

2.1.2 GluN2A$^{2B(CTR)/2B(CTR)}$ mouse breeding strategy

GluN2A$^{2B(CTR)/2B(CTR)}$ were maintained on a C57BL/6J background. For experimental purposes, homozygous and wild-type mice of both sexes were used and were generated as a result of heterozygous intercrosses and homozygous crosses. While heterozygous crosses provide the advantage of producing littermate controls, homozygous crosses were used in cases where genotyping was not possible prior to dark rearing experiments commencing. This was done to prevent non-experimentally usable heterogenous mice from undergoing dark rearing experiments, however, the result is a lack of blinding. Litters were used when they became available and, as such, mice were assigned to experimental groups as needed to ensure equal group sizes.

2.1.2 Genotyping of GluN2A$^{2B(CTR)/2B(CTR)}$

To determine the genotype of mice in the GluN2A$^{2B(CTR)/2B(CTR)}$ colony, the DNA was extracted from ear notches by boiling at 100ºC in 50 mM NaOH (600 µl) for 10 minutes. This was followed by the addition of 60 µl of 1M tris-HCl and centrifugation at max speed to remove contaminating protein. Each PCR reaction contained: 1 µl of DNA sample, 0.5 µL of 4 primers listed in **figure 2.1**, 12 µl HotStarTaq Master Mix (Qiagen) and 10 µl DNAase-free H_2O. The PCR conditions were as follows: 5 minutes at 95°C followed by 34 cycles of 94°C for 30 seconds, 55°C for 1 minute and 72°C for 1 minute, followed by an extension step at 72°C for 10 minutes. The PCR products were run on 1.5% agarose gel and visualized using SYBR Safe (Life Technologies) as a DNA stain (**Fig 2.1C**).

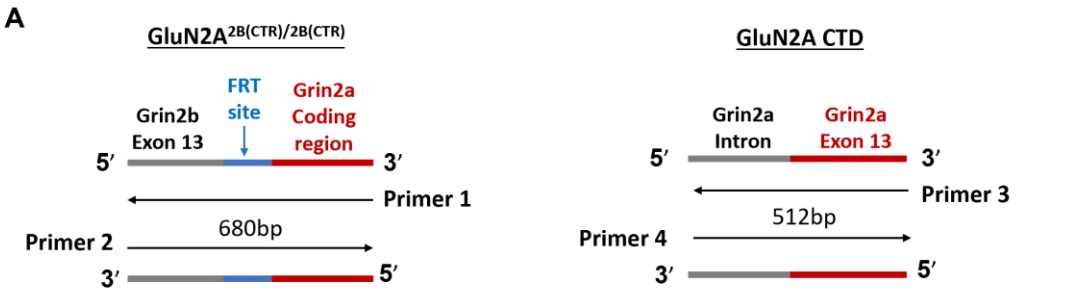

B

Primer	Primer sequence
1	GGGGAAGTTACATGGTGGATTG
2	GGGATGATCAGTGCTTGCTTC
3	CTTCTTTTCTTCAATGTGCACTCC
4	CTACATCATCAGAAGCCCACC

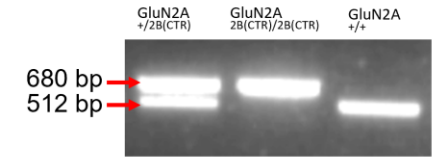

Figure 2.1 - Genotyping strategy to detect GluN2A$^{2B(CTR)}$ region.
(A) Primer set 1 and 2 were designed to amplify the *GRIN2B* exon coding for the Glun2B CTR inserted into the *GIRIN2a* gene. Primer set 3 and 4 were designed to amplify the beginning of the exon coding for the GluN2A CTR and the preceding intronic sequence. **(B)** The nucleotide sequence of primer pairs. **(C)** PCR products of mouse genomic DNA from a heterozygous/GluN2A$^{+/2B(CTR)}$ (left), complete knock-in of GluN2B CTR into GluN2A subunit/GluN2A$^{2B(CTR)/2B(CTR)}$ (middle), and a WT/GluN2A$^{+/+}$.

2.3 Dark rearing

To examine the sensory experience dependent changes to the GluN2A:GluN2B ratio, P21 mice were transferred to a dark cabinet in a light-proofed room and exposed to dark conditions for 7 days. Animals were checked daily using infrared night vision goggles and light sensitive film as a control for potential light infiltration. At the experimental end point half of the animals were anaesthetised in either the dark or light conditions and decapitated following the disappearance of reflexes. The other half were re-exposed to light for a 12 or 24 hr period before decapitation and tissue collection. In a separate set of experiments, the sensory dependent developmental trajectory of NMDAR composition was assessed by rearing animals in the dark from birth. Pregnant dams were transferred to the dark cabinet prior to giving birth. Tissue was collected as described previously at P7, P14, P21 and P28. A list of the equipment and control measures for dark rearing experiments is summarised in **table 2.1**.

Table 2.1 – summary of dark rearing protocol, control measures and sources of light infiltration

Equipment	Time points (postnatal days)	Re-exposure protocol	Control measures	Sources of light infiltration
Light proof room	P0-28 (From birth)	Dedicated room for 24Hr re-exposure	Light sensitive film	Failure to secure cabinet door
Blackout curtain around door	P21-P28 (7 day)	Lights set to permanently on	Record of films kept *supplemental **Fig S1**	Failure to close blackout curtain
Dark cabinet		LED lamp placed over cage	Immediate early gene expression	Use of red torches
Night vision goggles		Mice collected after 24HR constant light		Respiratory hoods with power lights
Red safety light (formerly)		Normal holding room for 12Hr re-exposure		Animal Unit Lighting system technical problems

2.4 Preparation of Postsynaptic density enriched fractions.

To isolate PSD-enriched proteins (containing synaptic NMDARs), a protocol adapted from Milnerwood et al, 2010 was used. Primary visual cortices from P28 light and dark reared mice were dissected, their cortices removed and snap frozen before being stored at -80ºC until fractionation. To obtain PSD enriched fractions, visual cortices were placed in 500µl ice-cold homogenization buffer (10 mM Sucrose, 10 mM HEPES, supplemented with Protease and Phosphatase Inhibitor Cocktail tablets (Roche, Burgess Hill, UK), (pH 7.4). Tissue samples were homogenized with a teflon/glass homogenizer, 125µl of homogenate was kept for RNA isolation while the remaining homogenate was centrifuged (1,000 g, 10 min, 4C). The supernatant was collected and centrifuged at 12,000 g (20 min, 4°C), after which the pellet was resuspended twice in 4mM HEPES (containing 1mM EDTA, pH 7.4) by repeating the last centrifugation step. To obtain the non-PSD enriched fraction, pellets were then resuspended (in 20 mM HEPES, 100 mM NaCl and 0.5% Triton X-100, pH 7.2). Samples were incubated for 15 min at 4°C while rotating gently, followed by centrifugation (12,000 g, 20 min, 4°C). The supernatant was collected (Non-PSD enriched fraction) and the pellet solubilized (in 20 mM HEPES, 0.15 mM NaCl, 1%

Triton X-100, 1% sodium deoxycholate (DOC), 1% SDS, 1 mM DTT, pH 7.5) for a further 1h at 4°C with gentle agitation. Finally, the samples were centrifuged at 10,000 g for 15 min (4°C) and the supernatants were collected as PSD-enriched fractions. Fractions were stored at −20°C until western blotting. The PSD fractionation protocol is outlined in **Figure 2.2**. It is important to note that, while care was taken during dissections to isolate V1, some V2 tissue may have been present in samples.

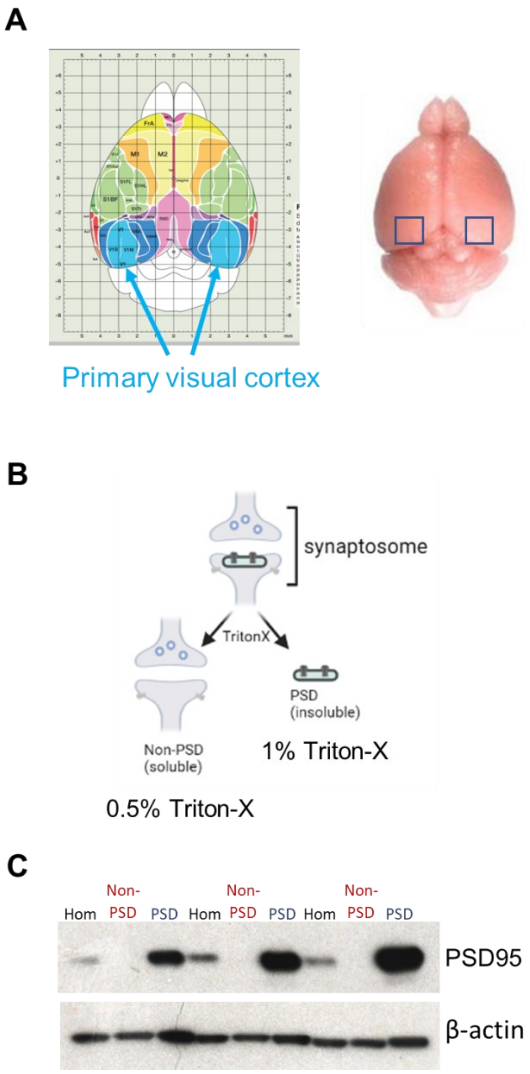

Figure 2.2 – Overview of PSD fractionation protocol.

A) Shows the primary visual cortex as indicated by mouse brain atlas and a representation of the dissection area. **B)** Diagrammatic representation of the PSD fractionation protocol displaying the components of each fraction. **C)** Representative western blot for PSD95 in total homogenate (Hom), Non-PSD fraction (Non-PSD) and PSD fraction (PSD).

2.5 Western blotting

On the day of use, the PSD, Non-PSD and total homogenate fractions were defrosted on ice and a colorimetric BCA assay (Pierce) was run to determine the protein concentration of the samples (measured with a FLUOstar Omega microplate reader). Aliquots of the samples were then taken and diluted in dH2O to a concentration of 25µg/48.75 µL. Reducing agent (7.5 µL, NuPAGE) and sample buffer (18.75 µL, NuPAGE) were added to 48.75 µL of the diluted sample (final protein concentration 5 µg/15 µL). The samples were then vortexed, spun down and boiled for 10 minutes. Samples were spun down again and 15 µL of sample was loaded onto a precast Bis-tris gradient gel (4%–12%)(NuPage) and subjected to electrophoresis at 120V. Following electrophoresis, proteins were transferred onto a methanol activated PVDF membrane using the Xcell Surelock system (Invitrogen) running at 80V for 1 hour. Following the protein transfer, the PVDF membranes were blocked for 1 hour at room temperature with 5% non-fat dried milk in TBS with 0.1% Tween 20. The membranes were incubated at 4°C overnight with the primary antibodies diluted in blocking solution (**Table 2.1**).

The following day membranes underwent 3 x 5min washes in TBS-T. Following the wash steps, membranes were incubated for 1 hour at room temperature with appropriate HRP-linked secondary antibodies diluted in 5% non-fat dried milk in TBS with 0.1% Tween 20. Secondary antibodies used were either rabbit HRP antibody (1:2000) or mouse HRP antibody (1:1000). Following incubation with secondaries, membranes were washed for 3 x 5min in TBS-T and incubated in enhanced chemiluminescence reagents for 1 minute. For visualization of western blots, blots were developed manually using chemiluminescent detection on Kodak Carestream BioMax light film. Western blots were digitally scanned and densitometric analysis was performed using ImageJ. A box was drawn around the band of interest and the mean grey value was measured; the same box was then used to take measurements from each sample on the blot. The mean grey value of the background was then measured and subtracted from sample values. All analysis involved normalising to either beta actin or total protein stain (Thermo Fisher Scientific) as a loading control. During initial experiments it was discovered that beta actin was more variable in

GluN2A$^{2B(CTR)/2B(CTR)}$ mice, and as such total protein was deemed to be a more appropriate loading control for experiments involving genotype comparisons.

Table 2.2 – Antibodies used.

Antibody	Host	Dilution	Source	Catalogue/Product#
Anti-GluN2A(N-terminal)	rabbit	1:2000	Thermo Fisher Scientific	480031
Anti-GluN2B(N-terminal)	rabbit	1:2000	Thermo Fisher Scientific	71-8600
Anti-GluN1	mouse	1:2000	Thermo Fisher scientific	32-0500
Anti-GluN2B (C-terminal domain)	mouse	1:2000	BD Bioscience	610416
PSD95	mouse	1:1000	BD Bioscience	610495
Synaptophysin	rabbit	1:2000	Abcam	ab14692
cFos	rabbit	1:500	Abcam	ab222699
Egr1	rabbit	1:250	Thermo Fisher scientific	MA5-15008
Beta actin	rabbit	1:20000	Abcam	ab8227

2.5.1 GluN2A and GluN2B N-terminal and C-terminal antibody validation

GluN2A and GluN2B have very similar molecular weights, and both produce a band of ~180kDa upon immunolabelling with their respective antibodies. The N-terminal GluN2A antibody (480031) that is used within this thesis has previously been validated in GluN2A KO rats (McKay et al. 2018), however, similar validations have not been conducted on the N-terminal GluN2B antibody (71-8600) used. This N-terminal GluN2B antibody was selected due to its use in similar experiments (McKay et al., 2018) and the initial characterisation of the GluN2A$^{2B(CTR)/2B(CTR)}$ mouse line (Ryan et al., 2013), however, this does not preclude the possibility of some cross-reactivity with GluN2A. The C-terminal specificity of the GluN2B C-terminal domain

antibody was previously validated in GluN2B$^{2A(CTR)/2A(CTR)}$ mice lacking the GluN2B CTD (Ryan et al., 2013; Frank et al., 2016).

2.5.2 Stripping and re-probing of membrane

To probe for multiple proteins, membranes were stripped using reblot plus strong stripping solution made up to a final concentration of 1X. Membranes were stripped for 15 minutes followed by a 5 minute wash in 1X TBS-T. To ensure that no residual signal remained, membranes were incubated with the appropriate secondary antibody for the previous protein and developed using the chemiluminescent detection method described previously. Membranes were then incubated with a new primary antibody and the detection steps repeated.

Stripping of the membrane multiple times may lead to the loss of some protein. Therefore, in cases where a direct comparison of two proteins on the same membrane was required (i.e. GluN2A:GluN2B ratio), care was taken to ensure that these proteins were probed first.

2.6 RNA Isolation and cDNA synthesis

RNA was isolated using the Roche High Pure RNA isolation reagents (including the optional DNase treatment) following passage of the homogenate through a High pure filter column. For qRT-PCR, cDNA was synthesized from 1-3 µg RNA using the Roche First Strand cDNA Synthesis kit (Roche) according to the manufacturer's instructions. Briefly, the required amount of RNA (up to 3 µg) was diluted in RNase-free water (up to 7 µl final volume) and mixed on ice with 2x cDNA Synthesis master mix (10 µl), random primers: oligo-dT primers 3:1 (total 2 µl- 200 ng) and either 1 µl RT/RNase block enzyme mixture (for RT reactions) or 1 µl water (for No RT control reactions). Reaction mixtures were mixed, spun down and incubated for 2 min at 25°C, 40 min at 42 °C and 5 min at 95°C. cDNA was stored at -20°C

2.7 qRT-PCR

The qt-PCRs were run using the Stratagene Mx3000P QPCR System (Agilent Technologies) using SYBR Green MasterRox (Roche) with 6 ng of cDNA per well of a 96-well plate, using the following programme: 10 min at 95 °C, 40 cycles of 30 s at 95 °C, 40 s at 60 °C and 30 s at 72 °C, with a subsequent cycle of 1 min at 95 °C and 30 s at 55 °C ramping up to 95 °C over 30 s (to measure the dissociation curve). Species-specific mouse primers were used (Table 2.3). Raw qt-PCR data was analysed using Microsoft excel by using the Δ/Δ Ct equation and normalising to the housekeeping gene Gapdh.

Table 2.3 – Primer sequences

Gene	Forward Primer sequence	Reverse Primer Sequence
Gapdh	CTTCCACCTTCGATGCC	TAGGCCCCTCCTGTTATTATG
Fos	GTTTCAACGCCGACTACGAG	CTGTCACCGTGGGGATAAAG
Arc	AGTGGTGGGAGTTCAAGCAG	TCCTCAGCGTCCACATACAG
Bdnf	AAAGTCCCGGTATCCAAAGG	CTTATGAATCGCCAGCCAAT
Nr4a1	CTTCAAGCGCACAGTACAG	CCTGGAACTTGGAATAGTCC
Kcnj3	GGGGACGATTACCAGGTAGTG	CGCTGCCGTTTCTTCTTGG
Kcnj4	ATGCACGGACACAACCGAAA	CTGGGACTTGTTGCTCAGG

2.8 RNA-seq and its analysis

RNA sequencing of mouse primary visual cortex was performed by Edinburgh Genomics (University of Edinburgh) using Trueseq Stranded Total RNA V2 library preparation along with next-generation sequencing on the Illumina Novaseq 6000 platform. At-least 1 µg RNA per sample was utilised, with RNA-integrity number (RIN) > 7. Per-gene read counts were summarised using featureCounts, and differential expression analysis performed using DESeq2, with a significance threshold calculated at a Benjamini–Hochberg-adjusted P value of <0.05.

Bioinformatics analysis was carried out by Dr Owen Dando, Dr Xin He and Dr Deepali Vasoya. Gene Ontology analysis was preformed using TopGO R package.

2.9 Statistical analysis

All results are presented as mean ± standard error of the mean unless otherwise stated. Statistical testing involved a 2-tailed student t-test, or for studies employing multiple testing, One-way or Two-way ANOVA was used followed by Tukey's multiple comparisons test . A Shapiro-Wilk test was used to assume statistical normality of data as it was the most appropriate method for the sample sizes of all experimental groups. All statistical analyses were conducted using GraphPad Prism version 10.1.2 for Windows. Statistical effects were considered significant if $p < 0.05$. Data points represent a single animal. Statistical details of each experiment can be found within the corresponding figure legends.

2.10 Statistical power

Power calculations were calculated based on data from pilot dark rearing studies using G*Power version 3.1.9.7 (Faul et al., 2007). The effect size in pilot experiments of dark rearing from P0-P28 was 0.533. With a significance criterion of $\alpha = .05$ and power = .80, the minimum sample size needed with this effect size is n = 9. Due to technical limitations, the sample size used was only 4 mice and as such this experiment is underpowered. This will be discussed in more detail in the appropriate section.

The effect size in pilot experiments of dark rearing from P21-P28 was 1.31. With a significance criterion of $\alpha = .05$ and power = .80, the minimum sample size needed with this effect size is n = 7. Thus, the obtained sample size of 10-12 is sufficient to detect differences between light groups.

Chapter 3

The role of sensory experience in changes to NMDAR GluN2A/2B subunit composition.

Chapter 3 - The role of sensory experience in changes to NMDAR GluN2A/2B subunit composition.

3.1 Introduction

It has been observed that the properties of NMDARs and their contribution to synaptic transmission within the VC undergo a change over the course of postnatal development. Over the course of postnatal development, the contribution of NMDARs to visually evoked responses is reduced and the duration of NMDAR-mediated currents shortens (Carmignoto and Vicini, 1992; Fox, Sato and Daw, 1989; Roberts and Ramoa, 1999; Tsumoto et al, 1987). The maturation of these properties occurs during the critical period of the VC, a window of time in which sensory experience influences synaptic plasticity (Daw et al, 1992; Fagiolini et al 1994; Guire, Lickey and Gordon, 1999). Moreover, depriving animals of sensory input by dark rearing them from birth delays both the onset of the critical period (Cyander and Mitchell, 1980; Cyander, 1983; Fagiolini et al 1994; Guire, Lickey and Gordon, 1999; Iwai et al, 2003; Mower, 1991) and the maturation of NMDAR properties (Carmignoto and Vicini, 1992; Fox, Sato and Daw, 1989).

One long standing hypothesis is that sensory experience influences NMDAR properties leading to a change in the relationship between NMDAR activation and the induction of either LTP or LTD (Cooper and Bear, 2012). According to the BCM theory of synaptic plasticity, the history of postsynaptic activity influences the crossover point between LTP and LTD, otherwise known as the θm (Bienenstock, Cooper and Munro, 1982; Cooper and Bear, 2012). Based on this theory, the expectation would be that dark reared animals, where VC activity is low, exhibit a shift in the θm that favours LTP. Indeed, Kirkwood, Rioult and Bear. (1996) demonstrated that dark rearing rats from birth induces an NMDA dependent reduction in the θm, thereby promoting the induction of LTD at a typically subthreshold frequency of 0.5Hz. In the pursuit of the molecular mechanisms underpinning this shift, attention turned to NMDAR subunit composition. As mentioned in **section 1.1.1**, GluN2A and GluN2B containing NMDARs exhibit faster and slower deactivation

kinetic respectively, as such, changes to subunit composition may serve as a mechanism for modifying the postsynaptic influx of Ca^{2+} and the subsequent induction of LTP/LTD. Moreover, over the course of postnatal development, there is a shift in NMDAR composition from predominantly GluN2B-containing to a greater inclusion of GluN2A containing receptors, which results in an increase in the GluN2A:GluN2B ratio. Therefore, this has led to the suggestion that the change in NMDAR subunit composition underpins the developmental change in NMDAR properties. As such, the observation that dark rearing delays maturation of NMDAR properties may reflect a delay in the developmental increase of GluN2A. Indeed, it has been demonstrated that rats dark reared from birth exhibit an attenuated increase in both the synaptic level of GluN2A and total GluN2A within V1 homogenates (Giannakopoulos, Kouvelas and Mitsacos, 2010; Quinlan et al, 1999a). Therefore dark rearing delays the rise in the GluN2A:GluN2B ratio but does not abolish it, suggesting that the subunit composition change is driven by both an intrinsic developmental programme and sensory experience. However, whereas the rat studies showed that GluN2A levels are markedly lower in P28 rats, one study conducted in mice observed that the effect of dark rearing on the GluN2A:GluN2B ratio was driven by an initial increase in GluN2B (~P28) followed by a later decrease in GluN2A (~P42) (Chen and Bear, 2007). However, this study used total V1 homogenate for its biochemical analysis, potentially masking synapse specific changes. Therefore, I first sought to investigate whether dark rearing WT mice from birth attenuated the increase in the synaptic GluN2A:GluN2B ratio. If sensory experience is required for the normal shift in the subunit ratio, then it could be predicted that WT mice dark reared from birth would exhibit an attenuated increase in GluN2A over the first 4 weeks of postnatal development and/or an increase in synaptic GluN2B.

Previous reports of brief dark exposure in juvenile rats beginning at P21-28 for 3-5 days, describe a reduction in the GluN2A:GluN2B ratio that is driven primarily by a decrease in the GluN2A subunit (Philpot et al, 2001;Quinlan et al, 1999a, Quinlan et al, 1999b,). On the other hand, it has also been reported that 3-day dark exposure of juvenile rats produces a decrease in the synaptic GluN2A:GluN2B ratio by increasing GluN2B expression, with no change to GluN2A (Chen and Bear, 2007). Collectively, these findings suggest that brief visual deprivation may lower the GluN2A:GluN2B

ratio through either an increase in GluN2B, a decrease in GluN2A, or both. Presumably the mechanisms for experience driven changes in the subunit ratio would be comparable between rats and mice, however, similar studies in mice are lacking. Therefore, I next sought to investigate the effect of brief dark exposure on the synaptic GluN2A:GluN2B ratio in the mouse V1. Additionally, as it has previously been demonstrated that the GluN2A:GluN2B ratio bidirectionally shifts in response deprivation and experience (Quinlan et al, 1999a), I also wanted to examine the effect of re-exposing mice to light following brief dark exposure. Based on the previous observations made in rats, I hypothesised that brief dark exposure and subsequent light re-exposure would shift the GluN2A:GluN2B ratio via changes in the synaptic expression of both GluN2A and GluN2B subunits. To test this hypothesis, I dark reared WT mice between P21-28 either with or without subsequent re-exposure to light for 24Hr. If the regulation of both subunits contributed to the ratio shift, then there would be a decrease in synaptic GluN2A and a corresponding increase in GluN2B following 7-day dark rearing. This would then be reversed by subsequent re-exposure to light for 24Hr.

3.2 The developmental increase in synaptic GluN2A is not attenuated by dark rearing WT mice from birth.

It is widely accepted that the level of GluN2A in rodents increases over the first four weeks of postnatal life. To investigate the effect of sensory experience in the mouse GluN2A:GluN2B ratio increase, I took pregnant WT mice and placed them in a photon-free room prior to littering down (**Fig3.1A**). V1 was then dissected from dark reared pups at P7, P14, P21 and P28 along with age-matched light reared controls. PSD enriched fractions were subject to western blot and the level of synaptic GluN2A and GluN2B analysed (**Fig3.1E**).

In agreement with what has been reported previously, I observed a significant age-dependent increase in the level of synaptic GluN2A in light reared mice. However, counter to the notion of a "switch", the level of GluN2B remained stable across the

first four weeks of development. This is in line with previous observations made in the cortex (McKay et al, 2018) and suggests that increased expression of GluN2A is the driving factor in the developmental subunit ratio shift. Surprisingly, I observed that dark rearing from birth did not attenuate the expected developmental increase in GluN2A (**Fig3.1B**). Similarly, dark rearing did not promote an increase in GluN2B (**Fig3.1C**). As a result the increase in the synaptic GluN2A:GluN2B ratio develops normally in the absence of visual input (**Fig3.1D**).

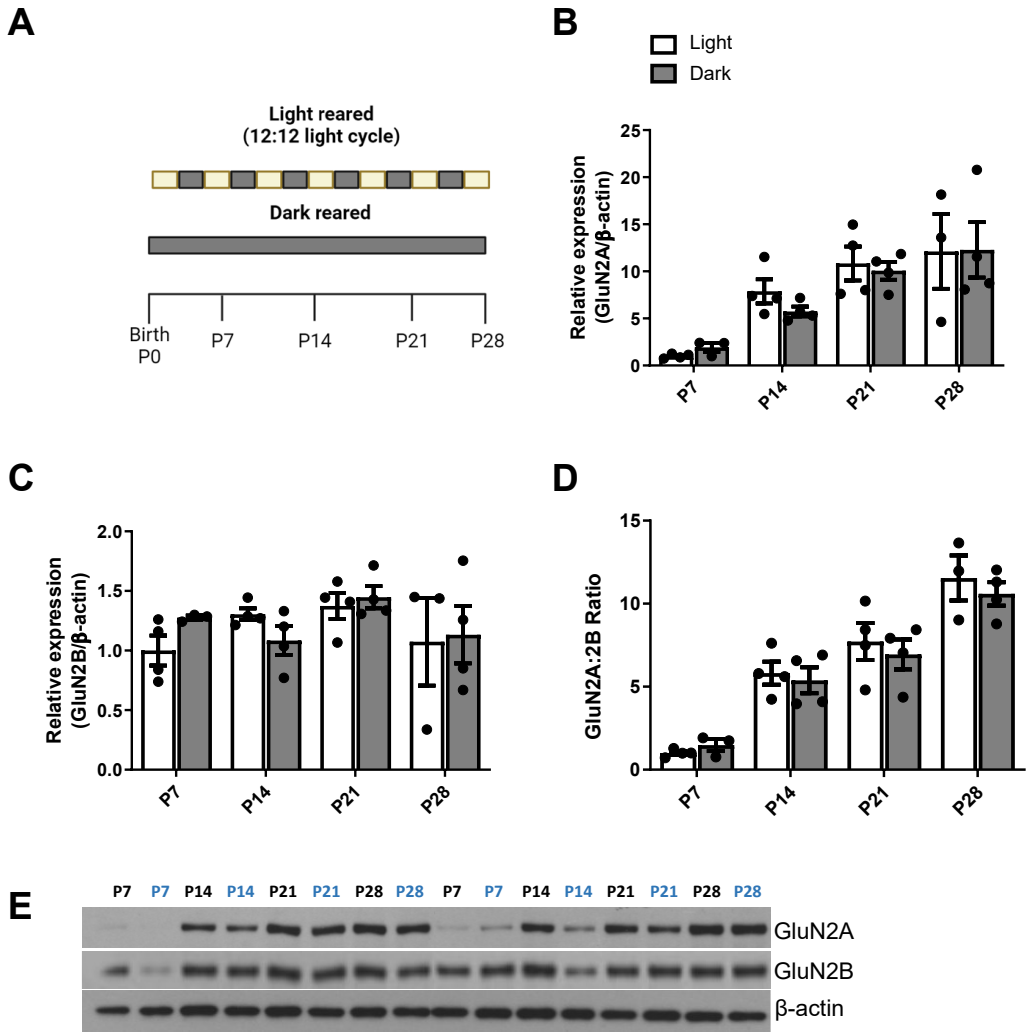

Figure 3.1 – The developmental increase of GluN2A levels is not attenuated by dark rearing.

A) Timeline for dark rearing experiments depicting light condition and age of mice. Postsynaptic density (PSD) enriched visual cortex extracts from either light reared or dark reared P7, P14, P21 , P28 mice were analysed for GluN2A and GluN2B protein expression. **B)** Quantitation of GluN2A., Two-way ANOVA (main Age effect) for GluN2A: $F(3, 23) = 46.50$, $p < 0.0001$; (light condition effect) for GluN2A: $F(1, 23) = 1.416$, $p = 0.2463$. **C)** Quantitation of GluN2B, Two-way ANOVA (main Age effect) for GluN2B: $F(3, 23) = 1.822$, $p = 0.1712$; (light condition effect) for GluN2B: $F(1, 23) = 0.02135$, $p = 0.8851$. **D)** In P7-28 light and dark reared mice, the ratio of subunits was calculated based on the expression of both GluN2A and GluN2B. Two-way ANOVA (main Age effect) for GluN2A:GluN2B ratio: $F(3, 23) = 51.80$., $p < 0.0001$; (light condition effect) for GluN2A:GluN2B ratio: $F(1, 23) = 0.6960$, $p = 0.4127$. **E)** Representative blot for WT GluN2A and GluN2B in light reared (blue) or dark reared (black) P7, P14, P21 , P28 mice, normalised to β-actin. P7 light $n=4$, P7 dark $n=3$, P14 light $n=4$, P14 dark $n=4$, P21 light $n=4$, P21 dark $n=4$, P28 light n=3, P28 dark n=4.

3.3 Expression of cFos and Egr1 protein and mRNA in P28 light and dark reared mice.

As seen in **section 3.1**, dark rearing failed to attenuate the developmental rise in the GluN2A:GluN2B ratio. In order to determine whether there were any differences in the level of activity between light and dark reared mice, I decided to investigate the expression of activity-dependent protein markers in light and dark reared mice. Both cFos and Egr1 (also known as Zif268) are well characterised markers of activity. To test their expression level, I took total homogenate fractions from P28 mice that had either been reared in normal 12:12 light or dark reared from birth and analysed them for cFos and Egr1 expression via western blot (**Fig3.2A**).

Analysis of the protein levels of both cFos and Egr1 revealed no difference in the expression level between light reared and dark reared mice (**Fig 3.2B-C**). However, expression of each protein was highly variable in both light and dark reared mice. The high variability even in light reared mice presented a challenge, making it difficult to power the experiment sufficiently to see any difference between the light reared and dark reared groups.

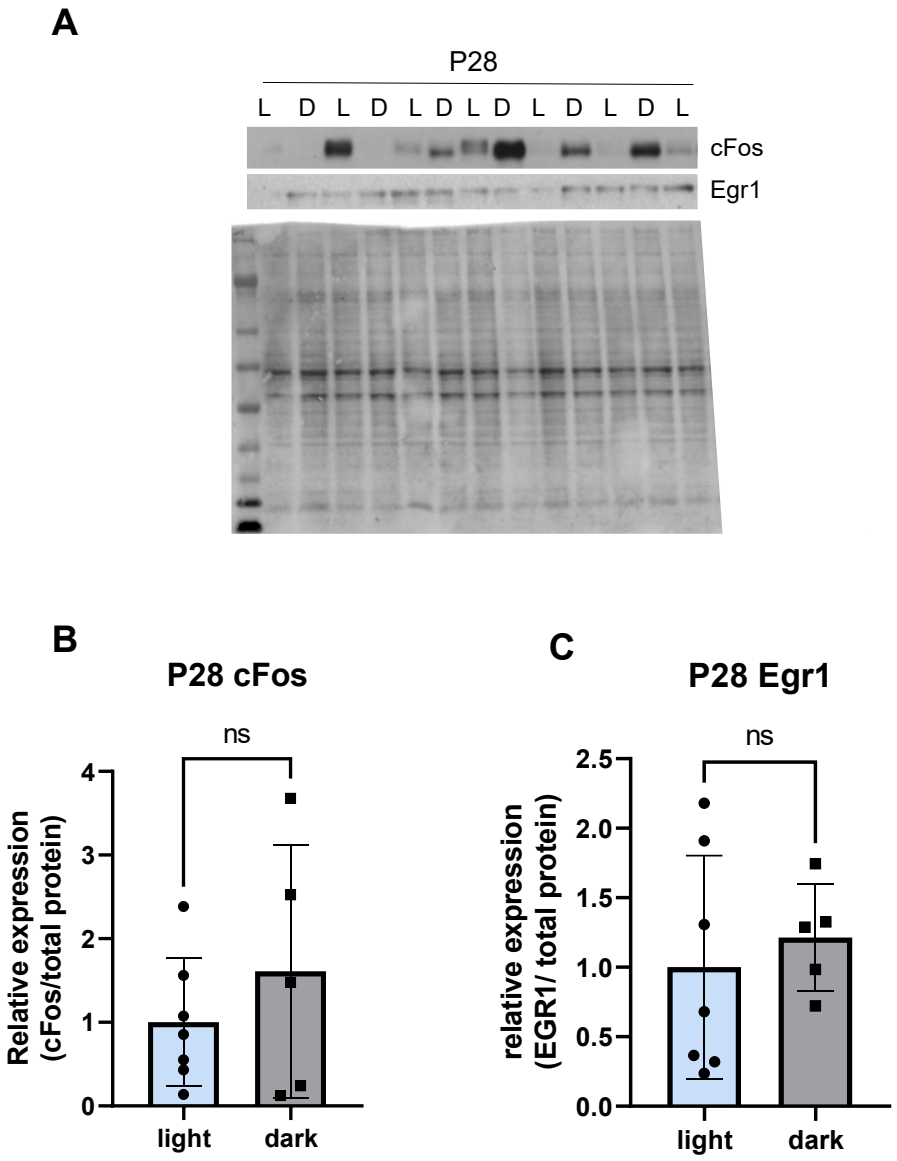

<u>Figure 3.2</u> – Protein levels of activity-dependent markers are not reduced in mice dark reared from birth.

Primary visual cortex homogenate taken from either light reared or dark reared P28 mice was analysed for cFos and Egr1 expression. **A)** Representative blot for cFos and Egr1 normalised to total protein. Protein expression of cFos (**B**) and Egr1 (**C**) in dark reared mice relative to light reared. Unpaired t test, $p = 0.3780$, $p = 0.5968$. Results are presented as mean (SD).

Based on the variability observed in protein expression, I next decided to look at the mRNA expression to see if there were any differences at the transcription level. Much like what was observed at the protein level, *Fos* and *Egr1* showed no differences in their levels of expression between light and dark (**Fig 3.3A-B**). I also examined mRNA expression of the CREB regulated gene *Bdnf*, a gene which is also regulated by neuronal activity. Again, I observed no difference in the expression of *Bdnf* in dark reared mice (**Fig 3.3C**). Taken together these results showed a surprising lack of any activity-dependent regulation with dark rearing from birth.

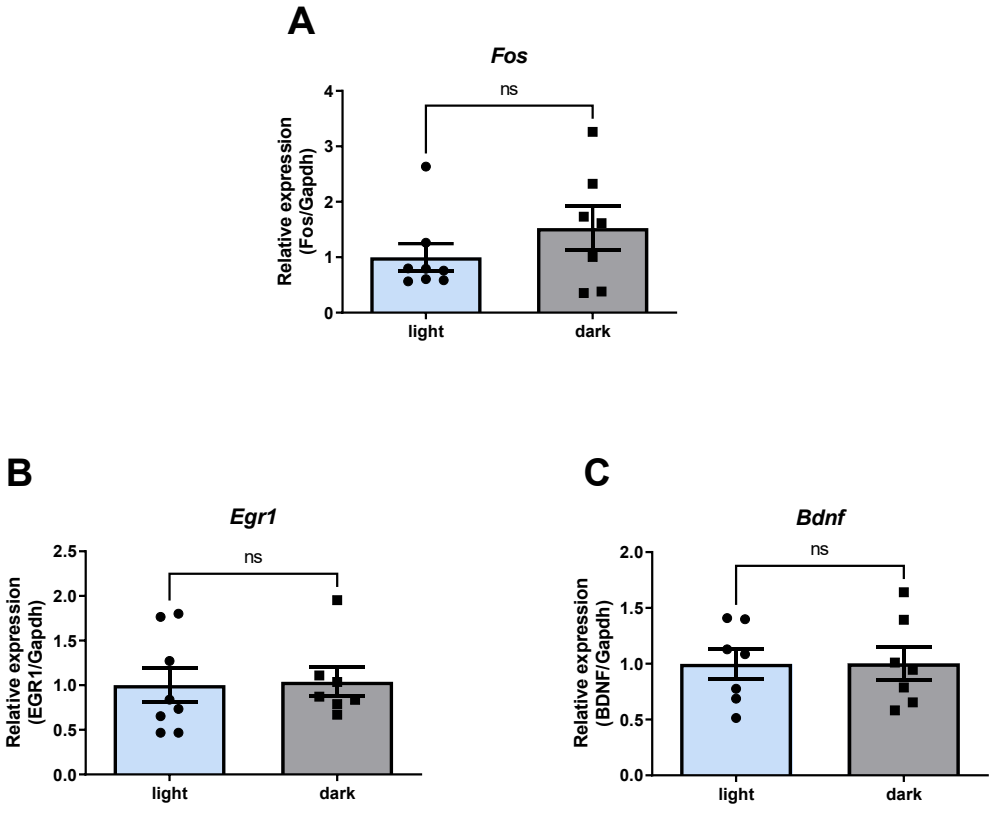

Figure 3.3 - mRNA levels of activity-dependent markers are not reduced in mice dark reared from birth.

RNA extracted from either light reared or dark reared P28 mice were analysed for *Fos*, *Egr1* and *Bdnf* mRNA expression. Expression was normalised to housekeeping gene *Gapdh*. The mRNA expression

of *Fos* (**A**) *Egr1* (**B**) and *Bdnf* (**C**) in dark reared relative to light reared mice. Unpaired t test, p = 0.2695, p = 0.8846, p = 0.9917. Light n=8, Dark n=7.

3.4 7 days of dark rearing during the critical period alters NMDAR subunit composition.

To examine whether 7-day dark rearing induced sensory experience dependent changes to the ratio of GluN2A:GluN2B, WT mice were dark reared for 7 days during the critical period (P21-P28) with or without subsequent re-exposure to light for 24Hr (**Fig3.4A**). PSD enriched fractions from V1 of WT mice were then analysed for synaptic GluN2A and GluN2B expression via western blotting (**Fig3.4E**). Analysis of GluN2A signal intensity revealed a robust decrease in the level of synaptic GluN2A following 7 days of dark rearing. In line with the bidirectional nature of the ratio shift, WT GluN2A returned to pre-dark levels following 24Hr light re-exposure (**Fig 3.4B**). Interestingly, a modest yet significant decrease was also observed in the level of synaptic GluN2B following dark rearing (**Fig 3.4C**). This combination of a robust decrease in synaptic GluN2A levels and a relatively smaller decrease in GluN2B resulted in a significant reduction to the GluN2A:GluN2B ratio (**Fig3.4D**).

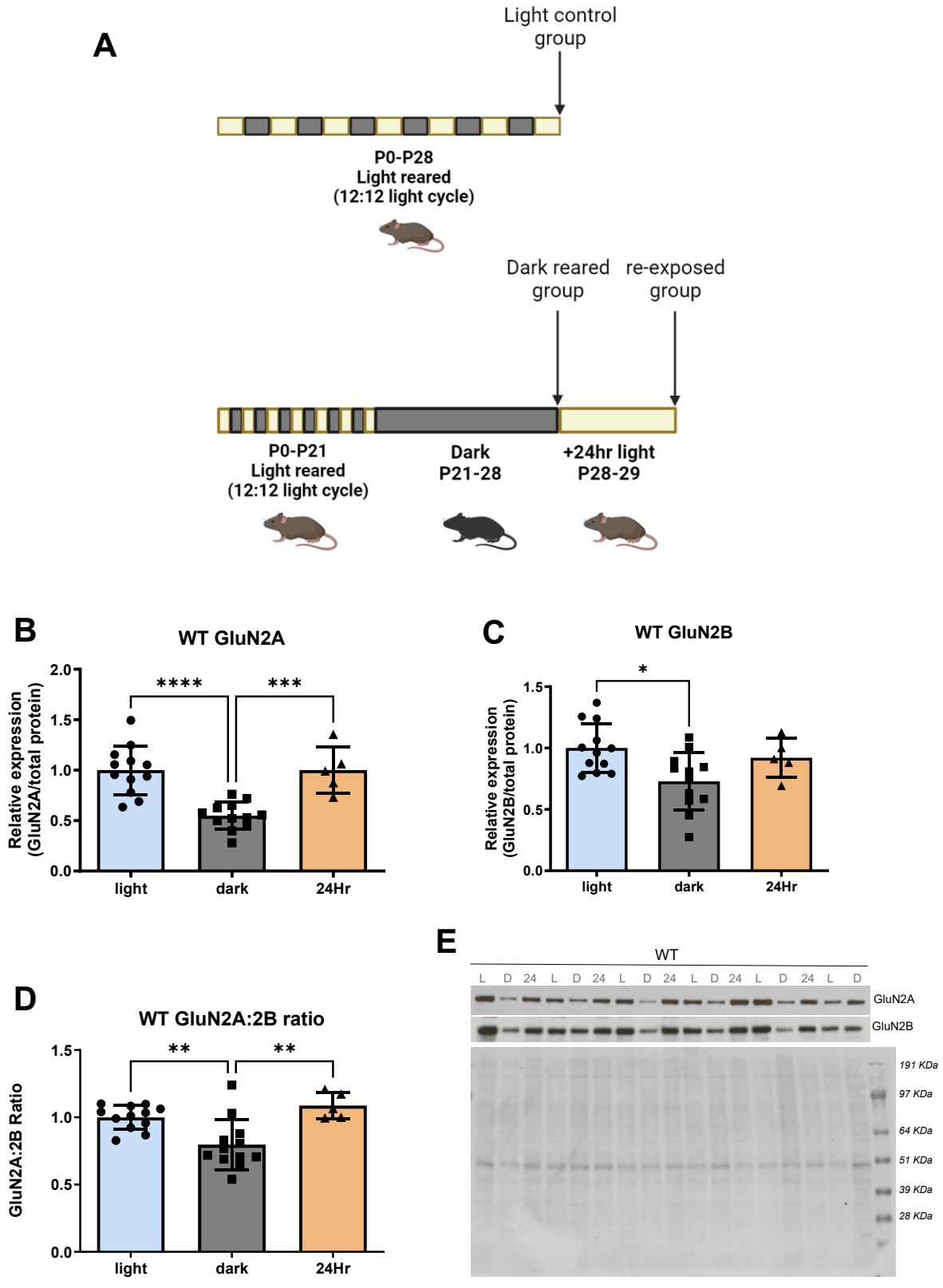

Figure 3.4 – 7-day dark rearing and 24Hr re-exposure alter GluN2A:GluN2B ratio.

PSD enriched visual cortex fractions from P28-29 mice either light reared, dark reared or dark reared with 24Hr light re-exposure were analysed for synaptic GluN2A and GluN2B expression. **A)** Outline

of 7-day dark rearing timeline **B)** GluN2A protein level exhibits a significant decrease following 7-day dark rearing and a significant rebound following re-exposure to light for 24Hr. One-way ANOVA for WT GluN2A: $F(2, 26) = 17.78$, $p < 0.0001$. **C)** Protein level of WT GluN2B exhibit a moderate decrease following dark rearing but no significant rebound following re-exposure to light. One-way ANOVA for WT GluN2B: $F(2, 26) = 5.219$, $p = 0.0124$. **D)** The ratio of GluN2A:GluN2B was calculated based on the relative levels of GluN2A and GluN2B for each light condition and found to be significantly lower in dark reared mice but comparable to the light ratio following 24Hr re-exposure. One-way ANOVA WT GluN2A:GluN2B ratio: $F(2, 26) = 10.10$, $p = 0.0006$. **E)** Representative blot for WT GluN2A and GluN2B, normalised to total protein. Tukey's test for multiple comparisons *P<0.05; **P < 0.01; ***P < 0.001; ****P<0.0001. WT light *n*=12, dark *n*=12, 24Hr *n*=5.

3.5 7-day dark rearing downregulates activity-dependent Immediate early gene expression.

Work conducted previously by colleagues showed that dark rearing WT mice for 7 days produced a robust downregulation of multiple IEGs. Therefore, this observation provided me with an additional control measure for assessing the quality of dark rearing. RNA was extracted from V1 tissue taken from P28-P29 mice who had either been kept under a normal 12:12 light cycle, reared in total darkness for 7 days, or dark reared for 7 days followed by re-exposure to light for 24Hr. RNA was then converted to cDNA and qRT-PCR utilised to determine the mRNA expression of *Arc, Fos, Nr4a1* and *Bdnf*.

In line with previous observations in our laboratory, I observed a significant downregulation of *Arc* mRNA in mice dark reared for 7 days, however, contrary to previous observations, 24Hr light re-exposure failed to produce a rebound in *Arc* mRNA expression (**Fig 3.5A**). Similar observations were also made for *Fos* (**Fig3.5B**) and *Nr4a1*(**Fig3.5C**). Of the IEGs tested, *Bdnf* was the only one that failed to exhibit any change in mRNA level in response to 7-day dark rearing (**Fig3.5D**).

Based on the robust down regulation of IEGs, it is clear that dark rearing over a 7-day period is effective in reducing synaptic activity within the VC. Surprisingly, in the case of these IEGs, it was also observed that subsequent re-exposure to light for 24Hr

failed to induce a rebound in IEG expression, with Fos and Nr4a1 expression remaining significantly lower than the light baseline. However, as these genes are rapidly activated in response to activity, it is possible that their peak expression occurs much earlier in the re-exposure period and begins to decline prior to the 24Hr end point. Indeed, subsequent time course experiments on dark reared mice re-exposed to light for 1, 3, 6 ,12 and 24Hr revealed that IEG expression peaked between 1-12Hr but began to decline thereafter (**supplementary Figure S6**).

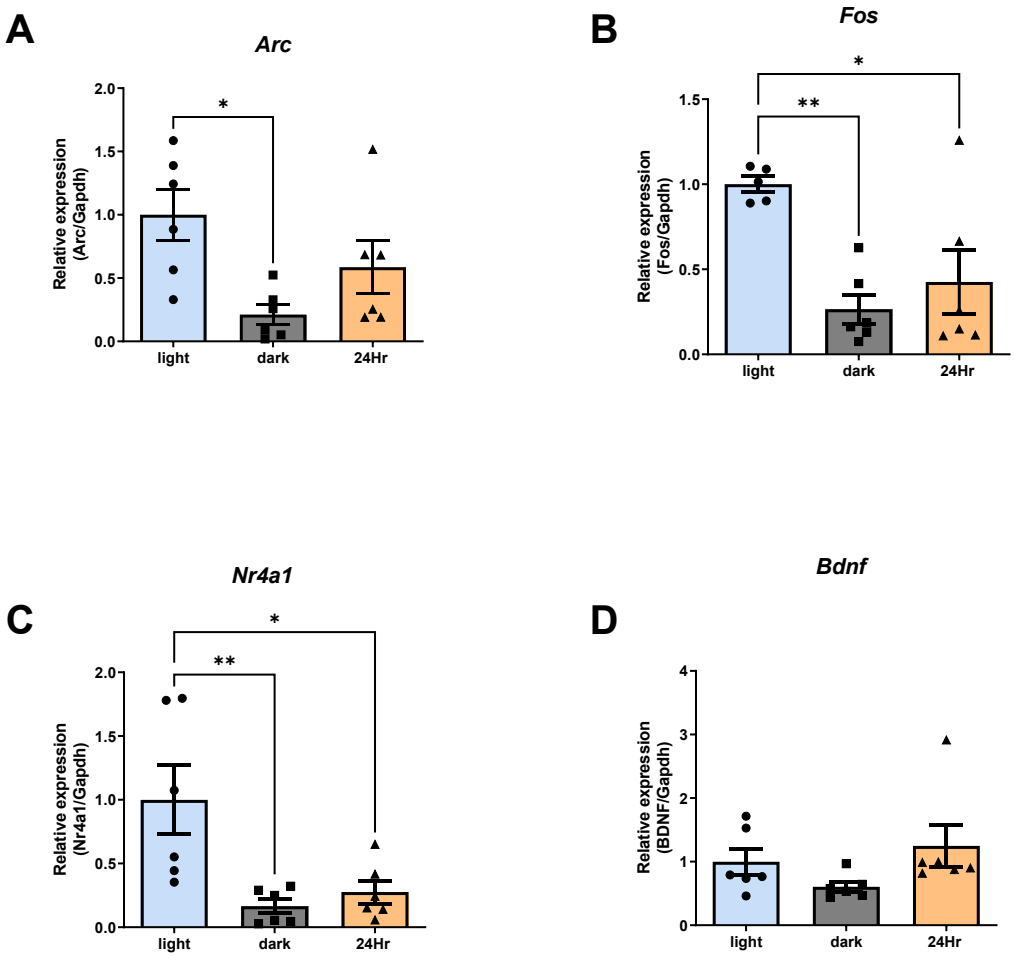

Figure 3.5– IEGs are downregulated by 7-day dark rearing in WT mice .

The mRNA expression of *Arc*, *Fos*, *Nr4a1* and *Bdnf* was measured in light reared mice and mice dark reared for 7 days (P21-28) with or without subsequent re-exposure to light for 24Hr. Expression relative to WT for *Arc* **(A)**, *Fos* **(B)** and *Nr4a1* **(C)** and *Bdnf* **(D)**. One-way ANOVA (*Arc*: F (2, 15) = 5.175, p = 0.0195; *Fos*: F (2, 14) = 8.427, p =

0.0040; *Nr4a1*: F (2, 15) = 7.365, p = 0.0059; *Bdnf*: F (2, 14) = 2.446, p = 0.1227). Tukey's test for multiple comparisons *P<0.05; **P < 0.01. WT light n = 6, dark n = 6, 24Hr n = 6.

3.6 7-day dark rearing downregulates intrinsic activity genes

Inward rectifying K^+ (K_{ir}) channels are an interesting class of K^+ channels that play a vital role in determining membrane excitability. They are so named for their ability to allow a greater influx rather than efflux of ions through their channel pore, so-called inward rectification. This inward rectification is mediated by the increased blockade of the channel pore by intracellular ions such as polyamines and Mg^{2+} upon depolarisation. This effectively impedes the outward flow of K^+ (Bichet, Haass and Jan, 2003). K_{ir} channels are believed to be critically involved in the maintenance of the resting membrane potential and neuronal excitability through their influence on membrane properties (Hibino et al, 2010). Indeed, blockade of K_{ir} channels has been shown to cause neuronal depolarisation and the initiation of action potential firing (Day et al, 2005). Therefore, greater expression of K_{ir} channels would appear to promote reduced neuronal excitability while lower expression favours increased neuronal excitability.

Both $K_{ir3.1}$(Kcnj3) and $K_{ir2.3}$(Kcnj4) are highly expressed within the cerebral cortex (Shcherbatyy et al, 2015). To investigate whether 7-day dark rearing induced changes in the expression of K_{ir} channels that may be representative of homeostatic changes in neuronal excitability, the level of *Kcnj3* and *Kcnj4* mRNA was compared between dark reared and light control mice. Interestingly, 7-day dark rearing triggered a significant decrease in the mRNA expression of both *Kcnj3* and *Kcnj4* in WT mice (**Fig 3.6**). Based upon their role in limiting neuronal excitability, it is possible that the removal of sensory input promotes a homeostatic decrease in K_{ir} channels in order to increase neuronal excitability. However, electrophysiological analysis will be required to robustly test this hypothesis.

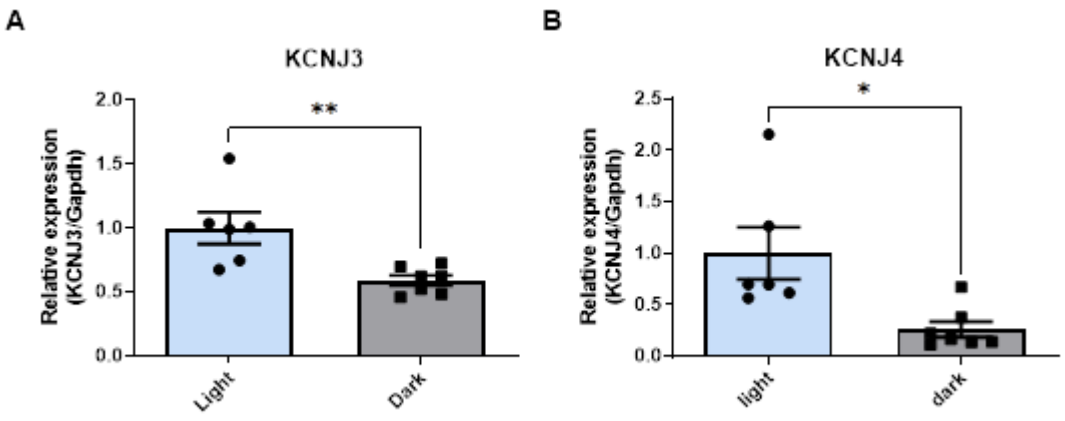

Figure 3.6 – Dark rearing reduces the m RNA expression of K_{ir} channels Kcnj3 and Kcnj4.

Using the qRT-PCR method, the mRNA expression of Kcnj3 and Kcnj4 was measured in light reared mice and mice dark reared for 7 days (P21-28). Relative mRNA expression of **(A)** *Kcnj3* and **(B)** *Kcnj4* in dark reared mice compared to light controls. Unpaired t test; **p = 0.0065, *p = 0.0123. WT light n = 6, dark n= 7

3.7 Red light is not suitable for dark rearing experiments.

It is a common misconception that mice are insensitive to red light. As such, this misunderstanding has led to the use of red light as a method for light/dark cycle reversal studies. While it is true that the mouse eye is 12 times less sensitive to a red-light stimulus of 600nm when compared to the human eye (Pierson et al, 2018), this does not mean that mice are wholly incapable of detecting red light. Indeed, multiple studies have demonstrated that while less sensitive, mice do indeed exhibit responses to bright red light (Butler and Silver, 2011, Hattar et al., 2003, Lucas et al., 2001). This calls into question the validity of using red light in dark rearing experiments. To investigate the effect of red light on NMDA subunit changes, WT mice were reared for 7-days in a light-proof room using either infrared night vision goggles (NV) or red-light lamps (RL) to observe the mice during welfare checks. The change in synaptic levels of GluN2A, GluN2B and the subunit ratio between light reared mice and the two dark rearing conditions was then directly compared.

In comparing the two dark rearing methods a striking difference emerged. Most noticeably, While GluN2A protein level exhibits a significant decrease following 7-

day dark rearing in the NV condition, a non-significant intermediate decrease is observed when RL is used. The synaptic level of GluN2B exhibits a slight, but non-significant decrease in both the RL and NV group. Furthermore, the ratio of GluN2A:GluN2B was calculated based on the relative levels of synaptic GluN2A and GluN2B for each light condition and found to be significantly lower in NV dark reared mice but not in RL dark reared mice. Taken together this would suggest that even brief exposure to RL during checks is sufficient to maintain enough activity within V1 to prevent NMDAR subunit composition changes.

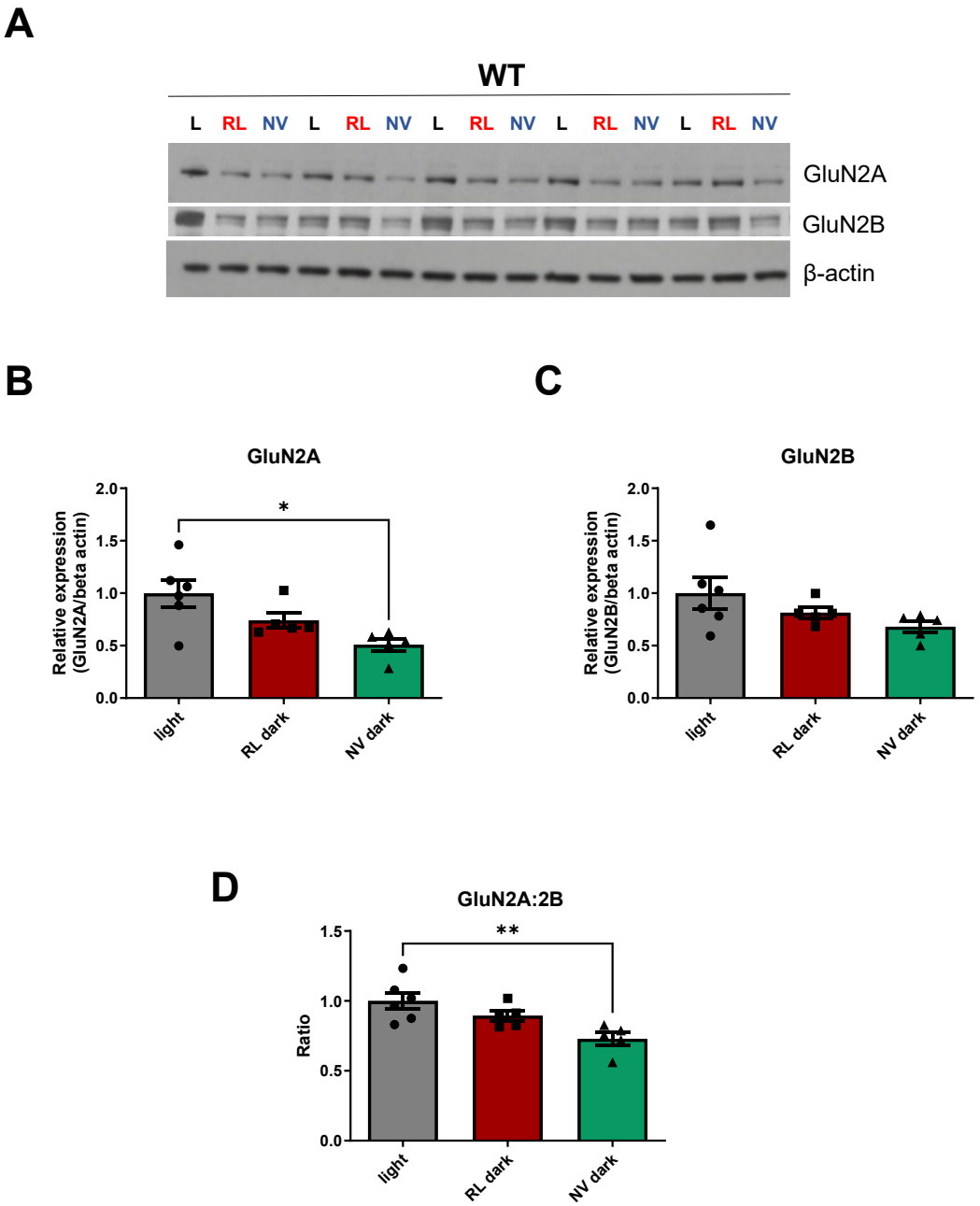

Figure 3.7 – Using red light for animal welfare checks during 7-day dark rearing prevents GluN2A:GluN2B ratio decrease.

PSD enriched visual cortex fractions from P28-29 mice either light reared, dark reared with red light (RL) or night vision goggles (NV) for animal checks were analysed for synaptic GluN2A and GluN2B expression. **A)** Representative blot for WT GluN2A and GluN2B, normalised to β-actin. **B)** Quantitation of GluN2A in RL and NV dark rearing groups compared to light controls. One-way ANOVA for WT GluN2A: $F(2, 14) = 5.507$, $p = 0.0172$. **C)**. Quantitation of GluN2B. One-way ANOVA for WT GluN2B: $F(2, 14) = 1.437$, $p = 0.2706$. **D)** Calculated GluN2A:GluN2B ratio. One-way ANOVA WT GluN2A:GluN2B ratio: $F(2, 14) = 9.103$, $p = 0.0029$. Tukey's test for multiple comparisons *P<0.05; **P < 0.01. light n = 6, RL n = 5, NV n = 5.

3.8 Exposure to red light preserves activity within the visual cortex.

The observations that dark rearing with RL fails to produce a significant decrease on the GluN2A:GluN2B ratio suggesting that some residual activity is maintained. To further investigate the effect of using RL during dark rearing experiments on activity within V1, the mRNA expression of activity-dependent genes was examined. In contrast to the previous observations made in NV cohorts, mice dark reared with RL exhibit no change in the expression of *Fos* and *Nr4a1*(**Fig3.8A-B**). Similarly, mice dark reared with RL exhibit no decrease in the mRNA expression of *Kcnj3* and *Kcnj4* (**Fig.C-D**). This would suggest that the brief exposure to RL during daily welfare checks is sufficient to produce responses that maintain activity within V1 and prevent homeostatic changes. Therefore, these results would argue against the suitability of RL for visual deprivation studies.

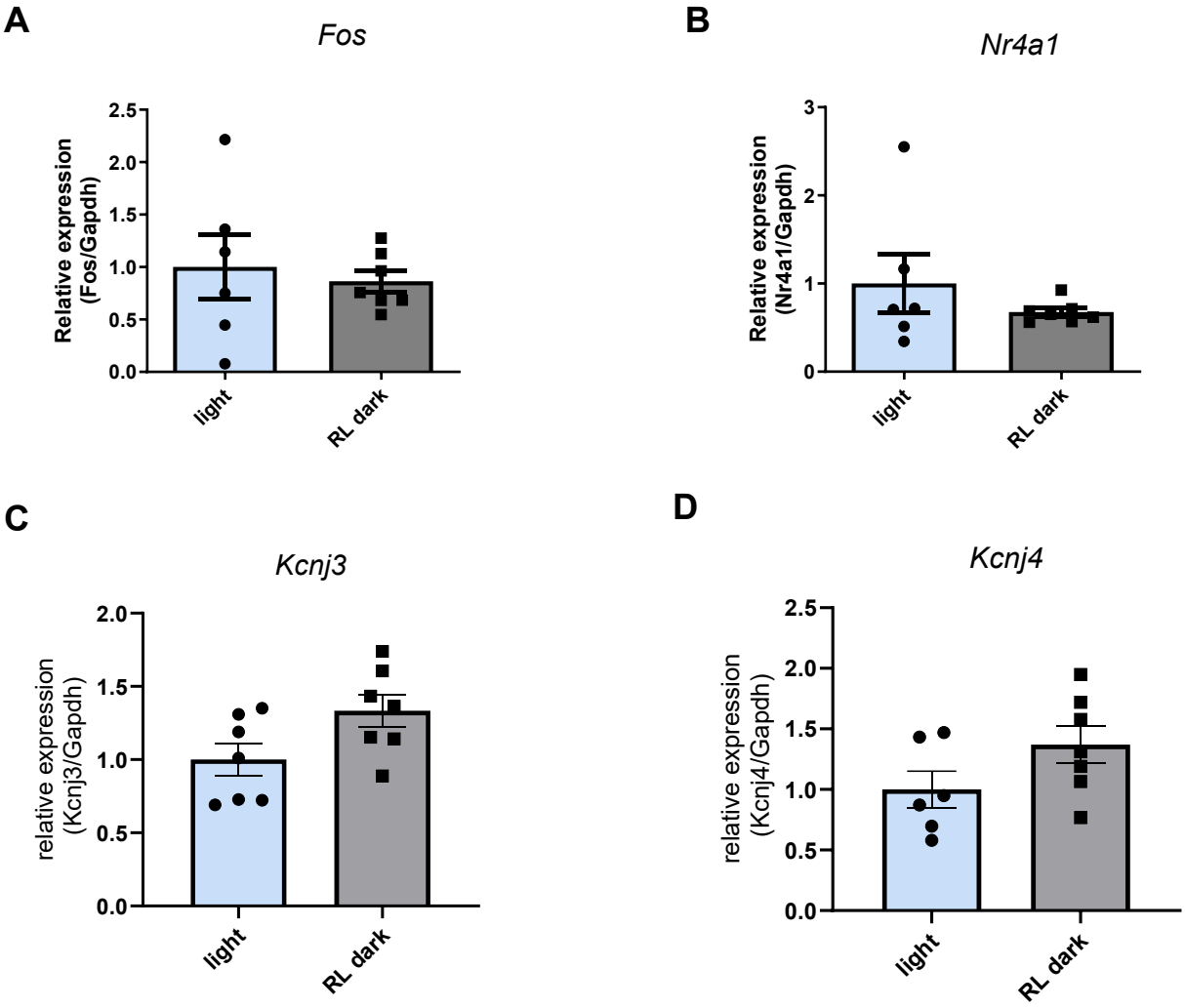

<u>Figure 3.8</u> – The expression of activity-dependent IEGs and Kir channels Kcnj3 and Kcnj4 is not downregulated in mice dark reared with red light checks.

Using the qRT-PCR method, the mRNA expression of activity-dependent and intrinsic activity associated markers was measured in light reared mice and mice dark reared for 7 days (P21-28) using red light lamps to perform animal checks. Relative expression of *Fos* **A)** and *Nr4a1* **B)** mRNA following dark rearing with red light. Unpaired t test; p=0.6601, p=0.3143, p=0.8368. Relative expression of *Kcnj3* **C)** and *Kcnj4* **D)** mRNA. Unpaired t test; p = 0.0540, p = 0.1181. WT light n = 7, RL dark n = 7.

3.6 Discussion

3.6.1 Summary – experimental findings in dark rearing from birth.

The current experiments provide compelling evidence for rising GluN2A levels as the driving factor in the developmental increase of the GluN2A:GluN2B ratio within the VC. As GluN2B remains constant over this time, this would reasonably argue against its removal as a key feature of the developmental subunit ratio increase. This is in agreement with the observation that the GluN2A:GluN2B ratio increase proceeds normally in the cortex and hippocampus of GluN2B$^{\Delta CaMKII\alpha}$ mice (McKay et al, 2018). Therefore, these observations argue against a subunit "switch" in which GluN2A levels rise while GluN2B levels fall. Furthermore, these results show that the developmental increase of the GluN2A:GluN2B ratio within the VC proceeds normally when mice are dark reared from birth. This finding is surprising, however, the lack of any influence of dark rearing on the normal ratio shift may be reflective of compensatory mechanisms that act to maintain normal development.

3.6.2 Does dark rearing from birth trigger compensatory mechanisms?

It was observed that the activity-dependent markers cFos and Egr1 showed no difference in expression between light and dark reared mice. This is not completely unexpected in the case of cFos, as previous immunohistochemical studies of cFos have shown that it has low basal expression that is not strongly influenced by dark rearing (Kaplan, Guo and Mower, 1996). However, Egr1 has been shown to be a much better indicator of the activity changes observed in dark rearing and in response to the non-competitive NMDAR antagonist MK801 (Kaplan, Guo and Mower, 1996 ;Worley et al, 1991). Light sensitive films that were used as controls during the period of dark rearing revealed no indication of light exposure, therefore raising questions as to the reason for the observations to both the subunit ratio and activity-dependent gene expression.

One possible explanation is that V1 also receives afferents from the primary motor cortex, and as a result elevated activity-dependent genes/protein expression may reflect increased motor activity in the dark. One other possibility is that long periods of dark rearing trigger a certain degree of compensation that ensures appropriate expression of GluN2A. There may be some hint of this in **Fig 4.1B**, where I witnessed that dark reared mice show slightly lower levels of GluN2A at P14. This is the point at which the eyes first open and as such the difference may be representative of the strong visual input being newly received by the light reared mice. However, by P21 the GluN2A levels in the dark reared and light reared mice are indistinguishable, suggesting that dark reared mice might be able to effectively "catch-up". Interestingly, it has been shown that dark rearing rats from birth prevents the typical developmental increase in GABAergic input to V1 layer II/III pyramidal neurons (Morales, Choi and Kirkwood, 2002). This lends the possibility that compensation may come in the form of an altered excitation/inhibition balance. In such a case, reduced inhibitory input may allow neurons to maintain a base level of activity that is sufficient to promote key developmental processes even in the absence of sensory input. This may involve the regulation of key molecular signals such as the Bdnf signalling pathway. Indeed, it has been observed that overexpression of Bdnf is sufficient to promote the normal development of the mouse VC even in the absence of visual experience (Gianfranceschi et al, 2003). Therefore, compensatory changes that boost key signalling pathways may block the effect of dark rearing.

3.6.3 Transcriptional regulation of *GRIN2A* and *GRIN2B* during development.

Transcription regulation of *GRIN2A* and *GRIN2B* has been implicated as a potential mechanism in mediating the developmental subunit shift. One potential scenario involves the regulation of *GRIN2B* expression during development via the epigenetic remodelling of chromatin. The Repressor element 1 silencing transcription factor (REST) is known to silence *GRIN2B* by acting through epigenetic mechanisms (Sasner and Buonanno, 1996). Interestingly, one study found that knockdown of REST *in vivo* prevented the subunit "switch" (Rodenas-Ruano et al, 2012). In a similar study,

it was proposed that microRNAs work in combination with REST to regulate the increase and decrease of *GRIN2A* and *GRIN2B* respectively (Corbel et al, 2015)

It has already been shown that the identity of the CTD does not influence the developmental ratio shift (McKay et al, 2018), suggesting that subunit specific mechanisms of insertion and removal are not required in this process. Therefore, it is possible that the developmental increase in GluN2A is primarily controlled by a developmental increase in transcription and translation of the subunit. However, as increasing the level of synaptic GluN2A alone is sufficient to raise the GluN2A:GluN2B ratio, it would be reasonable to suggest that mechanisms that promote *GRIN2A* transcription are more crucial than those involved in the suppression of *GRIN2B*.

3.6.5 Summary – 7-day dark rearing experimental findings

While dark rearing from birth had little impact on the typical GluN2A:GluN2B ratio increase, dark rearing for 7 days following 3 weeks of normal rearing proved to be a much more effective paradigm for the induction of deprivation mediated decreases in both the subunit ratio and activity dependent markers. Furthermore, this reduction in the GluN2A:GluN2B ratio was completely reversed by re-exposing dark reared mice to light for 24Hr. Crucially, this bidirectional shift in the ratio was observed to be driven by regulating the synaptic level of GluN2A, but not GluN2B. This would suggest that GluN2A is more dynamically regulated than GluN2B, with changes in synaptic activity potentially promoting a reduction/increase in synaptic GluN2A through influencing the balance between GluN2A recycling and its insertion/stability at the synapse.

3.6.6 Loss of GluN2B from triheteromeric NMDARs following 7-day dark rearing?

Although levels of GluN2B were also observed to change in response to both deprivation and subsequent re-exposure, the current findings argue against a

significant role for the regulation of GluN2B levels in the GluN2A:GluN2B ratio shift. Firstly, based on the models that have been put forward previously, one would expect that a decrease in activity (in this case light deprivation) would promote an increase in the levels GluN2B and that a subsequent increase in activity (24H re-exposure) would trigger a decrease in GluN2B expression. However, in the current study, the opposite is observed. This counterintuitive pattern of GluN2B expression in response to activity can reasonably be explained by the presence of triheteromeric NMDARs. In the case of triheteromeric NMDARS containing both a GluN2A and a GluN2B subunit, it would be reasonable to predict that GluN2B will be subject to removal from the synapse owing to its association with GluN2A. The degree to which the presence of GluN2A in a triheteromeric receptor complex influences removal of the receptor is uncertain and is something that would be of interest to investigate further. Based on the dominant influence of GluN2A on other properties of triheteromeric receptors and the significant, yet smaller loss of GluN2B observed in the current study, it may be the case that the presence of GluN2A promotes an intermediate loss of triheteromeric receptors.

Overall the current observations argue against the requirement for a mechanism that mediates insertion/removal of GluN2B in response to changing levels of sensory input. Previously it was demonstrated that CTD^{2B}/CaMKII/CK2 mediated events are not required for the developmental change in NMDAR subunit composition (McKay et al, 2018), the current findings suggest that this is also the case for dynamic experience dependent changes. As such, it is reasonable to predict that dark rearing $GluN2B^{\Delta CaMKII}$ for 7 days will produce a decrease in the GluN2A:GluN2B ratio that is comparable to WT.

3.6.4 Role of sensory experience in GluN2A:GluN2B ratio shift - Critical evaluation of methods

One of the benefits of using PSD enriched fractions is that it provides a better representation of experience/deprivation driven changes to NMDAR subunit composition at the synapse. Unlike PSD fractions, synaptoneurosome preparations contain presynaptic, postsynaptic and extrasynaptic components. As such, the use of synaptoneurosomes may account for some of the conflicting observations made in

earlier studies. On the other hand, the dissection and processing of whole V1 limits the ability to interrogate layer specific changes in NMDA expression. Taking slices of V1 and microdissecting specific layers may provide a better insight into how NMDAR composition changes across V1 circuitry.

In terms of the deprivation paradigm itself, the finding that red light negates the effect of dark rearing emphasises the importance of transparency when detailing the methods used for dark rearing experiments. Detailed dark rearing methods are often missing from the literature and, as such, it is often unclear how animal welfare checks were performed in the dark. This lends the possibility that variations in the methodology may contribute to conflicting results between studies. The dark rearing protocol outlined in this thesis was developed to account for as many sources of light infiltration as possible, which also considered the effect of red-light vs infrared light as the means of observing the animals in the dark. Taken together, I am confident that the dark rearing methods employed were as robust as possible. However, it cannot be said with complete certainty that the room was always completely photon-free. Therefore, the effect of very minor and transient light exposure, not detectable by light control film, could potentially account for the lack of any delay in the GluN2A:GluN2B ratio shift or downregulation of activity-dependent markers that was observed following dark rearing from birth. However, even when light exposure is detectable this too affects the interpretation of results as it leads to the loss of experimental data. Due to their duration, 28-day dark rearing experiments are both time consuming and highly sensitive to the slightest of error. As such, the data presented regarding the GluN2A:GluN2B ratio is based on relatively small group sizes. Therefore, while the normal developmental increase in the GluN2A:GluN2B ratio that is observed agrees with previous observations, this data lacks sufficient power to truly say that dark rearing does not have an effect on the developmental increase of the GluN2A:GluN2B ratio.

Chapter 4

Experience-dependent shift of the GluN2A:GluN2B ratio requires the presence of the GluN2A CTD

Chapter 4 – Experience-dependent shift of the GluN2A:GluN2B ratio requires the presence of the GluN2A CTD

4.1 Introduction

In **chapter 3** it was demonstrated that 7-day dark rearing and 24Hr light re-exposure during the critical period lower and increase the GluN2A:GluN2B ratio respectively through the regulation of synaptic GluN2A levels. Therefore, I next sought to investigate the mechanisms underpinning the experience-dependent changes in GluN2A expression. A potential scenario is that GluN2A containing NMDARs are in a dynamic equilibrium between synaptic and internal sites. The presence of synaptic activity may be required to promote GluN2A delivery to the synapse, with low activity promoting more GluN2A at internal sites through reduced trafficking to the surface and/or increased recycling. As sites on the CTD^{2A} have been implicated in trafficking and endocytosis of GluN2A containing NMDARs, it is reasonable to suggest that the CTD^{2A} may be critical for the activity-dependent regulation of the synaptic expression of GluN2A.

To investigate the role of the CTD^{2A} in experience dependent NMDAR composition changes, I utilised the $GluN2A^{2B(CTR)/2B(CTR)}$ KI mouse, in which the exon encoding the CTD of GluN2A is replaced with that of GluN2B (Ryan et al, 2013), meaning that both GluN2A and GluN2B have the same CTD. If CTD^{2A} specific events are responsible for altering subunit composition at the synapse in response to 7-day dark rearing and light re-exposure, changes in subunit composition should be reduced in mice where both GluN2 subunits possess the CTD^{2B}.

NB: All dark rearing experiments discussed in this chapter involve dark rearing for 7 days (P21-28) either with or without subsequent re-exposure to light for 24 hours.

GluN2A and GluN2B antibodies used in this chapter are against the N-terminal domain (NTD) of the subunit unless otherwise stated.

4.2 Relative levels of synaptic GluN2A and GluN2B are comparable between genotypes within the visual cortex.

As the one of the main aims of these experiments is to establish the role of the CTD^{2A} in subunit composition in response to altering sensory input to the VC, it was important to first establish whether $GluN2A^{2B(CTR)/2B(CTR)}$ mice exhibited any difference in the level of GluN2A subunits within the VC. To examine the relative levels of GluN2A and GluN2B in WT and $GluN2A2B^{(CTR)/2B(CTR)}$ mice, PSD enriched fraction were extracted from the V1 of P28 mice raised under standard 12:12 light conditions. Western blot analysis was then used to determine the synaptic levels of GluN2A and GluN2B. As both GluN2A and GluN2B subunits in the $GluN2A^{2B(CTR)/2B(CTR)}$ mice possess the same CTD, N-terminal antibodies were used for each subunit (**Fig 4.1B**). I observed that the levels of both GluN2A and GluN2B were comparable between genotypes (**Fig 4.1C-D**), as was the ratio of GluN2A:GluN2B (**Fig 4.1E**). Taken together, I was confident that the replacing the sequence of CTD^{2A} with that of the analogous sequence for CTD^{2B} did not alter expression levels of either subunit at VC synapses. As such, this removed a major confounding factor in any future observations made in 7-day dark rearing experiments.

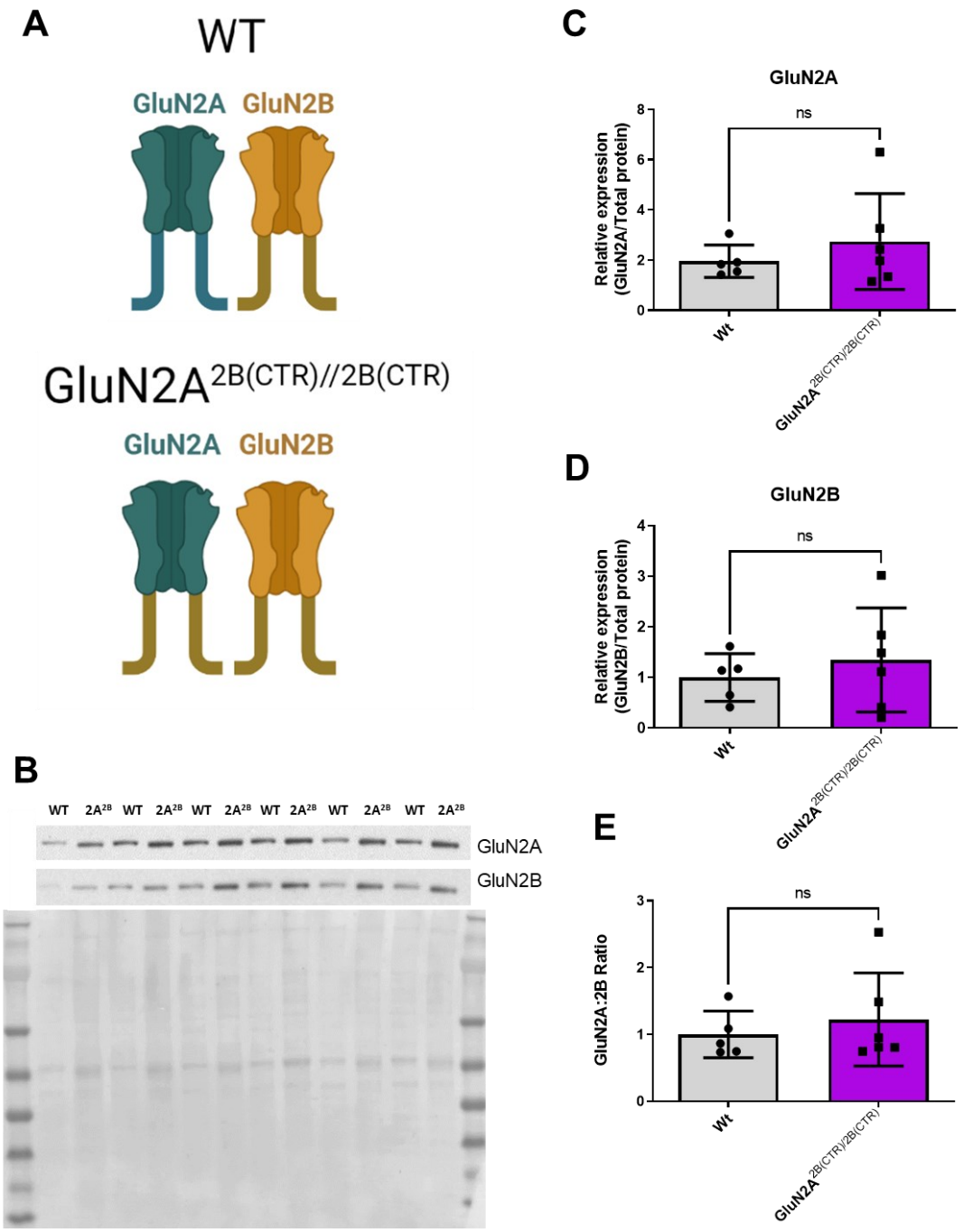

<u>Figure 4.1</u> – Synaptic GluN2A and GluN2B levels are not altered in the VC of GluN2A$^{2B(CTR)/2B(CTR)}$ mice.

A) Diagrammatic representation of the GluN2A$^{2B(CTR)/2B(CTR)}$ showing reciprocal swap of CTD^{2A} for CTD^{2B}. **B)** Postsynaptic density enriched visual cortex extracts from either WT or GluN2A$^{2B(CTR)/2B(CTR)}$ mice were analysed for GluN2A and GluN2B expression, normalised to total protein. Synaptic levels of GluN2A **(C)**, GluN2B **(D)** and GluN2A:GluN2B ratio **(E)** in GluN2A$^{2B(CTR)/2B(CTR)}$ mice relative to WT. Unpaired t test: $p = 0.4049$, $p = 0.5059$, $p = 0.5354$. WT n = 5, RL GluN2A$^{2B(CTR)/2B(CTR)}$ n = 6.

4.3 GluN2B is more abundant than GluN2A in mouse primary visual cortex.

The GluN2A$^{2B(CTR)/2B(CTR)}$ KI mouse serves as a unique tool for probing the relative abundance of GluN2A and GluN2B. Specifically, as all GluN2A and GluN2B subunits possess the CTD^{2B}, probing with a CTD^{2B} specific antibody provides a representation of the total population of GluN2A and GluN2B containing NMDARS. The difference in the level of CTD^{2B} observed between WT and the KI mice therefore represents the proportion of GluN2A$^{2B(CTR)}$ chimeric subunits. Previously, this method was utilised by Frank et al, (2016) to demonstrate that GluN2B is fourfold more abundant in the whole cortex. However, this study was conducted using whole lysates, thus masking synaptic expression. Therefore, I sought to utilise this technique to examine the relative abundance of synaptic GluN2A and GluN2B in the mouse V1 (**Fig 4.2A**). To achieve this, the PSD fractions extracted in **section 4.2** were probed with an antibody for the GluN2B CTD and normalised to the level of GluN2B NTD (**Fig 4.2C**). No significant difference in GluN2B CTD was observed between genotypes (**Fig4.2B**). This suggests that GluN2A containing NMDARs form a relatively small proportion of the overall NMDAR population in the mouse V1. This is in agreement with what has been observed previously in whole brain lysates (Frank et al, 2016) and suggests that changes to the level of synaptic GluN2A (as the less abundant unit) may have a greater contribution in shifting the GluN2A:GluN2B ratio in response to activity.

This would explain the observations made in WT mice dark reared for 7 days (**section 3.4)**. Since the population of GluN2B is already so much larger, a modest decrease in GluN2B would have relatively little effect in shifting the ratio whereas a modest decrease in GluN2A would have a much greater impact on the ratio. This is reflected by the fact that 7-day dark rearing mediates a drop in the GluN2A:GluN2B ratio even when both GluN2A and GluN2B levels are significantly decreased.

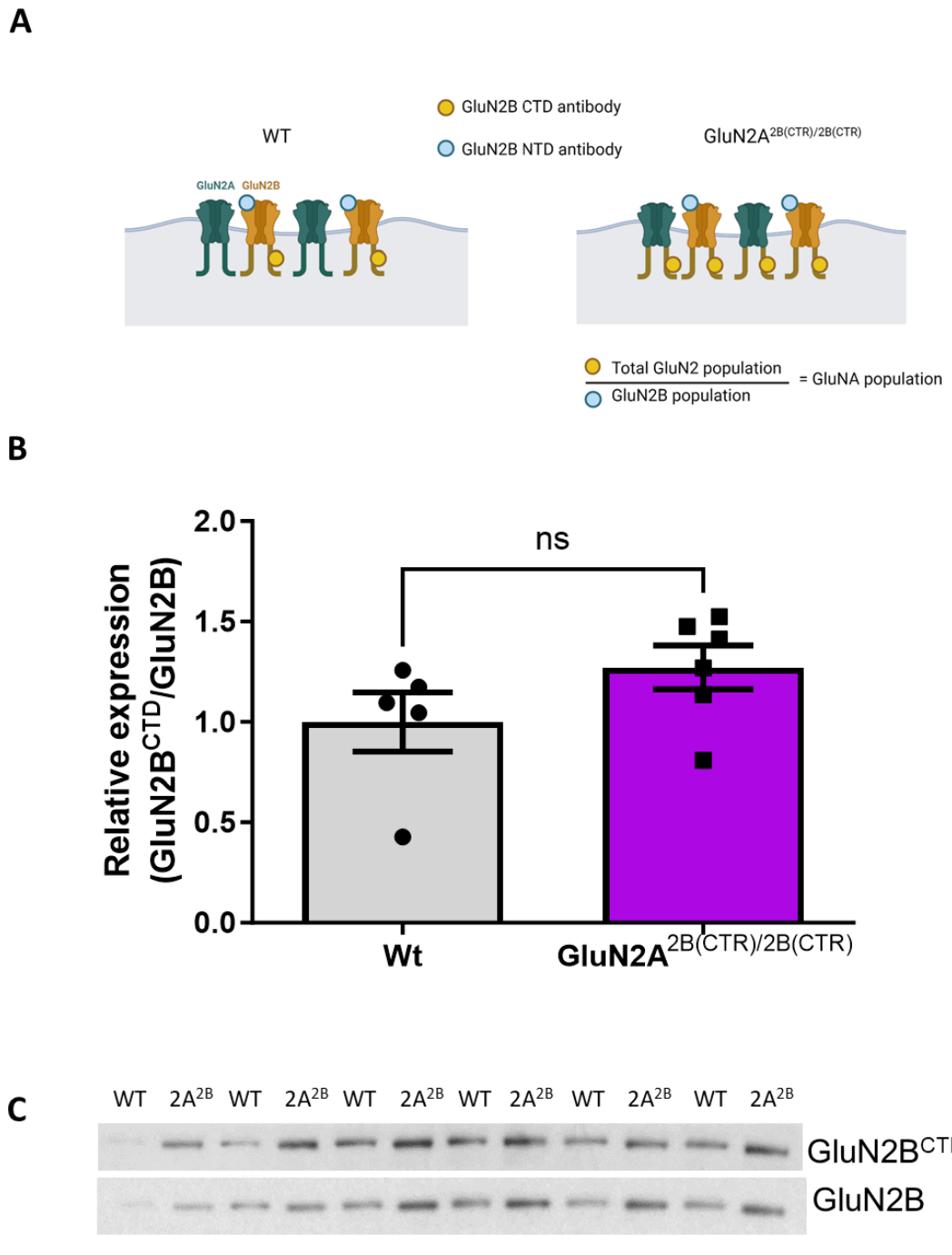

Figure 4.2 – GluN2A containing NMDARs make up a small proportion of the overall NMDAR population within the VC.

A) Outline of the strategy used to determine the relative population of GluN2A to GluN2B. **B)** Post synaptic visual cortex extracts were analysed for GluN2B CTD and normalised to the total GluN2B population as measured by the level of GluN2B NTD**. C)** Expression of GluN2B CTD at the synapse in mice expressing chimeric GluN2A$^{2B(CTR)}$ subunits relative to WT mice, Unpaired t test, $p = 0.1656$. WT n = 5, RL GluN2A$^{2B(CTR)/2B(CTR)}$ n = 6.

4.4 7-day dark rearing downregulates activity dependent Immediate early gene expression in GluN2A2B$^{(CTR)/2B(CTR)}$ mice.

In **chapter 3**, it was observed that IEG expression serves as a good marker of the changes to activity in the VC produced by dark rearing. As such, I also examined the expression of *Arc, Fos, Nr4a1* and *Bdnf* mRNA extracted from the VC of GluN2A$^{2B(CTR)/2B(CTR)}$ mice following normal rearing, 7-day dark rearing, and 7-day dark with subsequent 24Hr light re-exposure.

Interestingly, while IEG expression was also downregulated in GluN2A$^{2B(CTR)/2B(CTR)}$ mice, the regulation was less robust than that seen previously in WT. For instance, I observed that *Arc* mRNA was not significantly reduced in GluN2A$^{2B(CTR)/2B(CTR)}$ mice dark reared for 7 days (**Fig4.3A**). Additionally, when compared to previous observations in WT, GluN2A$^{2B(CTR)/2B(CTR)}$ mice exhibit a less-marked reduction in *Fos* mRNA expression following dark rearing (**Fig4.3B**). On the other hand, the change in the level of Nr4a1 mRNA that followed dark rearing was comparable to WT (**Fig4.3C**). The expression of *Bdnf* mRNA also exhibits a significant decrease following dark rearing (**Fig4.3D**). Similar to what was observed previously in WT, the majority of IEGs tested failed to exhibit a rebound following 24Hr re-exposure to light, with the only exception being *Bdnf*.

As robust control measures were in place, this weaker responses of *Arc* and *Fos* could not be accounted for by light infiltration during the dark period. Moreover, similar observations were observed in subsequent experiments and will be discussed in more detail in **chapter 5**.

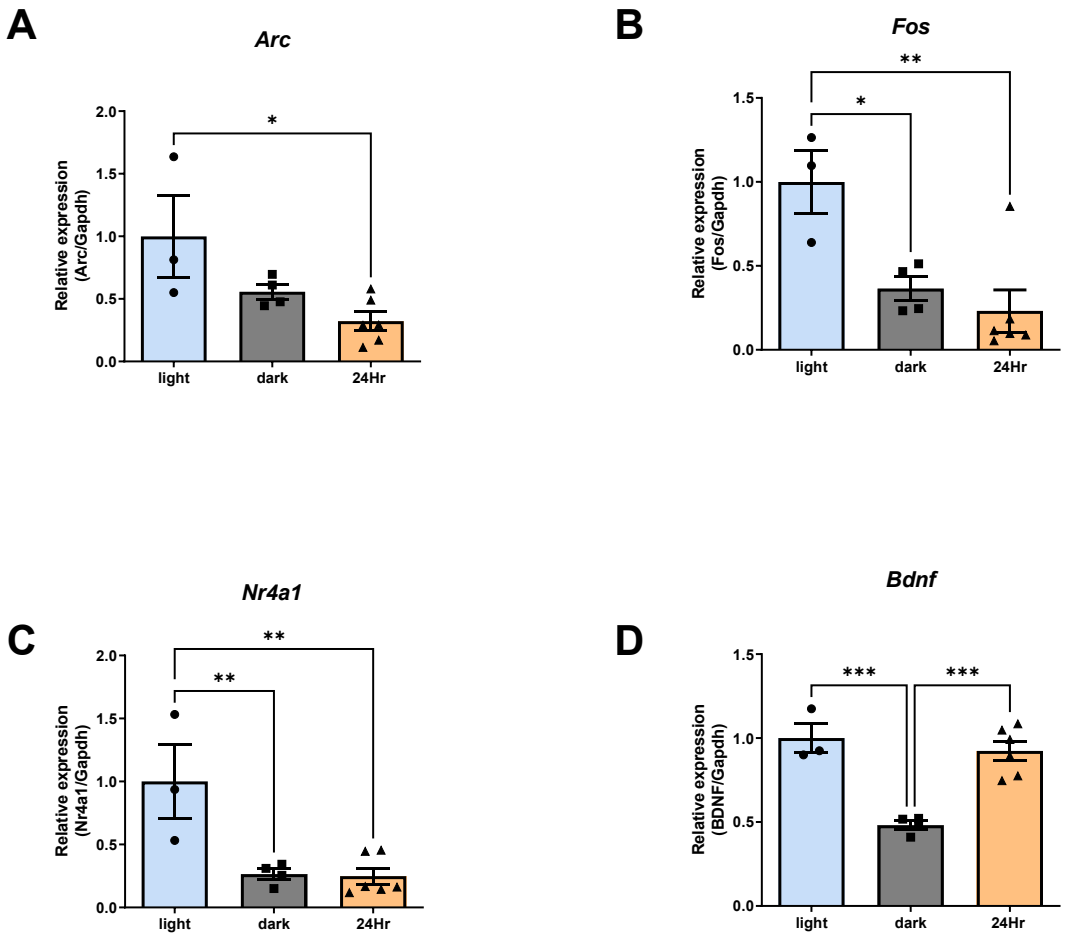

<u>Figure 4.3</u>– IEGs are downregulated by 7-day dark rearing in GluN2A$^{2B(CTR)/2B(CTR)}$ mice.

Using the qRT-PCR method, the mRNA expression of *Arc*, *Fos*, *Nr4a1* and *BDNF* were measured in GluN2A$^{2B(CTR)/2B(CTR)}$ mice that were either light reared or dark reared for 7 days (P21-28) with or without subsequent re-exposure to light for 24Hr. **A-D**) In GluN2A$^{2B(CTR)/2B(CTR)}$ mice, dark rearing reduced the relative expression of *Fos* **(B)**, *Nr4a1***(C)** and *Bdnf* **(D)**, but not *Arc* **(A)**. One-way ANOVA *Arc*: F (2, 10) = 5.435, p = 0.0253; *Fos*: F (2, 10) = 8.202, p = 0.0078; *Nr4a1*: F (2, 10) = 9.847, p = 0.0043; *Bdnf*: F (2, 10) = 19.97, p = 0.0003). Subsequent re-exposure to light only induced a significant rebound in *Bdnf*. Tukey's test for multiple comparisons *P<0.05; **P < 0.01; ***P < 0.001. GluN2A$^{2B(CTR)/2B(CTR)}$, light n=3, dark n=4, 24Hr n=6

4.5 The activity dependent shift in the GluN2A:2B ratio does not proceed in the absence of the GluN2A CTD

To examine whether the absence of the CTD^{2A} prevented activity dependent changes to the ratio of GluN2A:GluN2B, $GluN2A^{2B(CTR)/2B(CTR)}$ mice were dark reared using the 7-day dark rearing protocol outlined in **section 3.4**. PSD enriched fractions were then isolated from the VC and analysed for synaptic GluN2A and GluN2B (**Fig4.4**).

Western blot analysis revealed that $GluN2A^{2B(CTR)/2B(CTR)}$ mice showed no significant change in either the level of GluN2A or GluN2B in response to either 7-day dark rearing or subsequent re-exposure to light (**Fig 4.4 A-B**). As the synaptic expression of each subunit remained unchanged across the three light conditions so too did the GluN2A:GluN2B ratio (**Fig4.4C**). To determine whether the results observed in $GluN2A^{2B(CTR)/2B(CTR)}$ represent a statistically significant genotype effect, a direct comparison was made between genotypes using the percentage change from their respective light control groups as a conversion factor. Direct comparison between $GluN2A^{2B(CTR)/2B(CTR)}$ and WT mice revealed that the level of synaptic GluN2A is significantly influenced by both light condition and genotype (**Fig4.4D**). Similarly, GluN2B also exhibits a genotype-dependent difference in protein level following dark rearing (**Fig4.4E**). Comparison of the GluN2A:GluN2B ratio between genotypes reveals a light condition dependent effect, but no significant genotype effect (**Fig4.4F**). However, the light-dependent effect upon the ratio is solely driven by WT. This suggests that, while regulation of the GluN2A:GluN2B ratio in WT may be more dynamic, the overall change is modest.

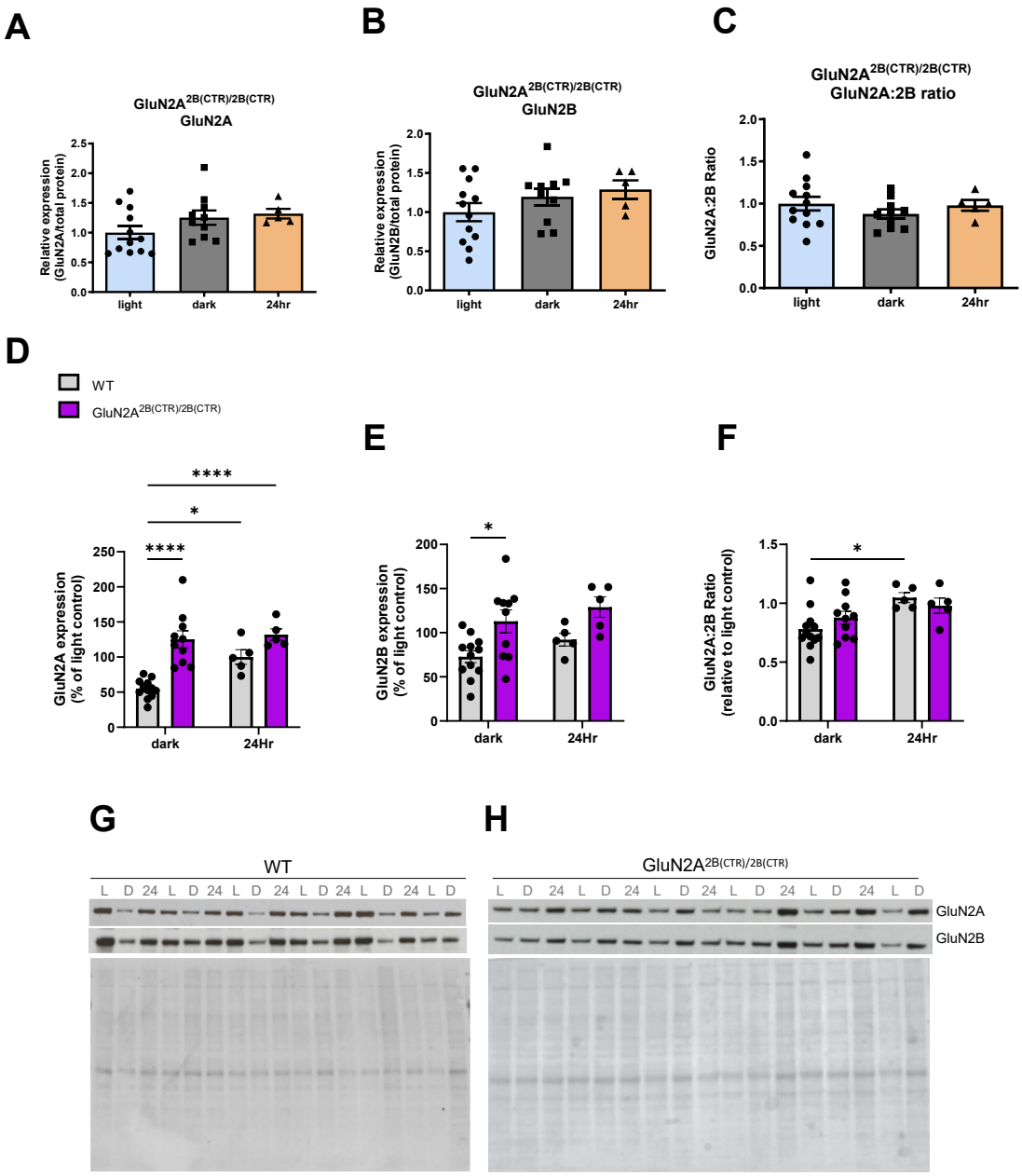

Figure 4.4 – Activity dependent changes in GluN2A:GluN2B ratio are not observed in GluN2A$^{2B(CTR)/2B(CTR)}$ mice.

PSD enriched visual cortex fractions from P28-29 GluN2A$^{2B(CTR)/2B(CTR)}$ mice either light reared, dark reared or dark reared with 24Hr light re-exposure were analysed for synaptic GluN2A and GluN2B expression **A)** Relative expression of GluN2A normalised to light. One-way ANOVA for GluN2A$^{2B(CTR)/2B(CTR)}$ GluN2A: $F(2, 26) = 1.976$, $p = 0.1589$. **B)** Relative expression of GluN2B**.** One-way ANOVA for GluN2A$^{2B(CTR)/2B(CTR)}$ GluN2B: $F(2, 26) = 0.3944$, $p = 0.6781$. **C)** Relative ratio of GluN2A:GluN2B. One-way ANOVA for GluN2A$^{2B(CTR)/2B(CTR)}$ GluN2A:GluN2B ratio: $F(2, 26) =$

0.7073, p = 0.5022. **D)** Two-way ANOVA (main genotpe effect) for GluN2A: F (1, 28) = 27.03, $p < 0.0001$; (light condition effect) for GluN2A: F (1, 28) = 6.993 $p = 0.0133$. **E)** Two-way ANOVA (main genotpe effect) for GluN2B: F (1, 28) = 11.35, $p = 0.0022$; (light condition effect) for GluN2B: F (1, 28) = 2.409 $p = 0.1319$. **F)** Two-way ANOVA (main genotpe effect) for GluN2A:GluN2B: F (1, 28) = 0.05647, $p = 0.8139$; (light condition effect) for GluN2A:GluN2B: F (1, 28) = 9.120, $p = 0.0053$.. **G-H)** Representative blot for WT and GluN2A$^{2B(CTR)/2B(CTR)}$ GluN2A and GluN2B protein, normalised to total protein. Tukey's test for multiple comparisons *P<0.05; **P < 0.01; ***P < 0.001; ****P<0.0001GluN2A$^{2B(CTR)/2B(CTR)}$, light n=12, dark n=11, 24Hr n=5

4.6 Dark rearing alters postsynaptic protein composition.

In addition to the observation that dark rearing lowered the ratio of GluN2A:GluN2B in WT mice (**Fig4.5A**), I also observed a moderate decrease in other synaptic proteins, including the principal NMDAR subunit GluN1 and the MAGUK family scaffolding protein PSD95 (**Fig 4.5C-D**). The loss of GluN1 is consistent with a decrease in both GluN2A and GluN2B subunits, possibly representing the loss of GluN2A from di-heteromeric $GluN1_2$-$GluN2A_2$ and GluN2B from tri-heteromeric $GluN1_2$-$GluN2A_1$-$GluN2B_1$. In addition, PSD95 is more strongly associated with CTD^{2A} and as such it's respective decrease may represent a consequence of the loss of GluN2A from the synapse. As was observed previously with the GluN2A:GluN2B ratio, GluN2A$^{2B(CTR)/2B(CTR)}$ also do not exhibit any changes in synaptic levels of GluN1 or PSD95 (**Fig 4.5 B, E-F**).

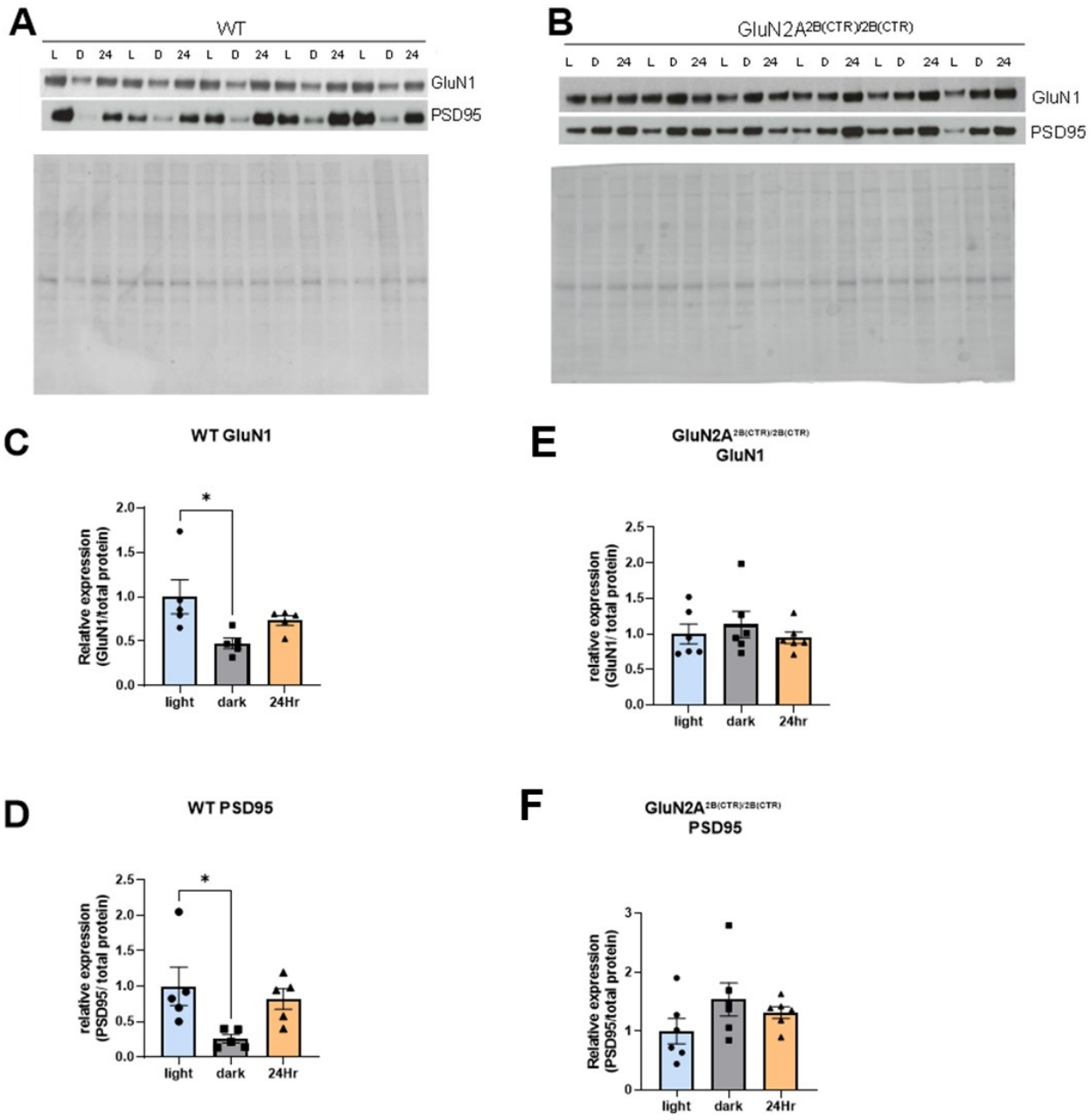

<u>Figure 4.5</u> - The activity dependent changes to postsynaptic protein composition does not occur in GluN2A$^{2B(CTR)/2B(CTR)}$ mice.

A-B) PSD enriched visual cortex extracts from P28-29 mice either light reared, dark reared or dark reared + 24Hr light re-exposure were analysed for GluN1, PSD95 and GluA1 expression, normalised to total protein. Representative blot for WT (**A**) and GluN2A$^{2B(CTR)/2B(CTR)}$ (**B**). **C**) In WT mice GluN1 protein level exhibits a significant decrease following 7-day dark rearing with a slight but non-significant rebound following re-exposure to light for 24Hr. One-way ANOVA for WT GluN1: F (2, 12) = 4.775, p = 0.0298. **D)** Protein level of WT PSD95 exhibit a moderate decrease following dark

rearing but no significant rebound following re-exposure to light. One-way ANOVA for WT PSD95: F (2, 12) = 4.599, p = 0.0329. **E)** GluN2A$^{2B(CTR)/2B(CTR)}$ do not exhibit any changes in the level of GluN1 across any of the light conditions. One-way ANOVA for GluN2A$^{2B(CTR)/2B(CTR)}$ GluN1: F (2, 15) = 0.4685, p = 0.6348. **F)** As with GluN1, GluN2A$^{2B(CTR)/2B(CTR)}$ show no difference in PSD95 expression across any light condition. One-way ANOVA for GluN2A$^{2B(CTR)/2B(CTR)}$ PSD95: F (2, 15) = 1.627, *p* = 0.2293. Tukey's test for multiple comparisons *P<0.05; WT light n=5. dark n=5, 24Hr n=5; GluN2A$^{2B(CTR)/2B(CTR),}$ light n=6, dark n=6, 24Hr n=6

4.7 Presynaptic marker synaptophysin is not reduced in dark reared mice.

One possibility that must be considered when faced with a robust loss of a multiple synaptic proteins is that dark rearing over 7 days is sufficient to induce the loss of synapses. Previously, it has been observed that both brief (4-7 days) and prolonged (>5 weeks) periods of monocular deprivation are sufficient to induce rapid withdrawal of the branches that serve the deprived eye (Antonini and Stryker, 1993; Antonini and Stryker, 1996). Binocular deprivation has a much milder effect when compared to that of monocular deprivation, with neurons maintaining responsiveness to both eyes. Importantly, however, this selectivity is lost if binocular deprivation is performed for longer durations (Cooper and Bear, 2012). As such, I investigated whether the loss of postsynaptic proteins was the result of synapse loss.

To determine whether synapses were being lost as a result of 7 days of dark rearing, western blots were run using non-PSD fractions collected from the same mice used in **section 4.6 (Fig4.6B)**. These fractions contain presynaptic, extrasynaptic and perisynaptic components. Blots were then probed for the presynaptic marker synaptophysin (**Fig4.6A,C,E**) Neither WT mice nor GluN2A$^{2B(CTR)/2B(CTR)}$ mice exhibited any difference in the levels of synaptophysin expression following dark rearing or subsequent light re-exposure (**Fig4.6D,F**). Therefore, the unchanged level of synaptophysin tentatively suggests that synapses are not being lost as a result of 7-day dark rearing. However, further immunohistochemical experiments that focus on quantifying the number of synapses present in both light and dark reared animals will be needed before any definitive conclusion can be made as to the effect of 7-day dark rearing on synapse loss.

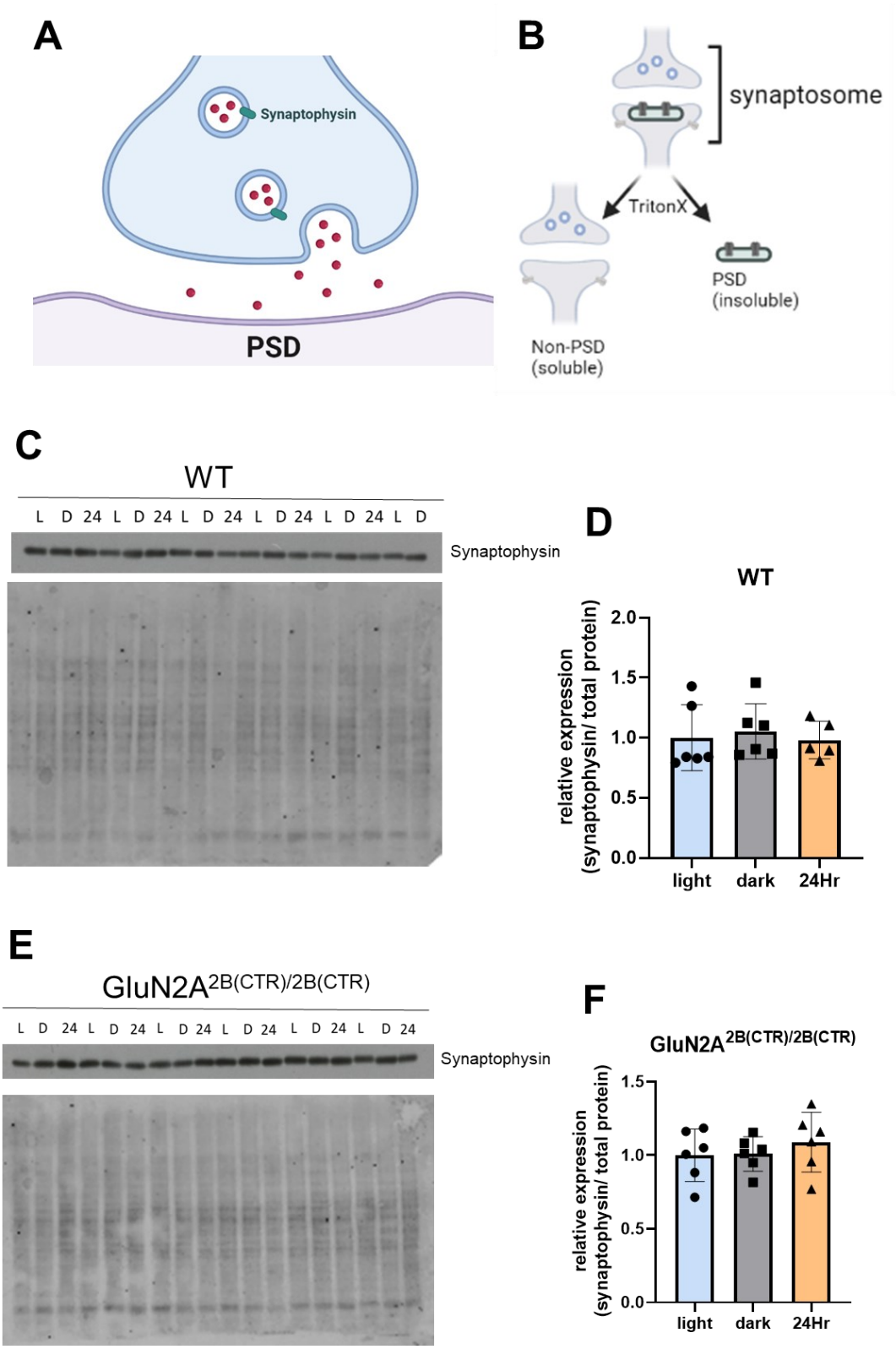

Figure 4.6 – Dark rearing does not induce a loss of presynaptic marker synaptophysin.

A) Diagrammatic representation of synaptophysin localisation at the pre-synapse. **B)** Non-PSD fractions containing presynaptic, extrasynaptic and perisynaptic components are obtained through

solubilisation of synaptosome in 0.5% Triton-x detergent. **C, E**) Representative blots of synaptophysin expression across light, dark and 24Hr light re-exposure for WT (**C**) and GluN2A$^{2B(CTR)/2B(CTR)}$ (**E**), normalised to total protein **D)** WT synaptophysin expression is unchanged across any of the 3 light conditions. One-way ANOVA for WT synaptophysin: F (2, 14) = 0.1464, p = 0.8651 **F)** GluN2A$^{2B(CTR)/2B(CTR)}$ synaptophysin levels do not change across light conditions. One-way ANOVA for GluN2A$^{2B(CTR)/2B(CTR)}$ synaptophysin: F (2, 15) = 0.4922, p = 0.6208. WT light n=6. dark n=6, 24Hr n=5; GluN2A$^{2B(CTR)/2B(CTR)}$, light n=6, dark n=6, 24Hr n=6.

4.8 Discussion

4.8.1 Summary

When considering the results obtained in this chapter, there is evidence to suggest that the CTD^{2A} is required for experience-dependent changes to NMDAR composition at the synapse. This raises the question – what is the precise role of CTD^{2A} in mediating these changes? It would be reasonable to assume that CTD^{2A} specific interactions, signalling or post-translational modifications are required to remove GluN2A from the synapse in response to changes in activity. However, it is also possible that greater anchoring mediated by CTD^{2B} recruited protein complexes may also account for the lack of change observed. Both possibilities are discussed in more detail below.

4.8.2 What is the role of CTD^{2A} in activity-dependent changes to subunit composition?

The recent identification of a CaMKII phosphorylation site at s1459 on CTD^{2A} and its role in activity-dependent removal and recycling of GluN2A *in vitro* could provide a potential mechanism to explain the observations made in the current dark rearing experiments. This model proposes that phosphorylation of S1459 increases GluN2A association with Sorting Nexin 27 (SNX27) which in turn leads to trafficking of GluN2A to the synapse. Once at the synapse, dephosphorylation facilitates increased PSD95 binding and stabilises the subunit (Mota Vieira et al, 2020). The phosphorylation state of this site is therefore proposed to determine the binding of

CTD^{2A} to either SNX27 or PSD95, with the outcomes of promoting membrane recycling and membrane anchoring respectively. Therefore, mechanisms that uncouple the CTD^{2A} from PSD95 may contribute to the activity driven decrease in GluN2A. It would therefore be of interest to investigate the effect of overexpressing or increasing endogenous expression of PSD95 on the activity-dependent ratio shift. However, retention of GluN2A at the PSD is also influenced by a number of other scaffolding proteins. For instance, the rab-effector protein Rabphilin3A (Rph3A) is known to bind to the CTD^{2A} . In response to LTP it forms a complex with PSD95 to promote GluN2A stability at the PSD, while the disruption of Rph3A binding rapidly reduces the levels of synaptic GluN2A (Stanic et al, 2015). Additionally, it has been shown that Scribble1 acts in an activity-dependent manner to control the synaptic expression of NMDARs; notably, binding of Scribble1 at the CTD^{2A} 1458-1464 site prevents GluN2A from undergoing lysosomal trafficking and degradation by increasing GluN2A recycling to the synaptic membrane via interplay with AP-2 (Piguel et al, 2014). Therefore, it can be appreciated that disruption of any number of these CTD^{2A}/scaffolding protein interactions may account for a reduction in synaptic expression.

4.8.3 Does the CTD^{2B} promote greater anchoring at the PSD?

As mentioned in **section 1.6**, the presence of the CTD^{2B} allows NMDARs to be selectively partitioned into large 1.5MDa supercomplexes (Frank et al, 2016). The $GluN2A^{2B(CTR)/2B(CTR)}$ mice represent a unique situation where the entire NMDAR population can form supercomplexes. Indeed, co-immunoprecipitation analysis revealed a significantly greater association of GluN2A with PSD95 and PSD93 in $GluN2A^{2B(CTR)/2B(CTR)}$ compared to WT (Ryan et al, 2013). The consequences for the loss of selectivity in supercomplex formation between GluN2A and GluN2B remains to be elucidated. However, it is possible that the results observed in dark reared $GluN2A^{2B(CTR)/2B(CTR)}$ mice are due to greater anchoring of GluN2A via the presence of the CTD^{2B} and its recruitment of supercomplexes which may provide greater stability at the synapse. This may also be evidenced by the lack of change to PSD95 following dark rearing of $GluN2A^{2B(CTR)/2B(CTR)}$ mice, suggesting a more “rigid”

protein scaffold that renders the synapse less flexible to experience-dependent changes of the postsynaptic proteome. Analysing the whole postsynaptic proteome via mass spectroscopy may provide some clues as to the broader picture of postsynaptic changes in response to activity. Based on the observations made in the western analysis, I would hypothesise that GluN2A$^{2B(CTR)/2B(CTR)}$ mice would show reduced postsynaptic proteome changes in response to dark rearing and subsequent light re-exposure.

4.8.4 Predictions for 7-day dark rearing in GluN2B$^{2A(CTR)/2A(CTR)}$ mice

The role of CTD^{2A} in sensory experience driven changes can be investigated further by using the GluN2B$^{2A(CTR)/2A(CTR)}$ KI mouse. Based on the observation that the dark rearing induced decrease in synaptic GluN2A is driven by the presence of the CTD^{2A}, a reasonable prediction might be that GluN2B$^{2A(CTR)/2A(CTR)}$ mice will demonstrate a robust decrease in both GluN2A and GluN2B in response to dark rearing. Similarly, levels of both subunits would then be predicted to exhibit a rebound following re-exposure to light (**Fig 4.7**). This would further support a CTD^{2A} mediated mechanism of activity-driven removal/insertion.

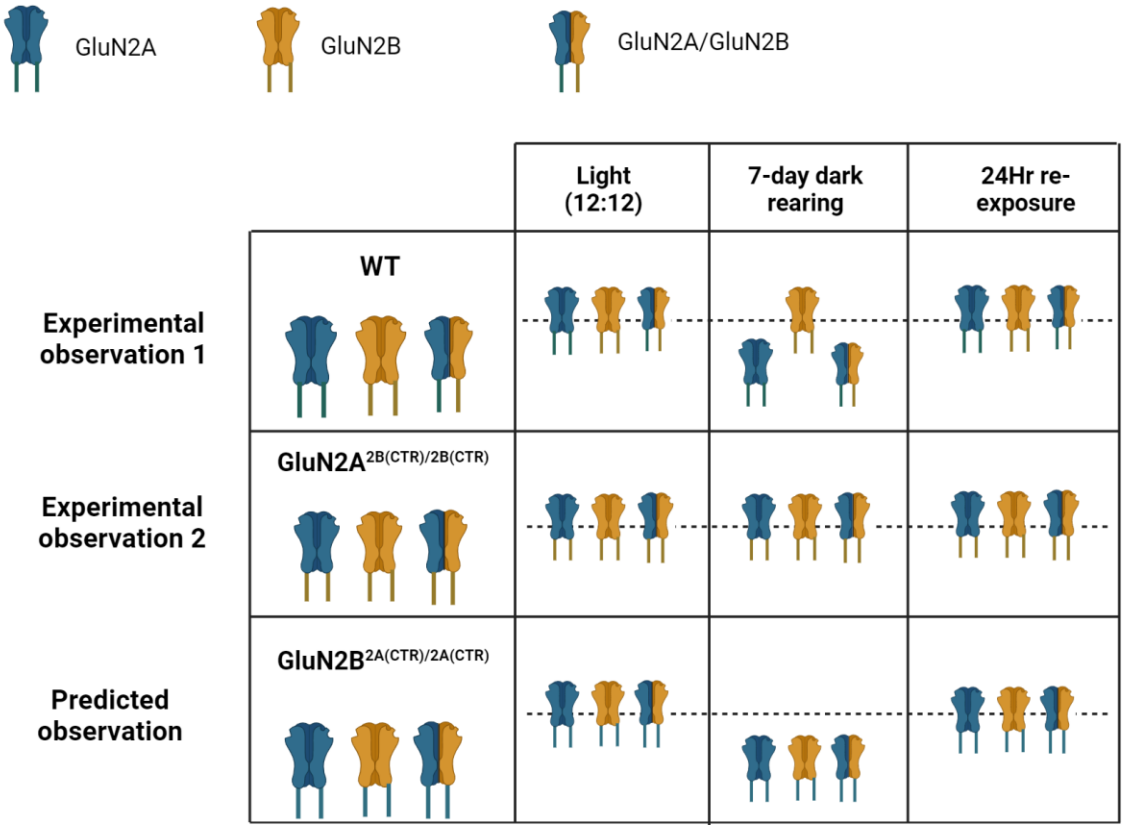

Figure 4.7 - Diagrammatic representation of the predicted effect of dark rearing GluN2B$^{2A(CTR)/2A(CTR)}$.

The experimental observations in Chapter 3 and the current chapter are summarised. Based on these observations, the predicted observation for 7-day dark rearing of GluN2B$^{2A(CTR)/2A(CTR)}$ is outlined.

4.8.5 The role of the CTD^{2A} in mediating activity-dependent changes of the GluN2A:GluN2B ratio - Critical evaluation of the methods

While useful, the approach used to investigate the relative proportion of GluN2A and GluN2B in V1 (**section 4.1**) only utilises the GluN2A$^{2B(CTR)/2B(CTR)}$ mouse model. Arguably, performing the same experiment in the GluN2B$^{2A(CTR)/2A(CTR)}$ would provide greater clarity on this issue. If the abundance of GluN2B is greater, it would be reasonable to predict that the level of CTD^{2A} in GluN2B$^{2A(CTR)/2A(CTR)}$ compared to WT would be significantly greater. This is due to the fact that in WT the CTD^{2A} signal would represent only the level of GluN2A, but in GluN2B$^{2A(CTR)/2A(CTR)}$ mice it would represent the population of GluN2A and GluN2B combined. Indeed, the study that used this technique previously showed subtle differences when comparing CTD^{2B}

expression between GluN2A$^{2B(CTR)/2B(CTR)}$ and WT, but more dramatic changes in CTD^{2A} expression between GluN2B$^{2A(CTR)/2A(CTR)}$ and WT (Frank et al., 2016). Taken together this provided compelling evidence for a larger proportion of GluN2B within the forebrain. Unfortunately, the lack of availability of GluN2B$^{2A(CTR)/2A(CTR)}$ mice prevented complementary experiments to be conducted in V1. Therefore, while the results presented currently suggest a higher proportion of GluN2B within V1, it would be beneficial to repeat these experiments in GluN2B$^{2A(CTR)/2A(CTR)}$ mice.

For GluN2A$^{2B(CTR)/2B(CTR)}$ mice, the absence of a deprivation mediated fall in GluN2A levels is consistent with a role for the CTD^{2A} in either mediating signalling that actively removes GluN2A in response to the absence of sensory input or by influencing synaptic stability of GluN2A. In addition, the lack of change in either subunit further argues against a CTD^{2B}-dependent mechanism of removal/insertion of GluN2B in response to changes in activity. This would also support the suggestion that the modest decrease in GluN2B that was observed in WT mice (**section 3.4**) is mediated by a CTD^{2A}-dependent loss of triheteromeric receptors. However, previous evidence has suggested that deprivation promotes an initial increase of GluN2B that is followed by a later decrease in GluN2A (Chen and Bear, 2007). Therefore, it is possible that dark rearing for a shorter period of time may reveal early changes in GluN2B. As such, it would be of interest to investigate subunit expression following shorter durations of dark rearing, possibly 3-day and 5-day. If similar observations are made and GluN2B levels remain stable across different durations of dark rearing, then this would strengthen the argument for dynamic changes to GluN2A levels as the key mechanism for experience-dependent control of the subunit ratio.

Chapter 5

Dynamic range in response to activity is reduced in GluN2A$^{2B(CTR)/2B(CTR)}$ mice.

Chapter 5– Dynamic range in response to activity is reduced in GluN2A$^{2B(CTR)/2B(CTR)}$ mice.

5.1 Introduction

In **chapter 4**, it was established that unique CTD sequences are not required for the developmental shift in NMDAR subunit composition, their role in other aspects of neuronal development is poorly understood. A previous study investigating the role of the CTD signalling in development revealed that swapping CTD^{2A} for CTD^{2B}, but not the reverse, resulted in changes to dendritic morphology, including lengthening of the total arbor path along with the average apical length and the total basal length (Keith et al, 2019). Therefore, this suggests that CTD identity influences key intracellular signalling pathways involved in establishing dendritic morphology. As the downstream consequences of these intracellular signalling pathways presumably involve the regulation of gene transcription, it is likely that these mice would exhibit transcriptomic differences when compared to WT. However, the transcriptomic difference in mice with the CTD^{2A} swapped for that of CTD^{2B} has not yet been studied. To explore impact of swapping the CTD^{2A} for CTD^{2B} on gene expression, I performed RNA-seq analysis on RNA isolated from V1 of P28 WT and GluN2A$^{2B(CTR)/2B(CTR)}$ mice reared under standard 12-hour light-dark cycle.

As discussed in **section 1.2**, Ca^{2+} influx mediated by synaptic NMDARs is critical for the induction of rapidly transcribed IEGs that facilitate a secondary wave of gene expression that mediates long term changes in neuronal function. Previously, our laboratory used RNA-seq analysis to probe gene expression changes in the VC of WT mice following 7-day dark rearing. Here it was found that sensory deprivation produced a robust downregulation of many IEGs including *Egr2*, *Npas4* and *Fos*. However, the influence of swapping the CTD^{2A} for that of CTD^{2B} on transcriptomic changes had not yet been tested. Using RNA-seq, I next sought to investigate whether the CTD^{2A} was required for the gene expression changes following 7-day dark rearing and subsequent re-exposure to light for 12Hr. Based on the qRT-PCR data presented in **chapter 4** that showed an attenuated dark rearing induced decrease of IEG

expression in GluN2A$^{2B(CTR)/2B(CTR)}$ mice, a reasonable hypothesis might be that activity-dependent transcriptional changes would be attenuated in the absence of the CTD^{2A}. To investigate whether the CTD^{2A} was required for the gene expression changes following 7-day dark rearing and subsequent re-exposure to light for 12Hr, RNA-seq data from WT and GluN2A$^{2B(CTR)/2B(CTR)}$ was analysed to identify sets of genes which exhibited significant genotype differences in response to changes in synaptic activity induced by dark rearing and re-exposure to light. Gene ontology (GO) analysis was then applied to identify the biological processes and potential signalling pathways associated with these differentially regulated genes.

Finally, I wanted to determine whether there was an association between the activity-dependent regulation of genes and the pattern of differential expression between genotypes under each light condition. For example, do genes that are typically induced by light exhibit lower expression in GluN2A$^{2B(CTR)/2B(CTR)}$ mice under light conditions, but more highly expressed in the dark? By using enrichment analysis of gene sets for both light induced and repressed genes I aimed to establish whether the pattern of differential expression between genotypes was reflective of weaker activity-dependent regulation in GluN2A$^{2B(CTR)/2B(CTR)}$.

NB: All dark rearing experiments discussed in this chapter involve dark rearing for 7 days either with or without subsequent re-exposure to light for 12 hours. This is a different re-exposure protocol to that used in **chapter 4.**

Bioinformatic analyses of the returned reads was undertaken by Dr Owen Dando, Dr Xin He and Dr Deepali Vasoya. This analysis was then used to curate gene sets for subsequent analysis.

5.2 Differential expression of genes between GluN2A$^{2B(CTR)/2B(CTR)}$ and WT mice.

To gain a better understanding of the role of the CTD^{2A} in development and normal biological function, RNA-seq was performed on RNA extracted from the VC of P28 WT and GluN2A$^{2B(CTR)/2B(CTR)}$ mice raised under standard light conditions (12:12), Raw read counts were summarised using featureCounts before differential expression analysis was performed using DESeq2. Following this, a list of genes that exhibited significant differential expression in GluN2A$^{2B(CTR)/2B(CTR)}$ mice under standard light conditions ($p\_adj<0.05$) was curated. A total of 206 genes were identified as being differentially regulated between WT and GluN2A$^{2B(CTR)/2B(CTR)}$ mice. Of this gene set, genes predominantly showed lower expression in GluN2A$^{2B(CTR)/2B(CTR)}$ (130) with relatively fewer genes showing higher expression (76) (**Table S1**).

To investigate the functional importance of these genes, I next performed ontology analysis of the core set of genes that showed differential expression in GluN2A2B$^{(CTR)/2B(CTR)}$ mice. For those genes that showed lower expression in GluN2A2B$^{(CTR)/2B(CTR)}$ mice (**Fig 5.1B**), GO Biological Processes were dominated by those associated with regulation of postsynaptic protein composition, synapse assembly, axon guidance, and actin filament assembly. GO Molecular Functions were dominated by cytoskeletal binding activity and binding to excitatory ion channels while GO Cellular Components included the actin cytoskeleton, excitatory synapses, and multiple dendritic sites. For those genes that showed higher expression in GluN2A$^{2B(CTR)/2B(CTR)}$ mice (**Fig5.1C**), GO Biological Processes were dominated by those associated with regulation of the circadian rhythm. GO Molecular Functions exhibited low overlap with the gene set, however, there was an association with transcription factor binding. GO Cellular Components included dendritic and intracellular vesical compartments.

Collectively, these analyses suggest a role for CTD^{2A} in regulating the postsynaptic proteome at excitatory synapses. Notably, multiple activity-dependent genes involved with the maintenance of circadian rhythm were identified amongst the smaller set of gene that were more highly expressed in GluN2A$^{2B(CTR)/2B(CTR)}$. As activity-dependent

genes appear to be both downregulated and upregulated in GluN2A$^{2B(CTR)/2B(CTR)}$, this raised the question of whether these mice have an altered basal level of activity.

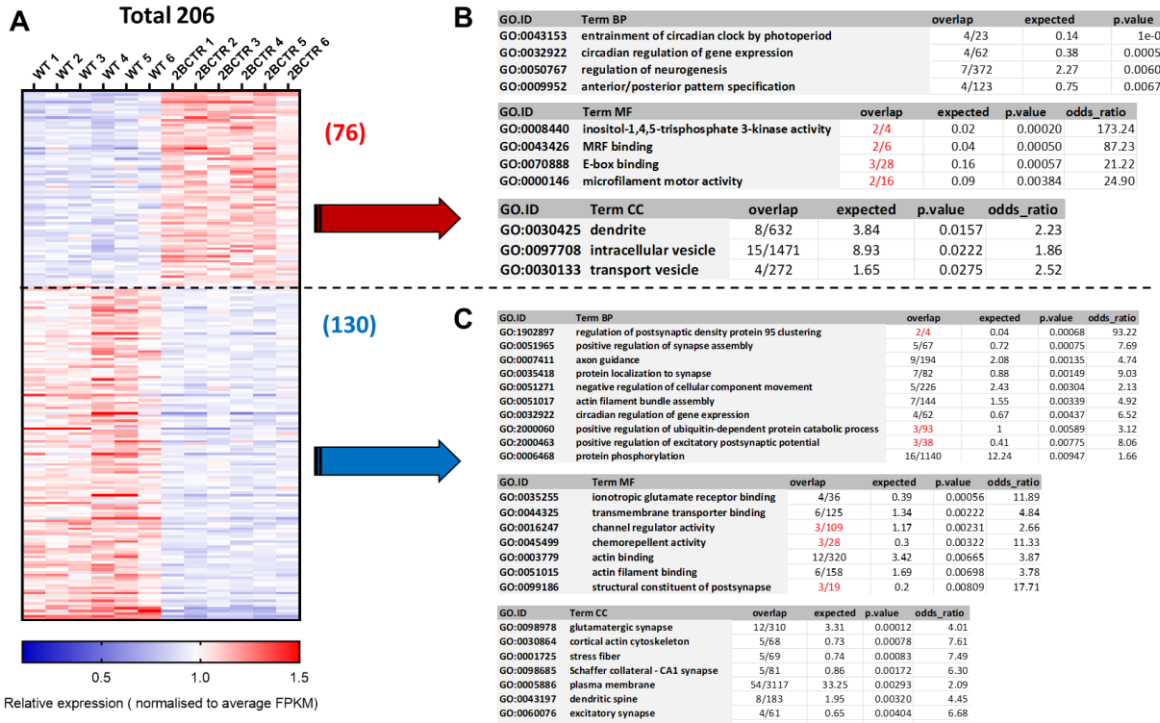

B

GO.ID	Term BP	overlap	expected	p.value	odds_ratio
GO:0043153	entrainment of circadian clock by photoperiod	4/23	0.14	1e-05	36.06
GO:0032922	circadian regulation of gene expression	4/62	0.38	0.00055	11.79
GO:0050767	regulation of neurogenesis	7/372	2.27	0.00602	3.34
GO:0009952	anterior/posterior pattern specification	4/123	0.75	0.00675	5.72

GO.ID	Term MF	overlap	expected	p.value	odds_ratio
GO:0008440	inositol-1,4,5-trisphosphate 3-kinase activity	2/4	0.02	0.00020	173.24
GO:0043426	MRF binding	2/6	0.04	0.00050	87.23
GO:0070888	E-box binding	3/28	0.16	0.00057	21.22
GO:0000146	microfilament motor activity	2/16	0.09	0.00384	24.90

GO.ID	Term CC	overlap	expected	p.value	odds_ratio
GO:0030425	dendrite	8/632	3.84	0.0157	2.23
GO:0097708	intracellular vesicle	15/1471	8.93	0.0222	1.86
GO:0030133	transport vesicle	4/272	1.65	0.0275	2.52

C

GO.ID	Term BP	overlap	expected	p.value	odds_ratio
GO:1902897	regulation of postsynaptic density protein 95 clustering	2/4	0.04	0.00068	93.22
GO:0051965	positive regulation of synapse assembly	5/67	0.72	0.00075	7.69
GO:0007411	axon guidance	9/194	2.08	0.00135	4.74
GO:0035418	protein localization to synapse	7/82	0.88	0.00149	9.03
GO:0051271	negative regulation of cellular component movement	5/226	2.43	0.00304	2.13
GO:0051017	actin filament bundle assembly	7/144	1.55	0.00339	4.92
GO:0032922	circadian regulation of gene expression	4/62	0.67	0.00437	6.52
GO:2000060	positive regulation of ubiquitin-dependent protein catabolic process	3/93	1	0.00589	3.12
GO:2000463	positive regulation of excitatory postsynaptic potential	3/38	0.41	0.00775	8.06
GO:0006468	protein phosphorylation	16/1140	12.24	0.00947	1.66

GO.ID	Term MF	overlap	expected	p.value	odds_ratio
GO:0035255	ionotropic glutamate receptor binding	4/36	0.39	0.00056	11.89
GO:0044325	transmembrane transporter binding	6/125	1.34	0.00222	4.84
GO:0016247	channel regulator activity	3/109	1.17	0.00231	2.66
GO:0045499	chemorepellent activity	3/28	0.3	0.00322	11.33
GO:0003779	actin binding	12/320	3.42	0.00665	3.87
GO:0051015	actin filament binding	6/158	1.69	0.00698	3.78
GO:0099186	structural constituent of postsynapse	3/19	0.2	0.00809	17.71

GO.ID	Term CC	overlap	expected	p.value	odds_ratio
GO:0098978	glutamatergic synapse	12/310	3.31	0.00012	4.01
GO:0030864	cortical actin cytoskeleton	5/68	0.73	0.00078	7.61
GO:0001725	stress fiber	5/69	0.74	0.00083	7.49
GO:0098685	Schaffer collateral - CA1 synapse	5/81	0.86	0.00172	6.30
GO:0005886	plasma membrane	54/3117	33.25	0.00293	2.09
GO:0043197	dendritic spine	8/183	1.95	0.00320	4.45
GO:0060076	excitatory synapse	4/61	0.65	0.00404	6.68
GO:0043198	dendritic shaft	4/68	0.73	0.00595	5.95
GO:0030027	lamellipodium	6/156	1.66	0.00649	3.84

Figure 5.1 – Differential regulation of genes in GluN2A$^{2B(CTR)/2B(CTR)}$ mice.

A) Heat map of genes that are differentially expressed between WT and GluN2A2B$^{(CTR)/2B(CTR)}$ in standard (12:12) light conditions: higher expression (red), lower expression (blue). FPKM of individual samples normalised to the average FPKM of all samples (>1 FPKM cut-off, p_adj<0.05). Ontology analysis of genes with higher expression **(B)** or lower expression **(C)** in GluN2A2B$^{(CTR)/2B(CTR)}$mice when compared to WT. Overlap genes highlighted in red represent genes with an overlap < 4 but which rank in the top ten ontology terms.

5.3 Activity-dependent regulation of gene expression is attenuated in the absence of CTD^{2A}.

I next addressed the role of CTD^{2A} in activity-dependent changes to the transcriptome. To establish the effect of dark rearing and subsequent 12Hr light re-exposure on gene expression in both genotypes, gene sets were generated from those genes identified as exhibiting significant differential expression for both light comparisons (Dark_vs_Light or 12Hr_vs_Dark) in each genotype ($p_{adj}<0.05$, FPKM>1).

In general, $GluN2A^{2B(CTR)/2B(CTR)}$ mice exhibited weaker regulation of gene expression in response to activity, with fewer genes being regulated in response to dark (WT: 543 genes, $GluN2A^{2B(CTR)/2B(CTR)}$: 314 genes). Notably, like the previous observations in RT-qPCR experiments performed in **Chapter 4**, IEG expression is not as robustly downregulated in dark reared $GluN2A^{2B(CTR)/2B(CTR)}$ mice when compared to WT mice (**Fig 5.2 B-C**). Re-exposure to light following dark rearing produced a much stronger regulation of gene expression when compared to the effect of going from standard light into the dark. However, while $GluN2A^{2B(CTR)/2B(CTR)}$ mice do show a more robust regulation of gene expression following re-exposure, the response is still smaller than that of WT (WT: 3790 genes, $GluN2A^{2B(CTR)/2B(CTR)}$: 1595 genes) (**Fig 5.2 D-E**).

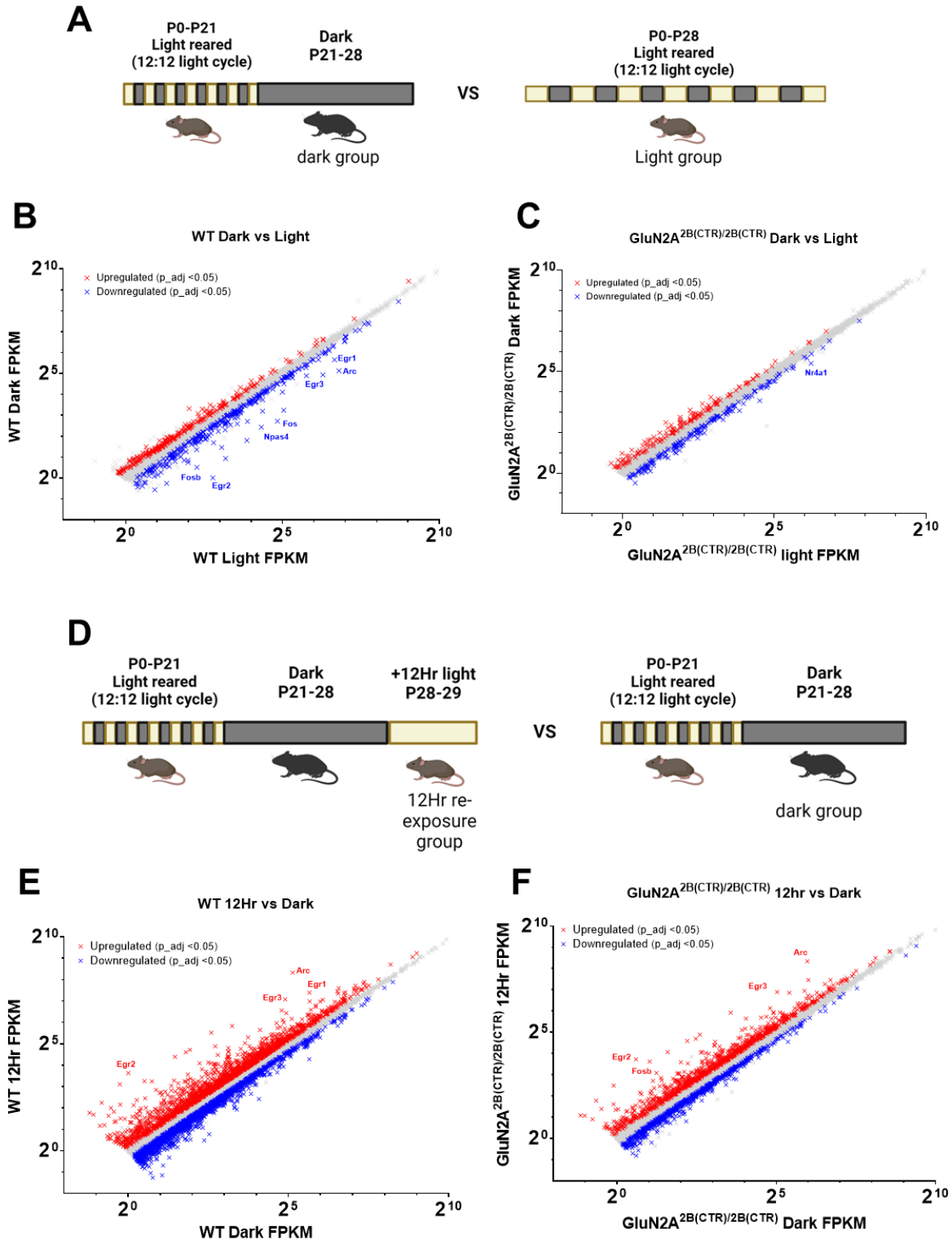

Figure 5.2 – Dark rearing and 12Hr re-exposure alter gene expression more robustly in WT mice compared to GluN2A$^{2B(CTR)/2B(CTR)}$

A) Diagrammatic representation of dark_vs_light comparison condition. Dark mice are reared in standard light until P21 and then dark reared from P21-P28, light mice remain in standard (12:12) light

until P28. RNAseq analysis performed in WT **(B)** and GluN2A$^{2B(CTR)/2B(CTR)}$ **(C)** following dark rearing for 7 days. Genes significantly upregulated (red) and downregulated (blue) are highlighted (expression cut-off >1FPKM, p values are adjusted for multiple testing by the Benjamini–Hochberg procedure to give a false discovery rate of 5% (p_adj < 0.05)). **D)** Diagrammatic representation of dark_vs_12Hr comparison condition. RNAseq analysis performed in WT **(E)** and GluN2A$^{2B(CTR)/2B(CTR)}$ **(F)** following dark rearing for 7 days with subsequent re-exposure to light for 12Hrs. Genes significantly upregulated (red) and downregulated (blue) are highlighted (expression cut-off 1FPKM, p values are adjusted for multiple testing by the Benjamini–Hochberg procedure to give a false discovery rate of 5% (p_adj < 0.05)). WT light n=6, dark n=5, 12Hr n=4; GluN2A$^{2B(CTR)/2B(CTR)}$, light n=6, dark n=6, 12Hr n=4.

5.4 Differential regulation of activity-dependent pathways

Having shown that activity-dependent changes in the transcriptome are attenuated in GluN2A$^{2B(CTR)/2B(CTR)}$ mice, I next set out to identify the biological processes involved. To address this, genes were analysed for significant genotype interactions in response to the two light comparisons. This yielded a set of genes that showed a genotype effect in response to dark vs light (495 genes) and 12Hr vs dark (878 genes) (genotype_interaction; p_adj<0.05) (**Table S2-3**). These sets were then further broken down into 3 subsets based on the light condition effect being: significant only in WT, only in GluN2A$^{2B(CTR)/2B(CTR)}$, or both (**Fig 5.3A, 5.4A**). For both light comparisons, the majority of genes that exhibited a genotype interaction fell into the subset of being exclusively regulated in WT (dark vs light: 371; 12Hr vs dark: 544), with relatively fewer being regulated only in GluN2A$^{2B(CTR)/2B(CTR)}$ (dark vs light: 91; 12Hr vs dark: 39) or regulated by both (dark vs light: 32; 12Hr vs dark: 297). This indicates that genotype differences are predominantly driven by stronger regulation of gene expression in WT, suggesting that the differences observed are more likely due to an attenuation of activity dependent changes rather than a qualitative difference in the response of GluN2A$^{2B(CTR)/2B(CTR)}$ mice.

To determine the biological role of these genotype differences, I performed ontology analysis of those genes that showed a genotype difference driven by WT (**Fig5.3B,**

5.4B). For genes that were downregulated in the dark (**Fig5.3C**), GO Biological Processes were dominated by those associated with regulation of excitatory post synaptic signalling, including the insertion of receptors and synaptic vesicle docking. GO Molecular Functions were dominated by those involved in vesicle docking, regulation of mRNA translation/stability and MAPK signalling. GO Cellular Components included the postsynaptic membrane and glutamatergic synapses. For those genes that were upregulated by dark (**Fig5.3D**), relatively few GO Biological Processes were identified, however, there was an association with remodelling of the cytoskeleton and protein binding. GO Molecular Functions also exhibited poor overlap, however, there was an association with axon guidance and TAP1/2 binding. GO Cellular Components included those of the plasma membrane and receptor complexes.

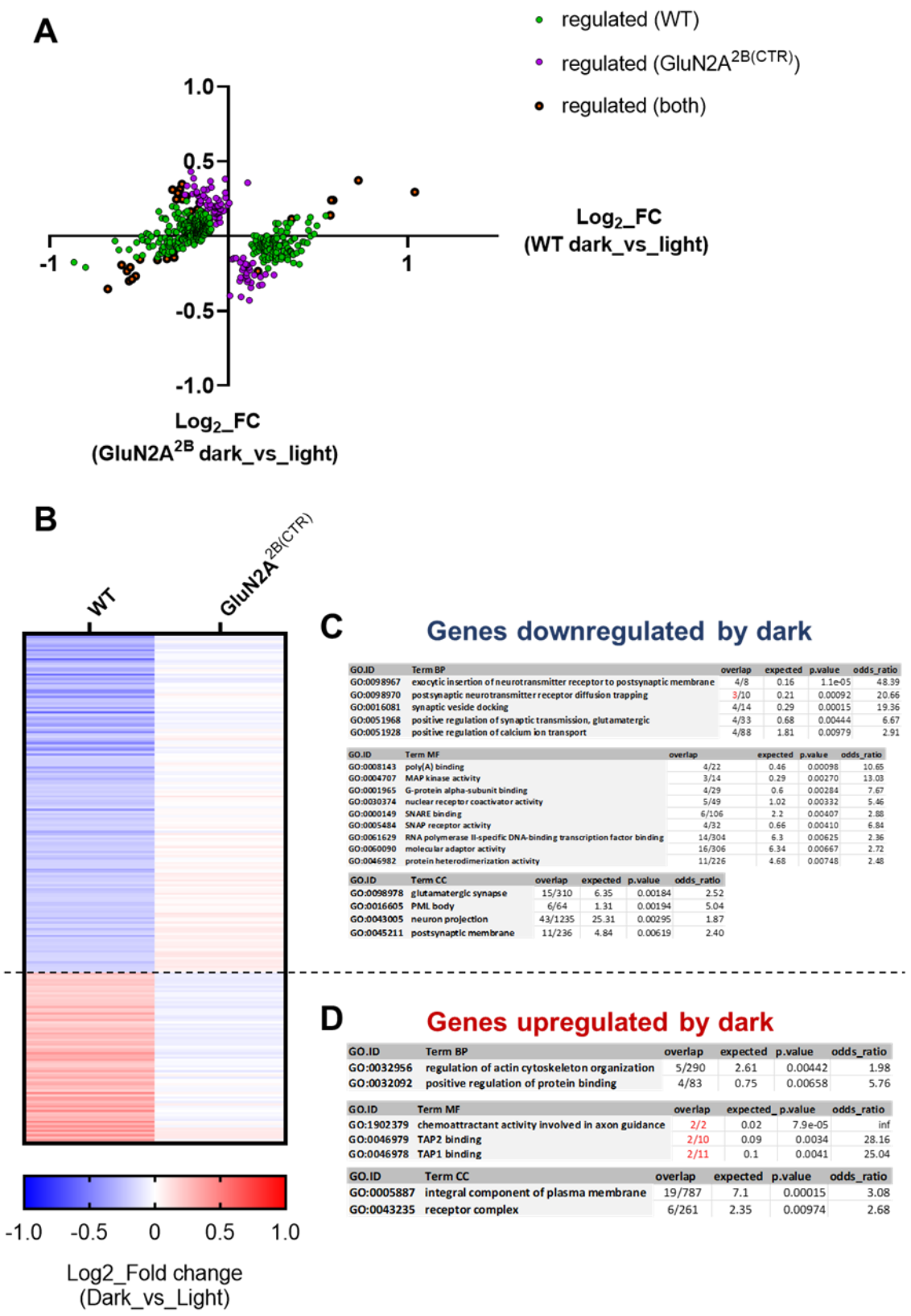

Figure 5.3 - Genotype differences in response to 7-day dark rearing are driven by greater magnitude of change in WT mice.

A) The Log2 fold change for genes in which genotype interaction is significant for dark_vs_light comparison is shown for both genotypes (y-axis: GluN2A$^{2B(CTR)/2B(CTR)}$; x-axis: WT). Genes significantly (p_adj < 0.05) regulated in WT (green), GluN2A$^{2B(CTR)/2B(CTR)}$(purple), or both genotypes (orange). **B)** Heat map of genes downregulated (blue) and upregulated (red) in WT mice dark reared for 7 days, which also exhibit a significant genotype interaction. Ontology analysis of genes downregulated **(C)** or upregulated **(D)** by dark rearing**.** Overlap genes highlighted in red represent genes with an overlap < 4 but which rank in the top ten ontology terms.

For genes that were upregulated by 12Hr re-exposure, GO Biological Processes were dominated by genes associated with regulation of synaptic signalling, including the negative regulation of receptor internalization and intracellular signalling cascades. GO Molecular Functions were dominated by tyrosine kinases and phosphatases, GTPase activity, and glutamate transporter activity. GO Cellular Components included the postsynaptic membranes and dendritic components (**Fig 5.4C**). For those genes that were downregulated by re-exposure, GO Biological Processes and GO Molecular Functions showed a weak enrichment for glycinergic signalling while GO Cellular Components also included glycinergic synapses (**Fig 5.4D**).

Taken together, these analyses suggest that GluN2A$^{2B(CTR)/2B(CTR)}$ might have a reduced ability to regulate excitatory signalling in response to changing levels of activity. Possibly due to an impaired ability to regulate insertion/removal of excitatory receptors from the post synapse and/or altered intracellular signalling pathways responsible for controlling protein synthesis.

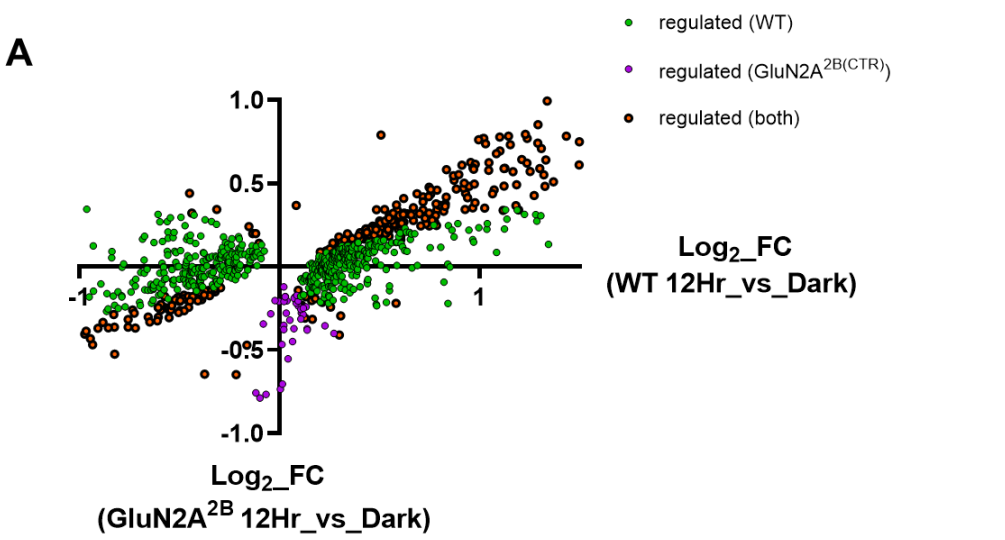

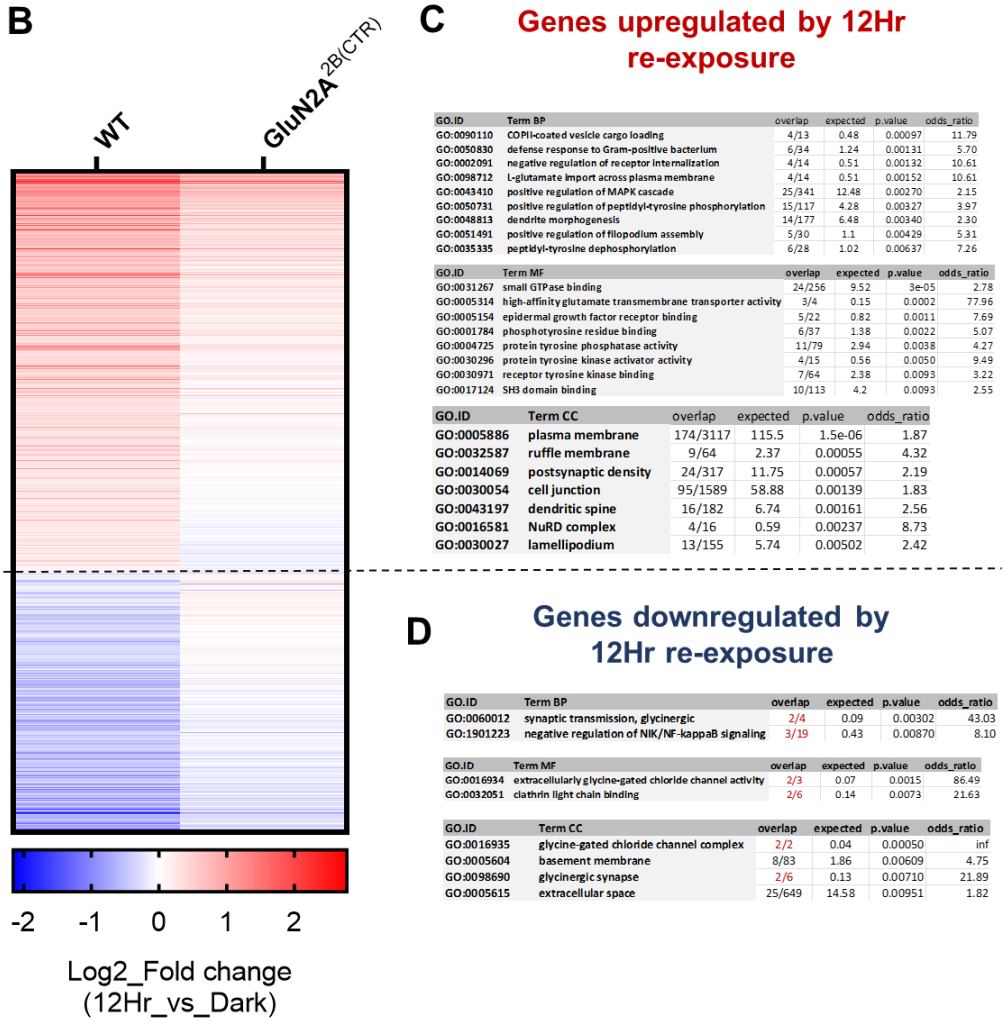

C

Genes upregulated by 12Hr re-exposure

GO.ID	Term BP	overlap	expected	p.value	odds_ratio
GO:0090110	COPII-coated vesicle cargo loading	4/13	0.48	0.00097	11.79
GO:0050830	defense response to Gram-positive bacterium	6/34	1.24	0.00131	5.70
GO:0002091	negative regulation of receptor internalization	4/14	0.51	0.00132	10.61
GO:0098712	L-glutamate import across plasma membrane	4/14	0.51	0.00152	10.61
GO:0043410	positive regulation of MAPK cascade	25/341	12.48	0.00270	2.15
GO:0050731	positive regulation of peptidyl-tyrosine phosphorylation	15/117	4.28	0.00327	3.97
GO:0048813	dendrite morphogenesis	14/177	6.48	0.00340	2.30
GO:0051491	positive regulation of filopodium assembly	5/30	1.1	0.00429	5.31
GO:0035335	peptidyl-tyrosine dephosphorylation	6/28	1.02	0.00637	7.26

GO.ID	Term MF	overlap	expected	p.value	odds_ratio
GO:0031267	small GTPase binding	24/256	9.52	3e-05	2.78
GO:0005314	high-affinity glutamate transmembrane transporter activity	3/4	0.15	0.0002	77.96
GO:0005154	epidermal growth factor receptor binding	5/22	0.82	0.0011	7.69
GO:0001784	phosphotyrosine residue binding	6/37	1.38	0.0022	5.07
GO:0004725	protein tyrosine phosphatase activity	11/79	2.94	0.0038	4.27
GO:0030296	protein tyrosine kinase activator activity	4/15	0.56	0.0050	9.49
GO:0030971	receptor tyrosine kinase binding	7/64	2.38	0.0093	3.22
GO:0017124	SH3 domain binding	10/113	4.2	0.0093	2.55

GO.ID	Term CC	overlap	expected	p.value	odds_ratio
GO:0005886	plasma membrane	174/3117	115.5	1.5e-06	1.87
GO:0032587	ruffle membrane	9/64	2.37	0.00055	4.32
GO:0014069	postsynaptic density	24/317	11.75	0.00057	2.19
GO:0030054	cell junction	95/1589	58.88	0.00139	1.83
GO:0043197	dendritic spine	16/182	6.74	0.00161	2.56
GO:0016581	NuRD complex	4/16	0.59	0.00237	8.73
GO:0030027	lamellipodium	13/155	5.74	0.00502	2.42

D

Genes downregulated by 12Hr re-exposure

GO.ID	Term BP	overlap	expected	p.value	odds_ratio
GO:0060012	synaptic transmission, glycinergic	2/4	0.09	0.00302	43.03
GO:1901223	negative regulation of NIK/NF-kappaB signaling	3/19	0.43	0.00870	8.10

GO.ID	Term MF	overlap	expected	p.value	odds_ratio
GO:0016934	extracellularly glycine-gated chloride channel activity	2/3	0.07	0.0015	86.49
GO:0032051	clathrin light chain binding	2/6	0.14	0.0073	21.63

GO.ID	Term CC	overlap	expected	p.value	odds_ratio
GO:0016935	glycine-gated chloride channel complex	2/2	0.04	0.00050	inf
GO:0005604	basement membrane	8/83	1.86	0.00609	4.75
GO:0098690	glycinergic synapse	2/6	0.13	0.00710	21.89
GO:0005615	extracellular space	25/649	14.58	0.00951	1.82

Figure 5.4 – Genotype differences in response to 12Hr re-exposure are driven by greater magnitude of change in WT mice.

A) The Log2 fold change for genes in which genotype interaction is significant for 12Hr_vs_dark comparison is shown for both genotypes (y-axis: GluN2A$^{2B(CTR)/2B(CTR)}$; x-axis: WT). Genes significantly ($p\_adj < 0.05$) regulated in WT (green), GluN2A$^{2B(CTR)/2B(CTR)}$(purple), or both genotypes (orange). **B)** heat map of genes downregulated (blue) and upregulated (red) in WT mice dark reared and re-exposed to light for 12Hr which exhibit a significant genotype interaction. Ontology analysis of genes upregulated **(C)** or downregulated **(D)** in WT mice following 12Hr re-exposure. Overlap genes highlighted in red represent genes with an overlap < 4 but which rank in the top ten ontology terms

5.5 GluN2A$^{2B(CTR)/2B(CTR)}$ mice exhibit a reduced dynamic range in response to activity.

Throughout the analyses of the transcriptome of GluN2A$^{2B(CTR)/2B(CTR)}$, a pattern was beginning to emerge of weaker activity driven responses. To probe this further, I wanted to determine whether genes that showed differential expression between genotypes under each of the three light conditions were enriched for a particular pattern of activity. In order to achieve this, I assembled two gene sets: those genes that were induced by both standard light and upon 12Hr re-exposure in either genotype (Gene set A) (**Fig 5.5A**) and those which were repressed by both standard light and 12Hr re-exposure in either genotype (Gene set B) (**Fig 5.6A**). Using these gene sets, I investigated whether there was any correlation between the nature of differential expression observed in GluN2A$^{2B(CTR)/2B(CTR)}$ mice for a given light condition and the activity-dependent pattern of regulation for those differentially expressed genes (Gene lists are included in **Table S4 – S10**)

I found that for genes that exhibited both lower and higher expression in GluN2A$^{2B(CTR)/2B(CTR)}$ mice under standard light conditions were enriched for genes induced by light, Gene set A. However, the enrichment was 3-fold greater for those genes that show lower expression in GluN2A$^{2B(CTR)/2B(CTR)}$ mice when compared to those which showed higher expression (**Fig5.5B**). In the dark condition, there was a strong enrichment for Gene set A in those genes that were more highly expressed in GluN2A$^{2B(CTR)/2B(CTR)}$(**Fig5.5C**). In the re-exposure condition, genes with lower expression in GluN2A$^{2B(CTR)/2B(CTR)}$ showed an enrichment for genes found in Gene set A (**Fig5.5D**). Taken together, this demonstrates a link between the pattern of

activity and the nature of differential expression between genotypes whereby, in GluN2A$^{2B(CTR)/2B(CTR)}$ mice, lower expression is more likely to be found in conditions where activity is positively regulated and higher expression in conditions where activity is negatively regulated.

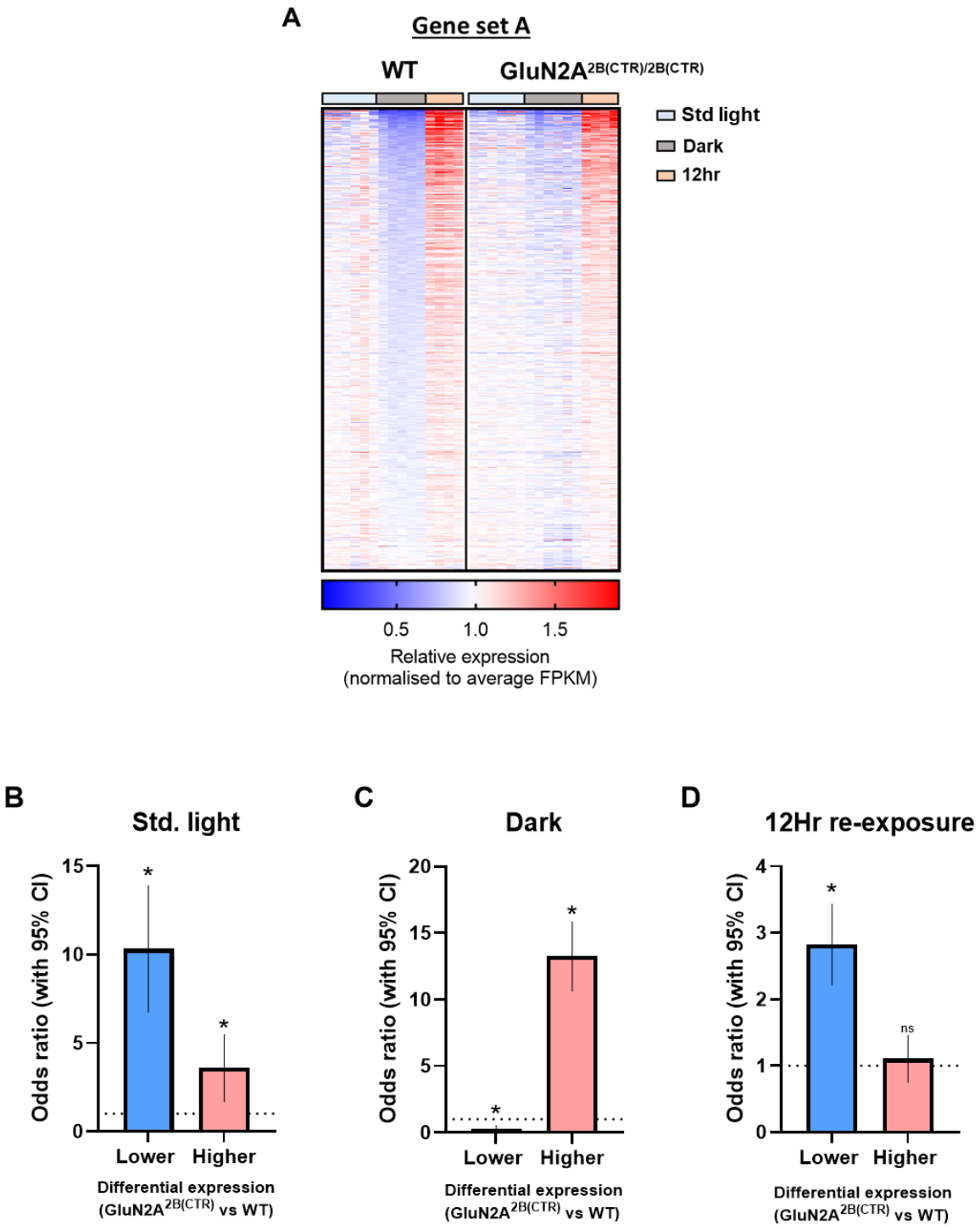

Figure 5.5 - Genes that are positively regulated by light have a reduced dynamic range in GluN2A$^{2B(CTR)/2B(CTR)}$ mice.

A) Heatmap of genes that are positively regulated by both standard light and 12Hr re-exposure (942), FPKM of individual samples normalised to the average FPKM of all samples (>1 FPKM cut-off).

B) Genes that exhibit lower and higher expression in GluN2A$^{2B(CTR)/2B(CTR)}$ under standard light conditions are enriched for gene set A (two-sided Fisher's exact test, lower: p<0.0001, odds ratio = 9.913; higher: p=0.0002, odds ratio = 3.239)

C) Genes that exhibit higher expression in GluN2A$^{2B(CTR)/2B(CTR)}$ in the dark are enriched for gene set A (two-sided Fisher's exact test, lower: p=0.0002, odds ratio = 0.2420; higher: p<0.0001, odds ratio = 13.09)

D) Genes that exhibit lower expression in GluN2A$^{2B(CTR)/2B(CTR)}$ following 12Hr light re-exposure enriched for gene set A (two-sided Fisher's exact test, lower: p<0.0001, odds ratio = 2.782; higher: p=0.6670, odds ratio = 1.076)

I next examined Gene set B; genes repressed by light. Based on the observations made in Gene set A, I anticipated to observe the opposite pattern of differential expression between genotypes in response to activity. Indeed, genes that were more highly expressed in GluN2A$^{2B(CTR)/2B(CTR)}$ mice under standard light conditions were enriched for Gene set B (**Fig 5.6B**), as were genes that exhibited lower expression in darkness (**Fig 5.6C**). As might be expected, genes that exhibited higher expression in GluN2A$^{2B(CTR)/2B(CTR)}$ following 12Hr re-exposure were also enriched for Gene set B (**Fig 5.6D**). This again demonstrates a link between activity and the nature of differential expression between genotypes. Simply, GluN2A$^{2B(CTR)/2B(CTR)}$ mice exhibit higher expression of activity repressed genes in light and lower expression in dark conditions, suggesting attenuated repression and induction respectively.

Overall, this presents a scenario in the GluN2A$^{2B(CTR)/2B(CTR)}$ mice where genes that are induced by activity are less so, and genes that are negatively regulated by activity are less repressed. As a result, GluN2A$^{2B(CTR)/2B(CTR)}$ mice possess a reduced dynamic range in response to activity. Therefore, this would suggest a crucial role for the CTD^{2A} in the regulation of this dynamic range.

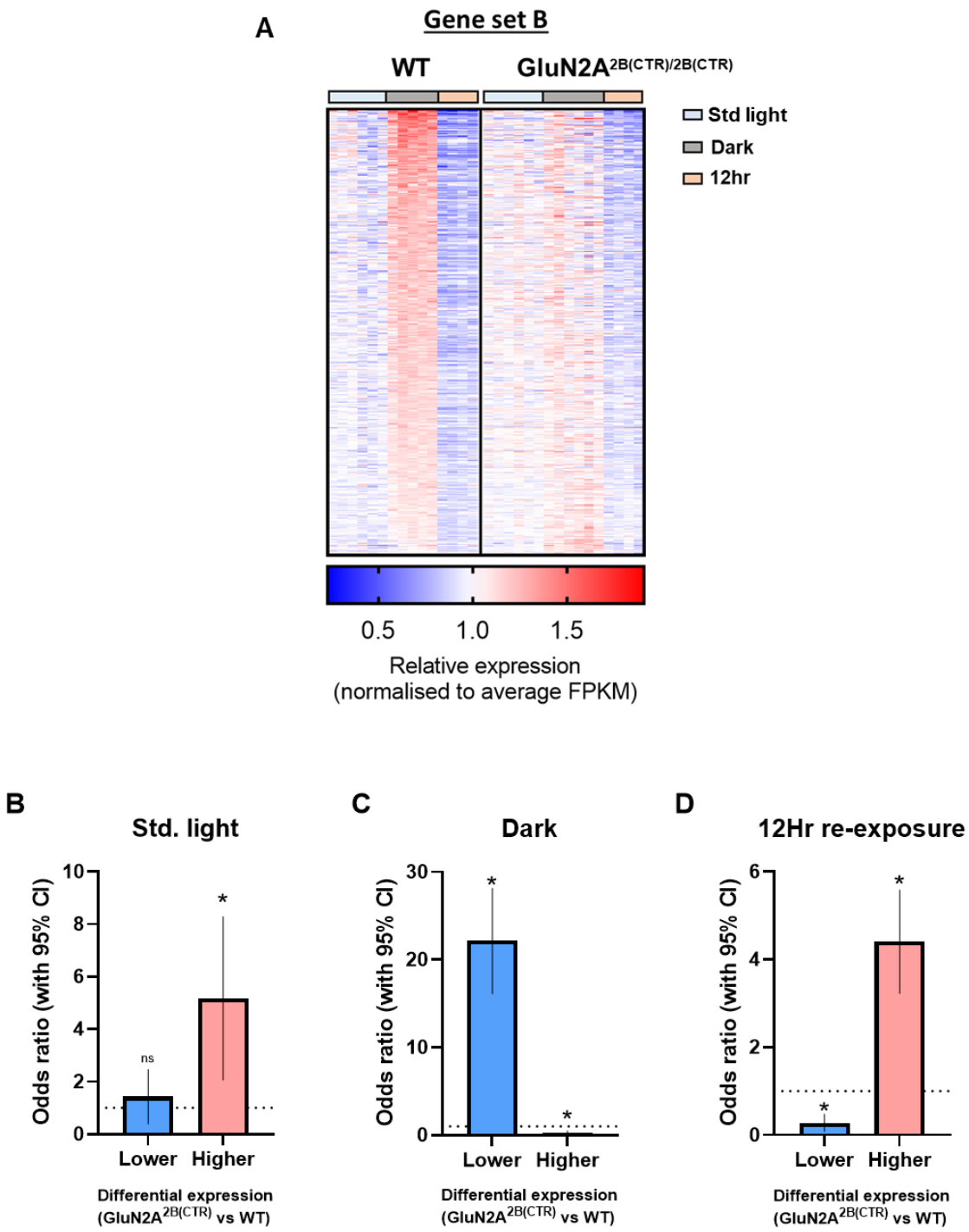

Figure 5.6 - Genes that are negatively regulated by light have a reduced dynamic range in GluN2A$^{2B(CTR)/2B(CTR)}$ mice.

A) Heatmap of genes that are positively regulated by both standard light and 12Hr re-exposure (942), FPKM of individual samples normalised to the average FPKM of all samples (>1 FPKM cut-off).

B) Genes that exhibit higher expression in GluN2A$^{2B(CTR)/2B(CTR)}$ under standard light conditions are enriched for gene set B(two-sided Fisher's exact test, lower: p = 0.6507, odds ratio = 1.163; higher: p<0.0001, odds ratio = 4.588)

C) Genes that exhibit lower expression in GluN2A$^{2B(CTR)/2B(CTR)}$ in the dark are enriched for gene set B (two-sided Fisher's exact test, lower: p<0.0001, odds ratio = 21.58; higher: p=0.0002, odds ratio = 0.2088)

D) Genes that exhibit higher expression in GluN2A$^{2B(CTR)/2B(CTR)}$ following 12Hr light re-exposure are enriched for gene set B (two-sided Fisher's exact test, lower: p<0.0001, odds ratio = 0.2262; higher: p<0.0001, odds ratio = 4.308)

5.6 Discussion

5.6.1 Summary

It can be concluded that CTD^{2A} plays an important role in the activity driven changes of the transcriptome. This is evidenced in **section 5.3** where it was demonstrated that GluN2A$^{2B(CTR)/2B(CTR)}$ exhibit reduced activity-dependent gene regulation as a whole and in **section 5.4** where it was demonstrated that genotype interaction differences in response to activity are predominantly driven by the magnitude of change in WT relative to GluN2A$^{2B(CTR)/2B(CTR)}$. Finally, enrichment analysis in **section 5.5** reveals that there is an association between the activity-dependent regulation of genes and their pattern of differential expression in GluN2A$^{2B(CTR)/2B(CTR)}$ mice that points towards weaker regulation. Taken together, this suggests that GluN2A$^{2B(CTR)/2B(CTR)}$ mice have a reduced dynamic range in response to activity. The proposed model of the dynamic range for both genotypes is summarised in **Figure 5.7**.

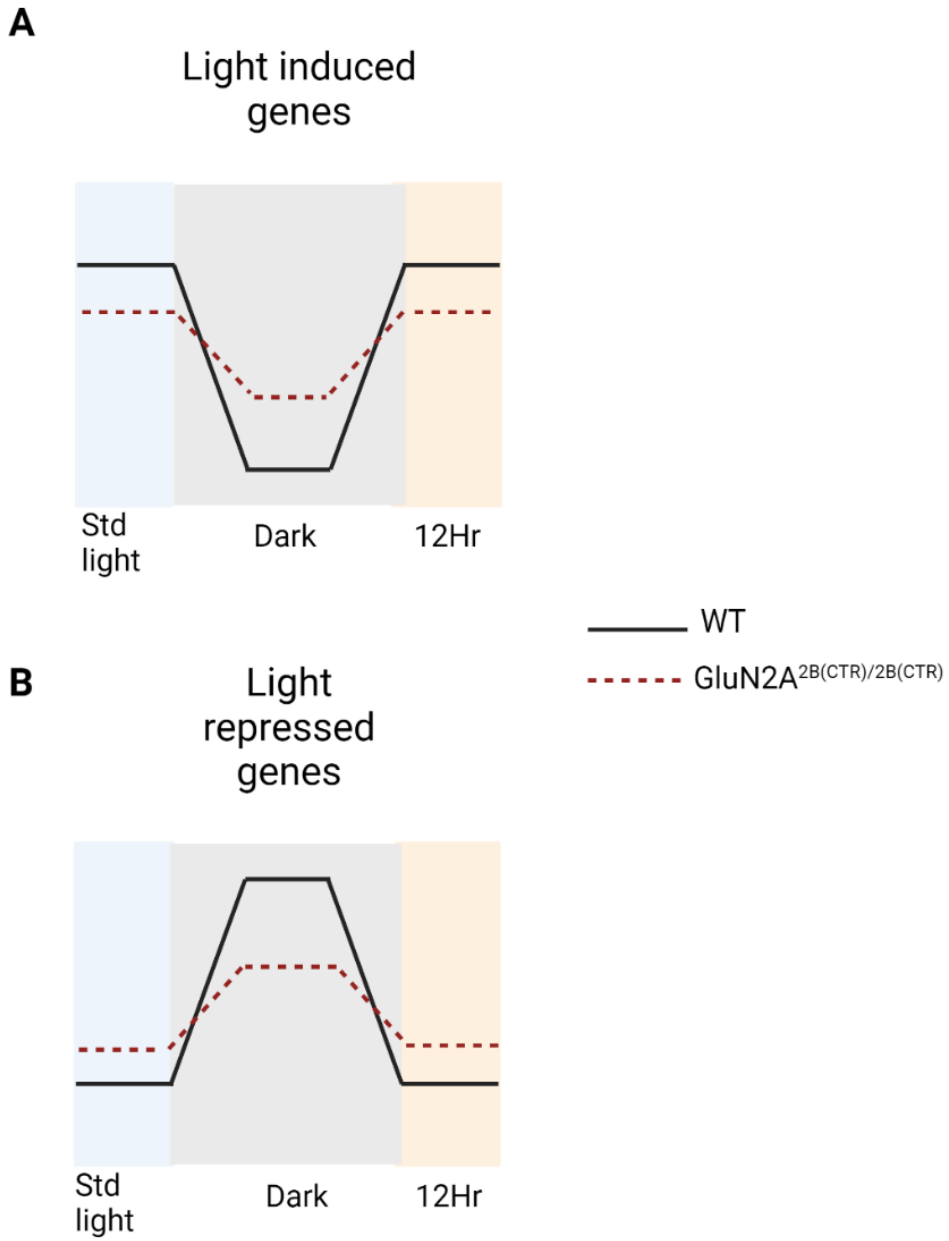

Figure 5.7 – Diagrammatic representation of the dynamic range of WT and GluN2A$^{2B(CTR)/2B(CTR)}$ mice.

A) Gene that are induced by light exhibit weaker induction in GluN2A$^{2B(CTR)/2B(CTR)}$ mice in standard light and following 12Hr re-exposure and reduced repression following 7-day dark rearing.

B) Gene that are repressed by light exhibit weaker repression in GluN2A$^{2B(CTR)/2B(CTR)}$ mice in standard light and following 12Hr re-exposure and reduced induction following 7-day dark rearing.

5.6.2 Role of CTD^{2A} in development

GO analysis of genes differentially expressed between WT and $GluN2A^{2B(CTR)/2B(CTR)}$ under normal light conditions revealed terms associated with neurodevelopmental processes. Specifically, genes that exhibited lower expression in the $GluN2A^{2B(CTR)/2B(CTR)}$ mice were associated with synapse assembly, axonal guidance, and cytoskeletal organisation. Interestingly, it has been shown that the CTDs of GluN2 subunits directly bind cytoskeletal proteins such as α-actinin (Sheng and Pak, 2000). Therefore, differential recruitment of cytoskeletal components may influence axon outgrowth and synaptogenesis. As such, $GluN2A^{2B(CTR)/2B(CTR)}$ mice may exhibit morphological differences. Based on this, it would be of great interest to carry out morphological analyses of axons and dendrites in the $GluN2A^{2B(CTR)/2B(CTR)}$.

5.6.3 Role of CTD^{2A} in sensory-dependent regulation of genes associated with post synaptic proteome.

While it is clear that the CTD^{2A} plays a role in the activity-dependent regulation of transcription, the precise mechanisms underpinning this are not yet clear. In **chapter 4** it was observed that $GluN2A^{2B(CTR)/2B(CTR)}$ show reduced proteomic changes in response to activity, as reflected in both the GluN2A:GluN2B ratio and other postsynaptic proteins. This is also indicated in the GO analysis of genes which show greater activity-dependent regulation in WT mice. For instance, in response to dark, WT mice exhibit a greater downregulation of genes associated with the insertion of neurotransmitter receptors whereas in in response to 12Hr re-exposure, there is a greater upregulation of genes associated with the negative regulation of receptor internalisation. Therefore, CTD^{2A}-dependent intracellular signalling cascades may regulate transcription in order to facilitate changes to the postsynaptic proteome that regulate excitatory signalling.

5.6.4 Role of CTD identity in mediating activity-dependent intracellular signalling cascades.

GO analysis also reveals difference in GTPase binding activity and MAPK signalling between the genotypes in response to activity. Both CTD^{2A} and CTD^{2B} are known to bind small GTPases as well as GTPase-activating protein and guanine nucleotide exchange factor, all of which are involved in mediating GTPase activity (Warnet et al, 2020). Therefore, the CTD serves as a scaffold that brings together key regulatory components of GTPase activity. As such GTPase activity depends on the binding occupancy of the CTD. Differential binding of protein complexes between the CTD^{2A} and CTD^{2B} may therefore determine their efficiency in mediating GTPase activity. One such example of this GTPase activity is the activation of Ras by Ras protein-specific guanine nucleotide-releasing factor (RasGRF1). Upon neuronal activity, RasGRF1 activates Ras which then goes on to activate MAPK/ERK1/2 pathway which in turn regulates the activation of transcription. Therefore, the CTD identity may influence activation of MAPK/ERK1/2 signalling and downstream activity-dependent gene transcription. Additionally, there is some evidence to suggest that GluN2B has an inhibitory effect on Ras-ERK signalling through preferential coupling of the RasGAP SynGAP to the CTD^{2B} (Kim et al, 2005). Therefore, differential recruitment of proteins at the CTDs could also influence downstream signalling in response to activity/experience. Interestingly, previous work done in primary neuronal cultures from $GluN2B^{2A(CTR)/2A(CTR)}$ KI mice found that activity-dependent signalling to ERK1/2 did not require CTD^{2B} specific sequences (McKay et al, 2018), however the role of CTD^{2A} has not yet been tested. Therefore, it would be of interest to investigate ERK1/2 phosphorylation in the $GluN2A^{2B(CTR)/2B(CTR)}$ mice following dark rearing.

Alternatively, the attenuated activity-dependent changes to gene expression may not be mediated by CTD dependent signalling, but rather by impaired changes to NMDAR composition at the synapse. For instance, in **chapter 4** it was observed that dark reared WT mice exhibit reduced GluN2A,GluN2B and GluN1 whereas $GluN2A^{2B(CTR)/2B(CTR)}$ mice do not. Therefore, the weaker changes to activity-dependent gene expression may be explained by differences in NMDAR-dependent Ca^{2+} signalling. As such, CTD^{2A} may influence activity-dependent transcription by either directly mediating

downstream signalling cascades and/or indirectly by influencing NMDAR expression at the synapse (**Fig 6.8**)

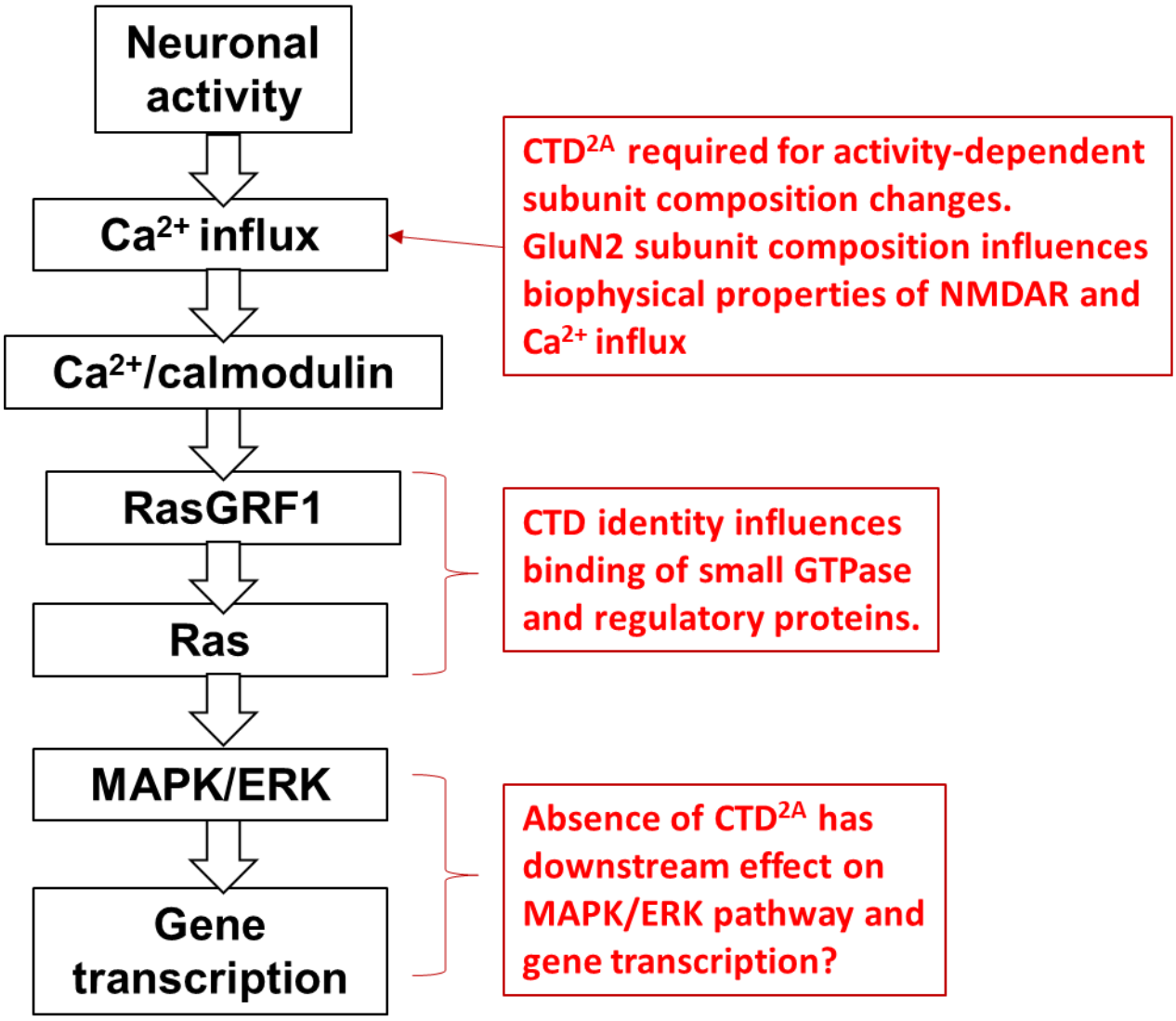

Figure 6.8 – Summary diagram depicting points at which CTD identity may influence MAPK signalling and downstream gene transcription.

5.6.5 Experimental approaches to answer new questions.

The current experiments have raised many new questions. Firstly, what is the role of the CTD^{2A} in regulating the dynamic range in response to activity? Does the reduced dynamic range in $GluN2A^{2B(CTR)/2B(CTR)}$ mice stem from a loss of key CTD^{2A} mediated signalling pathways or is it the result of the over expression of the CTD^{2B}? One approach to address the question of the role of CTD^{2A} would be perform mass spectroscopy on immunoprecipitated complexes of CTD^{2A}. This may provide answers as to protein interactions of CTD^{2A} under both light and dark conditions and may give some clue as to underlying signalling pathways. In addition, this method could also be applied to examine CTD^{2B} protein interactions. The influence of CTD^{2B}-mediated supercomplex assembly on downstream signalling has not been widely investigated. These complexes can be made up of many different protein combinations, with different combinations likely recruiting different downstream signalling pathways. In addition, little is known about how activity, or lack thereof, influences supercomplex composition. Therefore, it would be of great interest to establish how sensory experience influence supercomplex composition within the VC.

At the electrophysiological level, it would be of interest to measure visually evoked potentials (VEPs) in the $GluN2A^{2B(CTR)/2B(CTR)}$ mouse. As transcriptomic data suggests a reduced dynamic range, it might be expected that normally reared $GluN2A^{2B(CTR)/2B(CTR)}$ mice would exhibit reduced VEPs when compared to WT under standard light, but higher VEPs following dark rearing.

Chapter 6

Discussion

6.1 Translational implications of NMDAR CTDs in the context of neurodevelopment

Divergent evolution of the CTD^{2A} and CTD^{2B} allows them to preferentially couple to different signalling cascades and therefore differentially influence the downstream consequences of NMDAR activation. Despite the recognition that CTD identity contributes to the functional diversity of NMDAR signalling, the influence of CTD^{2A} and CTD^{2B} on activity-dependent changes in NMDAR composition and neuronal gene expression is still poorly understood. The results presented in this thesis have begun to shed some light on this issue and suggest an important role for CTD^{2A} in this activity-dependent change. This is small step in addressing the broader question - how might CTD translation contribute to neurodevelopmental disorders?

6.1.1 GluN2A/2B CTD mutations associated with neurodevelopmental disorders.

Genome sequencing studies have identified over 200 neuropathology associated variants in GRIN genes, with a large proportion of these variants being found in *GRIN2A* and *GRIN2B* (**Fig 1.13**). As may be expected, most of these variants are found within the highly conserved amino binding domain (ABD) and TMD, however, ~20% of these variants occur within the CTD (reviewed by (Ishchenko et al, 2021). Mutations are being discovered at a faster rate than the labour-intensive functional characterisation of these CTD variants, but some variants associated with autism spectrum disorder (ASD), intellectual disability (ID) and epilepsy have been studied in detail.

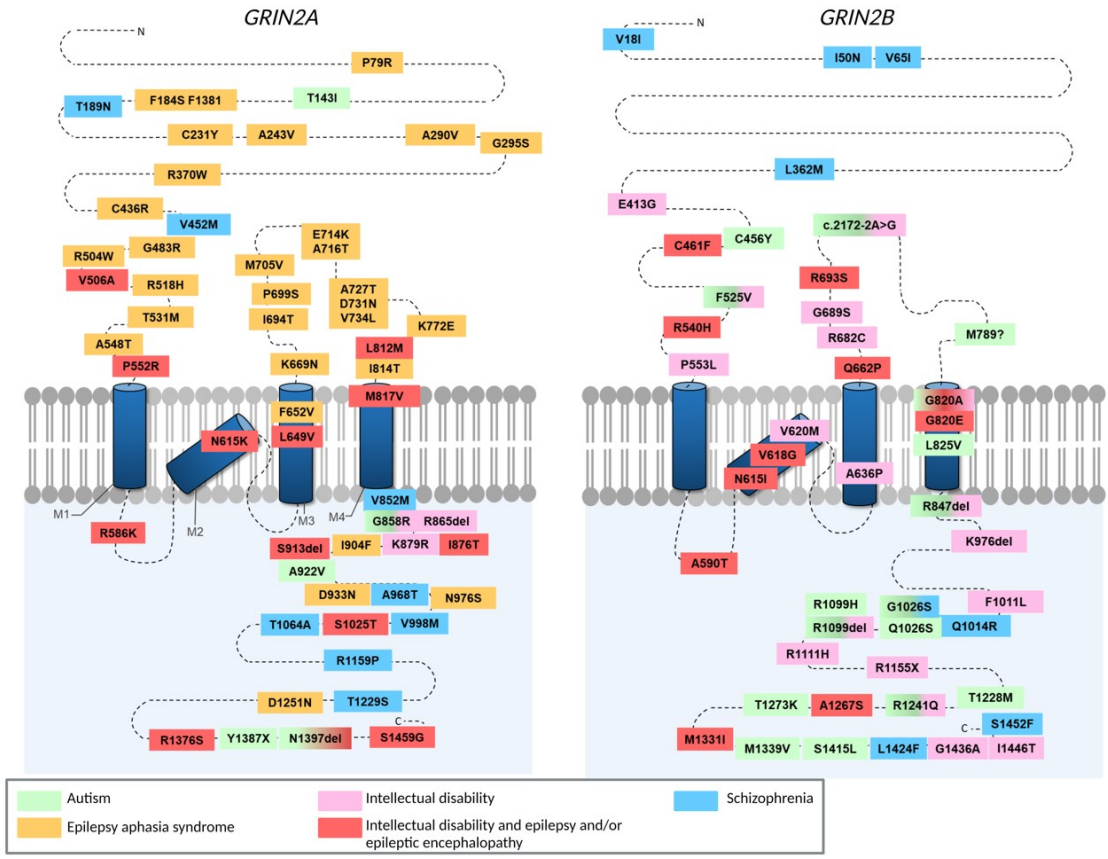

Figure 1.13 - Schematic showing the locations of heterozygous missense, nonsense and frameshift mutations in GRIN2A (glutamate receptor ionotropic NMDA 2A) and in GRIN2B (NMDA 2B) that have been identified in people with neurodevelopmental disorders.

The extreme extracellular amino terminus of these subunits contains allosteric modulation sites. The region between the N terminus and the M1 domain, plus the extracellular loop between the M3 and M4 domains, encode the glutamate-binding domain. The M2 domain features many side chains that point towards the receptor channel pore and dictate ion permeability. Finally, the long cytoplasmic carboxy-terminal domain is involved in receptor targeting and coupling to downstream signalling complexes. Figure based on refs (Bramswig et al, 2015; Chen et al, 2017; Dimassi et al, 2014; Endele et al, 2010; Firth et al, 2009; Freunscht et al, 2013; Grozeva et al, 2015; Lal et al, 2015; Lemke et al, 2014; Lemke et al, 2013; Lesca et al, 2013; Li et al, 2022; Liu et al, 2017; Mota Vieira et al, 2020; Myers et al, 2011; O'Roak et al, 2012; Pan et al, 2015; Platzer et al, 2017; Rauch et al, 2012; Stessman et al, 2017; Takasaki et al, 2016; Tarabeux et al, 2011; Venkateswaran et al, 2014; von Stulpnagel et al, 2017; Williams et al, 2012). Reprinted from Haddow, Hardingham and Kind, 2022.

6.1.2 *GRIN2B* mutations

Liu et al, 2017 characterised an autism associated GluN2B mutant occurring in the CTD of GluN2B (S1415L human, S1413L rodent). Rat hippocampal neurons transfected with mutant GluN2B showed a 30% reduction in receptor surface expression compared to GluN2B WT. In addition, GluN2B S1413L-expressing neurons also showed a reduction in spine density. From this it would appear that the CTD^{2B} plays an important role in the trafficking of GluN2B to the synaptic membrane which when impaired may lead to a reduction of dendritic spines. In contrast, in **chapter 4** it was observed that the VC of P28 $GluN2A^{2B(CTR)/2B(CTR)}$ mice exhibits no difference in the synaptic level of either GluN2A or GluN2B when compared to WT mice. This agrees with what has been observed previously in whole brain (McKay et al., 2018). As such, it suggests a level of redundancy between CTD^{2A} and CTD^{2B} with regards to trafficking. However, the effect of swapping the CTD^{2B} for that of CTD^{2A} ($GluN2B^{2A(CTR)/2A(CTR)}$) on the developmental subunit shift has not yet been investigated. Future experiments using this model would be beneficial to shed light on whether appropriate trafficking of GluN2B depends on CTD identity or simply the presence of an intact CTD.

For CTD^{2B} mutations in which trafficking deficits and morphological changes are observed, there is some question as to whether differences in morphology occur as a result of the loss of intracellular signalling linked to the CTD^{2B} or whether these changes are simply a consequence of altered NMDAR levels at the synapse. Using independently generated chimeric KI mice, Keith et al, 2019 found that replacing CTD^{2A} for CTD^{2B} in GluN2A resulted in longer total dendritic path, average apical length, and total basal length relative to WT mice. Additionally, they observed no differences in dendritic morphology when only CTD^{2A} was expressed. Lastly, replacing the ABD or TMD of GluN2A for that of GluN2B had no effect on morphology, thereby suggesting CTD^{2B} dependent signalling as the crucial factor in mediating the morphological differences observed. Interestingly, when looking at the transcriptomic data presented in **chapter 5**, there is an association between genes that are differentially expressed between normally reared WT and $GluN2A^{2B(CTR)/2B(CTR)}$

mice and GO terms related to cytoskeletal organisation, actin bundle assembly, axon guidance and synapse assembly. Taken together, these results tentatively support a role for CTD^{2B}-specific intracellular signalling pathways in the regulation of neuronal morphology during development. Therefore, this raises the possibility that deficits in CTD^{2B} signalling may contribute to altered development in ASD/ID. Further studies probing the role of the novel CTD^{2B} variants on dendritic complexity and spine morphology will help to shed light on the role of CTD^{2B} signalling in ASD/ID during neurodevelopment.

6.1.3 *GRIN2A* mutations

Mutations in *GRIN2A* are commonly associated with developmental delay and epileptic phenotypes (Addis et al, 2017; Lemke et al, 2013). While these mutations predominantly occur in the ABD or TMD resulting in functional changes to the subunits, a number of epilepsy-associated variants have also been identified within the CTD^{2A} (Lemke et al, 2013; Lesca et al, 2013; Mota Vieira et al, 2020). In addition to the NMDAR mediated Ca^{2+} influx that is required for the induction of plasticity, there is also some evidence to suggest that GluN2 CTD identity influences synaptic plasticity induced by different patterns of activity (Ryan et al, 2013). Therefore, mutations that either affect trafficking of the GluN2A subunit or that alter key interaction sites have the potential to impair synaptic plasticity. However, seemingly counterintuitively, mutations in the CTD^{2A} that enhance trafficking also negatively impact plasticity. Li et al, 2022 recently characterised a rare ID associated variant in the GluN2A subunit. The mutation, K879R, was found to occur within an endoplasmic retention signal motif and resulted in enhanced cell surface expression. The increased expression of GluN2A led to deficits in synaptic transmission both in GluN2A_K879R mouse hippocampal CA1 neurons and in K879R KI mice. Additionally, KI mice exhibited impairments in the induction of LTP and LTD as well as deficits in learning and memory.

6.1.4 Influence of *GRIN2A* and *GRIN2B* mutations in Seizures.

As mentioned previously, dynamic control of the GluN2A:GluN2B ratio has been proposed as one of the mechanisms by which neuronal activity is kept within a functional range in response to changing levels of activity. Considering the suggested role for NMDAR subunit composition in homeostatic regulation of activity, it could be suggested that mutations in GRIN2A promote epileptic phenotypes through either a reduction or loss of function of the GluN2A subunit itself, e.g., caused by mutations that affect agonist binding and channel properties, or through a reduction in subunit expression at the synapse. The result of any of these mutations would lead to a reduction in GluN2A activity, thereby leading to an impaired homeostatic ability of circuits and the facilitation of hyper-excitability. As shown in **chapter 3**, GluN2A would appear to be more dynamically regulated by activity when compared to GluN2B. Furthermore, in **chapter 4** it was demonstrated that activity-dependent changes in GluN2A do not occur in the absence of the CTD^{2A}. The mechanism that underpins the importance of CTD^{2A} in this process remains to be elucidated, but it would be reasonable to suggest that mutations that impair this activity-dependent regulation may result in epileptic phenotypes. Indeed, the epilepsy- associated variant GluN2A-S1459G has exhibited activity-dependent trafficking deficits (Mota Vieira et al, 2020

However, it should also be noted that a loss of excitatory drive from inhibitory interneurons and subsequent disinhibition as a result of a loss of GluN2A function may also contribute to hyper-excitability. Indeed, it was recently shown that enhancing GluN2A activity in both excitatory and inhibitory interneurons with the use of the positive allosteric modulator (PAM) GNE-0723 reduced epileptiform activity in mouse models of Alzheimer's disease and Dravet syndrome (Hanson et al, 2020). Overall, it appears that the GluN2A:GluN2B ratio is important in mediating seizure susceptibility. Specifically, a decrease in this ratio favours increased seizure susceptibility. In the hippocampus both a decrease in GluN2A expression (Acutain et al, 2021) and upregulation of GluN2B (Gorlewicz et al, 2022) have been implicated in contributing to seizure pathogenesis. In addition, selective blockade of GluN2B has

been shown to reduce seizure susceptibility (Chen et al, 2016; Mares et al, 2021) and dextromethorphan induced convulsive behaviours (Tran et al, 2017). However, it remains unclear whether the beneficial effect of modifying the relative activity of GluN2A/2B is solely the result of restoring homeostatic balance or whether subunit specific signalling pathways are also involved. Crucially, there is currently no evidence to suggest that CTD-dependent effects mediate the subunit-specific effect on seizure pathogenesis.

6.1.5 GRIN2A and GRIN2B mutation in Schizophrenia

Impaired NMDAR-mediated neurotransmission has been proposed as one of the contributing factors in schizophrenia (SZ) pathology, owing to the observation that psychomimetic compounds can transiently replicate SZ symptomology by blocking NMDAR neurotransmission (Javitt, 1987; Javitt & Zukin, 1991). Genetic evidence also points to a role for disrupted NMDAR signalling in SZ. For instance, GRIN2A has been implicated as a risk gene for SZ by a recent genome wide association study (Schizophrenia Working Group of the Psychiatric Genomics, 2014). In addition, exome sequencing has revealed several de novo SZ associated mutation in both the GRIN2A and GRIN2B genes, several of which occur in the CTD (Myers et al, 2011; Tarabeux et al, 2011). However, it remains to be seen whether these de novo CTD mutations are causative in SZ. If they do indeed contribute to the pathogenesis of SZ, the question then becomes by what means? Do these mutants disrupt key CTD dependent signalling pathways or do they simply impair trafficking and therefore synaptic NMDAR content. Robust characterisation of these variants will be required to address these key questions.

6.1.6 Influence of GRIN2A and GRIN2B mutations on sensory processing.

ASD and Fragile X syndrome (FXS) are associated with impaired sensory integration (reviewed by Robertson and Baron-Cohen, 2017). Although the mechanism that underpin aberrant sensory processing in individuals with ASD and FXS are not yet fully understood, there is some preliminary evidence to suggest that NMDAR mediated metaplasticity may play an important role. For instance, it has been observed

that mouse models of FXS show a precocious potentiation of open eye responses following MD (Dölen et al, 2007). Considering that the regulation of NMDAR composition has been implicated in the metaplastic changes that occur following MD, it is possible that mouse models of FXS possess aberrant developmental or activity-dependent control of the GluN2A:GluN2B ratio.

6.1.7 Gaps in the knowledge: GluN2/GluN2B CTDs and their influence on allosteric modulation.

Overall, understanding the molecular consequences of GRIN2A and GRIN2B mutations may provide an opportunity for targeted therapeutic strategies. Indeed, several preclinical pharmacological studies have highlighted the potential for the use of both negative allosteric modulators (NAMs) and PAMs in treating gain of function and loss of function GRIN variants respectively (Benke et al, 2021; Epi, 2015; Han et al, 2022; Strehlow et al, 2022). This begs the question - if changes in the GluN2A:GluN2B ratio are an important contributor to homeostatic plasticity, how could allosteric modulators be used in cases where activity-dependent control of the ratio is dysregulated? Reasonably, you would first need to understand how the ratio changes in order to identify the best target. The results in this thesis favour a model in which ratio changes are predominantly driven by GluN2A, and as such careful and targeted modulation of GluN2A activity may be enough to help keep activity within a functional range. However, it is also important to consider that allosteric modulators may be influenced by intracellular factors such as the phosphorylation, ubiquitination and palmitoylation states of CTDs. This was highlighted in a recent study in which it was demonstrated that GluN2 deletions robustly altered the activity of both PAMs and NAMs, likewise, agents altering phosphorylation state and intracellular Ca^{2+} levels were also observed to produce receptor-specific and compound specific changes to PAM activity (Sapkota et al, 2019). Therefore, further studies investigating the metabotropic influence of CTDs on the activity of allosteric modulator will be a crucial step in paving the way to developing appropriate treatment strategies for aberrant NMDAR activity.

6.2 Experimental summary

The work presented in this thesis was conducted to investigate the hypothesis that CTD^{2A} is required for activity-dependent changes in NMDA subunit composition. In the course of addressing this hypothesis the following key findings were established:

- Contrary to the idea of a subunit "switch", changes to the synaptic level of GluN2B do not contribute to either the developmental or activity-dependent GluN2A:GluN2B ratio shift. Furthermore, GluN2B abundance in the VC cortex is much greater than that of GluN2A, suggesting that regulation of GluN2B would have a minimal effect on altering the overall ratio of subunits. In both cases, changes to the level of synaptic GluN2A are what drives the ratio shift.

- Genetically replacing the GluN2A CTD with that of GluN2B prevents experience-dependent changes in synaptic levels of GluN2A. Therefore, the CTD^{2A} plays a critical role in the mechanisms underpinning activity driven changes to the expression of GluN2A at the synapse.

- Replacing the CTD^{2A} with CTD^{2B} attenuates activity-dependent changes in the transcriptome, resulting in a reduced dynamic range.

6.2.1 Switch or shift – Nature of the GluN2A:GluN2B ratio change.

The data presented in **chapter 4** demonstrates that GluN2A containing NMDARs make up a relatively small proportion of the overall NMDAR population within the VC. This finding is in agreement with previous observations made in the whole forebrain (Frank et al, 2016) and argues against the prevailing theory that GluN2A replaces GluN2B as the most abundant subunit in the forebrain during development (Monyer et al, 1992; Sanz-Clemente, Nicoll and Roche, 2013). This casts doubt on an equal role for GluN2B insertion/removal as a key mechanism in mediating activity-dependent changes in the GluN2A:GluN2B ratio as the degree of change would need to be substantial. This is further supported by the observation that 7-day dark rearing mediates a decrease in the GluN2A:GluN2B ratio even when there is a significant loss of GluN2A and a smaller, yet significant loss of GluN2B. Therefore, this presents the regulation of GluN2A as the key determinant in experience-dependent changes to NMDAR subunit composition. However, the duration of dark rearing used in these experiments was longer than that of similar studies that did observe an upregulation of GluN2B. That being said, if the mechanism driving an increase in synaptic expression of GluN2B is driven by a loss of activity then presumably this mechanism would still be at play as long as activity is low, whether it be 5-days or 7-days of dark rearing. A more pressing concern with 7-day dark rearing is the possibility of synapse loss. The significant decrease in synaptic GluN2A, GluN2B, GluN1 and PSD95 could indicate this as a possible scenario. However, the relatively stable expression of the presynaptic marker synaptophysin coupled with the subsequent rebound of proteins following 24Hr re-exposure makes this scenario seem unlikely.

Given that the results presented above argue in favour of the regulation of synaptic GluN2A as the key driver in altering the GluN2A:GluN2B ratio, it is maybe not surprising that GluN2A$^{2B(CTR)/2B(CTR)}$ mice fail to exhibit dynamic changes in the GluN2A:GluN2B ratio. Overall, this would suggest a role for the CTD^{2A} in regulating synaptic GluN2A levels in response to deprivation/experience. The precise nature of this role remains to be ascertained; however, it is possible that the loss of critical CTD^{2A} required for removal/insertion of GluN2A and/or increased synaptic anchoring through the overexpression of CTD^{2B} accounts for the observations made in

GluN2A$^{2B(CTR)/2B(CTR)}$ mice (**Fig 6.1**). Future experiments will focus on assessing both possibilities.

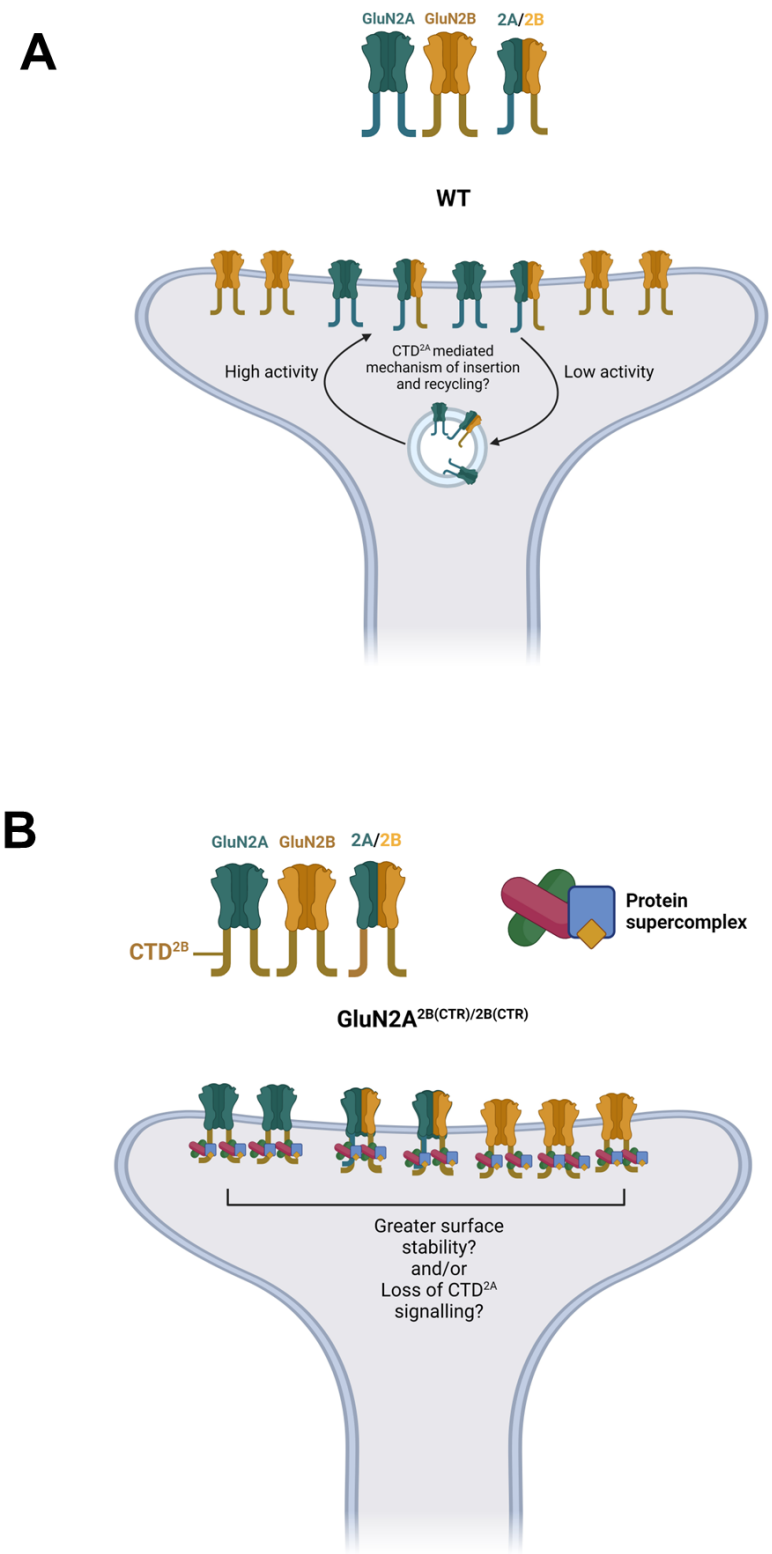

Figure 6.1 – Proposed mechanisms by which CTD identity influences sensory-dependent changes in GluN2A:GluN2B ratio.

A) In WT, 7-day dark rearing promotes a shift in the GluN2A:GluN2B ratio through the removal of GluN2A from diheteromeric receptors and triheteromeric receptors (also resulting in a moderate decrease of synaptic GluN2B) via CTD^{2A} -dependent mechanisms. Future work will be aimed at investigating sensory-dependent protein interactions at the CTD^{2A}.

B) In $GluN2A^{2B(CTR)/2B(CTR)}$, 7-day dark rearing fails to produce any change in the synaptic expression of either GluN2A or GluN2B. This could be due to the loss of, as yet unknown, CTD^{2A} mediated protein interactions and signalling and/or increased subunit stability at the synapse owing to greater recruitment of large supercomplexes. Future work to establish the influence of activity on supercomplex composition and their influence on downstream signalling will be required.

6.2.2 Activity-dependent transcription – How might CTD^{2A} influence gene expression?

The results presented in **Chapter 5** suggest that sensory experience-driven transcriptomic changes require the presence of the CTD^{2A}. Indeed, replacing the CTD^{2A} with that of CTD^{2B} was observed to attenuate transcriptional changes to many IEGs as well as genes involved with synaptic modification and intracellular signalling pathways. As discussed in **section 1.2.2,** CREB-mediated transcription is controlled by both a fast Ca^{2+}/calmodulin pathway and a slower MAPK pathway. Taken together, it is possible that the consequences of swapping the CTD^{2A} stem from the loss of key binding sites for signalling proteins and their regulatory proteins and/or impaired ability to modify NMDAR subunit composition and Ca^{2+} influx. Previous *in vitro* work conducted within our lab showed that synaptic activity produced a robust induction of IEGs in $GluN2A^{2B(CTR)/2B(CTR)}$ neurons that was indistinguishable from WT neurons. This suggests that the main determinant in IEG induction was the level of nuclear Ca^{2+} and not CTD^{2A} mediated signalling (McKay, unpublished observation). Naturally, dark rearing presents a more complex scenario where longer durations of low activity promote homeostatic changes to NMDAR composition. Therefore, it is possible that the weaker regulation of gene expression in $GluN2A^{2B(CTR)/2B(CTR)}$ mice is partly due to its inability to dynamically regulate

NMDAR subunit composition and, therefore, Ca^{2+} influx. That being said, our understanding of the role of CTD^{2A} signalling during sensory deprivation is lacking. Therefore, further experiments probing the CTD^{2A} interactions and signalling in response to 7-day dark rearing and light re-exposure will be required. In addition, it would also be of benefit to investigate sensory-dependent CTD^{2B}-supercomplex recruitment. For instance, does activity influence which proteins are recruited into the supercomplex? How does this effect downstream signalling and gene transcription?

6.2.3 Concluding remarks

It is hoped that the findings of the current study will set the groundwork for future experiments probing the role of the CTD^{2A} in mediating the downstream consequences of altering sensory experience. At the start of this thesis I outlined the following hypothesis: CTD^{2A} specific events are required for changes in NMDAR subunit composition at the synapse in response to sensory stimulation/deprivation. The results presented in this thesis do support a role for the CTD^{2A} in the mechanisms underpinning experience-dependent changes in NMDAR subunit composition. However, it must be noted that, while experience-dependent regulation of the GluN2A:GluN2B ratio does appear to be less dynamic in $GluN2A^{2B(CTR)/2B(CTR)}$ mice, the overall ratio is not significantly different between genotypes following dark rearing. This is likely due to the smaller concomitant decrease in GluN2B that occurs in WT following 7-day dark rearing. However, the fact that changes in both GluN2A and GluN2B are absent in $GluN2A^{2B(CTR)/2B(CTR)}$ mice suggests that the CTD^{2A} is driving a reduction in both subunits. As such, it is possible that GluN2B is being removed as part of GluN2A containing triheteromeric NMDARs. To investigate whether GluN2B is being lost from diheteromeric or triheteromeric NMDARs, it would be useful to take electrophysiological recordings from brain slices following application of Spermine. Spermine has been shown to only potentiate diheteromeric GluN2B receptors, therefore, it could be predicted that the level of spermine potentiation will be comparable between light and dark reared mice if GluN2B is being lost from triheteromeric receptors.

If GluN2B is subject to the same regulation as GluN2A via its incorporation into triheteromeric NMDARs, then this raises questions about the effectiveness of a GluN2A:GluN2B ratio mediated mechanism of shifting the modification threshold. This is especially true if triheteromeric receptors make up a large proportion of NMDARs in V1. The work conducted in this thesis focuses on the molecular mechanisms and as such cannot comment on whether metaplasticity is affected in the absence of the CTD^{2A}. This could be achieved by measuring field potentials in VC slices of mice following dark rearing. Based on the observations made at the protein level, it could be predicted that these mice will exhibit impaired deprivation-induced metaplasticity. Indeed, it has previously been shown that deprivation fails to produce metaplastic changes in GluN2A KO mice (Philpot, Cho and Bear, 2007). Similar observations in $GluN2A^{2B(CTR)/2B(CTR)}$ would confirm an important role for both GluN2A and its CTD in experience-dependent metaplasticity.

References

Acutain, M. F., Griebler Luft, J., Vazquez, C. A., Popik, B., Cercato, M. C., Epstein, A., Salvetti, A., Jerusalinsky, D. A., de Oliveira Alvares, L. & Baez, M. V. (2021) Reduced Expression of Hippocampal GluN2A-NMDAR Increases Seizure Susceptibility and Causes Deficits in Contextual Memory. Front Neurosci, 15, 644100.

Addis, L., Virdee, J. K., Vidler, L. R., Collier, D. A., Pal, D. K. & Ursu, D. (2017) Epilepsy-associated GRIN2A mutations reduce NMDA receptor trafficking and agonist potency - molecular profiling and functional rescue. Sci Rep, 7(1), 66.

Alsaad, H. A., DeKorver, N. W., Mao, Z., Dravid, S. M., Arikkath, J. & Monaghan, D. T. (2019) In the Telencephalon, GluN2C NMDA Receptor Subunit mRNA is Predominately Expressed in Glial Cells and GluN2D mRNA in Interneurons. Neurochem Res, 44(1), 61-77.

Amador, A., Bostick, C. D., Olson, H., Peters, J., Camp, C. R., Krizay, D., Chen, W., Han, W., Tang, W., Kanber, A., Kim, S., Teoh, J., Sah, M., Petri, S., Paek, H., Kim, A., Lutz, C. M., Yang, M., Myers, S. J., Bhattacharya, S., Yuan, H., Goldstein, D. B., Poduri, A., Boland, M. J., Traynelis, S. F. & Frankel, W. N. (2020) Modelling and treating GRIN2A developmental and epileptic encephalopathy in mice. Brain, 143(7), 2039-2057.

Andras, I. E., Deli, M. A., Veszelka, S., Hayashi, K., Hennig, B. & Toborek, M. (2007) The NMDA and AMPA/KA receptors are involved in glutamate-induced alterations of occludin expression and phosphorylation in brain endothelial cells. J Cereb Blood Flow Metab, 27(8), 1431-43.

Antonini, A., Fagiolini, M. & Stryker, M. P. (1999) Anatomical correlates of functional plasticity in mouse visual cortex. J Neurosci, 19(11), 4388-406.

Antonini, A. & Stryker, M. P. (1993) Rapid remodeling of axonal arbors in the visual cortex. Science, 260(5115), 1819-21.

Antonini, A. & Stryker, M. P. (1996) Plasticity of geniculocortical afferents following brief or prolonged monocular occlusion in the cat. J Comp Neurol, 369(1), 64-82.

Arnold, F. J., Hofmann, F., Bengtson, C. P., Wittmann, M., Vanhoutte, P. & Bading, H. (2005) Microelectrode array recordings of cultured hippocampal networks reveal a simple model for transcription and protein synthesis-dependent plasticity. J Physiol, 564(Pt 1), 3-19.

Atallah, B. V., Bruns, W., Carandini, M. & Scanziani, M. (2012) Parvalbumin-expressing interneurons linearly transform cortical responses to visual stimuli. Neuron, 73(1), 159-70.

Babiec, W. E., Guglietta, R., Jami, S. A., Morishita, W., Malenka, R. C. & O'Dell, T. J. (2014) Ionotropic NMDA receptor signaling is required for the induction of long-term depression in the mouse hippocampal CA1 region. J Neurosci, 34(15), 5285-90.

Bading, H. & Greenberg, M. E. (1991) Stimulation of protein tyrosine phosphorylation by NMDA receptor activation. Science, 253(5022), 912-4.

Balasuriya, D., Stewart, A. P. & Edwardson, J. M. (2013) The sigma-1 receptor interacts directly with GluN1 but not GluN2A in the GluN1/GluN2A NMDA receptor. J Neurosci, 33(46), 18219-24.

Banke, T. G., Dravid, S. M. & Traynelis, S. F. (2005) Protons trap NR1/NR2B NMDA receptors in a nonconducting state. J Neurosci, 25(1), 42-51.

Barnby, G., Abbott, A., Sykes, N., Morris, A., Weeks, D. E., Mott, R., Lamb, J., Bailey, A. J., Monaco, A. P. & International Molecular Genetics Study of Autism, C. (2005) Candidate-gene screening and association analysis at the autism-susceptibility locus on chromosome 16p: evidence of association at GRIN2A and ABAT. Am J Hum Genet, 76(6), 950-66.

Bear, M. F. (1995) Mechanism for a sliding synaptic modification threshold. Neuron, 15(1), 1-4.

Bear, M. F. & Malenka, R. C. (1994) Synaptic plasticity: LTP and LTD. Curr Opin Neurobiol, 4(3), 389-99.

Bell, K. F. & Hardingham, G. E. (2011) The influence of synaptic activity on neuronal health. Curr Opin Neurobiol, 21(2), 299-305.

Benke, T. A., Park, K., Krey, I., Camp, C. R., Song, R., Ramsey, A. J., Yuan, H., Traynelis, S. F. & Lemke, J. (2021) Clinical and therapeutic significance of genetic variation in the GRIN gene family encoding NMDARs. Neuropharmacology, 199, 108805.

Berberich, S., Punnakkal, P., Jensen, V., Pawlak, V., Seeburg, P. H., Hvalby, O. & Kohr, G. (2005) Lack of NMDA receptor subtype selectivity for hippocampal long-term potentiation. J Neurosci, 25(29), 6907-10.

Berl, S. & Waelsch, H. (1958) Determination of glutamic acid, glutamine, glutathione and gamma-aminobutyric acid and their distribution in brain tissue. J Neurochem, 3(2), 161-9.

Bichet, D., Haass, F. A. & Jan, L. Y. (2003) Merging functional studies with structures of inward-rectifier K(+) channels. Nat Rev Neurosci, 4(12), 957-67.

Bienenstock, E. L., Cooper, L. N. & Munro, P. W. (1982) Theory for the development of neuron selectivity: orientation specificity and binocular interaction in visual cortex. J Neurosci, 2(1), 32-48.

Biscoe, T. J., Davies, J., Dray, A., Evans, R. H., Francis, A. A., Martin, M. R. & Watkins, J. C. (1977) Depression of synaptic excitation and of amino acid induced excitatory responses of spinal neurones by D-alpha-aminoadipate, alpha,epsilon-diaminopimelic acid and HA-966. Eur J Pharmacol, 45(3), 315-6.

Blais, B. S., Shouval, H. Z. & Cooper, L. N. (1999) The role of presynaptic activity in monocular deprivation: comparison of homosynaptic and heterosynaptic mechanisms. Proc Natl Acad Sci U S A, 96(3), 1083-7.

Bock, D. D., Lee, W. C., Kerlin, A. M., Andermann, M. L., Hood, G., Wetzel, A. W., Yurgenson, S., Soucy, E. R., Kim, H. S. & Reid, R. C. (2011) Network anatomy and in vivo physiology of visual cortical neurons. Nature, 471(7337), 177-82.

Borgdorff, A. J. & Choquet, D. (2002) Regulation of AMPA receptor lateral movements. Nature, 417(6889), 649-53.

Bortone, D. S., Olsen, S. R. & Scanziani, M. (2014) Translaminar inhibitory cells recruited by layer 6 corticothalamic neurons suppress visual cortex. Neuron, 82(2), 474-85.

Bosch, M., Castro, J., Saneyoshi, T., Matsuno, H., Sur, M. & Hayashi, Y. (2014) Structural and molecular remodeling of dendritic spine substructures during long-term potentiation. Neuron, 82(2), 444-59.

Bramswig, N. C., Ludecke, H. J., Alanay, Y., Albrecht, B., Barthelmie, A., Boduroglu, K., Braunholz, D., Caliebe, A., Chrzanowska, K. H., Czeschik, J. C., Endele, S., Graf, E., Guillen-Navarro, E., Kiper, P. O., Lopez-Gonzalez, V., Parenti, I., Pozojevic, J., Utine, G. E., Wieland, T., Kaiser, F. J., Wollnik, B., Strom, T. M. & Wieczorek, D. (2015) Exome sequencing unravels unexpected differential diagnoses in individuals with the tentative diagnosis of Coffin-Siris and Nicolaides-Baraitser syndromes. Hum Genet, 134(6), 553-68.

Burzomato, V., Frugier, G., Perez-Otano, I., Kittler, J. T. & Attwell, D. (2010) The receptor subunits generating NMDA receptor mediated currents in oligodendrocytes. J Physiol, 588(Pt 18), 3403-14.

Butler, M. P. & Silver, R. (2011) Divergent photic thresholds in the non-image-forming visual system: entrainment, masking and pupillary light reflex. Proc Biol Sci, 278(1706), 745-50.

Callaway, E. M. & Borrell, V. (2011) Developmental sculpting of dendritic morphology of layer 4 neurons in visual cortex: influence of retinal input. J Neurosci, 31(20), 7456-70.

Carmignoto, G. & Vicini, S. (1992) Activity-dependent decrease in NMDA receptor responses during development of the visual cortex. Science, 258(5084), 1007-11.

Chang, N., Li, L., Hu, R., Shan, Y., Liu, B., Li, L., Wang, H., Feng, H., Wang, D., Cheung, C., Liao, M. & Wan, Q. (2010) Differential regulation of NMDA receptor function by DJ-1 and PINK1. Aging Cell, 9(5), 837-50.

Chatterton, J. E., Awobuluyi, M., Premkumar, L. S., Takahashi, H., Talantova, M., Shin, Y., Cui, J., Tu, S., Sevarino, K. A., Nakanishi, N., Tong, G., Lipton, S. A. & Zhang, D. (2002) Excitatory glycine receptors containing the NR3 family of NMDA receptor subunits. Nature, 415(6873), 793-8.

Chawla, S., Hardingham, G. E., Quinn, D. R. & Bading, H. (1998) CBP: a signal-regulated transcriptional coactivator controlled by nuclear calcium and CaM kinase IV. Science, 281(5382), 1505-9.

Chen, B., Feng, B., Tang, Y., You, Y., Wang, Y., Hou, W., Hu, W. & Chen, Z. (2016) Blocking GluN2B subunits reverses the enhanced seizure susceptibility after prolonged febrile seizures with a wide therapeutic time-window. Exp Neurol, 283(Pt A), 29-38.

Chen, B. S., Gray, J. A., Sanz-Clemente, A., Wei, Z., Thomas, E. V., Nicoll, R. A. & Roche, K. W. (2012) SAP102 mediates synaptic clearance of NMDA receptors. Cell Rep, 2(5), 1120-8.

Chen, W., Shieh, C., Swanger, S. A., Tankovic, A., Au, M., McGuire, M., Tagliati, M., Graham, J. M., Madan-Khetarpal, S., Traynelis, S. F., Yuan, H. & Pierson, T. M. (2017) GRIN1 mutation associated with intellectual disability alters NMDA receptor trafficking and function. J Hum Genet, 62(6), 589-597.

Chen, W. S. & Bear, M. F. (2007) Activity-dependent regulation of NR2B translation contributes to metaplasticity in mouse visual cortex. Neuropharmacology, 52(1), 200-14.

Chrivia, J. C., Kwok, R. P., Lamb, N., Hagiwara, M., Montminy, M. R. & Goodman, R. H. (1993) Phosphorylated CREB binds specifically to the nuclear protein CBP. Nature, 365(6449), 855-9.

Clasca, F., Rubio-Garrido, P. & Jabaudon, D. (2012) Unveiling the diversity of thalamocortical neuron subtypes. Eur J Neurosci, 35(10), 1524-32.

Cole, A. J., Saffen, D. W., Baraban, J. M. & Worley, P. F. (1989) Rapid increase of an immediate early gene messenger RNA in hippocampal neurons by synaptic NMDA receptor activation. Nature, 340(6233), 474-6.

Coleman, J. E., Nahmani, M., Gavornik, J. P., Haslinger, R., Heynen, A. J., Erisir, A. & Bear, M. F. (2010) Rapid structural remodeling of thalamocortical synapses parallels experience-dependent functional plasticity in mouse primary visual cortex. J Neurosci, 30(29), 9670-82.

Collingridge, G. L., Kehl, S. J. & McLennan, H. (1983) Excitatory amino acids in synaptic transmission in the Schaffer collateral-commissural pathway of the rat hippocampus. J Physiol, 334, 33-46.

Collins, M. O. & Grant, S. G. (2007) Supramolecular signalling complexes in the nervous system. Subcell Biochem, 43, 185-207.

Conti, F., DeBiasi, S., Minelli, A. & Melone, M. (1996) Expression of NR1 and NR2A/B subunits of the NMDA receptor in cortical astrocytes. Glia, 17(3), 254-8.

Cooper, L. N. & Bear, M. F. (2012) The BCM theory of synapse modification at 30: interaction of theory with experiment. Nat Rev Neurosci, 13(11), 798-810.

Cooper, L. N., Liberman, F. & Oja, E. (1979) A theory for the acquisition and loss of neuron specificity in visual cortex. Biol Cybern, 33(1), 9-28.

Corbel, C., Hernandez, I., Wu, B. & Kosik, K. S. (2015) Developmental attenuation of N-methyl-D-aspartate receptor subunit expression by microRNAs. Neural Dev, 10, 20.

Cruz-Martin, A., El-Danaf, R. N., Osakada, F., Sriram, B., Dhande, O. S., Nguyen, P. L., Callaway, E. M., Ghosh, A. & Huberman, A. D. (2014) A dedicated circuit links direction-selective retinal ganglion cells to the primary visual cortex. Nature, 507(7492), 358-61.

Curtis, D. R. (1963) The pharmacology of central and peripheral inhibition. Pharmacol Rev, 15, 333-64.

Curtis, D. R. & Johnston, G. A. (1974) Amino acid transmitters in the mammalian central nervous system. Ergeb Physiol, 69(0), 97-188.

Curtis, D. R., Phillis, J. W. & Watkins, J. C. (1959) Chemical excitation of spinal neurones. Nature, 183(4661), 611-2.

Curtis, D. R., Phillis, J. W. & Watkins, J. C. (1960) The chemical excitation of spinal neurones by certain acidic amino acids. J Physiol, 150(3), 656-82.

Curtis, D. R. & Watkins, J. C. (1963) Acidic amino acids with strong excitatory actions on mammalian neurones. J Physiol, 166(1), 1-14.

Cynader, M. (1983) Prolonged sensitivity to monocular deprivation in dark-reared cats: effects of age and visual exposure. Brain Res, 284(2-3), 155-64.

Cynader, M. & Mitchell, D. E. (1980) Prolonged sensitivity to monocular deprivation in dark-reared cats. J Neurophysiol, 43(4), 1026-40.

Davies, J. & Watkins, J. C. (1979) Selective antagonism of amino acid-induced and synaptic excitation in the cat spinal cord. J Physiol, 297(0), 621-35.

Davies, J. & Watkins, J. C. (1981) Differentiation of kainate and quisqualate receptors in the cat spinal cord by selective antagonism with gamma-D(and L)-glutamylglycine. Brain Res, 206(1), 172-7.

Daw, N. W., Fox, K., Sato, H. & Czepita, D. (1992) Critical period for monocular deprivation in the cat visual cortex. J Neurophysiol, 67(1), 197-202.

Day, M., Carr, D. B., Ulrich, S., Ilijic, E., Tkatch, T. & Surmeier, D. J. (2005) Dendritic excitability of mouse frontal cortex pyramidal neurons is shaped by the interaction among HCN, Kir2, and Kleak channels. J Neurosci, 25(38), 8776-87.

Di Cristo, G., Wu, C., Chattopadhyaya, B., Ango, F., Knott, G., Welker, E., Svoboda, K. & Huang, Z. J. (2004) Subcellular domain-restricted GABAergic innervation in primary visual cortex in the absence of sensory and thalamic inputs. Nat Neurosci, 7(11), 1184-6.

Diering, G. H., Gustina, A. S. & Huganir, R. L. (2014) PKA-GluA1 coupling via AKAP5 controls AMPA receptor phosphorylation and cell-surface targeting during bidirectional homeostatic plasticity. Neuron, 84(4), 790-805.

Dimassi, S., Labalme, A., Lesca, G., Rudolf, G., Bruneau, N., Hirsch, E., Arzimanoglou, A., Motte, J., de Saint Martin, A., Boutry-Kryza, N., Cloarec, R., Benitto, A., Ameil, A., Edery, P., Ryvlin, P., De Bellescize, J., Szepetowski, P. & Sanlaville, D. (2014) A subset of genomic alterations detected in rolandic epilepsies contains candidate or known epilepsy genes including GRIN2A and PRRT2. Epilepsia, 55(2), 370-8.

Dolen, G., Osterweil, E., Rao, B. S., Smith, G. B., Auerbach, B. D., Chattarji, S. & Bear, M. F. (2007) Correction of fragile X syndrome in mice. Neuron, 56(6), 955-62.

Dudek, S. M. & Bear, M. F. (1992) Homosynaptic long-term depression in area CA1 of hippocampus and effects of N-methyl-D-aspartate receptor blockade. Proc Natl Acad Sci U S A, 89(10), 4363-7.

Duggan, A. W. & Johnston, G. A. (1970) Glutamate and related amino acids in cat spinal roots, dorsal root ganglia and peripheral nerves. J Neurochem, 17(8), 1205-8.

Edman, S., McKay, S., Macdonald, L. J., Samadi, M., Livesey, M. R., Hardingham, G. E. & Wyllie, D. J. (2012) TCN 201 selectively blocks GluN2A-containing NMDARs in a GluN1 co-agonist dependent but non-competitive manner. Neuropharmacology, 63(3), 441-9.

Ehlers, M. D. (2003) Activity level controls postsynaptic composition and signaling via the ubiquitin-proteasome system. Nat Neurosci, 6(3), 231-42.

Endele, S., Rosenberger, G., Geider, K., Popp, B., Tamer, C., Stefanova, I., Milh, M., Kortum, F., Fritsch, A., Pientka, F. K., Hellenbroich, Y., Kalscheuer, V. M., Kohlhase, J., Moog, U., Rappold, G., Rauch, A., Ropers, H. H., von Spiczak, S., Tonnies, H., Villeneuve, N., Villard, L., Zabel, B., Zenker, M., Laube, B., Reis, A., Wieczorek, D., Van Maldergem, L. & Kutsche, K. (2010) Mutations in GRIN2A and GRIN2B encoding regulatory subunits of NMDA receptors cause variable neurodevelopmental phenotypes. Nat Genet, 42(11), 1021-6.

Epi, P. M. C. (2015) A roadmap for precision medicine in the epilepsies. Lancet Neurol, 14(12), 1219-28.

Evans, R. H., Francis, A. A. & Watkins, J. C. (1977) Selective antagonism by Mg2+ of amino acid-induced depolarization of spinal neurones. Experientia, 33(4), 489-91.

Fagiolini, M., Pizzorusso, T., Berardi, N., Domenici, L. & Maffei, L. (1994) Functional postnatal development of the rat primary visual cortex and the role of visual experience: dark rearing and monocular deprivation. Vision Res, 34(6), 709-20.

Feldman, M. L. & Peters, A. (1978) The forms of non-pyramidal neurons in the visual cortex of the rat. J Comp Neurol, 179(4), 761-93.

Finkbeiner, S. & Greenberg, M. E. (1996) Ca(2+)-dependent routes to Ras: mechanisms for neuronal survival, differentiation, and plasticity? Neuron, 16(2), 233-6.

Firth, H. V., Richards, S. M., Bevan, A. P., Clayton, S., Corpas, M., Rajan, D., Van Vooren, S., Moreau, Y., Pettett, R. M. & Carter, N. P. (2009) DECIPHER: Database of Chromosomal Imbalance and Phenotype in Humans Using Ensembl Resources. Am J Hum Genet, 84(4), 524-33.

Fiuza, M., Rostosky, C. M., Parkinson, G. T., Bygrave, A. M., Halemani, N., Baptista, M., Milosevic, I. & Hanley, J. G. (2017) PICK1 regulates AMPA receptor endocytosis via direct interactions with AP2 alpha-appendage and dynamin. J Cell Biol, 216(10), 3323-3338.

Fong, M. F., Finnie, P. S., Kim, T., Thomazeau, A., Kaplan, E. S., Cooke, S. F. & Bear, M. F. (2020) Distinct Laminar Requirements for NMDA Receptors in Experience-Dependent Visual Cortical Plasticity. Cereb Cortex, 30(4), 2555-2572.

Fox, K., Sato, H. & Daw, N. (1989) The location and function of NMDA receptors in cat and kitten visual cortex. J Neurosci, 9(7), 2443-54.

Frank, R. A. & Grant, S. G. (2017) Supramolecular organization of NMDA receptors and the postsynaptic density. Curr Opin Neurobiol, 45, 139-147.

Frank, R. A., Komiyama, N. H., Ryan, T. J., Zhu, F., O'Dell, T. J. & Grant, S. G. (2016) NMDA receptors are selectively partitioned into complexes and supercomplexes during synapse maturation. Nat Commun, 7, 11264.

Frenkel, M. Y. & Bear, M. F. (2004) How monocular deprivation shifts ocular dominance in visual cortex of young mice. Neuron, 44(6), 917-23.

Freunscht, I., Popp, B., Blank, R., Endele, S., Moog, U., Petri, H., Prott, E. C., Reis, A., Rubo, J., Zabel, B., Zenker, M., Hebebrand, J. & Wieczorek, D. (2013) Behavioral phenotype in five individuals with de novo mutations within the GRIN2B gene. Behav Brain Funct, 9, 20.

Frizelle, P. A., Chen, P. E. & Wyllie, D. J. (2006) Equilibrium constants for (R)-[(S)-1-(4-bromo-phenyl)-ethylamino]-(2,3-dioxo-1,2,3,4-tetrahydroquinoxalin-5-yl)-methyl]-phosphonic acid (NVP-AAM077) acting at recombinant NR1/NR2A and NR1/NR2B N-methyl-D-aspartate receptors: Implications for studies of synaptic transmission. Mol Pharmacol, 70(3), 1022-32.

Garner, C. C., Nash, J. & Huganir, R. L. (2000) PDZ domains in synapse assembly and signalling. Trends Cell Biol, 10(7), 274-80.

Gianfranceschi, L., Siciliano, R., Walls, J., Morales, B., Kirkwood, A., Huang, Z. J., Tonegawa, S. & Maffei, L. (2003) Visual cortex is rescued from the effects of dark rearing by overexpression of BDNF. Proc Natl Acad Sci U S A, 100(21), 12486-91.

Giannakopoulos, M., Kouvelas, E. D. & Mitsacos, A. (2010) Experience-dependent regulation of NMDA receptor subunit composition and phosphorylation in the retina and visual cortex. Invest Ophthalmol Vis Sci, 51(4), 1817-22.

Gonchar, Y., Wang, Q. & Burkhalter, A. (2007) Multiple distinct subtypes of GABAergic neurons in mouse visual cortex identified by triple immunostaining. Front Neuroanat, 1, 3.

Gonzalez, G. A. & Montminy, M. R. (1989) Cyclic AMP stimulates somatostatin gene transcription by phosphorylation of CREB at serine 133. Cell, 59(4), 675-80.

Gorlewicz, A., Pijet, B., Orlova, K., Kaczmarek, L. & Knapska, E. (2022) Epileptiform GluN2B-driven excitation in hippocampus as a therapeutic target against temporal lobe epilepsy. Exp Neurol, 354, 114087.

Graham, L. T., Jr., Shank, R. P., Werman, R. & Aprison, M. H. (1967) Distribution of some synaptic transmitter suspects in cat spinal cord: glutamic acid, aspartic acid, gamma-aminobutyric acid, glycine and glutamine. J Neurochem, 14(4), 465-72.

Groc, L., Choquet, D., Stephenson, F. A., Verrier, D., Manzoni, O. J. & Chavis, P. (2007) NMDA receptor surface trafficking and synaptic subunit composition are developmentally regulated by the extracellular matrix protein Reelin. J Neurosci, 27(38), 10165-75.

Groc, L., Heine, M., Cousins, S. L., Stephenson, F. A., Lounis, B., Cognet, L. & Choquet, D. (2006) NMDA receptor surface mobility depends on NR2A-2B subunits. Proc Natl Acad Sci U S A, 103(49), 18769-74.

Grozeva, D., Carss, K., Spasic-Boskovic, O., Tejada, M. I., Gecz, J., Shaw, M., Corbett, M., Haan, E., Thompson, E., Friend, K., Hussain, Z., Hackett, A., Field, M., Renieri, A., Stevenson, R., Schwartz, C., Floyd, J. A., Bentham, J., Cosgrove, C., Keavney, B., Bhattacharya, S., Italian, X. l. M. R. P., Consortium, U. K., Consortium, G., Hurles, M. & Raymond, F. L. (2015) Targeted Next-Generation Sequencing Analysis of 1,000 Individuals with Intellectual Disability. Hum Mutat, 36(12), 1197-204.

Gu, Q. A., Bear, M. F. & Singer, W. (1989) Blockade of NMDA-receptors prevents ocularity changes in kitten visual cortex after reversed monocular deprivation. Brain Res Dev Brain Res, 47(2), 281-8.

Guire, E. S., Lickey, M. E. & Gordon, B. (1999) Critical period for the monocular deprivation effect in rats: assessment with sweep visually evoked potentials. J Neurophysiol, 81(1), 121-8.

Hagenston, A. M. & Bading, H. (2011) Calcium signaling in synapse-to-nucleus communication. Cold Spring Harb Perspect Biol, 3(11), a004564.

Haldeman, S. & McLennan, H. (1972) The antagonistic action of glutamic acid diethylester towards amino acid-induced and synaptic excitations of central neurones. Brain Res, 45(2), 393-400.

Halt, A. R., Dallapiazza, R. F., Zhou, Y., Stein, I. S., Qian, H., Juntti, S., Wojcik, S., Brose, N., Silva, A. J. & Hell, J. W. (2012) CaMKII binding to GluN2B is critical during memory consolidation. EMBO J, 31(5), 1203-16.

Han, W., Yuan, H., Allen, J. P., Kim, S., Shaulsky, G. H., Perszyk, R. E., Traynelis, S. F. & Myers, S. J. (2022) Opportunities for Precision Treatment of GRIN2A and

GRIN2B Gain-of-Function Variants in Triheteromeric N-Methyl-D-Aspartate Receptors. J Pharmacol Exp Ther, 381(1), 54-66.

Hansen, K. B., Ogden, K. K., Yuan, H. & Traynelis, S. F. (2014) Distinct functional and pharmacological properties of Triheteromeric GluN1/GluN2A/GluN2B NMDA receptors. Neuron, 81(5), 1084-1096.

Hardingham, G. E. & Bading, H. (1998) Nuclear calcium: a key regulator of gene expression. Biometals, 11(4), 345-58.

Hardingham, G. E., Arnold, F. J. & Bading, H. (2001a) Nuclear calcium signaling controls CREB-mediated gene expression triggered by synaptic activity. Nat Neurosci, 4(3), 261-7.

Hardingham, G.E., Arnold, F.J. & Bading, H. (2001b). A calcium microdomain near NMDA receptors: on switch for ERK-dependent synapse-to-nucleus communication. Nature neuroscience, 4(6), 565-566.

Hardingham, G. E. & Bading, H. (2003) The Yin and Yang of NMDA receptor signalling. Trends Neurosci, 26(2), 81-9.

Hardingham, G. E., Chawla, S., Johnson, C. M. & Bading, H. (1997) Distinct functions of nuclear and cytoplasmic calcium in the control of gene expression. Nature, 385(6613), 260-5.

Hattar, S., Lucas, R. J., Mrosovsky, N., Thompson, S., Douglas, R. H., Hankins, M. W., Lem, J., Biel, M., Hofmann, F., Foster, R. G. & Yau, K. W. (2003) Melanopsin and rod-cone photoreceptive systems account for all major accessory visual functions in mice. Nature, 424(6944), 76-81.

Hattox, A. M. & Nelson, S. B. (2007) Layer V neurons in mouse cortex projecting to different targets have distinct physiological properties. J Neurophysiol, 98(6), 3330-40.

Hayashi, T. (1952) A physiological study of epileptic seizures following cortical stimulation in animals and its application to human clinics. Jpn J Physiol, 3(1), 46-64.

Hayashi, Y., Shi, S. H., Esteban, J. A., Piccini, A., Poncer, J. C. & Malinow, R. (2000) Driving AMPA receptors into synapses by LTP and CaMKII: requirement for GluR1 and PDZ domain interaction. Science, 287(5461), 2262-7.

He, K., Song, L., Cummings, L. W., Goldman, J., Huganir, R. L. & Lee, H. K. (2009) Stabilization of Ca2+-permeable AMPA receptors at perisynaptic sites by GluR1-S845 phosphorylation. Proc Natl Acad Sci U S A, 106(47), 20033-8.

Herring, B. E. & Nicoll, R. A. (2016) Long-Term Potentiation: From CaMKII to AMPA Receptor Trafficking. Annu Rev Physiol, 78, 351-65.

Hibino, H., Inanobe, A., Furutani, K., Murakami, S., Findlay, I. & Kurachi, Y. (2010) Inwardly rectifying potassium channels: their structure, function, and physiological roles. Physiol Rev, 90(1), 291-366.

Higley, M. J. & Contreras, D. (2006) Balanced excitation and inhibition determine spike timing during frequency adaptation. J Neurosci, 26(2), 448-57.

Hoffmann, H., Gremme, T., Hatt, H. & Gottmann, K. (2000) Synaptic activity-dependent developmental regulation of NMDA receptor subunit expression in cultured neocortical neurons. J Neurochem, 75(4), 1590-9.

Hu, S. C., Chrivia, J. & Ghosh, A. (1999) Regulation of CBP-mediated transcription by neuronal calcium signaling. Neuron, 22(4), 799-808.

Hubalkova, P., Ladislav, M., Vyklicky, V., Smejkalova, T., Hrcka Krausova, B., Kysilov, B., Krusek, J., Naimova, Z., Korinek, M., Chodounska, H., Kudova, E., Cerny, J. & Vyklicky, L., Jr. (2021) Palmitoylation Controls NMDA Receptor Function and Steroid Sensitivity. J Neurosci, 41(10), 2119-2134.

Hubel, D. H. & Wiesel, T. N. (1972) Laminar and columnar distribution of geniculo-cortical fibers in the macaque monkey. J Comp Neurol, 146(4), 421-50.

Ibata, K., Sun, Q. & Turrigiano, G. G. (2008) Rapid synaptic scaling induced by changes in postsynaptic firing. Neuron, 57(6), 819-26.

Ikeda, K., Nagasawa, M., Mori, H., Araki, K., Sakimura, K., Watanabe, M., Inoue, Y. & Mishina, M. (1992) Cloning and expression of the epsilon 4 subunit of the NMDA receptor channel. FEBS Lett, 313(1), 34-8.

Impey, S. & Goodman, R. H. (2001) CREB signaling--timing is everything. Sci STKE, 2001(82), pe1.

Ishchenko, Y., Carrizales, M. G. & Koleske, A. J. (2021) Regulation of the NMDA receptor by its cytoplasmic domains: (How) is the tail wagging the dog? Neuropharmacology, 195, 108634.

Ishii, T., Moriyoshi, K., Sugihara, H., Sakurada, K., Kadotani, H., Yokoi, M., Akazawa, C., Shigemoto, R., Mizuno, N., Masu, M. & et al. (1993) Molecular characterization of the family of the N-methyl-D-aspartate receptor subunits. J Biol Chem, 268(4), 2836-43.

Iwai, Y., Fagiolini, M., Obata, K. & Hensch, T. K. (2003) Rapid critical period induction by tonic inhibition in visual cortex. J Neurosci, 23(17), 6695-702.

Javitt, D. C. (1987) Negative schizophrenic symptomatology and the PCP (phencyclidine) model of schizophrenia. Hillside J Clin Psychiatry, 9(1), 12-35.

Javitt, D. C. & Zukin, S. R. (1991) Recent advances in the phencyclidine model of schizophrenia. Am J Psychiatry, 148(10), 1301-8.

Ji, W., Gamanut, R., Bista, P., D'Souza, R. D., Wang, Q. & Burkhalter, A. (2015) Modularity in the Organization of Mouse Primary Visual Cortex. Neuron, 87(3), 632-43.

Jiang, X., Shen, S., Cadwell, C. R., Berens, P., Sinz, F., Ecker, A. S., Patel, S. & Tolias, A. S. (2015) Principles of connectivity among morphologically defined cell types in adult neocortex. Science, 350(6264), aac9462.

Jimenez-Blasco, D., Santofimia-Castano, P., Gonzalez, A., Almeida, A. & Bolanos, J. P. (2015) Astrocyte NMDA receptors' activity sustains neuronal survival through a Cdk5-Nrf2 pathway. Cell Death Differ, 22(11), 1877-89.

Johnston, G. A. (1968) The intraspinal distribution of some depressant amino acids. J Neurochem, 15(9), 1013-7.

Kaplan, I. V., Guo, Y. & Mower, G. D. (1996) Immediate early gene expression in cat visual cortex during and after the critical period: differences between EGR-1 and Fos proteins. Brain Res Mol Brain Res, 36(1), 12-22.

Karadottir, R., Cavelier, P., Bergersen, L. H. & Attwell, D. (2005) NMDA receptors are expressed in oligodendrocytes and activated in ischaemia. Nature, 438(7071), 1162-6.

Kawaguchi, Y. & Kubota, Y. (1997) GABAergic cell subtypes and their synaptic connections in rat frontal cortex. Cereb Cortex, 7(6), 476-86.

Keith, R. E., Azcarate, J. M., Keith, M. J., Hung, C. W., Badakhsh, M. F. & Dumas, T. C. (2019) Direct Intracellular Signaling by the Carboxy terminus of NMDA Receptor GluN2 Subunits Regulates Dendritic Morphology in Hippocampal CA1 Pyramidal Neurons. Neuroscience, 396, 138-153.

Kessels, H. W., Nabavi, S. & Malinow, R. (2013) Metabotropic NMDA receptor function is required for beta-amyloid-induced synaptic depression. Proc Natl Acad Sci U S A, 110(10), 4033-8.

Kim, M. J., Dunah, A. W., Wang, Y. T. & Sheng, M. (2005) Differential roles of NR2A- and NR2B-containing NMDA receptors in Ras-ERK signaling and AMPA receptor trafficking. Neuron, 46(5), 745-60.

Kirkwood, A., Rioult, M. C. & Bear, M. F. (1996) Experience-dependent modification of synaptic plasticity in visual cortex. Nature, 381(6582), 526-8.

Kleinschmidt, A., Bear, M. F. & Singer, W. (1987) Blockade of "NMDA" receptors disrupts experience-dependent plasticity of kitten striate cortex. Science, 238(4825), 355-8.

Kohr, G., Jensen, V., Koester, H. J., Mihaljevic, A. L., Utvik, J. K., Kvello, A., Ottersen, O. P., Seeburg, P. H., Sprengel, R. & Hvalby, O. (2003) Intracellular domains of NMDA receptor subtypes are determinants for long-term potentiation induction. J Neurosci, 23(34), 10791-9.

Krizbai, I. A., Deli, M. A., Pestenacz, A., Siklos, L., Szabo, C. A., Andras, I. & Joo, F. (1998) Expression of glutamate receptors on cultured cerebral endothelial cells. J Neurosci Res, 54(6), 814-9.

Krogsgaard-Larsen, P., Honore, T., Hansen, J. J., Curtis, D. R. & Lodge, D. (1980) New class of glutamate agonist structurally related to ibotenic acid. Nature, 284(5751), 64-6.

Kuner, T. & Schoepfer, R. (1996) Multiple structural elements determine subunit specificity of Mg2+ block in NMDA receptor channels. J Neurosci, 16(11), 3549-58.

Kutsuwada, T., Kashiwabuchi, N., Mori, H., Sakimura, K., Kushiya, E., Araki, K., Meguro, H., Masaki, H., Kumanishi, T., Arakawa, M. & et al. (1992) Molecular diversity of the NMDA receptor channel. Nature, 358(6381), 36-41.

Lal, D., Steinbrucker, S., Schubert, J., Sander, T., Becker, F., Weber, Y., Lerche, H., Thiele, H., Krause, R., Lehesjoki, A. E., Nurnberg, P., Palotie, A., Neubauer, B. A., Muhle, H., Stephani, U., Helbig, I., Becker, A. J., Schoch, S., Hansen, J., Dorn, T., Hohl, C., Luscher, N., Epicure, c., Euro, E.-C. c., von Spiczak, S. & Lemke, J. R. (2015) Investigation of GRIN2A in common epilepsy phenotypes. Epilepsy Res, 115, 95-9.

Lalo, U., Pankratov, Y., Kirchhoff, F., North, R. A. & Verkhratsky, A. (2006) NMDA receptors mediate neuron-to-glia signaling in mouse cortical astrocytes. J Neurosci, 26(10), 2673-83.

Lan, J. Y., Skeberdis, V. A., Jover, T., Grooms, S. Y., Lin, Y., Araneda, R. C., Zheng, X., Bennett, M. V. & Zukin, R. S. (2001) Protein kinase C modulates NMDA receptor trafficking and gating. Nat Neurosci, 4(4), 382-90.

Lavezzari, G., McCallum, J., Dewey, C. M. & Roche, K. W. (2004) Subunit-specific regulation of NMDA receptor endocytosis. J Neurosci, 24(28), 6383-91.

Lee, C. H., Lu, W., Michel, J. C., Goehring, A., Du, J., Song, X. & Gouaux, E. (2014) NMDA receptor structures reveal subunit arrangement and pore architecture. Nature, 511(7508), 191-7.

Lee, H. K., Barbarosie, M., Kameyama, K., Bear, M. F. & Huganir, R. L. (2000) Regulation of distinct AMPA receptor phosphorylation sites during bidirectional synaptic plasticity. Nature, 405(6789), 955-9.

Lee, M. C., Yasuda, R. & Ehlers, M. D. (2010) Metaplasticity at single glutamatergic synapses. Neuron, 66(6), 859-70.

Lemke, J. R., Hendrickx, R., Geider, K., Laube, B., Schwake, M., Harvey, R. J., James, V. M., Pepler, A., Steiner, I., Hortnagel, K., Neidhardt, J., Ruf, S., Wolff, M., Bartholdi, D., Caraballo, R., Platzer, K., Suls, A., De Jonghe, P., Biskup, S. & Weckhuysen, S. (2014) GRIN2B mutations in West syndrome and intellectual disability with focal epilepsy. Ann Neurol, 75(1), 147-54.

Lemke, J. R., Lal, D., Reinthaler, E. M., Steiner, I., Nothnagel, M., Alber, M., Geider, K., Laube, B., Schwake, M., Finsterwalder, K., Franke, A., Schilhabel, M., Jahn, J. A., Muhle, H., Boor, R., Van Paesschen, W., Caraballo, R., Fejerman, N., Weckhuysen, S., De Jonghe, P., Larsen, J., Moller, R. S., Hjalgrim, H., Addis, L., Tang, S., Hughes, E., Pal, D. K., Veri, K., Vaher, U., Talvik, T., Dimova, P., Guerrero Lopez, R., Serratosa, J. M., Linnankivi, T., Lehesjoki, A. E., Ruf, S., Wolff, M., Buerki, S., Wohlrab, G., Kroell, J., Datta, A. N., Fiedler, B., Kurlemann, G., Kluger, G., Hahn, A., Haberlandt, D. E., Kutzer, C., Sperner, J., Becker, F., Weber, Y. G., Feucht, M., Steinbock, H., Neophythou, B., Ronen, G. M., Gruber-Sedlmayr, U., Geldner, J., Harvey, R. J., Hoffmann, P., Herms, S., Altmuller, J., Toliat, M. R., Thiele, H., Nurnberg, P., Wilhelm, C., Stephani, U., Helbig, I., Lerche, H., Zimprich, F., Neubauer, B. A., Biskup, S. & von Spiczak, S. (2013) Mutations in GRIN2A cause idiopathic focal epilepsy with rolandic spikes. Nat Genet, 45(9), 1067-72.

Lesca, G., Rudolf, G., Bruneau, N., Lozovaya, N., Labalme, A., Boutry-Kryza, N., Salmi, M., Tsintsadze, T., Addis, L., Motte, J., Wright, S., Tsintsadze, V., Michel, A., Doummar, D., Lascelles, K., Strug, L., Waters, P., de Bellescize, J., Vrielynck, P., de Saint Martin, A., Ville, D., Ryvlin, P., Arzimanoglou, A., Hirsch, E., Vincent, A., Pal, D., Burnashev, N., Sanlaville, D. & Szepetowski, P. (2013) GRIN2A mutations in acquired epileptic aphasia and related childhood focal epilepsies and encephalopathies with speech and language dysfunction. Nat Genet, 45(9), 1061-6.

Li, Q. Q., Chen, J., Hu, P., Jia, M., Sun, J. H., Feng, H. Y., Qiao, F. C., Zang, Y. Y., Shi, Y. Y., Chen, G., Sheng, N., Xu, Y., Yang, J. J., Xu, Z. & Shi, Y. S. (2022) Enhancing GluN2A-type NMDA receptors impairs long-term synaptic plasticity and learning and memory. Mol Psychiatry, 27(8), 3468-3478.

Linden, M. L., Heynen, A. J., Haslinger, R. H. & Bear, M. F. (2009) Thalamic activity that drives visual cortical plasticity. Nat Neurosci, 12(4), 390-2.

Lipton, S. A. & Kater, S. B. (1989) Neurotransmitter regulation of neuronal outgrowth, plasticity and survival. Trends Neurosci, 12(7), 265-70.

Liu, L., Wong, T. P., Pozza, M. F., Lingenhoehl, K., Wang, Y., Sheng, M., Auberson, Y. P. & Wang, Y. T. (2004) Role of NMDA receptor subtypes in governing the direction of hippocampal synaptic plasticity. Science, 304(5673), 1021-4.

Liu, S., Zhou, L., Yuan, H., Vieira, M., Sanz-Clemente, A., Badger, J. D., 2nd, Lu, W., Traynelis, S. F. & Roche, K. W. (2017) A Rare Variant Identified Within the GluN2B C-Terminus in a Patient with Autism Affects NMDA Receptor Surface Expression and Spine Density. J Neurosci, 37(15), 4093-4102.

Lodge, D. (2009) The history of the pharmacology and cloning of ionotropic glutamate receptors and the development of idiosyncratic nomenclature. Neuropharmacology, 56(1), 6-21.

Lucas, R. J., Douglas, R. H. & Foster, R. G. (2001) Characterization of an ocular photopigment capable of driving pupillary constriction in mice. Nat Neurosci, 4(6), 621-6.

Lund, J. S., Lund, R. D., Hendrickson, A. E., Bunt, A. H. & Fuchs, A. F. (1975) The origin of efferent pathways from the primary visual cortex, area 17, of the macaque monkey as shown by retrograde transport of horseradish peroxidase. J Comp Neurol, 164(3), 287-303.

Luscher, C. & Malenka, R. C. (2012) NMDA receptor-dependent long-term potentiation and long-term depression (LTP/LTD). Cold Spring Harb Perspect Biol, 4(6).

Lyons, M. R. & West, A. E. (2011) Mechanisms of specificity in neuronal activity-regulated gene transcription. Prog Neurobiol, 94(3), 259-95.

Maki, B. A., Aman, T. K., Amico-Ruvio, S. A., Kussius, C. L. & Popescu, G. K. (2012) C-terminal domains of N-methyl-D-aspartic acid receptor modulate unitary channel conductance and gating. J Biol Chem, 287(43), 36071-80.

Mares, P., Kozlova, L., Mikulecka, A. & Kubova, H. (2021) The GluN2B-Selective Antagonist Ro 25-6981 Is Effective against PTZ-Induced Seizures and Safe for Further Development in Infantile Rats. Pharmaceutics, 13(9).

Massey, P. V., Johnson, B. E., Moult, P. R., Auberson, Y. P., Brown, M. W., Molnar, E., Collingridge, G. L. & Bashir, Z. I. (2004) Differential roles of NR2A and NR2B-containing NMDA receptors in cortical long-term potentiation and long-term depression. J Neurosci, 24(36), 7821-8.

Matsuda, S., Mikawa, S. & Hirai, H. (1999) Phosphorylation of serine-880 in GluR2 by protein kinase C prevents its C terminus from binding with glutamate receptor-interacting protein. J Neurochem, 73(4), 1765-8.

McKay, S., Griffiths, N. H., Butters, P. A., Thubron, E. B., Hardingham, G. E. & Wyllie, D. J. (2012) Direct pharmacological monitoring of the developmental switch in NMDA receptor subunit composition using TCN 213, a GluN2A-selective, glycine-dependent antagonist. Br J Pharmacol, 166(3), 924-37.

McKay, S., Ryan, T. J., McQueen, J., Indersmitten, T., Marwick, K. F. M., Hasel, P., Kopanitsa, M. V., Baxter, P. S., Martel, M. A., Kind, P. C., Wyllie, D. J. A., O'Dell, T. J., Grant, S. G. N., Hardingham, G. E. & Komiyama, N. H. (2018) The Developmental Shift of NMDA Receptor Composition Proceeds Independently of GluN2 Subunit-Specific GluN2 C-Terminal Sequences. Cell Rep, 25(4), 841-851 e4.

McKenzie, G. J., Stevenson, P., Ward, G., Papadia, S., Bading, H., Chawla, S., Privalsky, M. & Hardingham, G. E. (2005) Nuclear Ca2+ and CaM kinase IV specify hormonal- and Notch-responsiveness. J Neurochem, 93(1), 171-85.

McLennan, H. & Lodge, D. (1979) The antagonism of amino acid-induced excitation of spinal neurones in the cat. Brain Res, 169(1), 83-90.

Meguro, H., Mori, H., Araki, K., Kushiya, E., Kutsuwada, T., Yamazaki, M., Kumanishi, T., Arakawa, M., Sakimura, K. & Mishina, M. (1992) Functional characterization of a heteromeric NMDA receptor channel expressed from cloned cDNAs. Nature, 357(6373), 70-4.

Miller, K. D. (1996) Synaptic economics: competition and cooperation in synaptic plasticity. Neuron, 17(3), 371-4.

Milnerwood, A. J., Gladding, C. M., Pouladi, M. A., Kaufman, A. M., Hines, R. M., Boyd, J. D., Ko, R. W., Vasuta, O. C., Graham, R. K., Hayden, M. R., Murphy, T. H. & Raymond, L. A. (2010) Early increase in extrasynaptic NMDA receptor signaling and expression contributes to phenotype onset in Huntington's disease mice. Neuron, 65(2), 178-90.

Mony, L., Zhu, S., Carvalho, S. & Paoletti, P. (2011) Molecular basis of positive allosteric modulation of GluN2B NMDA receptors by polyamines. EMBO J, 30(15), 3134-46.

Monyer, H., Burnashev, N., Laurie, D. J., Sakmann, B. & Seeburg, P. H. (1994) Developmental and regional expression in the rat brain and functional properties of four NMDA receptors. Neuron, 12(3), 529-40.

Monyer, H. & Seeburg, P. H. (1993) Constituents involved in glutamate receptor signaling. Hippocampus, 3 Spec No, 125-9.

Monyer, H., Sprengel, R., Schoepfer, R., Herb, A., Higuchi, M., Lomeli, H., Burnashev, N., Sakmann, B. & Seeburg, P. H. (1992) Heteromeric NMDA receptors: molecular and functional distinction of subtypes. Science, 256(5060), 1217-21.

Moody, T. D., Watabe, A. M., Indersmitten, T., Komiyama, N. H., Grant, S. G. & O'Dell, T. J. (2011) Beta-adrenergic receptor activation rescues theta frequency stimulation-induced LTP deficits in mice expressing C-terminally truncated NMDA receptor GluN2A subunits. Learn Mem, 18(2), 118-27.

Morales, B., Choi, S. Y. & Kirkwood, A. (2002) Dark rearing alters the development of GABAergic transmission in visual cortex. J Neurosci, 22(18), 8084-90.

Morris, R. G. (1989) Synaptic plasticity and learning: selective impairment of learning rats and blockade of long-term potentiation in vivo by the N-methyl-D-aspartate receptor antagonist AP5. J Neurosci, 9(9), 3040-57.

Mota Vieira, M., Nguyen, T. A., Wu, K., Badger, J. D., 2nd, Collins, B. M., Anggono, V., Lu, W. & Roche, K. W. (2020) An Epilepsy-Associated GRIN2A Rare Variant Disrupts CaMKIIalpha Phosphorylation of GluN2A and NMDA Receptor Trafficking. Cell Rep, 32(9), 108104.

Mower, G. D. (1991) The effect of dark rearing on the time course of the critical period in cat visual cortex. Brain Res Dev Brain Res, 58(2), 151-8.

Muller, T., Grosche, J., Ohlemeyer, C. & Kettenmann, H. (1993) NMDA-activated currents in Bergmann glial cells. Neuroreport, 4(6), 671-4.

Myers, R. A., Casals, F., Gauthier, J., Hamdan, F. F., Keebler, J., Boyko, A. R., Bustamante, C. D., Piton, A. M., Spiegelman, D., Henrion, E., Zilversmit, M., Hussin, J., Quinlan, J., Yang, Y., Lafreniere, R. G., Griffing, A. R., Stone, E. A., Rouleau, G. A. & Awadalla, P. (2011) A population genetic approach to mapping neurological disorder genes using deep resequencing. PLoS Genet, 7(2), e1001318.

Nabavi, S., Kessels, H. W., Alfonso, S., Aow, J., Fox, R. & Malinow, R. (2013) Metabotropic NMDA receptor function is required for NMDA receptor-dependent long-term depression. Proc Natl Acad Sci U S A, 110(10), 4027-32.

Nguyen, P. V., Abel, T. & Kandel, E. R. (1994) Requirement of a critical period of transcription for induction of a late phase of LTP. Science, 265(5175), 1104-7.

Nicoletti, F., Meek, J. L., Iadarola, M. J., Chuang, D. M., Roth, B. L. & Costa, E. (1986) Coupling of inositol phospholipid metabolism with excitatory amino acid recognition sites in rat hippocampus. J Neurochem, 46(1), 40-6.

O'Kusky, J. & Colonnier, M. (1982) A laminar analysis of the number of neurons, glia, and synapses in the adult cortex (area 17) of adult macaque monkeys. J Comp Neurol, 210(3), 278-90.

O'Roak, B. J., Deriziotis, P., Lee, C., Vives, L., Schwartz, J. J., Girirajan, S., Karakoc, E., Mackenzie, A. P., Ng, S. B., Baker, C., Rieder, M. J., Nickerson, D. A., Bernier,

R., Fisher, S. E., Shendure, J. & Eichler, E. E. (2011) Exome sequencing in sporadic autism spectrum disorders identifies severe de novo mutations. Nat Genet, 43(6), 585-9.

O'Roak, B. J., Vives, L., Fu, W., Egertson, J. D., Stanaway, I. B., Phelps, I. G., Carvill, G., Kumar, A., Lee, C., Ankenman, K., Munson, J., Hiatt, J. B., Turner, E. H., Levy, R., O'Day, D. R., Krumm, N., Coe, B. P., Martin, B. K., Borenstein, E., Nickerson, D. A., Mefford, H. C., Doherty, D., Akey, J. M., Bernier, R., Eichler, E. E. & Shendure, J. (2012) Multiplex targeted sequencing identifies recurrently mutated genes in autism spectrum disorders. Science, 338(6114), 1619-22.

Obara-Michlewska, M., Ruszkiewicz, J., Zielinska, M., Verkhratsky, A. & Albrecht, J. (2015) Astroglial NMDA receptors inhibit expression of Kir4.1 channels in glutamate-overexposed astrocytes in vitro and in the brain of rats with acute liver failure. Neurochem Int, 88, 20-5.

Oja, E. (1982) A simplified neuron model as a principal component analyzer. J Math Biol, 15(3), 267-73.

Olney, J. W. (1969) Brain lesions, obesity, and other disturbances in mice treated with monosodium glutamate. Science, 164(3880), 719-21.

Olsen, S. R., Bortone, D. S., Adesnik, H. & Scanziani, M. (2012) Gain control by layer six in cortical circuits of vision. Nature, 483(7387), 47-52.

Olverman, H. J., Jones, A. W. & Watkins, J. C. (1984) L-glutamate has higher affinity than other amino acids for [3H]-D-AP5 binding sites in rat brain membranes. Nature, 307(5950), 460-2.

Opazo, P., Labrecque, S., Tigaret, C. M., Frouin, A., Wiseman, P. W., De Koninck, P. & Choquet, D. (2010) CaMKII triggers the diffusional trapping of surface AMPARs through phosphorylation of stargazin. Neuron, 67(2), 239-52.

Opazo, P., Sainlos, M. & Choquet, D. (2012) Regulation of AMPA receptor surface diffusion by PSD-95 slots. Curr Opin Neurobiol, 22(3), 453-60.

Orban, G. A. (2008) Higher order visual processing in macaque extrastriate cortex. Physiol Rev, 88(1), 59-89.

Osten, P., Khatri, L., Perez, J. L., Kohr, G., Giese, G., Daly, C., Schulz, T. W., Wensky, A., Lee, L. M. & Ziff, E. B. (2000) Mutagenesis reveals a role for ABP/GRIP binding to GluR2 in synaptic surface accumulation of the AMPA receptor. Neuron, 27(2), 313-25.

Palygin, O., Lalo, U. & Pankratov, Y. (2011) Distinct pharmacological and functional properties of NMDA receptors in mouse cortical astrocytes. Br J Pharmacol, 163(8), 1755-66.

Pan, Y., Chen, J., Guo, H., Ou, J., Peng, Y., Liu, Q., Shen, Y., Shi, L., Liu, Y., Xiong, Z., Zhu, T., Luo, S., Hu, Z., Zhao, J. & Xia, K. (2015) Association of genetic variants of GRIN2B with autism. Sci Rep, 5, 8296.

Paoletti, P., Ascher, P. & Neyton, J. (1997) High-affinity zinc inhibition of NMDA NR1-NR2A receptors. J Neurosci, 17(15), 5711-25.

Paoletti, P., Bellone, C. & Zhou, Q. (2013) NMDA receptor subunit diversity: impact on receptor properties, synaptic plasticity and disease. Nat Rev Neurosci, 14(6), 383-400.

Park, M., Penick, E. C., Edwards, J. G., Kauer, J. A. & Ehlers, M. D. (2004) Recycling endosomes supply AMPA receptors for LTP. Science, 305(5692), 1972-5.

Parsons, M. P. & Raymond, L. A. (2014) Extrasynaptic NMDA receptor involvement in central nervous system disorders. Neuron, 82(2), 279-93.

Passafaro, M., Piech, V. & Sheng, M. (2001) Subunit-specific temporal and spatial patterns of AMPA receptor exocytosis in hippocampal neurons. Nat Neurosci, 4(9), 917-26.

Patterson, M. & Yasuda, R. (2011) Signalling pathways underlying structural plasticity of dendritic spines. Br J Pharmacol, 163(8), 1626-38.

Patterson, M. A., Szatmari, E. M. & Yasuda, R. (2010) AMPA receptors are exocytosed in stimulated spines and adjacent dendrites in a Ras-ERK-dependent manner during long-term potentiation. Proc Natl Acad Sci U S A, 107(36), 15951-6.

Pawlak, V., Schupp, B. J., Single, F. N., Seeburg, P. H. & Kohr, G. (2005) Impaired synaptic scaling in mouse hippocampal neurones expressing NMDA receptors with reduced calcium permeability. J Physiol, 562(Pt 3), 771-83.

Peirson, S. N., Brown, L. A., Pothecary, C. A., Benson, L. A. & Fisk, A. S. (2018) Light and the laboratory mouse. J Neurosci Methods, 300, 26-36.

Perez-Otano, I. & Ehlers, M. D. (2005) Homeostatic plasticity and NMDA receptor trafficking. Trends Neurosci, 28(5), 229-38.

Philpot, B. D., Cho, K. K. & Bear, M. F. (2007) Obligatory role of NR2A for metaplasticity in visual cortex. Neuron, 53(4), 495-502.

Philpot, B. D., Espinosa, J. S. & Bear, M. F. (2003) Evidence for altered NMDA receptor function as a basis for metaplasticity in visual cortex. J Neurosci, 23(13), 5583-8.

Philpot, B. D., Weisberg, M. P., Ramos, M. S., Sawtell, N. B., Tang, Y. P., Tsien, J. Z. & Bear, M. F. (2001) Effect of transgenic overexpression of NR2B on NMDA receptor function and synaptic plasticity in visual cortex. Neuropharmacology, 41(6), 762-70.

Piguel, N. H., Fievre, S., Blanc, J. M., Carta, M., Moreau, M. M., Moutin, E., Pinheiro, V. L., Medina, C., Ezan, J., Lasvaux, L., Loll, F., Durand, C. M., Chang, K., Petralia, R. S., Wenthold, R. J., Stephenson, F. A., Vuillard, L., Darbon, H., Perroy, J., Mulle, C., Montcouquiol, M., Racca, C. & Sans, N. (2014) Scribble1/AP2 complex coordinates NMDA receptor endocytic recycling. Cell Rep, 9(2), 712-27.

Plath, N., Ohana, O., Dammermann, B., Errington, M. L., Schmitz, D., Gross, C., Mao, X., Engelsberg, A., Mahlke, C., Welzl, H., Kobalz, U., Stawrakakis, A., Fernandez, E., Waltereit, R., Bick-Sander, A., Therstappen, E., Cooke, S. F., Blanquet, V., Wurst, W., Salmen, B., Bosl, M. R., Lipp, H. P., Grant, S. G., Bliss, T. V., Wolfer, D. P. & Kuhl, D. (2006) Arc/Arg3.1 is essential for the consolidation of synaptic plasticity and memories. Neuron, 52(3), 437-44.

Platzer, K., Yuan, H., Schutz, H., Winschel, A., Chen, W., Hu, C., Kusumoto, H., Heyne, H. O., Helbig, K. L., Tang, S., Willing, M. C., Tinkle, B. T., Adams, D. J., Depienne, C., Keren, B., Mignot, C., Frengen, E., Stromme, P., Biskup, S., Docker, D., Strom, T. M., Mefford, H. C., Myers, C. T., Muir, A. M., LaCroix, A., Sadleir, L., Scheffer, I. E., Brilstra, E., van Haelst, M. M., van der Smagt, J. J., Bok, L. A., Moller, R. S., Jensen, U. B., Millichap, J. J., Berg, A. T., Goldberg, E. M., De Bie, I., Fox, S., Major, P., Jones, J. R., Zackai, E. H., Abou Jamra, R., Rolfs, A., Leventer, R. J., Lawson, J. A., Roscioli, T., Jansen, F. E., Ranza, E., Korff, C. M., Lehesjoki, A. E., Courage, C., Linnankivi, T., Smith, D. R., Stanley, C., Mintz, M., McKnight, D., Decker, A., Tan, W. H., Tarnopolsky, M. A., Brady, L. I., Wolff, M., Dondit, L., Pedro, H. F., Parisotto, S. E., Jones, K. L., Patel, A. D., Franz, D. N., Vanzo, R., Marco, E., Ranells, J. D., Di Donato, N., Dobyns, W. B., Laube, B., Traynelis, S. F. & Lemke, J. R. (2017) GRIN2B encephalopathy: novel findings on phenotype, variant clustering, functional consequences and treatment aspects. J Med Genet, 54(7), 460-470.

Pouille, F. & Scanziani, M. (2001) Enforcement of temporal fidelity in pyramidal cells by somatic feed-forward inhibition. Science, 293(5532), 1159-63.

Punnakkal, P., Jendritza, P. & Kohr, G. (2012) Influence of the intracellular GluN2 C-terminal domain on NMDA receptor function. Neuropharmacology, 62(5-6), 1985-92.

Purpura, D. P., Girado, M., Smith, T. G., Callan, D. A. & Grundfest, H. (1959) Structure-activity determinants of pharmacological effects of amino acids and related compounds on central synapses. J Neurochem, 3(3), 238-68.

Quinlan, E. M., Olstein, D. H. & Bear, M. F. (1999a) Bidirectional, experience-dependent regulation of N-methyl-D-aspartate receptor subunit composition in the rat visual cortex during postnatal development. Proc Natl Acad Sci U S A, 96(22), 12876-80.

Quinlan, E. M., Philpot, B. D., Huganir, R. L. & Bear, M. F. (1999b) Rapid, experience-dependent expression of synaptic NMDA receptors in visual cortex in vivo. Nat Neurosci, 2(4), 352-7.

Rauch, A., Wieczorek, D., Graf, E., Wieland, T., Endele, S., Schwarzmayr, T., Albrecht, B., Bartholdi, D., Beygo, J., Di Donato, N., Dufke, A., Cremer, K., Hempel, M., Horn, D., Hoyer, J., Joset, P., Ropke, A., Moog, U., Riess, A., Thiel, C. T., Tzschach, A., Wiesener, A., Wohlleber, E., Zweier, C., Ekici, A. B., Zink, A. M., Rump, A., Meisinger, C., Grallert, H., Sticht, H., Schenck, A., Engels, H., Rappold, G., Schrock, E., Wieacker, P., Riess, O., Meitinger, T., Reis, A. & Strom, T. M. (2012) Range of genetic mutations associated with severe non-syndromic sporadic intellectual disability: an exome sequencing study. Lancet, 380(9854), 1674-82.

Rauner, C. & Kohr, G. (2011) Triheteromeric NR1/NR2A/NR2B receptors constitute the major N-methyl-D-aspartate receptor population in adult hippocampal synapses. J Biol Chem, 286(9), 7558-66.

Ravikrishnan, A., Gandhi, P. J., Shelkar, G. P., Liu, J., Pavuluri, R. & Dravid, S. M. (2018) Region-specific Expression of NMDA Receptor GluN2C Subunit in Parvalbumin-Positive Neurons and Astrocytes: Analysis of GluN2C Expression using a Novel Reporter Model. Neuroscience, 380, 49-62.

Riou, M., Stroebel, D., Edwardson, J. M. & Paoletti, P. (2012) An alternating GluN1-2-1-2 subunit arrangement in mature NMDA receptors. PLoS One, 7(4), e35134.

Rittenhouse, C. D., Shouval, H. Z., Paradiso, M. A. & Bear, M. F. (1999) Monocular deprivation induces homosynaptic long-term depression in visual cortex. Nature, 397(6717), 347-50.

Roberts, E. B. & Ramoa, A. S. (1999) Enhanced NR2A subunit expression and decreased NMDA receptor decay time at the onset of ocular dominance plasticity in the ferret. J Neurophysiol, 81(5), 2587-91.

Robertson, C. E. & Baron-Cohen, S. (2017) Sensory perception in autism. Nat Rev Neurosci, 18(11), 671-684.

Roche, K. W., O'Brien, R. J., Mammen, A. L., Bernhardt, J. & Huganir, R. L. (1996) Characterization of multiple phosphorylation sites on the AMPA receptor GluR1 subunit. Neuron, 16(6), 1179-88.

Roche, K. W., Standley, S., McCallum, J., Dune Ly, C., Ehlers, M. D. & Wenthold, R. J. (2001) Molecular determinants of NMDA receptor internalization. Nat Neurosci, 4(8), 794-802.

Rodenas-Ruano, A., Chavez, A. E., Cossio, M. J., Castillo, P. E. & Zukin, R. S. (2012) REST-dependent epigenetic remodeling promotes the developmental switch in synaptic NMDA receptors. Nat Neurosci, 15(10), 1382-90.

Rodriguez, G., Mesik, L., Gao, M., Parkins, S., Saha, R. & Lee, H. K. (2019) Disruption of NMDAR Function Prevents Normal Experience-Dependent Homeostatic Synaptic Plasticity in Mouse Primary Visual Cortex. J Neurosci, 39(39), 7664-7673.

Rosier, A. M., Arckens, L., Orban, G. A. & Vandesande, F. (1993) Laminar distribution of NMDA receptors in cat and monkey visual cortex visualized by [3H]-MK-801 binding. J Comp Neurol, 335(3), 369-80.

Roth, M. M., Dahmen, J. C., Muir, D. R., Imhof, F., Martini, F. J. & Hofer, S. B. (2016) Thalamic nuclei convey diverse contextual information to layer 1 of visual cortex. Nat Neurosci, 19(2), 299-307.

Ryan, T. J., Emes, R. D., Grant, S. G. & Komiyama, N. H. (2008) Evolution of NMDA receptor cytoplasmic interaction domains: implications for organisation of synaptic signalling complexes. BMC Neurosci, 9, 6.

Ryan, T. J., Kopanitsa, M. V., Indersmitten, T., Nithianantharajah, J., Afinowi, N. O., Pettit, C., Stanford, L. E., Sprengel, R., Saksida, L. M., Bussey, T. J., O'Dell, T. J., Grant, S. G. & Komiyama, N. H. (2013) Evolution of GluN2A/B cytoplasmic domains diversified vertebrate synaptic plasticity and behavior. Nat Neurosci, 16(1), 25-32.

Sanderson, J. L., Gorski, J. A. & Dell'Acqua, M. L. (2016) NMDA Receptor-Dependent LTD Requires Transient Synaptic Incorporation of Ca(2)(+)-Permeable AMPARs Mediated by AKAP150-Anchored PKA and Calcineurin. Neuron, 89(5), 1000-15.

Sanz-Clemente, A., Gray, J. A., Ogilvie, K. A., Nicoll, R. A. & Roche, K. W. (2013a) Activated CaMKII couples GluN2B and casein kinase 2 to control synaptic NMDA receptors. Cell Rep, 3(3), 607-14.

Sanz-Clemente, A., Matta, J. A., Isaac, J. T. & Roche, K. W. (2010) Casein kinase 2 regulates the NR2 subunit composition of synaptic NMDA receptors. Neuron, 67(6), 984-96.

Sanz-Clemente, A., Nicoll, R. A. & Roche, K. W. (2013b) Diversity in NMDA receptor composition: many regulators, many consequences. Neuroscientist, 19(1), 62-75.

Sapkota, K., Dore, K., Tang, K., Irvine, M., Fang, G., Burnell, E. S., Malinow, R., Jane, D. E. & Monaghan, D. T. (2019) The NMDA receptor intracellular C-terminal domains reciprocally interact with allosteric modulators. Biochem Pharmacol, 159, 140-153.

Scala, F., Kobak, D., Shan, S., Bernaerts, Y., Laturnus, S., Cadwell, C. R., Hartmanis, L., Froudarakis, E., Castro, J. R., Tan, Z. H., Papadopoulos, S., Patel, S. S., Sandberg, R., Berens, P., Jiang, X. & Tolias, A. S. (2019) Layer 4 of mouse neocortex differs in cell types and circuit organization between sensory areas. Nat Commun, 10(1), 4174.

Scannevin, R. H. & Huganir, R. L. (2000) Postsynaptic organization and regulation of excitatory synapses. Nat Rev Neurosci, 1(2), 133-41.

Schipke, C. G., Ohlemeyer, C., Matyash, M., Nolte, C., Kettenmann, H. & Kirchhoff, F. (2001) Astrocytes of the mouse neocortex express functional N-methyl-D-aspartate receptors. FASEB J, 15(7), 1270-2.

Schizophrenia Working Group of the Psychiatric Genomics, C. (2014) Biological insights from 108 schizophrenia-associated genetic loci. Nature, 511(7510), 421-7.

Schneggenburger, R. (1996) Simultaneous measurement of Ca2+ influx and reversal potentials in recombinant N-methyl-D-aspartate receptor channels. Biophys J, 70(5), 2165-74.

Seeburg, P. H., Burnashev, N., Kohr, G., Kuner, T., Sprengel, R. & Monyer, H. (1995) The NMDA receptor channel: molecular design of a coincidence detector. Recent Prog Horm Res, 50, 19-34.

Sharp, C. D., Hines, I., Houghton, J., Warren, A., Jackson, T. H. t., Jawahar, A., Nanda, A., Elrod, J. W., Long, A., Chi, A., Minagar, A. & Alexander, J. S. (2003) Glutamate causes a loss in human cerebral endothelial barrier integrity through activation of NMDA receptor. Am J Physiol Heart Circ Physiol, 285(6), H2592-8.

Shcherbatyy, V., Carson, J., Yaylaoglu, M., Jackle, K., Grabbe, F., Brockmeyer, M., Yavuz, H. & Eichele, G. (2015) A digital atlas of ion channel expression patterns in the two-week-old rat brain. Neuroinformatics, 13(1), 111-25.

Sheng, M. & Kim, M. J. (2002) Postsynaptic signaling and plasticity mechanisms. Science, 298(5594), 776-80.

Sheng, M. & Pak, D. T. (2000) Ligand-gated ion channel interactions with cytoskeletal and signaling proteins. Annu Rev Physiol, 62, 755-78.

Shinozaki, H. & Konishi, S. (1970) Actions of several anthelmintics and insecticides on rat cortical neurones. Brain Res, 24(2), 368-71.

Shinozaki, H. & Shibuya, I. (1974) A new potent excitant, quisqualic acid: effects on crayfish neuromuscular junction. Neuropharmacology, 13(7), 665-72.

Shipp, S. & Zeki, S. (1989) The Organization of Connections between Areas V5 and V1 in Macaque Monkey Visual Cortex. Eur J Neurosci, 1(4), 309-32.

Simons, D. J. & Woolsey, T. A. (1984) Morphology of Golgi-Cox-impregnated barrel neurons in rat SmI cortex. J Comp Neurol, 230(1), 119-32.

Skowronska, K., Obara-Michlewska, M., Czarnecka, A., Dabrowska, K., Zielinska, M. & Albrecht, J. (2019) Persistent Overexposure to N-Methyl-D-Aspartate (NMDA) Calcium-Dependently Downregulates Glutamine Synthetase, Aquaporin 4, and Kir4.1 Channel in Mouse Cortical Astrocytes. Neurotox Res, 35(1), 271-280.

Sladeczek, F., Pin, J. P., Recasens, M., Bockaert, J. & Weiss, S. (1985) Glutamate stimulates inositol phosphate formation in striatal neurones. Nature, 317(6039), 717-9.

Smith, G. B., Heynen, A. J. & Bear, M. F. (2009) Bidirectional synaptic mechanisms of ocular dominance plasticity in visual cortex. Philos Trans R Soc Lond B Biol Sci, 364(1515), 357-67.

Soares, C., Lee, K. F., Nassrallah, W. & Beique, J. C. (2013) Differential subcellular targeting of glutamate receptor subtypes during homeostatic synaptic plasticity. J Neurosci, 33(33), 13547-59.

Soriano, F. X. & Hardingham, G. E. (2007) Compartmentalized NMDA receptor signalling to survival and death. J Physiol, 584(Pt 2), 381-7.

Sprengel, R., Suchanek, B., Amico, C., Brusa, R., Burnashev, N., Rozov, A., Hvalby, O., Jensen, V., Paulsen, O., Andersen, P., Kim, J. J., Thompson, R. F., Sun, W., Webster, L. C., Grant, S. G., Eilers, J., Konnerth, A., Li, J., McNamara, J. O. & Seeburg, P. H. (1998) Importance of the intracellular domain of NR2 subunits for NMDA receptor function in vivo. Cell, 92(2), 279-89.

Stanic, J., Carta, M., Eberini, I., Pelucchi, S., Marcello, E., Genazzani, A. A., Racca, C., Mulle, C., Di Luca, M. & Gardoni, F. (2015) Rabphilin 3A retains NMDA receptors at synaptic sites through interaction with GluN2A/PSD-95 complex. Nat Commun, 6, 10181.

Stein, I. S., Gray, J. A. & Zito, K. (2015) Non-Ionotropic NMDA Receptor Signaling Drives Activity-Induced Dendritic Spine Shrinkage. J Neurosci, 35(35), 12303-8.

Strehlow, V., Rieubland, C., Gallati, S., Kim, S., Myers, S. J., Peterson, V., Ramsey, A. J., Teuscher, D. D., Traynelis, S. F. & Lemke, J. R. (2022) Compound-heterozygous GRIN2A null variants associated with severe developmental and epileptic encephalopathy. Epilepsia.

Stroebel, D., Casado, M. & Paoletti, P. (2018) Triheteromeric NMDA receptors: from structure to synaptic physiology. Curr Opin Physiol, 2, 1-12.

Sullivan, T. J. & de Sa, V. R. (2006) Homeostatic synaptic scaling in self-organizing maps. Neural Netw, 19(6-7), 734-43.

Sutton, M. A., Ito, H. T., Cressy, P., Kempf, C., Woo, J. C. & Schuman, E. M. (2006) Miniature neurotransmission stabilizes synaptic function via tonic suppression of local dendritic protein synthesis. Cell, 125(4), 785-99.

Takasaki, Y., Koide, T., Wang, C., Kimura, H., Xing, J., Kushima, I., Ishizuka, K., Mori, D., Sekiguchi, M., Ikeda, M., Aizawa, M., Tsurumaru, N., Iwayama, Y., Yoshimi, A., Arioka, Y., Yoshida, M., Noma, H., Oya-Ito, T., Nakamura, Y., Kunimoto, S., Aleksic, B., Uno, Y., Okada, T., Ujike, H., Egawa, J., Kuwabara, H., Someya, T., Yoshikawa, T., Iwata, N. & Ozaki, N. (2016) Mutation screening of GRIN2B in schizophrenia and autism spectrum disorder in a Japanese population. Sci Rep, 6, 33311.

Tarabeux, J., Kebir, O., Gauthier, J., Hamdan, F. F., Xiong, L., Piton, A., Spiegelman, D., Henrion, E., Millet, B., team, S. D., Fathalli, F., Joober, R., Rapoport, J. L., DeLisi, L. E., Fombonne, E., Mottron, L., Forget-Dubois, N., Boivin, M., Michaud, J. L., Drapeau, P., Lafreniere, R. G., Rouleau, G. A. & Krebs, M. O. (2011) Rare mutations in N-methyl-D-aspartate glutamate receptors in autism spectrum disorders and schizophrenia. Transl Psychiatry, 1, e55.

Tovar, K. R., McGinley, M. J. & Westbrook, G. L. (2013) Triheteromeric NMDA receptors at hippocampal synapses. J Neurosci, 33(21), 9150-60.

Townsend, M., Yoshii, A., Mishina, M. & Constantine-Paton, M. (2003) Developmental loss of miniature N-methyl-D-aspartate receptor currents in NR2A knockout mice. Proc Natl Acad Sci U S A, 100(3), 1340-5.

Tran, H. Q., Chung, Y. H., Shin, E. J., Tran, T. V., Jeong, J. H., Jang, C. G., Nah, S. Y., Yamada, K., Nabeshima, T. & Kim, H. C. (2017) MK-801, but not naloxone, attenuates high-dose dextromethorphan-induced convulsive behavior: Possible involvement of the GluN2B receptor. Toxicol Appl Pharmacol, 334, 158-166.

Tsiola, A., Hamzei-Sichani, F., Peterlin, Z. & Yuste, R. (2003) Quantitative morphologic classification of layer 5 neurons from mouse primary visual cortex. J Comp Neurol, 461(4), 415-28.

Tsumoto, T., Hagihara, K., Sato, H. & Hata, Y. (1987) NMDA receptors in the visual cortex of young kittens are more effective than those of adult cats. Nature, 327(6122), 513-4.

Turrigiano, G. G. (2008) The self-tuning neuron: synaptic scaling of excitatory synapses. Cell, 135(3), 422-35.

Turrigiano, G. G., Leslie, K. R., Desai, N. S., Rutherford, L. C. & Nelson, S. B. (1998) Activity-dependent scaling of quantal amplitude in neocortical neurons. Nature, 391(6670), 892-6.

Tymianski, M. (2011) Emerging mechanisms of disrupted cellular signaling in brain ischemia. Nat Neurosci, 14(11), 1369-73.

Van Harreveld, A. (1959) Compounds in brain extracts causing spreading depression of cerebral cortical activity and contraction of crustacean muscle. J Neurochem, 3(4), 300-15.

Vicini, S., Wang, J. F., Li, J. H., Zhu, W. J., Wang, Y. H., Luo, J. H., Wolfe, B. B. & Grayson, D. R. (1998) Functional and pharmacological differences between recombinant N-methyl-D-aspartate receptors. J Neurophysiol, 79(2), 555-66.

Volianskis, A., France, G., Jensen, M. S., Bortolotto, Z. A., Jane, D. E. & Collingridge, G. L. (2015) Long-term potentiation and the role of N-methyl-D-aspartate receptors. Brain Res, 1621, 5-16.

von Stulpnagel, C., Ensslen, M., Moller, R. S., Pal, D. K., Masnada, S., Veggiotti, P., Piazza, E., Dreesmann, M., Hartlieb, T., Herberhold, T., Hughes, E., Koch, M., Kutzer, C., Hoertnagel, K., Nitanda, J., Pohl, M., Rostasy, K., Haack, T. B., Stohr, K., Kluger, G. & Borggraefe, I. (2017) Epilepsy in patients with GRIN2A alterations: Genetics, neurodevelopment, epileptic phenotype and response to anticonvulsive drugs. Eur J Paediatr Neurol, 21(3), 530-541.

Wahl, A. S., Buchthal, B., Rode, F., Bomholt, S. F., Freitag, H. E., Hardingham, G. E., Ronn, L. C. & Bading, H. (2009) Hypoxic/ischemic conditions induce expression of the putative pro-death gene Clca1 via activation of extrasynaptic N-methyl-D-aspartate receptors. Neuroscience, 158(1), 344-52.

Wang, C., Pralong, W. F., Schulz, M. F., Rougon, G., Aubry, J. M., Pagliusi, S., Robert, A. & Kiss, J. Z. (1996) Functional N-methyl-D-aspartate receptors in O-2A glial precursor cells: a critical role in regulating polysialic acid-neural cell adhesion molecule expression and cell migration. J Cell Biol, 135(6 Pt 1), 1565-81.

Warnet, X. L., Bakke Krog, H., Sevillano-Quispe, O. G., Poulsen, H. & Kjaergaard, M. (2021) The C-terminal domains of the NMDA receptor: How intrinsically

disordered tails affect signalling, plasticity and disease. Eur J Neurosci, 54(8), 6713-6739.

Weitlauf, C., Honse, Y., Auberson, Y. P., Mishina, M., Lovinger, D. M. & Winder, D. G. (2005) Activation of NR2A-containing NMDA receptors is not obligatory for NMDA receptor-dependent long-term potentiation. J Neurosci, 25(37), 8386-90.

Wiesel, T. N. & Hubel, D. H. (1965) Comparison of the effects of unilateral and bilateral eye closure on cortical unit responses in kittens. J Neurophysiol, 28(6), 1029-40.

Williams, H. J., Georgieva, L., Dwyer, S., Kirov, G., Owen, M. J. & O'Donovan, M. C. (2012) Absence of de novo point mutations in exons of GRIN2B in a large schizophrenia trio sample. Schizophr Res, 141(2-3), 274-6.

Wisden, W., Errington, M. L., Williams, S., Dunnett, S. B., Waters, C., Hitchcock, D., Evan, G., Bliss, T. V. & Hunt, S. P. (1990) Differential expression of immediate early genes in the hippocampus and spinal cord. Neuron, 4(4), 603-14.

Worley, P. F., Christy, B. A., Nakabeppu, Y., Bhat, R. V., Cole, A. J. & Baraban, J. M. (1991) Constitutive expression of zif268 in neocortex is regulated by synaptic activity. Proc Natl Acad Sci U S A, 88(12), 5106-10.

Wu, G. Y., Deisseroth, K. & Tsien, R. W. (2001) Activity-dependent CREB phosphorylation: convergence of a fast, sensitive calmodulin kinase pathway and a slow, less sensitive mitogen-activated protein kinase pathway. Proc Natl Acad Sci U S A, 98(5), 2808-13.

Wyllie, D. J., Livesey, M. R. & Hardingham, G. E. (2013) Influence of GluN2 subunit identity on NMDA receptor function. Neuropharmacology, 74, 4-17.

Xia, J., Zhang, X., Staudinger, J. & Huganir, R. L. (1999) Clustering of AMPA receptors by the synaptic PDZ domain-containing protein PICK1. Neuron, 22(1), 179-87.

Xia, Z., Dudek, H., Miranti, C. K. & Greenberg, M. E. (1996) Calcium influx via the NMDA receptor induces immediate early gene transcription by a MAP kinase/ERK-dependent mechanism. J Neurosci, 16(17), 5425-36.

Yang, W., Carrasquillo, Y., Hooks, B. M., Nerbonne, J. M. & Burkhalter, A. (2013) Distinct balance of excitation and inhibition in an interareal feedforward and feedback circuit of mouse visual cortex. J Neurosci, 33(44), 17373-84.

Yong, X. L. H., Zhang, L., Yang, L., Chen, X., Tan, J. Z. A., Yu, X., Chandra, M., Livingstone, E., Widagdo, J., Vieira, M. M., Roche, K. W., Lynch, J. W., Keramidas, A., Collins, B. M. & Anggono, V. (2021) Regulation of NMDA receptor trafficking

and gating by activity-dependent CaMKIIalpha phosphorylation of the GluN2A subunit. Cell Rep, 36(1), 109338.

Zhao, M. G., Toyoda, H., Lee, Y. S., Wu, L. J., Ko, S. W., Zhang, X. H., Jia, Y., Shum, F., Xu, H., Li, B. M., Kaang, B. K. & Zhuo, M. (2005) Roles of NMDA NR2B subtype receptor in prefrontal long-term potentiation and contextual fear memory. Neuron, 47(6), 859-72.

Figures created with BioRender.com.

Supplemental information

Figure S1

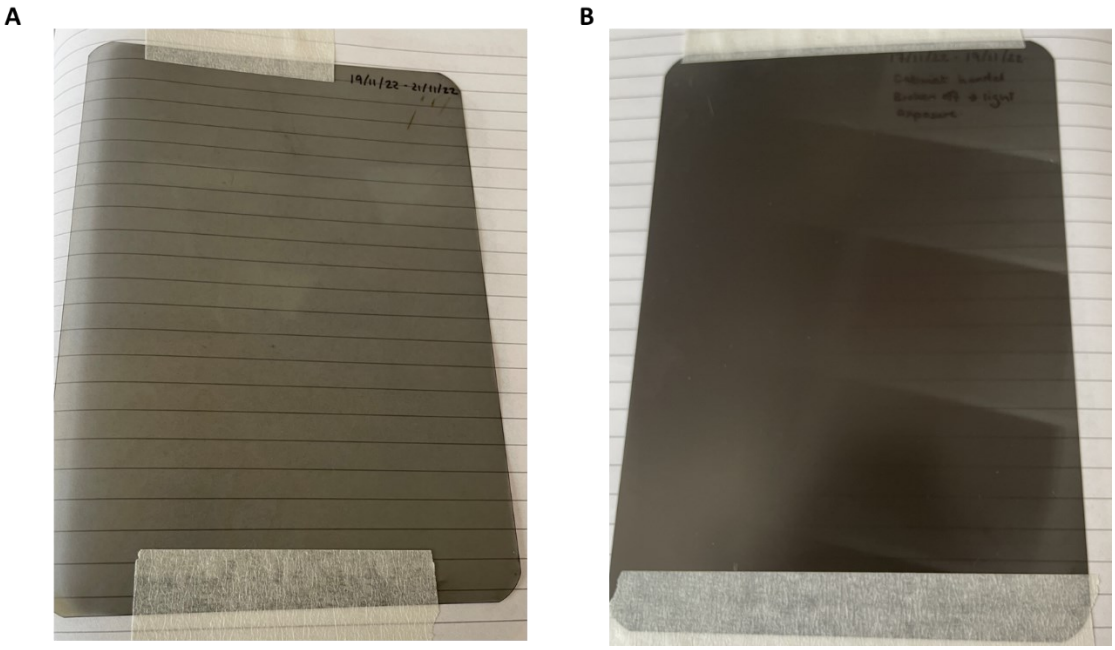

Figure S1 – Images of light sensitive film used as a control measure for light infiltration in the dark cabinet.

A) Example of non-exposed film indicating that there has been no light infiltration during the period in which the film was placed in the cabinet.

B) Example of film that has been exposed to light while in the dark cabinet. Darkness of the film and the distinct grid pattern indicate that the film was exposed to light while it was sitting on the shelves of the dark cabinet. Notes are made detailing the cause of the exposure and the standard operating procedure updated if required.

Figure S2

Figure S6

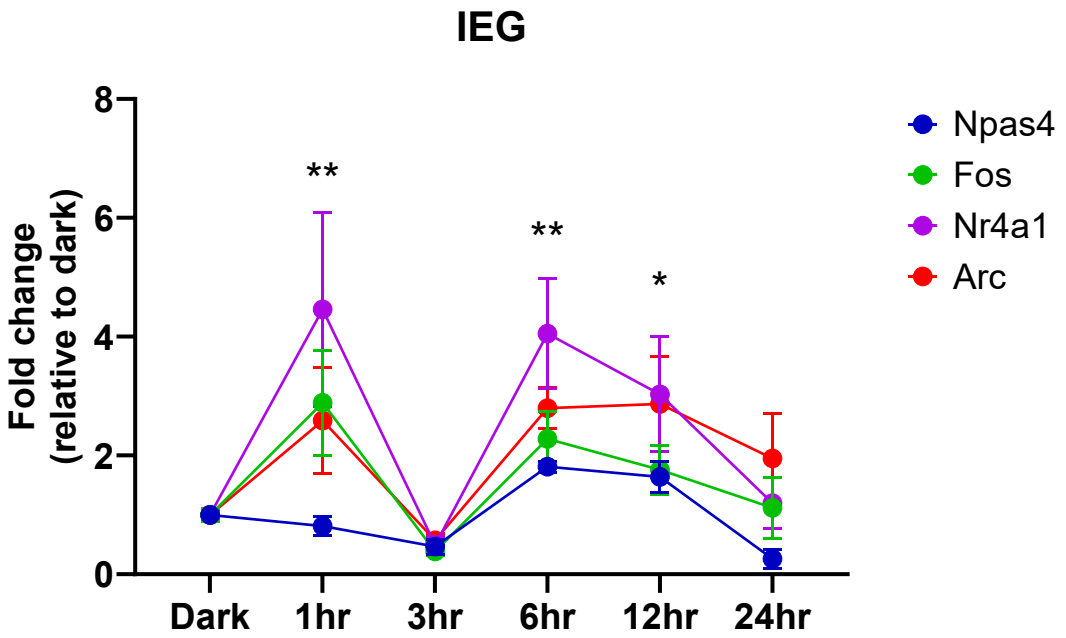

Figure S6– Time course of IEG following 7-day dark rearing.

The length of time that mice are re-exposed to light influences IEG expression. Most IEGs exhibit a peak in expression within the first hour of re-exposure, this then drops off by the third hour of exposure. Anecdotal observations suggest that the decrease observed at 3hr may be due to the animals sleeping. IEG expression rebounds again by 6hr where it remains elevated until 12Hrs, from which point expression begins to decline. Two-way ANOVA; re-exposure duration effect for IEG expression: $F(5, 124) = 5.601$, $p = 0.0001$. Dunnett's multiple comparisons test against dark, **P<0.01. *P<0.05.

Table S1 (1/2) – Genes differentially expressed in GluN2A$^{2B(CTR)/2B(CTR)}$ (Swap) under standard light

gene_name	WT_light_avg_fpkm	SWAP_light_avg_fpkm	light_SWAP_vs_WT.l2fc	light_SWAP_vs_WT.padj
Clec16a	17.05	24.79	0.50	8.76E-58
Hyi	2.73	4.24	0.33	1.53E-04
Per1	27.00	36.01	0.32	1.04E-06
Tnfrsf25	5.93	8.44	0.30	6.15E-04
Gpr3	2.80	3.69	0.28	5.27E-04
Tiparp	3.02	3.91	0.27	4.31E-04
Frmd6	6.71	8.70	0.27	1.11E-03
Xkr7	0.93	1.45	0.26	7.08E-03
Stk40	9.12	11.30	0.26	1.44E-06
Crlf3	4.22	5.34	0.26	1.53E-04
Jade2	7.73	9.70	0.26	1.15E-04
Bok	10.81	13.75	0.25	1.40E-03
Map3k14	1.05	1.40	0.25	9.44E-03
Celsr1	0.91	1.18	0.24	1.04E-02
Tnfaip3	0.90	1.19	0.24	1.26E-02
Sik1	2.88	3.83	0.24	1.72E-02
Phf13	5.57	6.86	0.24	1.15E-03
Wdr31	2.18	2.75	0.23	1.37E-02
Il33	5.14	6.48	0.22	1.55E-02
Tnnt2	1.48	1.91	0.22	2.24E-02
Serinc2	2.64	3.46	0.22	3.56E-02
Calhm2	1.35	1.73	0.22	3.38E-02
Bhlhe40	32.99	40.26	0.22	6.26E-03
Itpkc	2.52	3.15	0.21	3.03E-02
Rara	3.14	3.98	0.21	3.57E-02
Nnat	67.56	82.58	0.21	1.37E-02
Ier5	21.87	27.02	0.21	2.86E-02
Crhbp	11.13	13.56	0.21	1.19E-02
Spry4	2.62	3.23	0.21	2.18E-02
Pvr	3.00	3.66	0.21	1.69E-02
Cav2	17.51	20.87	0.20	1.25E-03
Tpd52l1	7.11	8.79	0.20	3.47E-02
Erich3	2.23	2.70	0.20	1.38E-02
Usp35	5.36	6.36	0.20	5.15E-03
Htr7	2.36	2.91	0.20	4.80E-02
Hebp1	6.02	7.32	0.20	3.38E-02
Cdc42ep4	9.93	11.68	0.20	6.15E-04
Zfp667	3.18	3.82	0.20	2.09E-02
Nab2	13.50	16.08	0.20	8.73E-03
Myo1c	4.67	5.57	0.19	2.33E-02
Lmbr1l	5.28	6.21	0.19	1.86E-02
Azin2	14.48	16.96	0.19	3.77E-03
Wnt7b	7.46	8.85	0.19	2.33E-02
Irf2bpl	14.61	17.23	0.18	2.18E-02
Arhgef26	5.48	6.39	0.18	3.43E-03
Ak4	7.53	8.87	0.18	3.21E-02
Map2k3	5.49	6.47	0.18	4.77E-02
Smad1	4.65	5.43	0.18	2.33E-02
Crkl	10.11	11.68	0.18	2.38E-04
Rassf5	6.59	7.72	0.18	3.57E-02
Bhlhe41	4.91	5.72	0.17	3.03E-02
Crebl2	8.04	9.27	0.17	4.16E-03
Cep164	4.16	4.83	0.17	3.12E-02
Rbm3	19.55	22.59	0.17	9.86E-03
Nipa1	18.77	21.44	0.16	5.31E-03
Mthfd1l	5.24	6.03	0.16	4.44E-02
Synpr	17.98	20.65	0.16	4.07E-02
Ipmk	5.82	6.65	0.16	2.31E-02
Lrig2	5.66	6.48	0.16	3.03E-02
Doc2a	22.09	25.13	0.15	3.30E-02
Zfp316	4.79	5.44	0.15	2.90E-02
Slc6a15	15.36	17.48	0.15	1.41E-02
Chst15	7.55	8.59	0.15	1.85E-02
Ache	17.03	19.24	0.14	4.95E-02
Neurl1a	37.48	42.00	0.14	4.00E-03
Alkbh5	10.04	11.22	0.13	2.31E-02
Dner	38.06	42.56	0.13	4.68E-02
Fam210a	4.11	4.58	0.13	4.26E-02
Pkia	46.73	51.74	0.12	1.11E-02
Trappc12	17.56	19.43	0.12	2.18E-02
Slc25a25	15.42	17.09	0.12	5.00E-02
Hpcal4	229.12	253.00	0.12	3.53E-02
Mturn	28.23	31.11	0.12	3.03E-02
Cry2	41.08	44.92	0.11	4.95E-02
Eif1ax	33.43	36.47	0.11	1.91E-02
Syn2	128.29	138.42	0.09	1.13E-02
Parp6	40.40	38.39	-0.09	2.86E-02
Smarcd1	55.62	52.26	-0.10	2.40E-02
Ndrg3	147.47	138.65	-0.10	5.10E-03
Dbn1	94.04	87.76	-0.11	2.18E-02
Cd47	34.78	32.43	-0.11	3.56E-02
Asic2	20.66	19.28	-0.11	3.47E-02
Coro2b	64.02	59.62	-0.11	9.28E-03
Wac	19.85	18.38	-0.12	1.07E-02
Map4k3	21.11	19.52	-0.12	1.85E-02
Ctxn1	285.64	264.27	-0.12	2.24E-03
Cdk5r2	121.30	111.80	-0.12	1.94E-02
Dlgap4	65.89	60.73	-0.12	6.40E-03
Itpk1	19.37	17.76	-0.13	4.92E-02
Zmynd8	27.69	25.40	-0.13	1.89E-02
Nlk	33.87	31.03	-0.13	4.95E-02
Snx3	75.95	69.41	-0.13	4.47E-02
Rabl2	19.18	17.56	-0.13	3.57E-02
Rnpep	19.80	18.09	-0.13	3.57E-02
Plcl2	18.92	17.30	-0.13	3.66E-02
Stx1b	166.54	152.15	-0.13	8.50E-03
Id2	58.24	53.00	-0.14	2.61E-02
Cacng2	19.05	17.37	-0.14	9.91E-03
Sik3	29.17	26.64	-0.14	2.05E-04

Table S1 (2/2)

Arpp21	100.09	91.41	-0.14	5.84E-05
Sel1l3	23.14	21.01	-0.14	8.43E-03
Cacng3	53.50	48.53	-0.14	8.67E-03
Kcnip2	32.99	29.93	-0.14	3.26E-02
Ccl27a	59.35	53.79	-0.14	1.65E-02
Med15	22.63	20.47	-0.14	2.67E-02
Flrt2	15.68	14.17	-0.14	3.54E-02
Slc30a3	62.79	56.54	-0.15	3.57E-02
Clvs1	14.15	12.80	-0.15	1.41E-02
Lingo1	125.79	112.86	-0.15	4.34E-02
Rnf126	36.57	32.98	-0.15	7.22E-03
Osbpl10	16.51	14.88	-0.15	1.15E-02
Mapk4	18.72	16.79	-0.15	4.46E-02
Baiap2	73.99	66.73	-0.15	4.10E-03
Sulf2	34.38	31.06	-0.15	1.85E-04
Kazn	15.81	14.21	-0.15	7.09E-03
Omg	67.71	60.66	-0.15	2.58E-02
Med14	13.27	11.85	-0.15	3.72E-02
Actn1	28.63	25.61	-0.16	1.05E-02
Ina	68.59	61.28	-0.16	1.42E-02
Cd34	39.39	35.37	-0.16	9.31E-04
Wee1	7.16	6.35	-0.16	4.59E-02
Trim9	86.32	76.48	-0.16	4.69E-02
Garnl3	35.07	31.34	-0.16	3.20E-03
Vip	18.66	16.57	-0.16	2.87E-02
Fscn1	96.08	85.51	-0.16	1.63E-02
Dynlrb1	108.16	96.25	-0.16	2.09E-02
Lrrtm3	15.63	13.90	-0.16	1.87E-02
Ly6e	87.12	77.49	-0.16	1.35E-02
Mical2	81.75	72.93	-0.16	4.90E-03
Nectin1	10.05	8.91	-0.17	1.64E-02
Lhfp	8.13	7.18	-0.17	1.91E-02
Plp1	590.93	517.66	-0.17	4.95E-02
Arntl	9.60	8.51	-0.17	9.81E-03
Nfatc3	3.04	2.65	-0.17	3.30E-02
Actn4	46.19	41.02	-0.17	2.98E-04
R3hdm1	64.91	56.85	-0.17	2.87E-02
Cwc22	5.43	4.75	-0.17	3.57E-02
Zfp386	4.80	4.20	-0.18	3.24E-02
Neto2	14.27	12.50	-0.18	8.73E-03
mt-Nd2	2952.31	2588.67	-0.18	6.40E-03
Fem1c	5.55	4.86	-0.18	1.55E-02
Prrt1	80.41	70.83	-0.18	7.26E-04
St8sia5	16.62	14.56	-0.18	2.44E-03
Dscaml1	10.97	9.50	-0.18	1.85E-02
Lrrk2	7.17	6.21	-0.18	1.26E-02
Fmnl1	41.72	36.15	-0.19	1.11E-02
Arhgap31	5.99	5.13	-0.19	3.12E-02
Gstm1	110.21	95.20	-0.19	1.35E-02
Galnt9	37.50	32.07	-0.19	3.47E-02
Fbxw7	61.48	54.06	-0.19	5.69E-06
Chrm2	2.91	2.49	-0.19	2.61E-02
Sdk2	5.37	4.51	-0.19	4.95E-02
Adam19	5.52	4.80	-0.20	6.15E-04
Ptk2	38.95	33.48	-0.20	5.54E-03
Zfpm1	8.72	7.42	-0.20	2.12E-02
Inhba	2.47	1.27	-0.20	1.81E-02
AI593442	43.84	38.25	-0.20	1.04E-06
Asap2	10.40	8.96	-0.20	1.62E-03
Ddx3x	58.81	50.61	-0.20	2.44E-03
Npas2	13.17	11.30	-0.20	5.56E-03
Colgalt2	2.12	1.78	-0.20	2.32E-02
Slc9a5	12.56	10.33	-0.20	4.34E-02
Tamalin	20.65	17.69	-0.21	1.17E-03
Dnajc1	5.00	4.13	-0.21	3.12E-02
Rasgef1b	19.97	17.21	-0.21	6.47E-05
Plekhh2	1.62	1.31	-0.21	4.44E-02
Med8	12.76	10.70	-0.21	9.73E-03
B3galt2	7.22	6.14	-0.21	2.94E-03
Dipk2a	13.50	11.28	-0.21	1.45E-02
Gfpt2	4.46	3.69	-0.21	2.12E-02
Adamts17	1.21	0.99	-0.21	1.86E-02
Hdac1	10.18	8.48	-0.22	8.20E-03
Epha10	15.06	12.38	-0.22	1.64E-02
mt-Nd4	1912.36	1612.12	-0.22	1.27E-03
Hs3st1	20.19	16.99	-0.22	1.23E-03
Fosb	4.81	2.78	-0.22	1.55E-02
Robo3	14.81	12.01	-0.22	1.76E-02
Mamld1	10.24	8.62	-0.22	6.15E-04
Zfp143	3.96	3.18	-0.23	2.27E-02
Dapk2	1.70	1.23	-0.23	3.54E-02
Sema3f	5.36	4.34	-0.23	1.03E-02
Flrt3	8.57	7.13	-0.23	1.40E-03
Sp2	6.17	5.13	-0.24	6.15E-04
Edn1	1.38	0.96	-0.24	1.91E-02
Npnt	17.89	14.83	-0.24	1.12E-04
Scnn1a	3.51	2.80	-0.25	3.53E-03
Kdm6a	6.96	5.57	-0.25	3.75E-03
Tpbg	5.91	4.86	-0.25	3.72E-04
Tnfrsf12a	3.37	2.36	-0.25	1.35E-02
Rnd1	17.56	14.03	-0.25	2.17E-03
Sult1a1	5.16	3.73	-0.25	1.13E-02
Zdhhc14	12.05	9.63	-0.26	1.11E-03
Eif2s3x	5.48	4.13	-0.26	6.25E-03
Egr3	54.18	35.35	-0.26	7.08E-03
Cited4	6.45	4.96	-0.26	3.06E-03
Zfp39	3.15	2.47	-0.27	6.15E-04
Homer1	39.82	27.54	-0.28	3.75E-03
Tmem254	23.10	17.81	-0.28	5.30E-04
Scube1	11.91	9.07	-0.33	5.09E-07
Fhip1a	3.38	2.47	-0.35	1.11E-06
Pim1	1.50	0.96	-0.35	5.97E-05
Ddit4l	16.60	12.12	-0.38	9.58E-10
Tekt5	4.36	2.75	-0.42	1.07E-07
Kcnj2	4.93	3.05	-0.42	1.02E-07
Bfar	11.91	7.50	-0.61	6.80E-47
Emp2	5.60	3.21	-0.63	6.58E-29

Table S2 (1/4) – Light_vs_Dark significant genotype interaction

gene_name	WT_light_vs_dark.l2fc	WT_light_vs_dark.padj	SWAP_light_vs_dark.l2fc	SWAP_light_vs_dark.padj	light_dark_genotype_interaction.l2fc	light_dark_genotype_interaction.padj
Fosb	0.86	8.60E-15	0.18	2.48E-01	1.35	2.60E-03
Gm15721	0.80	1.35E-14	0.21	1.01E-01	0.89	1.32E-03
Ptgs2	0.67	4.21E-09	0.35	1.10E-03	0.79	1.86E-02
Serpinb8	0.63	7.72E-10	0.03	8.75E-01	0.84	5.28E-03
Baz1a	0.61	1.38E-08	0.09	5.80E-01	0.77	4.99E-03
Tamalin	0.60	1.68E-21	0.19	3.56E-02	0.43	2.44E-03
Gcnt4	0.57	6.64E-15	0.23	8.33E-03	0.37	2.05E-02
Egr3	0.56	1.12E-06	0.09	4.98E-01	0.78	3.42E-03
Inhba	0.56	1.04E-06	0.30	1.44E-02	1.15	1.08E-02
Strip2	0.55	3.80E-15	0.21	4.17E-02	0.36	3.82E-02
Hkdc1	0.54	3.76E-14	0.29	8.05E-06	0.30	3.27E-02
Pmepa1	0.52	2.43E-23	0.27	6.22E-06	0.26	1.29E-02
Stard8	0.52	9.68E-14	0.14	2.28E-01	0.40	2.15E-02
Tnfrsf12a	0.51	4.18E-06	0.04	8.27E-01	0.70	1.29E-02
Prmt8	0.50	5.36E-12	0.16	5.64E-04	0.40	8.95E-04
Net1	0.49	7.79E-11	0.00	9.83E-01	0.55	4.64E-04
Pparg	0.48	1.58E-06	0.13	3.48E-01	0.46	4.22E-02
Asb11	0.48	5.64E-06	0.03	8.81E-01	0.63	3.62E-03
Rnd1	0.46	1.64E-07	-0.02	9.05E-01	0.57	1.20E-03
Slc9a5	0.46	7.71E-08	0.04	7.68E-01	0.50	2.38E-03
Ism1	0.45	1.36E-05	0.03	8.63E-01	0.55	1.40E-02
Smim43	0.45	7.18E-08	-0.01	9.43E-01	0.54	2.24E-03
Scube1	0.44	6.65E-18	0.07	5.36E-01	0.38	3.92E-03
Tmem267	0.43	1.52E-05	0.00	9.82E-01	0.55	2.20E-02
Camk1g	0.42	1.11E-06	0.07	5.90E-01	0.43	1.77E-02
Homer1	0.40	3.64E-04	-0.02	9.14E-01	0.59	3.17E-02
Dusp14	0.40	1.10E-10	0.16	5.37E-03	0.27	1.53E-02
Rgs4	0.40	4.16E-18	0.14	9.33E-02	0.26	3.13E-02
Rnd3	0.39	2.72E-06	0.04	7.50E-01	0.41	1.26E-02
Mfsd2a	0.39	2.21E-07	-0.16	2.96E-01	0.73	2.38E-03
Nrn1	0.39	1.26E-06	0.12	9.43E-02	0.32	3.65E-02
Mapk4	0.38	3.84E-08	0.02	8.79E-01	0.40	5.90E-04
St8sia5	0.37	1.65E-15	0.12	5.34E-02	0.27	1.38E-03
Gm42528	0.37	8.25E-04	-0.12	2.81E-01	0.65	2.38E-03
Hmgb3	0.37	9.56E-06	0.09	3.68E-01	0.34	2.17E-02
Pak6	0.37	1.38E-11	0.10	1.03E-01	0.29	2.38E-03
Mir22hg	0.37	3.02E-08	0.09	3.88E-01	0.30	4.76E-02
Rgs2	0.36	7.95E-10	0.07	3.21E-01	0.32	1.38E-03
Rgs7	0.36	1.23E-12	0.11	5.31E-02	0.26	2.44E-03
Scg2	0.36	3.01E-05	0.01	8.96E-01	0.40	5.82E-03
Tob1	0.35	1.92E-04	-0.12	3.85E-01	0.58	7.46E-03
Gimap6	0.35	4.69E-03	-0.11	4.92E-01	0.70	1.53E-02
Cacng3	0.35	1.69E-14	0.15	1.88E-02	0.20	4.56E-02
Ppm1h	0.34	5.02E-06	0.03	7.42E-01	0.35	1.08E-02
Marchf1	0.34	1.47E-06	0.05	7.34E-01	0.33	4.88E-02
Klf9	0.34	2.83E-09	-0.03	7.85E-01	0.40	8.17E-04
Mpp3	0.34	9.85E-11	0.12	1.06E-01	0.23	3.24E-02
Mapk6	0.34	2.36E-06	0.06	3.96E-01	0.31	1.36E-02
Erg	0.33	1.40E-03	-0.03	8.77E-01	0.46	2.17E-02
Gm10419	0.33	6.34E-08	0.10	9.50E-02	0.25	2.03E-02
Zfp36	0.33	7.42E-03	-0.07	6.92E-01	0.58	3.24E-02
Fos	0.33	5.69E-04	0.07	6.67E-01	1.86	2.66E-02
Pspc1	0.33	2.81E-09	0.05	5.57E-01	0.29	4.34E-03
Plcl2	0.33	1.42E-10	0.02	7.45E-01	0.32	1.25E-05
Gbe1	0.33	4.36E-05	0.04	7.63E-01	0.33	3.80E-02
Arpp19	0.32	4.81E-09	0.10	1.86E-01	0.22	4.96E-02
Mamld1	0.31	4.90E-07	-0.20	8.41E-02	0.59	5.72E-04
St3gal5	0.31	1.11E-07	0.11	3.98E-02	0.22	2.51E-02
Lancl2	0.30	2.00E-17	0.14	4.36E-03	0.16	2.05E-02
mt-Nd4	0.30	3.42E-06	-0.03	7.96E-01	0.37	6.22E-03
Fam107a	0.30	1.35E-07	-0.14	2.28E-01	0.50	1.85E-03
Ifrd1	0.30	9.45E-05	0.04	7.16E-01	0.30	2.33E-02
Nlk	0.30	6.00E-13	0.06	4.59E-01	0.24	1.33E-02
Tbc1d4	0.29	3.66E-03	-0.19	1.76E-01	0.65	1.33E-02
Fbxw7	0.29	3.76E-14	0.07	3.65E-01	0.22	1.36E-02
Zbtb1	0.29	4.92E-03	-0.03	8.46E-01	0.39	3.81E-02
Rps24-ps3	0.29	3.42E-02	-0.12	4.71E-01	0.67	3.73E-02
Scg3	0.29	1.28E-10	0.07	1.53E-01	0.23	1.22E-03
Rnf115	0.28	2.05E-08	0.04	6.84E-01	0.26	3.15E-03
Smyd2	0.28	1.45E-06	0.04	6.55E-01	0.26	1.08E-02
Chrm2	0.28	8.50E-04	-0.16	1.21E-01	0.50	1.21E-03
Tsnax	0.28	1.43E-03	0.01	8.71E-01	0.31	2.51E-02
Snap25	0.28	3.15E-11	0.08	7.97E-02	0.20	3.71E-03
Slc35f3	0.27	5.83E-04	-0.08	4.94E-01	0.39	8.01E-03
Npnt	0.27	1.17E-07	-0.05	6.35E-01	0.35	3.77E-03
Epha10	0.27	8.39E-04	-0.11	2.80E-01	0.43	5.22E-03
Npas4	0.26	5.65E-03	-0.08	5.44E-01	2.36	8.34E-03
Mchr1	0.26	1.13E-03	0.02	8.56E-01	0.28	3.17E-02
Slc6a17	0.26	3.65E-18	0.07	4.28E-01	0.19	4.66E-02
Denr	0.26	1.02E-06	0.03	7.96E-01	0.25	1.08E-02
Dipk2a	0.26	9.79E-04	-0.04	7.74E-01	0.33	3.81E-02
Ift57	0.26	2.01E-06	0.02	7.96E-01	0.25	5.02E-03
Ppp1r15a	0.26	9.54E-03	-0.11	2.50E-01	0.43	7.46E-03
Sun1	0.25	3.56E-08	0.08	1.61E-01	0.18	3.63E-02
Zfp39	0.25	5.21E-03	-0.08	4.13E-01	0.39	6.18E-03
Ubtd2	0.25	1.87E-03	-0.03	8.34E-01	0.30	2.19E-02
Rbbp8	0.25	2.83E-02	-0.08	5.41E-01	0.40	3.43E-02
Ptprj	0.25	4.41E-06	-0.07	2.38E-01	0.34	5.36E-05
Slc2a1	0.24	2.98E-03	-0.15	3.19E-01	0.52	4.84E-02
Sulf2	0.24	8.76E-09	0.00	9.69E-01	0.26	8.98E-04
Stx1b	0.24	2.39E-10	0.02	8.13E-01	0.23	4.64E-04
Ndrg3	0.24	3.78E-13	-0.02	7.57E-01	0.27	1.98E-06
Kcnk1	0.24	3.05E-04	-0.01	9.53E-01	0.26	2.64E-02
Mllt11	0.24	6.01E-08	0.03	6.96E-01	0.21	8.34E-03
Sgms1	0.23	6.37E-04	-0.05	7.34E-01	0.31	4.59E-02
Gm37885	0.23	3.04E-02	-0.23	5.39E-02	0.61	7.55E-03
Rasgrp1	0.23	5.32E-05	0.00	9.99E-01	0.25	4.16E-02
Ccdc141	0.23	2.10E-02	-0.16	1.90E-01	0.49	2.15E-02
Lhx6	0.23	2.75E-04	-0.09	4.76E-01	0.36	1.95E-02

Table S2 (2/4)

Phtf2	0.23	1.71E-03	-0.06	6.28E-01	0.32	2.36E-02
Trpc3	0.23	4.68E-04	-0.02	9.04E-01	0.27	2.17E-02
Scrt2	0.23	1.28E-02	-0.07	5.34E-01	0.35	2.43E-02
Zfp711	0.23	3.34E-03	-0.01	9.17E-01	0.27	4.59E-02
Cacng2	0.23	9.48E-10	0.05	5.65E-01	0.18	3.48E-02
Grsf1	0.23	8.10E-06	-0.02	8.29E-01	0.26	4.32E-03
Atf6	0.23	4.39E-04	-0.03	8.34E-01	0.27	3.06E-02
Usp49	0.23	2.34E-03	-0.03	7.63E-01	0.29	1.73E-02
Map9	0.23	3.07E-05	-0.01	8.99E-01	0.25	7.71E-03
Vip	0.23	4.35E-03	-0.02	8.79E-01	0.27	3.80E-02
Fndc3b	0.22	3.57E-03	-0.05	6.27E-01	0.31	2.03E-02
Actn4	0.22	2.51E-07	0.01	9.30E-01	0.22	3.07E-03
Smap1	0.22	3.41E-07	0.01	9.44E-01	0.23	2.44E-03
Elovl4	0.22	1.03E-04	-0.02	8.06E-01	0.26	8.38E-03
Lhfp	0.22	1.83E-03	-0.07	4.93E-01	0.31	8.38E-03
Nkapd1	0.22	8.39E-04	0.00	9.81E-01	0.24	4.87E-02
Mxi1	0.22	5.87E-06	-0.11	2.34E-01	0.35	1.25E-03
Dynlrb1	0.22	3.04E-04	-0.01	8.96E-01	0.25	1.46E-02
Adipor2	0.22	3.58E-03	-0.14	1.76E-01	0.40	7.49E-03
Zmiz1	0.22	9.89E-04	-0.05	6.68E-01	0.29	3.83E-02
Etv5	0.22	8.74E-04	-0.02	8.71E-01	0.26	4.69E-02
Uvrag	0.22	4.21E-06	0.00	9.69E-01	0.23	3.07E-03
Phyhipl	0.22	9.52E-05	0.04	4.96E-01	0.19	3.06E-02
R3hdm2	0.21	5.49E-08	0.01	9.46E-01	0.21	1.08E-02
Sh3rf3	0.21	2.84E-03	-0.11	4.09E-01	0.37	4.69E-02
Actr3b	0.21	1.11E-06	-0.01	9.62E-01	0.23	5.95E-03
Ptpn3	0.21	9.90E-05	-0.13	8.59E-02	0.36	2.71E-04
Dclk1	0.21	1.10E-06	0.00	9.89E-01	0.22	1.95E-02
Zfp617	0.21	1.44E-02	-0.12	2.21E-01	0.38	8.01E-03
Kcnn2	0.21	1.11E-03	-0.12	6.50E-02	0.35	4.64E-04
Omg	0.20	2.22E-04	-0.03	6.89E-01	0.25	8.07E-03
Ddx1	0.20	5.20E-04	-0.02	8.10E-01	0.23	1.29E-02
Exosc9	0.20	8.44E-03	-0.03	7.14E-01	0.26	2.45E-02
Myo1e	0.20	4.33E-03	-0.02	8.45E-01	0.24	2.61E-02
Ndufs1	0.20	1.71E-04	0.04	4.16E-01	0.16	3.06E-02
Cul3	0.20	4.73E-04	-0.02	8.10E-01	0.23	1.81E-02
Atp1b1	0.20	4.40E-05	0.05	3.05E-01	0.16	2.51E-02
Plpbp	0.20	1.89E-05	0.02	7.58E-01	0.18	1.08E-02
Usp2	0.19	3.07E-04	0.00	9.88E-01	0.21	4.98E-02
Cap2	0.19	2.78E-06	0.04	4.52E-01	0.16	2.15E-02
Nrg3	0.19	1.16E-02	-0.07	4.86E-01	0.29	2.86E-02
Gabra4	0.19	1.45E-05	0.06	2.63E-01	0.14	4.87E-02
Cd34	0.19	9.00E-04	-0.08	1.72E-01	0.29	8.98E-04
Psmd12	0.19	1.74E-03	-0.08	2.34E-01	0.29	1.82E-03
Hip1	0.19	4.65E-03	-0.10	3.43E-01	0.32	2.03E-02
Dbndd2	0.19	3.56E-03	-0.11	2.86E-01	0.33	1.73E-02
Gphn	0.19	4.81E-03	-0.08	2.24E-01	0.28	3.56E-03
Gnl2	0.19	1.73E-03	-0.03	7.24E-01	0.23	1.86E-02
Actn1	0.19	9.68E-05	-0.11	3.54E-01	0.32	2.57E-02
Enpp6	0.19	3.21E-02	-0.12	2.68E-01	0.35	2.80E-02
Elmo1	0.18	1.71E-05	0.00	9.99E-01	0.19	3.47E-03
Hmgn3	0.18	5.11E-03	-0.02	8.34E-01	0.22	2.82E-02
Atp6v1g2	0.18	2.80E-05	-0.02	7.46E-01	0.22	3.42E-03
Stx3	0.18	5.73E-03	-0.08	4.73E-01	0.28	2.97E-02
Rbm3	0.18	2.54E-03	-0.09	4.54E-01	0.31	4.84E-02
Abcg2	0.18	8.44E-03	-0.05	5.76E-01	0.26	2.26E-02
Pnpla2	0.18	2.04E-02	-0.11	2.80E-01	0.33	1.95E-02
Mboat2	0.18	5.32E-04	0.00	9.71E-01	0.19	2.90E-02
Pi4ka	0.18	1.47E-09	-0.01	9.06E-01	0.20	2.27E-02
Etv6	0.18	2.94E-02	-0.07	4.86E-01	0.28	4.88E-02
Mak16	0.18	1.16E-02	-0.02	8.18E-01	0.22	4.84E-02
Asic2	0.18	2.02E-04	-0.01	9.25E-01	0.20	1.56E-02
Fam216a	0.18	4.00E-03	-0.01	8.91E-01	0.20	1.96E-02
Atxn2	0.18	1.30E-03	-0.03	8.20E-01	0.22	4.87E-02
Atp1a1	0.18	9.00E-04	0.00	9.99E-01	0.19	2.45E-02
Septin7	0.18	1.15E-03	0.01	8.87E-01	0.17	4.13E-02
Cox10	0.18	2.70E-03	-0.02	8.34E-01	0.21	1.49E-02
Alas1	0.18	1.22E-03	-0.05	5.53E-01	0.24	9.23E-03
Nkrf	0.18	9.93E-03	-0.06	5.98E-01	0.25	4.25E-02
Zfp386	0.17	3.27E-02	-0.10	1.82E-01	0.30	7.73E-03
AI593442	0.17	7.26E-04	-0.03	7.26E-01	0.21	1.09E-02
Tmem108	0.17	3.93E-02	-0.12	2.42E-01	0.33	2.96E-02
Eif5b	0.17	7.52E-03	-0.07	1.86E-01	0.26	3.42E-03
Itpk1	0.17	5.00E-04	-0.12	2.12E-01	0.31	6.38E-03
Atf2	0.17	4.41E-06	-0.04	7.12E-01	0.22	2.43E-02
Phospho2	0.17	1.48E-02	-0.14	2.20E-01	0.35	2.05E-02
Csnk2b	0.17	1.39E-03	-0.05	4.44E-01	0.23	2.44E-03
Chfr	0.17	1.12E-03	-0.16	1.68E-01	0.37	1.67E-02
Med8	0.17	4.17E-02	-0.14	1.30E-01	0.34	1.28E-02
Hepacam	0.17	3.03E-04	-0.02	7.81E-01	0.20	1.29E-02
Ppp5c	0.17	4.57E-04	0.03	6.45E-01	0.15	4.85E-02
Fem1c	0.17	3.31E-02	-0.06	5.01E-01	0.25	3.63E-02
Nudt4	0.17	2.40E-04	0.00	9.82E-01	0.18	2.45E-02
Slc2a13	0.17	3.33E-03	-0.01	8.54E-01	0.19	2.43E-02
Hnrnph2	0.17	5.00E-04	-0.01	9.22E-01	0.18	3.71E-03
Ube2g1	0.17	1.66E-03	-0.07	2.65E-01	0.25	1.68E-03
Smarcd1	0.17	1.24E-06	0.03	6.90E-01	0.14	1.36E-02
Nop56	0.17	1.31E-04	0.01	9.26E-01	0.17	1.46E-02
Ccdc6	0.16	1.33E-02	-0.10	3.86E-01	0.29	4.84E-02
Max	0.16	2.77E-03	-0.04	5.49E-01	0.22	8.07E-03
Rims2	0.16	5.28E-04	-0.05	5.62E-01	0.22	1.54E-02
Utp4	0.16	1.61E-02	-0.10	3.04E-01	0.28	1.71E-02
Sra1	0.16	4.29E-02	-0.05	5.64E-01	0.23	4.88E-02
Tpgs2	0.16	6.21E-04	0.00	9.95E-01	0.17	1.84E-02
Fam81a	0.16	9.79E-04	-0.02	8.20E-01	0.19	1.53E-02
Map7d2	0.16	5.51E-03	-0.02	8.12E-01	0.19	2.51E-02
Pitpna	0.16	1.65E-05	-0.01	8.77E-01	0.17	7.08E-04
Atp2b1	0.16	2.75E-02	-0.08	3.76E-01	0.26	4.25E-02
Paqr8	0.16	4.26E-02	-0.17	5.56E-02	0.37	9.66E-03
Tfg	0.16	5.56E-03	-0.06	4.61E-01	0.23	1.49E-02

Table S2 (3/4)

Idh3a	0.16	3.14E-04	0.04	4.56E-01	0.13	4.46E-02
Vapa	0.15	1.86E-03	-0.01	8.91E-01	0.17	1.53E-02
Fkbp3	0.15	1.79E-03	-0.02	8.00E-01	0.18	1.08E-02
Fbxo45	0.15	6.38E-03	-0.03	7.23E-01	0.19	2.19E-02
Cdc42se2	0.15	3.83E-04	-0.02	8.54E-01	0.18	2.16E-02
Ppil4	0.15	9.54E-03	-0.15	1.58E-01	0.34	1.66E-02
Otulinl	0.15	4.58E-02	-0.12	2.49E-01	0.31	3.20E-02
Sec13	0.15	1.76E-02	-0.04	5.97E-01	0.20	2.85E-02
Dlst	0.15	3.20E-04	0.03	5.55E-01	0.13	1.29E-02
Rnf4	0.15	8.09E-04	-0.02	8.11E-01	0.17	1.38E-02
Cstf2	0.15	1.10E-02	-0.09	2.89E-01	0.26	1.87E-02
Tbk1	0.15	5.33E-03	-0.06	3.24E-01	0.21	2.44E-03
Utp15	0.15	2.93E-02	-0.04	6.09E-01	0.20	4.76E-02
Pias2	0.15	3.94E-02	-0.11	2.83E-01	0.28	3.82E-02
Ntrk2	0.14	3.76E-02	-0.05	4.70E-01	0.21	4.97E-02
Ranbp9	0.14	2.54E-03	-0.13	1.64E-01	0.29	9.95E-03
Psmc1	0.14	3.12E-02	-0.09	9.55E-02	0.25	6.39E-03
Timm9	0.14	3.96E-02	-0.11	1.22E-01	0.28	9.14E-03
Hnrnpu	0.14	2.97E-02	-0.04	5.36E-01	0.20	4.53E-02
Psma1	0.14	1.90E-02	-0.06	3.84E-01	0.21	1.53E-02
Hars	0.14	1.25E-02	-0.04	6.11E-01	0.19	3.61E-02
Vamp2	0.14	3.63E-05	-0.01	9.10E-01	0.16	1.36E-02
Map4k3	0.14	2.45E-03	-0.14	8.65E-02	0.30	3.62E-03
Snrpn	0.14	4.78E-03	-0.07	3.58E-01	0.22	1.36E-02
Cdc27	0.14	6.63E-03	-0.09	1.83E-01	0.24	3.72E-03
Kpna3	0.14	1.99E-03	-0.01	8.50E-01	0.16	2.05E-02
Psme3	0.14	6.29E-03	-0.03	6.61E-01	0.18	2.13E-02
Rad23b	0.14	2.26E-03	0.00	9.66E-01	0.15	4.50E-02
Mtmr2	0.14	2.61E-03	-0.09	1.43E-01	0.23	7.08E-04
Smc3	0.14	1.89E-02	-0.09	2.62E-01	0.25	1.76E-02
Cfap36	0.14	3.67E-02	-0.06	2.77E-01	0.20	1.36E-02
Gclc	0.13	2.05E-02	-0.08	3.52E-01	0.23	3.08E-02
Etf1	0.13	8.43E-03	-0.01	9.29E-01	0.15	4.59E-02
Slu7	0.13	2.67E-02	-0.03	6.88E-01	0.17	4.84E-02
Hs6st1	0.13	4.39E-03	-0.02	7.87E-01	0.16	2.79E-02
Rars	0.13	3.96E-02	-0.07	3.97E-01	0.22	3.57E-02
Eif3a	0.13	1.42E-02	-0.05	3.30E-01	0.19	9.08E-03
Zfr	0.13	5.23E-03	-0.04	3.99E-01	0.18	6.15E-03
Mark3	0.13	9.01E-03	-0.07	3.65E-01	0.21	2.03E-02
Adam9	0.13	7.10E-03	-0.07	3.63E-01	0.21	1.73E-02
Tax1bp1	0.13	2.22E-02	-0.06	3.15E-01	0.19	1.18E-02
Mat2a	0.13	4.80E-02	-0.15	8.32E-02	0.30	1.36E-02
Ivns1abp	0.13	1.59E-02	-0.06	4.29E-01	0.20	3.68E-02
Herpud1	0.13	4.26E-02	-0.11	2.31E-01	0.25	2.90E-02
Atp6v1d	0.13	7.70E-03	-0.02	7.14E-01	0.15	1.79E-02
Mta1	0.12	1.23E-02	-0.04	6.19E-01	0.17	4.35E-02
Pabpc1	0.12	4.59E-02	-0.07	2.12E-01	0.21	1.66E-02
Zc3h14	0.12	1.94E-02	-0.06	3.82E-01	0.18	1.61E-02
Rabgap1	0.12	6.80E-03	-0.08	2.88E-01	0.21	1.56E-02
Acsl3	0.12	3.71E-02	-0.07	3.60E-01	0.20	4.08E-02
Zmym2	0.12	3.62E-02	-0.06	3.74E-01	0.19	3.14E-02
Picalm	0.12	7.94E-03	-0.10	1.61E-01	0.22	6.39E-03
Dlgap4	0.11	6.67E-03	-0.02	7.09E-01	0.14	2.79E-02
Cdk17	0.11	9.21E-03	-0.03	6.47E-01	0.15	4.50E-02
Sik3	0.11	1.44E-02	-0.11	1.12E-01	0.24	8.01E-03
Pik3ca	0.11	3.29E-02	-0.07	4.23E-01	0.19	5.00E-02
Sumo3	0.11	3.57E-02	-0.08	3.38E-01	0.20	4.77E-02
Spire1	0.11	3.03E-02	-0.12	6.17E-02	0.25	5.39E-03
Ppp2r5c	0.11	1.35E-02	-0.03	5.20E-01	0.14	9.23E-03
Mia3	0.11	3.03E-02	-0.03	6.42E-01	0.14	3.83E-02
Csde1	0.10	3.42E-02	-0.04	5.22E-01	0.14	2.66E-02
Clip1	0.10	1.83E-02	-0.08	3.16E-01	0.20	3.81E-02
Dnm1l	0.10	2.53E-02	-0.05	5.05E-01	0.15	4.43E-02
Gga1	-0.13	2.49E-02	0.06	4.70E-01	-0.19	3.81E-02
Pwwp3a	-0.14	1.39E-02	0.07	3.57E-01	-0.22	1.43E-02
Atp8b2	-0.14	3.51E-02	0.12	6.91E-02	-0.27	6.62E-03
Zfp512	-0.14	8.41E-03	0.00	9.80E-01	-0.14	4.84E-02
Zfp316	-0.14	2.47E-02	0.08	3.56E-01	-0.24	2.82E-02
Zfp513	-0.15	1.51E-02	0.03	7.48E-01	-0.19	4.84E-02
Wdr41	-0.16	5.65E-03	0.00	9.91E-01	-0.16	4.84E-02
Rpl11	-0.16	1.67E-02	0.11	3.23E-01	-0.29	3.81E-02
Gtf2ird1	-0.16	3.69E-02	0.06	4.44E-01	-0.24	2.79E-02
Cmtm6	-0.17	1.80E-02	0.10	2.97E-01	-0.29	1.84E-02
Cep164	-0.17	2.62E-02	0.08	3.03E-01	-0.27	1.53E-02
Vps51	-0.17	1.38E-02	0.07	4.01E-01	-0.26	2.02E-02
Adck2	-0.18	1.70E-02	0.05	5.23E-01	-0.25	1.69E-02
Neurl1a	-0.18	9.45E-05	0.03	6.85E-01	-0.22	6.66E-03
Sema4f	-0.18	1.83E-03	0.01	8.79E-01	-0.20	1.43E-02
Mapk7	-0.18	9.95E-03	0.05	6.18E-01	-0.25	3.24E-02
Arhgef40	-0.19	2.28E-03	0.07	4.73E-01	-0.27	1.13E-02
Mob3a	-0.19	4.54E-02	0.15	1.53E-01	-0.38	1.33E-02
Nat14	-0.19	5.38E-03	0.08	4.32E-01	-0.29	2.05E-02
Pcdhb17	-0.19	1.33E-02	0.04	7.42E-01	-0.25	4.22E-02
Cep63	-0.19	8.34E-04	0.02	8.91E-01	-0.22	3.80E-02
Coa6	-0.20	4.72E-02	0.18	9.46E-02	-0.44	8.68E-03
Mccc2	-0.20	5.35E-03	0.04	6.96E-01	-0.26	2.47E-02
Tspan17	-0.20	1.50E-02	0.11	2.81E-01	-0.34	1.77E-02
Ddr1	-0.20	3.18E-02	0.11	3.38E-01	-0.35	4.84E-02
Trpm2	-0.20	1.32E-02	0.07	2.88E-01	-0.30	1.08E-02
Tnfrsf1a	-0.20	3.39E-02	0.13	2.69E-01	-0.39	2.45E-02
Engase	-0.20	8.46E-03	0.04	7.47E-01	-0.27	3.88E-02
Zfp358	-0.20	8.07E-04	0.05	6.57E-01	-0.26	1.53E-02
Kcnk10	-0.20	1.48E-02	0.10	4.52E-01	-0.36	5.00E-02
Igsf8	-0.20	2.14E-02	0.08	4.46E-01	-0.32	4.59E-02
Nfatc2	-0.20	1.41E-02	0.03	7.85E-01	-0.27	4.87E-02
Sh2d3c	-0.21	2.72E-02	0.16	1.42E-01	-0.43	1.67E-02
Ppcdc	-0.21	1.18E-02	0.06	5.34E-01	-0.30	1.84E-02
Kank2	-0.21	3.20E-02	0.10	3.76E-01	-0.36	3.81E-02
Nelfb	-0.21	3.62E-04	0.00	9.99E-01	-0.22	3.27E-02
Pik3ip1	-0.21	5.87E-04	0.01	9.08E-01	-0.24	3.34E-02

Table S2 (4/4)

Fam181b	-0.21	1.69E-02	0.10	3.66E-01	-0.36	1.69E-02
Zfp219	-0.21	6.00E-05	0.00	9.99E-01	-0.23	4.59E-02
Smo	-0.22	7.11E-03	0.06	5.73E-01	-0.31	2.54E-02
Gm10736	-0.22	3.08E-02	0.22	7.47E-02	-0.55	1.07E-02
2810459M11Rik	-0.22	6.68E-03	0.16	2.65E-01	-0.47	4.14E-02
Wnt7b	-0.22	3.51E-03	0.05	7.23E-01	-0.30	4.84E-02
Vtn	-0.22	1.01E-03	0.14	2.36E-01	-0.42	1.54E-02
D130017N08Rik	-0.23	8.86E-04	0.03	8.31E-01	-0.28	2.76E-02
Dhtkd1	-0.23	2.26E-02	0.08	4.20E-01	-0.36	2.61E-02
5031434O11Rik	-0.23	6.92E-03	0.09	3.78E-01	-0.36	9.66E-03
Jrk	-0.24	7.56E-03	0.14	2.81E-01	-0.47	1.77E-02
Tmem80	-0.24	1.11E-05	0.03	7.72E-01	-0.30	4.80E-03
Zic4	-0.25	2.61E-02	0.12	4.02E-01	-0.47	3.75E-02
Cdkl1	-0.25	2.11E-02	0.05	6.23E-01	-0.35	3.53E-02
Tep1	-0.25	8.61E-03	0.10	4.16E-01	-0.42	1.36E-02
Azin2	-0.25	1.87E-04	0.03	8.33E-01	-0.30	1.79E-02
Cul9	-0.25	7.04E-06	0.02	8.18E-01	-0.29	1.25E-03
Tapbp	-0.26	1.65E-03	0.04	7.26E-01	-0.32	1.36E-02
Trappc6a	-0.26	3.94E-02	0.09	5.05E-01	-0.46	4.69E-02
Hsf4	-0.26	2.35E-02	0.18	1.14E-01	-0.55	8.55E-03
Ly6h	-0.26	1.52E-04	0.04	7.29E-01	-0.33	1.29E-02
Trim45	-0.26	2.40E-03	0.05	6.87E-01	-0.36	1.76E-02
Acat3	-0.26	4.44E-02	0.15	3.11E-01	-0.60	2.66E-02
Pnma8b	-0.26	4.84E-10	-0.09	1.60E-01	-0.18	2.80E-02
Bbc3	-0.26	4.04E-02	0.13	3.56E-01	-0.54	4.65E-02
Isyna1	-0.26	2.38E-03	0.08	5.06E-01	-0.40	2.45E-02
Pdgfrb	-0.26	3.81E-05	0.06	5.64E-01	-0.36	7.46E-03
Rps21	-0.26	1.95E-03	0.07	6.21E-01	-0.38	3.53E-02
Tap2	-0.27	4.01E-03	0.08	5.17E-01	-0.41	1.12E-02
Emilin1	-0.27	4.50E-02	0.16	2.79E-01	-0.62	4.09E-02
Cc2d2a	-0.27	4.86E-04	-0.04	5.90E-01	-0.25	4.14E-02
Qrfpr	-0.27	3.12E-02	0.14	3.52E-01	-0.56	3.34E-02
Ccdc61	-0.27	1.30E-02	0.11	3.49E-01	-0.46	1.22E-02
Exosc5	-0.27	7.45E-04	0.00	9.99E-01	-0.30	2.97E-02
Kirrel3	-0.27	1.85E-05	0.02	8.88E-01	-0.31	7.46E-03
Slc22a6	-0.28	7.31E-03	0.15	2.65E-01	-0.55	1.85E-02
Plppr3	-0.28	2.92E-06	0.08	4.32E-01	-0.38	1.13E-03
Cpne4	-0.28	1.61E-08	-0.08	2.29E-01	-0.20	2.80E-02
Igfbp5	-0.28	1.52E-03	0.06	5.51E-01	-0.40	1.56E-02
Ccdc159	-0.28	1.90E-03	0.07	5.76E-01	-0.41	1.35E-02
Htra3	-0.29	1.28E-02	0.15	2.90E-01	-0.62	2.51E-02
Pck2	-0.29	2.65E-06	-0.03	7.33E-01	-0.28	8.38E-03
Atp2a3	-0.29	1.25E-02	0.13	3.26E-01	-0.56	2.05E-02
Neil2	-0.30	1.44E-02	0.14	2.79E-01	-0.59	6.77E-03
Pigv	-0.30	3.35E-04	0.01	9.65E-01	-0.36	2.05E-02
Lepr	-0.31	9.97E-03	0.10	4.94E-01	-0.55	2.66E-02
Bnip5	-0.31	1.09E-03	0.10	3.79E-01	-0.48	5.82E-03
Arhgef19	-0.31	5.61E-06	0.04	7.85E-01	-0.40	2.51E-02
Slc6a20a	-0.32	1.21E-03	0.05	7.71E-01	-0.44	4.22E-02
Slc9b2	-0.32	6.54E-03	0.06	7.14E-01	-0.51	2.44E-02
Gpr88	-0.32	1.06E-07	-0.09	3.57E-01	-0.25	5.00E-02
Pold1	-0.33	2.64E-04	-0.03	8.65E-01	-0.35	3.81E-02
Slc6a13	-0.33	1.59E-02	0.11	5.18E-01	-0.82	4.70E-02
Cdkn1c	-0.33	2.71E-03	0.15	3.38E-01	-0.65	1.63E-02
Mttp	-0.33	2.84E-05	-0.06	5.92E-01	-0.31	2.71E-02
Cldn5	-0.33	8.02E-04	0.16	2.55E-01	-0.63	2.86E-02
Tle6	-0.33	3.07E-03	0.08	6.39E-01	-0.58	4.71E-02
Slc13a4	-0.33	3.86E-04	0.08	6.13E-01	-0.51	2.80E-02
Mmp11	-0.34	8.25E-03	0.10	5.69E-01	-0.75	3.47E-02
Trp53i11	-0.35	3.29E-13	-0.09	2.77E-01	-0.27	6.39E-03
Bmp6	-0.35	6.37E-04	0.10	5.35E-01	-0.58	2.37E-02
Cchcr1	-0.35	8.74E-04	0.11	3.59E-01	-0.57	1.68E-03
Gm47171	-0.35	8.12E-03	0.03	8.69E-01	-0.66	3.12E-02
Mgat5b	-0.35	1.85E-06	-0.11	1.76E-02	-0.27	2.60E-02
Aldh1a2	-0.36	3.14E-04	0.12	4.47E-01	-0.61	1.45E-02
Col8a2	-0.36	2.53E-03	0.12	4.58E-01	-0.76	3.79E-02
Gm11611	-0.36	2.10E-03	0.12	3.86E-01	-0.68	6.47E-03
Celsr1	-0.36	4.91E-05	0.18	1.17E-01	-0.65	5.49E-04
Ccdc171	-0.36	1.00E-03	0.02	9.32E-01	-0.51	2.80E-02
Crocc	-0.37	4.21E-05	0.01	9.35E-01	-0.46	2.11E-02
Gm37233	-0.38	1.64E-03	0.11	4.78E-01	-0.73	1.33E-02
Glt8d2	-0.38	6.09E-07	-0.12	1.55E-01	-0.30	4.84E-02
Col20a1	-0.39	5.25E-05	0.06	7.30E-01	-0.57	2.69E-02
Ptgdr	-0.39	1.64E-03	0.19	2.08E-01	-0.98	2.38E-03
Asgr1	-0.41	1.22E-03	0.10	5.41E-01	-1.00	4.59E-02
Rskr	-0.41	2.23E-05	0.04	8.12E-01	-0.56	9.15E-03
Mmp14	-0.42	6.20E-07	0.04	8.20E-01	-0.56	1.22E-02
Nnat	-0.44	1.82E-12	0.05	7.91E-01	-0.54	5.56E-03
Rprm	-0.44	6.57E-10	-0.09	2.77E-01	-0.40	2.44E-03
Col8a1	-0.45	9.34E-05	-0.04	8.13E-01	-0.60	1.73E-02
Wnt5a	-0.46	3.15E-09	-0.13	1.84E-01	-0.38	9.95E-03
Vstm4	-0.46	1.80E-05	0.00	9.95E-01	-0.62	2.17E-02
Sec1	-0.48	2.71E-06	-0.01	9.52E-01	-0.60	4.68E-02
Timeless	-0.49	3.56E-08	-0.07	6.40E-01	-0.51	7.46E-03
Pcdh19	-0.54	9.91E-12	-0.14	1.58E-01	-0.48	3.82E-03
Nos1	-0.57	2.83E-14	-0.14	4.17E-02	-0.50	2.94E-04
Cfap44	-0.57	8.71E-08	-0.24	3.67E-02	-0.51	4.14E-02
Evc2	-0.58	1.66E-18	-0.24	7.56E-03	-0.37	1.92E-02
Otof	-0.72	1.32E-22	-0.37	4.20E-06	-0.40	2.36E-02
Plk5	-1.04	1.34E-36	-0.29	2.04E-03	-0.91	7.80E-08

Table S3 (1/9) – 12Hr_vs_Dark significant genotype interaction

gene_name	WT_hr12_vs_dark.l2fc	WT_hr12_vs_dark.padj	SWAP_hr12_vs_dark.l2fc	SWAP_hr12_vs_dark.padj	hr12_dark_genotype_interaction.l2fc	hr12_dark_genotype_interaction.padj
Ccn4	2.77	2.97E-120	1.97	6.77E-76	-0.77	2.20E-03
Cdkn1a	2.72	7.65E-110	2.02	4.42E-79	-0.68	1.65E-02
F2rl2	2.34	2.09E-42	1.04	2.79E-10	-1.30	3.37E-03
Trh	2.23	5.85E-50	0.66	1.93E-04	-1.57	2.00E-05
Baz1a	2.09	9.13E-68	1.02	4.16E-12	-0.92	5.21E-03
Tmem40	2.07	4.58E-51	0.60	4.26E-04	-1.49	4.23E-07
Serpinb8	2.07	4.71E-124	0.91	2.62E-11	-1.03	7.63E-05
Megf11	1.98	5.71E-133	1.30	8.67E-35	-0.57	9.54E-03
Mybpc3	1.91	2.53E-32	0.89	1.20E-09	-1.17	6.46E-04
Bdnf	1.85	1.39E-108	1.29	4.93E-37	-0.48	3.74E-02
Fkbp5	1.73	6.45E-227	0.42	2.85E-02	-1.11	8.28E-04
Pmepa1	1.72	1.13E-142	1.12	8.65E-95	-0.61	1.16E-07
Hif3a	1.71	3.32E-53	0.27	2.17E-01	-1.24	3.36E-02
Klhl40	1.69	3.89E-79	0.72	3.83E-07	-0.86	1.32E-03
Maff	1.66	3.07E-16	0.31	1.44E-01	-1.88	1.86E-03
Tamalin	1.58	1.51E-97	1.13	2.86E-37	-0.40	4.03E-02
Scube1	1.55	7.33E-175	0.89	7.14E-38	-0.64	6.25E-09
Fancd2	1.50	9.76E-56	0.75	1.20E-11	-0.73	4.42E-04
Rasa4	1.50	9.11E-32	0.61	3.50E-06	-0.93	1.08E-03
Camk1g	1.43	7.38E-124	0.78	1.24E-22	-0.63	2.95E-06
Kcna5	1.37	2.43E-19	0.51	1.29E-03	-0.94	3.25E-03
Fam167a	1.34	3.55E-18	0.13	5.58E-01	-1.40	1.02E-04
Dnajb5	1.34	1.80E-94	0.99	3.22E-46	-0.32	3.80E-02
Sstr2	1.33	2.73E-58	0.64	3.34E-08	-0.65	3.29E-03
Itga5	1.33	4.54E-33	0.48	3.88E-04	-0.85	6.32E-04
A630023P12Rik	1.32	4.42E-19	0.55	4.95E-04	-0.80	1.66E-02
Htr2a	1.31	3.23E-99	0.71	4.90E-26	-0.59	7.52E-08
Smim3	1.31	2.54E-62	0.31	7.05E-02	-0.96	1.55E-04
Trib2	1.30	5.42E-107	0.59	4.79E-10	-0.68	4.91E-06
Slc9a5	1.29	5.39E-101	0.85	7.74E-47	-0.43	1.45E-04
Rnd3	1.29	1.14E-59	0.74	5.18E-20	-0.55	4.39E-04
Ctla2a	1.29	2.13E-15	0.27	1.24E-01	-1.20	3.43E-04
Mfsd2a	1.28	6.07E-81	0.31	1.08E-01	-0.87	5.73E-03
Rem2	1.27	9.32E-20	0.43	7.13E-03	-0.90	9.62E-03
Tet3	1.25	5.91E-150	0.57	1.73E-07	-0.63	3.30E-04
Gcnt4	1.24	2.96E-111	0.77	5.60E-19	-0.42	3.29E-03
Rasd1	1.24	2.27E-14	0.62	3.77E-07	-0.75	8.71E-03
Stard8	1.23	2.68E-73	0.79	1.03E-24	-0.41	7.79E-03
Fam83d	1.22	3.71E-16	0.31	1.07E-01	-0.97	1.62E-02
Lsm11	1.21	3.91E-93	0.64	8.38E-19	-0.56	4.50E-06
Prr5	1.19	1.08E-32	0.34	9.34E-03	-0.88	1.38E-05
Wipf3	1.19	9.92E-100	0.34	6.95E-02	-0.73	2.10E-02
Htr5b	1.18	5.73E-18	0.49	5.91E-04	-0.73	1.38E-02
4833422C13Rik	1.18	4.57E-21	0.37	7.10E-03	-0.87	3.01E-04
Mapk12	1.17	2.55E-35	0.57	1.92E-06	-0.57	8.98E-03
Syt12	1.15	1.56E-84	0.73	2.51E-29	-0.41	5.25E-04
Pdp1	1.14	5.66E-105	0.78	5.08E-23	-0.32	3.15E-02
Gm15832	1.14	6.30E-18	0.28	8.21E-02	-0.92	3.30E-04
Paqr5	1.13	1.20E-19	0.34	5.58E-02	-0.79	2.43E-02
Skil	1.13	8.91E-85	0.59	1.55E-10	-0.51	1.36E-03
Rhbdl3	1.12	1.87E-72	0.23	1.72E-01	-0.88	7.33E-05
Tnfaip6	1.12	6.44E-29	0.48	1.26E-03	-0.59	4.66E-02
Fat3	1.12	1.93E-94	0.59	1.52E-08	-0.49	7.49E-03
Pglyrp1	1.12	3.75E-25	0.34	3.21E-02	-0.78	2.21E-03
Inf2	1.10	7.06E-92	0.69	3.60E-26	-0.39	1.04E-03
Nrn1	1.10	5.25E-132	0.78	1.33E-46	-0.31	1.22E-03
Gm30938	1.08	3.64E-08	0.09	7.57E-01	-1.34	9.04E-03
Osbpl3	1.08	2.14E-51	0.68	1.61E-22	-0.40	7.68E-03
Map2k3	1.07	4.68E-29	0.46	1.04E-04	-0.61	9.04E-03
Cdyl2	1.06	2.33E-25	0.44	2.66E-03	-0.60	2.96E-02
Scg2	1.05	2.39E-83	0.62	3.71E-34	-0.42	1.71E-05
Chga	1.05	3.40E-82	0.58	1.40E-18	-0.46	6.39E-05
Gm15344	1.04	7.60E-09	0.26	2.20E-01	-0.93	4.42E-02
Gm42608	1.04	6.86E-18	0.22	2.43E-01	-0.84	7.49E-03
Ifrd1	1.03	5.07E-69	0.74	8.66E-35	-0.28	1.71E-02
Notch4	1.03	1.57E-24	0.35	4.00E-03	-0.69	8.28E-04
Slc2a1	1.02	3.41E-95	0.35	3.46E-02	-0.58	2.74E-02
Gfra2	1.02	1.84E-100	0.77	8.61E-53	-0.24	1.43E-02
Tsnax	1.01	5.77E-134	0.77	3.28E-69	-0.24	2.23E-03
Nostrin	1.00	6.10E-14	0.23	2.32E-01	-0.79	2.17E-02
Lingo1	1.00	7.83E-101	0.76	1.04E-43	-0.22	4.66E-02
Mapk4	0.98	2.54E-40	0.61	4.79E-29	-0.37	8.65E-03
Mamld1	0.98	3.63E-47	0.38	3.41E-03	-0.56	1.28E-02
Spred2	0.97	5.97E-73	0.50	1.92E-06	-0.44	1.36E-02
Pdgfb	0.97	6.97E-14	0.58	5.32E-11	-0.44	4.25E-02
Tincr	0.97	8.89E-10	0.15	5.29E-01	-0.93	3.74E-02
Smim43	0.97	5.52E-82	0.59	3.54E-12	-0.34	2.41E-02
Slc29a4	0.97	1.12E-21	0.16	3.08E-01	-0.84	3.30E-04
Hectd2	0.97	4.73E-41	0.35	7.40E-04	-0.61	3.30E-04
Kcnip3	0.96	8.11E-89	0.63	4.12E-25	-0.32	3.44E-03
Tpbg	0.95	2.78E-44	0.48	8.28E-08	-0.45	3.85E-03
Gipr	0.95	4.52E-14	0.22	2.04E-01	-0.77	4.31E-03
Gfod1	0.94	9.43E-69	0.41	5.32E-04	-0.48	1.57E-02
Hkdc1	0.93	8.13E-33	0.44	4.39E-11	-0.50	1.55E-04
Atp10a	0.93	2.12E-26	0.34	2.06E-02	-0.55	4.33E-02
Lhfp	0.92	3.16E-42	0.50	1.40E-09	-0.41	7.15E-03
Nectin1	0.92	4.95E-82	0.47	9.32E-08	-0.42	2.32E-03
Inka2	0.91	1.52E-89	0.61	8.43E-29	-0.29	2.32E-03
Lratd1	0.90	5.07E-38	0.55	3.47E-14	-0.34	3.15E-02
Gm27004	0.89	2.28E-11	0.26	1.01E-01	-0.68	1.52E-02
Dot1l	0.88	5.97E-45	0.47	3.09E-09	-0.41	5.73E-03
Wif1	0.87	2.95E-06	0.18	4.10E-01	-0.88	3.06E-02
Rph3a	0.87	1.82E-124	0.52	2.84E-43	-0.35	2.25E-09
Etv5	0.87	4.31E-144	0.55	3.96E-14	-0.30	7.49E-03
Hivep3	0.86	1.58E-82	0.22	2.34E-01	-0.59	2.07E-02
Gimap6	0.85	2.29E-10	0.00	9.90E-01	-0.96	1.57E-04
Pcdh15	0.84	4.82E-51	0.25	6.09E-02	-0.58	1.54E-03
Gm37111	0.84	3.38E-16	-0.22	2.35E-01	-1.19	7.73E-06
Epha2	0.84	1.03E-06	0.02	9.60E-01	-1.01	9.43E-03

Table S3 (2/9)

Sema7a	0.83	1.64E-95	0.58	3.09E-25	-0.24	1.39E-02
Rrp8	0.83	2.45E-18	0.42	3.88E-05	-0.42	4.05E-02
Sdc4	0.83	2.95E-42	0.38	5.86E-04	-0.43	2.23E-02
Myd88	0.83	1.34E-15	0.36	3.30E-03	-0.47	4.03E-02
Ltbp2	0.82	5.79E-05	-0.09	7.32E-01	-1.32	1.63E-02
Ccdc6	0.82	5.53E-53	0.33	9.39E-04	-0.48	1.66E-03
Sdk1	0.81	7.42E-32	0.12	3.60E-01	-0.70	2.24E-07
Kmt5a	0.80	1.12E-48	0.37	4.58E-05	-0.41	3.85E-03
Mat2a	0.79	5.32E-68	0.34	4.22E-05	-0.43	4.70E-04
Kif9	0.79	5.69E-141	0.46	1.05E-09	-0.31	8.02E-03
Cort	0.78	5.99E-18	0.25	1.30E-02	-0.56	1.93E-04
Ipmk	0.78	1.19E-33	0.38	1.08E-05	-0.40	7.81E-03
Lrrc8c	0.78	6.68E-54	0.31	2.45E-02	-0.44	4.80E-02
Rgs9	0.77	3.08E-34	0.27	1.30E-02	-0.50	1.42E-03
Gse1	0.77	2.00E-85	0.25	9.70E-02	-0.49	2.99E-02
Dnajc1	0.76	4.64E-21	0.28	4.09E-02	-0.47	4.93E-02
Sema5b	0.76	2.90E-32	0.29	1.29E-04	-0.47	1.26E-04
Pde4a	0.76	1.89E-91	0.46	8.39E-12	-0.28	1.04E-02
Kcnk1	0.76	5.39E-81	0.43	4.07E-12	-0.31	1.07E-03
Golm1	0.75	1.28E-22	0.11	5.18E-01	-0.65	5.39E-03
Uck2	0.75	2.02E-49	0.24	6.00E-04	-0.51	8.38E-08
Spns2	0.75	1.27E-59	0.32	1.16E-03	-0.41	6.23E-03
St8sia5	0.75	3.66E-106	0.48	1.43E-13	-0.26	9.00E-03
Slc35f3	0.75	9.67E-47	0.42	2.13E-07	-0.31	1.65E-02
Grk5	0.73	8.19E-45	0.26	5.16E-03	-0.47	5.64E-05
Adipor2	0.73	2.51E-50	0.29	3.77E-03	-0.42	4.31E-03
Adam19	0.72	1.72E-49	0.34	9.15E-05	-0.36	4.27E-03
Slc6a17	0.72	7.31E-109	0.39	7.45E-08	-0.31	3.56E-03
Slc7a5	0.72	4.07E-44	0.42	7.25E-21	-0.30	6.38E-04
Ubtd2	0.71	8.57E-27	0.24	6.14E-03	-0.46	2.65E-04
Lrp8	0.70	1.09E-52	0.32	3.99E-04	-0.37	6.72E-03
Pdlim3	0.69	2.39E-05	0.01	9.80E-01	-0.80	1.63E-02
Ssbp3	0.69	3.75E-49	0.44	7.04E-12	-0.24	4.03E-02
Siah3	0.68	9.36E-23	0.20	1.29E-01	-0.47	8.07E-03
Cacna1g	0.67	2.42E-42	0.28	8.76E-05	-0.39	3.43E-04
Rin1	0.67	6.20E-54	0.35	2.54E-06	-0.30	9.61E-03
Plce1	0.66	3.38E-15	-0.01	9.73E-01	-0.70	3.30E-04
Tac1	0.66	1.90E-09	0.20	8.29E-02	-0.49	2.00E-02
Furin	0.66	7.00E-39	0.31	2.37E-04	-0.34	1.01E-02
Gm6206	0.65	5.38E-07	0.16	2.85E-01	-0.53	4.03E-02
Sec24d	0.65	8.11E-18	0.21	6.54E-02	-0.45	9.96E-03
Sulf2	0.64	2.51E-50	0.32	5.24E-09	-0.32	1.99E-04
Lrfn2	0.64	2.35E-18	0.09	4.66E-01	-0.55	3.43E-04
Arl5b	0.63	4.57E-20	0.21	7.73E-02	-0.43	1.75E-02
Nxn	0.63	6.27E-16	0.23	6.40E-02	-0.40	3.75E-02
Prkd2	0.63	3.79E-09	0.10	6.23E-01	-0.55	4.11E-02
Mcl1	0.62	9.27E-27	0.32	9.83E-08	-0.30	8.99E-03
Pitpnm3	0.62	2.11E-52	0.27	2.90E-03	-0.34	9.84E-03
Actn4	0.62	2.31E-57	0.41	4.68E-18	-0.21	1.07E-02
Gramd1b	0.62	1.94E-56	0.31	6.47E-05	-0.29	1.43E-02
Tafa1	0.61	3.98E-30	0.12	1.23E-01	-0.50	7.52E-08
Fam53b	0.61	2.47E-30	0.26	1.37E-02	-0.34	4.33E-02
Pak6	0.61	2.14E-27	0.29	2.13E-07	-0.32	3.70E-03
Rnf165	0.61	3.28E-35	0.14	3.75E-01	-0.46	2.47E-02
Dclk1	0.61	1.36E-69	0.18	2.60E-02	-0.42	1.96E-05
Snx30	0.61	7.07E-42	0.16	2.96E-02	-0.45	7.93E-07
Htra1	0.60	9.20E-25	0.24	1.50E-02	-0.36	2.47E-02
1110018N20Rik	0.60	8.36E-14	0.20	1.07E-01	-0.40	2.62E-02
Sgms1	0.60	2.38E-20	0.26	9.34E-03	-0.34	3.82E-02
Ptpn12	0.60	7.13E-25	0.26	5.03E-03	-0.33	2.81E-02
Noct	0.60	1.35E-29	0.31	7.95E-08	-0.29	3.72E-03
Hbegf	0.60	3.70E-09	0.18	1.41E-01	-0.43	4.22E-02
Dpf1	0.59	3.16E-29	0.22	1.69E-02	-0.36	9.14E-03
Tspan5	0.59	1.13E-66	0.34	3.54E-12	-0.24	7.00E-04
BC034090	0.59	4.08E-11	0.15	2.68E-01	-0.45	2.77E-02
Ksr1	0.59	1.33E-34	0.01	9.83E-01	-0.59	4.48E-02
Stt3b	0.58	2.82E-44	0.37	3.09E-11	-0.21	3.06E-02
Plekhg5	0.58	3.01E-42	0.14	1.89E-01	-0.43	1.21E-03
Ptpn1	0.57	3.37E-24	0.26	4.09E-03	-0.31	3.28E-02
Smox	0.57	1.03E-29	0.09	5.93E-01	-0.48	8.88E-03
Plcl2	0.57	1.19E-41	0.28	1.35E-08	-0.29	1.02E-04
Tgfbr1	0.57	1.94E-24	0.25	2.98E-04	-0.32	2.95E-03
Cinp	0.57	2.70E-34	0.32	1.20E-10	-0.25	2.59E-03
Elmo2	0.56	2.50E-56	0.29	3.29E-07	-0.26	1.76E-03
Fam171a1	0.56	8.30E-45	0.28	1.35E-03	-0.27	3.33E-02
Garem1	0.56	3.28E-15	0.14	1.98E-01	-0.42	9.83E-03
Mex3c	0.56	3.43E-27	0.25	1.44E-03	-0.30	1.03E-02
Gimap8	0.55	6.22E-03	-0.12	6.30E-01	-0.90	4.89E-02
Igfbp3	0.55	6.30E-12	-0.14	4.43E-01	-0.75	3.08E-03
Ptprn	0.55	5.04E-48	0.31	1.73E-11	-0.24	1.63E-03
Dgcr2	0.55	9.91E-37	0.18	5.43E-04	-0.37	4.53E-07
Tdg	0.55	8.95E-16	0.29	8.46E-06	-0.26	4.28E-02
Arhgef7	0.55	1.26E-37	0.21	1.85E-02	-0.32	1.37E-02
Mirg	0.54	5.50E-10	0.13	2.77E-01	-0.43	2.35E-02
Ankrd52	0.54	2.76E-40	0.22	2.85E-02	-0.31	3.72E-02
Gvin-ps7	0.53	9.09E-04	-0.22	2.71E-01	-0.91	9.15E-03
Sall3	0.53	2.18E-09	-0.02	9.36E-01	-0.58	4.96E-03
Arpc2	0.53	1.93E-42	0.22	1.35E-04	-0.31	9.97E-05
Prkag2	0.53	1.78E-46	0.20	2.82E-02	-0.32	6.75E-03
Mir9-3hg	0.53	7.31E-27	0.09	5.49E-01	-0.43	2.52E-02
Insyn1	0.53	5.07E-28	0.27	6.49E-06	-0.25	1.78E-02
Cdc42se1	0.52	3.63E-38	0.26	3.08E-06	-0.26	1.57E-03
Stx1b	0.52	2.70E-72	0.34	6.23E-17	-0.18	3.51E-03
Dgkz	0.52	1.65E-60	0.20	1.74E-02	-0.31	4.31E-03
Lrrc58	0.52	1.74E-30	0.16	1.73E-01	-0.36	2.04E-02
Cotl1	0.51	1.16E-16	0.11	3.58E-01	-0.40	1.49E-02
Itpk1	0.51	3.01E-29	0.23	9.11E-03	-0.27	4.17E-02
Plekhf2	0.51	1.92E-07	0.15	1.82E-01	-0.37	3.76E-02
H2-T23	0.51	5.05E-12	0.79	2.24E-22	0.33	2.58E-02
Zhx3	0.51	6.67E-30	0.01	9.67E-01	-0.50	1.57E-03

Table S3 (3/9)

Uvrag	0.51	3.17E-24	0.23	1.52E-04	-0.27	2.62E-03
Zfp651	0.50	2.74E-35	0.26	3.09E-05	-0.24	1.42E-02
Ptpn3	0.50	1.29E-23	0.20	3.08E-03	-0.29	4.89E-03
Rbbp7	0.50	5.53E-36	0.27	1.79E-08	-0.22	3.60E-03
Wwc1	0.49	1.81E-37	0.17	2.58E-02	-0.32	1.01E-03
Hip1	0.49	9.24E-34	0.12	2.88E-01	-0.37	4.57E-03
Ccdc88c	0.49	3.70E-25	0.20	1.85E-03	-0.29	2.31E-03
Phtf2	0.49	1.19E-15	0.16	1.63E-01	-0.33	3.20E-02
Etf1	0.49	7.49E-42	0.19	2.25E-04	-0.29	4.91E-06
Entpd7	0.49	3.24E-11	0.15	1.92E-01	-0.35	2.94E-02
Ly75	0.49	7.40E-03	-0.23	2.57E-01	-0.93	3.02E-02
Grb2	0.48	2.29E-46	0.34	2.17E-23	-0.14	1.31E-02
Ttll8	0.48	3.69E-03	-0.23	3.03E-01	-0.94	3.28E-02
Utp4	0.48	5.17E-21	0.22	1.09E-02	-0.25	4.63E-02
Erc2	0.48	9.08E-27	0.14	7.10E-02	-0.35	3.57E-04
Fam78b	0.48	6.45E-27	0.24	1.74E-03	-0.24	2.60E-02
Cep76	0.48	1.99E-07	0.03	8.56E-01	-0.46	2.02E-02
Sipa1l2	0.48	3.95E-17	0.15	9.23E-02	-0.33	1.62E-02
Fam81a	0.48	2.60E-24	0.21	1.78E-05	-0.27	1.19E-03
Gm26747	0.48	9.94E-03	-0.19	3.94E-01	-0.88	4.94E-02
Myo1e	0.48	3.91E-13	0.13	9.72E-02	-0.36	8.28E-04
Ppp4r4	0.47	2.94E-13	0.09	4.69E-01	-0.39	1.53E-02
Hey1	0.47	2.35E-18	0.24	1.64E-05	-0.23	2.10E-02
Ptprf	0.47	1.12E-19	0.19	2.85E-02	-0.28	3.90E-02
Ttyh3	0.47	1.58E-34	0.23	1.03E-03	-0.24	2.04E-02
D630045J12Rik	0.47	1.57E-24	0.08	5.33E-01	-0.38	1.27E-02
Ncbp1	0.47	8.55E-27	0.17	3.82E-02	-0.30	5.37E-03
Slc6a8	0.46	1.67E-28	0.24	6.21E-06	-0.22	1.10E-02
Fhod3	0.46	9.70E-20	0.17	3.65E-02	-0.29	1.58E-02
Sec14l2	0.46	7.70E-17	0.17	3.73E-02	-0.29	1.91E-02
Mark1	0.46	2.08E-41	0.21	5.89E-05	-0.25	1.58E-04
Pde9a	0.46	8.03E-12	0.13	2.77E-01	-0.33	4.38E-02
Nrxn3	0.45	1.05E-42	0.21	2.25E-03	-0.24	9.13E-03
Rab3ip	0.45	5.15E-16	0.22	3.49E-04	-0.23	2.94E-02
Elovl4	0.45	3.61E-16	0.17	3.75E-02	-0.28	2.25E-02
Arhgap39	0.45	6.24E-26	0.08	5.07E-01	-0.37	7.49E-03
Cggbp1	0.45	4.96E-21	0.19	1.02E-02	-0.25	2.35E-02
Smurf1	0.45	4.71E-21	0.13	9.74E-02	-0.32	1.39E-03
Nup153	0.45	4.55E-19	0.13	2.70E-01	-0.32	3.74E-02
Patl1	0.45	4.15E-14	0.11	3.57E-01	-0.34	3.00E-02
Mtmr4	0.45	4.88E-29	0.14	1.34E-01	-0.30	1.80E-02
Cbl	0.45	2.88E-17	0.10	4.32E-01	-0.34	4.59E-02
Mark3	0.44	1.38E-28	0.11	2.04E-01	-0.33	1.35E-03
Ddx21	0.44	2.26E-16	0.05	6.93E-01	-0.40	1.65E-03
Ccdc141	0.44	3.97E-08	-0.08	6.49E-01	-0.54	1.02E-02
Azin1	0.44	1.46E-39	0.23	1.88E-05	-0.21	4.89E-03
Gad2	0.44	3.16E-35	0.18	4.88E-03	-0.26	1.60E-03
Ptprj	0.44	5.84E-23	0.17	1.63E-02	-0.27	8.01E-03
Vangl1	0.44	6.24E-05	-0.10	5.39E-01	-0.59	4.92E-03
Slc35e2	0.44	1.27E-20	0.06	5.98E-01	-0.38	3.56E-03
Dnmt3a	0.44	2.97E-26	-0.09	3.81E-01	-0.54	2.24E-07
Ivns1abp	0.44	1.46E-25	0.21	5.96E-03	-0.23	4.84E-02
AI506816	0.44	2.10E-04	-0.01	9.65E-01	-0.48	2.23E-02
Gm42528	0.44	3.59E-05	0.05	7.05E-01	-0.41	3.00E-02
Hacd2	0.44	4.41E-18	0.06	6.00E-01	-0.38	3.24E-04
Nav2	0.43	2.03E-23	0.08	4.59E-01	-0.35	5.44E-03
Sh3rf3	0.43	4.23E-14	0.01	9.62E-01	-0.43	4.59E-02
Naa25	0.43	4.10E-27	0.22	3.81E-04	-0.21	1.40E-02
Foxk2	0.43	1.89E-28	0.23	5.80E-05	-0.20	2.14E-02
Wdr4	0.43	1.48E-15	0.22	3.49E-04	-0.21	4.05E-02
Abl2	0.43	4.13E-25	0.09	2.74E-01	-0.33	5.55E-04
Brsk2	0.43	1.70E-49	0.18	8.36E-03	-0.24	6.43E-03
Arhgap44	0.43	9.49E-23	0.20	2.43E-03	-0.23	2.45E-02
Slc9a3r2	0.42	1.53E-10	0.09	3.17E-01	-0.34	1.30E-02
Hmgb3	0.42	9.09E-06	0.03	8.37E-01	-0.42	1.43E-02
Syncrip	0.42	1.09E-17	0.17	5.43E-03	-0.26	7.07E-03
Psmd12	0.42	1.25E-20	0.18	4.55E-03	-0.24	7.35E-03
Khdc4	0.42	4.18E-17	0.06	6.81E-01	-0.36	3.20E-02
Ppfibp1	0.42	1.08E-11	0.01	9.52E-01	-0.42	3.37E-04
Atxn2	0.41	2.58E-26	0.11	2.42E-01	-0.30	5.63E-03
Sccpdh	0.40	5.62E-16	0.17	7.71E-03	-0.24	1.36E-02
Bzw1	0.40	5.98E-23	0.20	1.48E-04	-0.20	2.43E-02
Smim36	0.40	1.51E-03	-0.12	5.45E-01	-0.59	4.59E-02
Dcaf10	0.40	1.71E-10	0.07	6.23E-01	-0.34	4.32E-02
Dock9	0.40	1.66E-18	0.02	9.14E-01	-0.38	7.82E-03
Tars	0.40	3.60E-14	0.19	1.91E-03	-0.21	2.65E-02
Plaa	0.39	2.40E-15	0.07	5.13E-01	-0.32	8.72E-03
B4galt5	0.39	6.87E-22	0.14	9.56E-02	-0.24	3.07E-02
Ankrd13b	0.39	2.27E-17	0.14	5.37E-02	-0.25	2.05E-02
Arpc5	0.39	4.22E-19	0.07	5.57E-01	-0.32	1.40E-02
Sla	0.39	5.49E-06	-0.02	9.39E-01	-0.42	4.44E-02
Svil	0.39	7.17E-07	-0.03	8.68E-01	-0.43	8.88E-03
Pik3r3	0.39	1.70E-11	0.02	9.08E-01	-0.38	8.88E-03
Ftsj3	0.39	4.96E-13	0.11	1.71E-01	-0.28	6.72E-03
Tmem117	0.38	3.99E-04	-0.05	7.32E-01	-0.47	1.65E-02
Ssh2	0.38	8.46E-12	0.01	9.75E-01	-0.38	3.00E-02
Csmd1	0.38	4.65E-29	0.02	8.80E-01	-0.36	1.78E-03
Abcg2	0.38	2.97E-09	0.07	5.15E-01	-0.31	1.37E-02
Selenoi	0.38	7.24E-20	0.15	4.93E-02	-0.23	2.52E-02
Ube2g1	0.37	4.03E-17	0.06	4.91E-01	-0.32	1.42E-04
Nsd2	0.37	2.40E-17	0.13	9.32E-02	-0.25	1.99E-02
Robo4	0.37	3.34E-04	0.00	1.00E+00	-0.40	3.96E-02
Cdk6	0.37	5.96E-04	-0.14	4.42E-01	-0.56	2.29E-02
Tnpo1	0.36	1.73E-14	0.12	2.17E-01	-0.25	4.92E-02
Kcmf1	0.36	1.87E-17	0.17	1.53E-02	-0.19	4.63E-02
Pld1	0.36	1.34E-06	-0.05	7.28E-01	-0.43	5.87E-03
Ddx50	0.36	2.04E-11	0.09	2.48E-01	-0.27	1.57E-02
1810055G02Rik	0.36	1.72E-11	0.11	1.75E-01	-0.26	1.06E-02
Max	0.36	8.93E-16	0.14	2.69E-02	-0.22	1.09E-02
Dhx33	0.36	1.84E-15	0.09	3.69E-01	-0.27	3.15E-02

Table S3 (4/9)

Garnl3	0.36	8.63E-16	0.01	9.66E-01	-0.35	1.90E-02
Chfr	0.35	6.44E-15	-0.12	3.83E-01	-0.49	2.76E-03
Ttll4	0.35	3.20E-06	-0.02	9.21E-01	-0.38	3.96E-02
Phf8	0.35	3.54E-12	0.06	6.46E-01	-0.30	4.38E-02
Hivep2	0.35	9.77E-17	0.06	6.28E-01	-0.29	2.33E-02
Traf3	0.35	1.10E-08	-0.16	2.93E-01	-0.54	7.61E-03
Klhl2	0.35	6.71E-17	0.18	1.43E-04	-0.17	3.20E-02
Ripor2	0.35	2.86E-15	0.02	8.93E-01	-0.33	2.80E-02
Lats1	0.35	3.70E-10	0.01	9.37E-01	-0.35	1.19E-02
Tollip	0.35	4.88E-26	0.10	1.93E-01	-0.24	1.01E-02
Txndc11	0.35	3.65E-10	0.07	4.16E-01	-0.27	1.49E-02
Ankrd13a	0.35	1.32E-13	0.05	7.45E-01	-0.30	4.90E-02
Pcgf3	0.34	1.79E-17	0.04	7.43E-01	-0.30	2.19E-02
Sptlc2	0.34	7.42E-11	0.11	1.49E-01	-0.24	2.04E-02
Serp1	0.34	1.48E-10	0.13	7.86E-02	-0.22	4.27E-02
Ildr2	0.34	3.02E-19	0.10	2.77E-01	-0.24	3.42E-02
Tmem229b	0.34	4.48E-10	0.03	7.54E-01	-0.32	3.63E-04
Set	0.34	8.37E-17	0.20	6.30E-07	-0.14	4.65E-02
Zfp410	0.34	2.48E-09	0.06	5.76E-01	-0.27	4.03E-02
Gphn	0.34	6.41E-16	0.15	8.53E-03	-0.18	2.93E-02
Sh3rf1	0.33	7.54E-14	0.01	9.43E-01	-0.32	7.07E-03
Scg3	0.33	6.78E-24	0.15	3.23E-03	-0.17	1.61E-02
Sec13	0.33	5.14E-14	0.13	2.85E-02	-0.20	1.12E-02
Rars	0.33	4.85E-10	0.12	1.10E-01	-0.21	4.31E-02
Ciapin1	0.33	1.53E-12	0.10	1.29E-01	-0.23	1.10E-02
Hrk	0.33	8.79E-14	-0.14	2.78E-01	-0.49	1.42E-03
Slc2a13	0.33	1.76E-17	0.15	2.76E-03	-0.18	1.16E-02
Eml4	0.33	1.38E-09	0.09	3.11E-01	-0.24	3.79E-02
Fgd1	0.33	2.74E-08	0.04	6.74E-01	-0.29	4.96E-03
Mtmr2	0.33	5.38E-15	0.05	6.02E-01	-0.28	9.88E-04
D5Ertd579e	0.33	1.38E-18	0.15	3.37E-03	-0.18	1.41E-02
Adora1	0.32	3.32E-19	0.16	2.14E-03	-0.16	4.18E-02
Purg	0.32	1.42E-05	-0.01	9.48E-01	-0.35	3.51E-02
Lair1	0.32	1.67E-04	-0.10	5.38E-01	-0.45	2.57E-02
Snx25	0.32	1.36E-12	0.09	1.67E-01	-0.24	1.76E-03
Usp38	0.32	1.01E-09	0.07	4.22E-01	-0.25	2.05E-02
Cramp1	0.32	1.50E-11	0.07	5.29E-01	-0.26	3.41E-02
Cd24a	0.32	2.40E-03	-0.20	1.31E-01	-0.56	4.21E-03
Wdr26	0.32	9.31E-12	0.03	7.28E-01	-0.29	5.86E-03
Eprs	0.32	9.44E-18	0.16	3.14E-04	-0.16	2.05E-02
Wapl	0.32	1.39E-08	0.08	2.89E-01	-0.24	2.57E-02
Kcnip1	0.32	4.58E-08	0.08	4.46E-01	-0.24	4.65E-02
Ybx1	0.31	5.24E-13	0.11	6.05E-02	-0.21	9.27E-03
Nol4l	0.31	4.44E-09	-0.06	5.61E-01	-0.38	5.83E-04
1700025G04Rik	0.31	1.34E-12	0.09	2.79E-01	-0.22	4.95E-02
Tnks1bp1	0.31	4.13E-16	0.12	5.68E-02	-0.19	3.32E-02
Cdk11b	0.31	3.55E-13	0.15	4.09E-03	-0.16	3.48E-02
Dock11	0.31	1.38E-03	-0.09	5.69E-01	-0.43	4.33E-02
Kctd3	0.31	5.55E-14	0.14	2.08E-03	-0.17	1.76E-02
Maml2	0.31	4.21E-03	-0.13	3.77E-01	-0.47	4.62E-02
Abi1	0.30	4.03E-17	0.11	1.50E-01	-0.20	3.15E-02
Rnf168	0.30	3.39E-08	0.06	5.18E-01	-0.25	1.62E-02
Sox11	0.30	3.03E-04	-0.05	7.11E-01	-0.37	4.44E-02
Psmc2	0.30	4.72E-13	0.14	1.03E-02	-0.17	3.27E-02
Fam163b	0.30	6.07E-07	0.01	9.15E-01	-0.29	2.49E-02
Erc1	0.30	2.98E-11	0.02	8.46E-01	-0.28	2.47E-02
Shisal1	0.30	1.31E-14	-0.04	7.29E-01	-0.35	1.04E-03
Lgalsl	0.30	1.26E-11	0.09	1.33E-01	-0.21	1.70E-02
Lig3	0.30	1.23E-09	0.10	1.27E-01	-0.19	4.01E-02
Psmb2	0.30	1.11E-06	0.05	5.56E-01	-0.25	4.45E-02
Ppp2ca	0.30	1.24E-19	0.18	2.21E-08	-0.12	3.10E-02
Plppr5	0.30	1.77E-07	0.08	2.14E-01	-0.22	2.41E-02
Ptpn11	0.30	4.93E-19	0.10	6.94E-02	-0.19	6.43E-03
Picalm	0.29	5.22E-14	0.04	6.87E-01	-0.26	1.06E-02
Pitpna	0.29	8.07E-19	0.14	1.08E-03	-0.15	1.29E-02
Pabpc1	0.29	6.60E-12	0.06	3.85E-01	-0.23	3.70E-03
Rap1b	0.29	5.02E-10	0.03	8.08E-01	-0.27	1.02E-02
Peli1	0.29	3.03E-09	0.00	9.90E-01	-0.29	7.49E-03
Ppp1r18	0.28	5.53E-03	-0.06	6.49E-01	-0.36	4.23E-02
Camk2b	0.28	9.70E-12	0.04	6.54E-01	-0.25	6.14E-03
Ndst1	0.28	7.42E-16	-0.05	6.70E-01	-0.34	6.14E-03
Cbs	0.28	7.02E-05	-0.09	4.61E-01	-0.38	2.01E-02
Tm9sf3	0.28	4.14E-11	0.09	1.13E-01	-0.19	1.65E-02
Uso1	0.28	2.60E-09	0.07	3.90E-01	-0.21	3.49E-02
Senp6	0.28	2.92E-08	0.05	5.69E-01	-0.23	2.77E-02
Psme4	0.28	1.35E-07	0.03	7.36E-01	-0.24	3.63E-02
Heatr3	0.28	3.45E-08	0.05	5.92E-01	-0.23	2.48E-02
Prpf38a	0.27	2.03E-05	-0.02	8.14E-01	-0.30	3.64E-03
Psma6	0.27	2.59E-10	0.09	1.91E-01	-0.18	4.03E-02
Dlst	0.27	6.95E-15	0.14	2.62E-04	-0.14	1.38E-02
Crmp1	0.27	6.37E-11	-0.07	3.76E-01	-0.35	4.96E-05
Tbk1	0.27	4.05E-09	0.08	1.61E-01	-0.19	1.66E-02
Plekha1	0.27	1.30E-10	-0.14	1.38E-01	-0.41	1.07E-04
Smap1	0.27	2.66E-13	0.08	1.40E-01	-0.19	5.87E-03
Gpr161	0.27	3.82E-03	-0.20	1.40E-01	-0.51	2.50E-02
Ahcyl1	0.27	1.86E-24	0.14	1.51E-03	-0.12	3.53E-02
Eif3a	0.26	1.56E-12	0.08	1.51E-01	-0.18	1.63E-02
Slc1a1	0.26	1.87E-12	0.04	6.44E-01	-0.22	1.65E-02
Vhl	0.26	1.09E-08	0.08	2.16E-01	-0.19	2.23E-02
Atrip	0.26	8.68E-06	0.03	8.06E-01	-0.24	4.66E-02
Dnajc7	0.26	5.29E-09	0.08	2.03E-01	-0.18	4.51E-02
Slx4	0.26	4.89E-08	0.04	6.64E-01	-0.22	4.44E-02
2900026A02Rik	0.26	8.07E-08	-0.03	7.64E-01	-0.30	1.03E-02
Marchf4	0.26	2.12E-05	-0.13	3.27E-01	-0.40	1.37E-02
Grpel2	0.26	8.17E-05	0.01	9.33E-01	-0.25	4.47E-02
Frmpd1	0.26	1.97E-03	-0.12	2.17E-01	-0.39	6.05E-03
Srgap2	0.26	4.77E-10	-0.04	7.07E-01	-0.31	1.07E-02
Tdp1	0.26	1.03E-04	-0.12	2.79E-01	-0.39	3.65E-03
Desi2	0.26	1.80E-05	0.00	9.90E-01	-0.26	2.46E-02
Dlg3	0.25	3.93E-11	0.11	2.05E-02	-0.14	4.58E-02

Table S3 (5/9)

Wdr5	0.25	3.38E-05	-0.03	7.63E-01	-0.29	8.72E-03
Pxk	0.25	1.45E-06	0.02	8.51E-01	-0.23	1.80E-02
Fras1	0.25	4.52E-06	-0.03	7.94E-01	-0.29	3.09E-02
Gatad1	0.25	6.65E-07	0.06	4.16E-01	-0.19	3.84E-02
Ccdc28b	0.25	1.15E-04	-0.18	2.00E-01	-0.46	1.94E-02
Xpo6	0.25	1.38E-12	-0.06	6.67E-01	-0.31	3.23E-02
Orai2	0.25	5.36E-05	-0.17	2.41E-01	-0.45	3.45E-02
Col4a1	0.25	3.18E-05	-0.12	2.00E-01	-0.37	2.98E-03
Dcaf5	0.25	2.15E-11	-0.03	7.23E-01	-0.28	1.54E-03
Cfap100	0.24	4.88E-02	-0.22	1.42E-01	-0.52	3.99E-02
Vcam1	0.24	1.73E-04	-0.09	3.45E-01	-0.34	6.45E-03
Ralgps2	0.24	6.06E-07	-0.09	5.08E-01	-0.34	2.99E-02
Fam98a	0.24	1.20E-06	0.01	9.29E-01	-0.23	1.32E-02
Cdc42se2	0.24	1.41E-14	-0.04	6.21E-01	-0.28	2.28E-04
Strn	0.24	4.75E-05	-0.09	3.86E-01	-0.34	1.23E-02
Actr3b	0.24	4.79E-09	-0.01	9.35E-01	-0.25	2.34E-02
Psmd2	0.24	8.20E-11	0.08	1.46E-01	-0.15	4.65E-02
Dip2a	0.23	1.00E-08	0.03	6.94E-01	-0.20	3.43E-02
Usp12	0.23	3.34E-07	-0.01	9.21E-01	-0.25	2.71E-02
Agpat3	0.23	2.03E-13	0.09	4.37E-02	-0.14	2.53E-02
Pdhx	0.23	3.28E-07	0.00	9.82E-01	-0.24	8.28E-04
Ctnnbip1	0.23	2.52E-06	-0.05	6.02E-01	-0.28	3.37E-03
Gng12	0.23	1.65E-07	-0.07	4.57E-01	-0.30	2.10E-03
Atl2	0.23	4.03E-08	0.05	5.59E-01	-0.18	4.05E-02
Cemip2	0.23	5.45E-05	-0.01	9.56E-01	-0.24	4.03E-02
Mmadhc	0.23	1.49E-05	0.02	8.38E-01	-0.21	1.65E-02
Garre1	0.23	2.82E-07	0.00	9.87E-01	-0.23	1.76E-02
Elovl1	0.23	7.91E-05	-0.16	7.26E-02	-0.40	3.42E-04
Sec23b	0.22	8.01E-07	0.03	7.51E-01	-0.20	3.00E-02
Anks1b	0.22	2.77E-12	0.06	3.50E-01	-0.17	1.19E-02
Kctd5	0.22	1.47E-04	-0.13	1.44E-01	-0.37	1.08E-03
Srl	0.22	2.78E-02	-0.19	1.78E-01	-0.45	3.57E-02
Trak2	0.22	5.54E-11	-0.11	1.10E-01	-0.34	9.25E-06
Mapre1	0.22	2.67E-07	-0.05	5.78E-01	-0.27	1.90E-03
Frmd5	0.22	1.88E-06	0.02	8.49E-01	-0.20	3.43E-02
Ncan	0.22	4.01E-10	0.02	8.41E-01	-0.20	1.46E-02
5031439G07Rik	0.21	5.43E-12	0.06	3.21E-01	-0.15	1.51E-02
Tspan14	0.21	2.50E-05	-0.02	8.10E-01	-0.24	1.52E-02
Gnl2	0.21	9.05E-06	-0.02	8.62E-01	-0.23	2.14E-02
Tns3	0.21	6.59E-06	-0.12	2.97E-01	-0.34	1.40E-02
Mboat2	0.21	4.14E-07	-0.03	7.05E-01	-0.24	4.08E-04
Prr14	0.21	1.36E-04	-0.01	9.53E-01	-0.22	2.51E-02
Zfp91	0.21	1.13E-07	0.01	8.81E-01	-0.20	8.88E-03
Gatad2b	0.21	1.07E-06	-0.01	9.36E-01	-0.22	4.94E-02
Pak2	0.21	7.24E-07	0.03	6.82E-01	-0.18	3.14E-02
Mllt11	0.21	3.55E-08	-0.02	8.68E-01	-0.22	6.51E-03
Slc1a2	0.21	5.65E-06	-0.03	7.32E-01	-0.24	1.82E-02
Spaca6	0.20	8.08E-04	-0.21	1.28E-01	-0.45	3.00E-02
Idh3a	0.20	2.22E-11	0.09	4.80E-02	-0.11	3.88E-02
Purb	0.20	1.80E-04	-0.01	9.44E-01	-0.21	4.45E-02
Nudt21	0.20	6.32E-05	0.01	9.11E-01	-0.19	3.91E-02
Kif5c	0.20	3.24E-12	0.06	2.08E-01	-0.13	1.59E-02
Prickle1	0.20	4.60E-08	0.04	5.13E-01	-0.15	4.22E-02
Znrf3	0.19	4.85E-03	-0.06	6.16E-01	-0.26	4.87E-02
Ubac2	0.19	1.55E-04	-0.03	7.89E-01	-0.22	2.59E-02
Mkrn1	0.19	8.61E-08	0.03	7.32E-01	-0.16	4.18E-02
Grk6	0.19	1.13E-05	-0.02	7.88E-01	-0.22	1.40E-02
Nfasc	0.19	1.42E-04	-0.10	2.32E-01	-0.30	8.05E-03
Gna13	0.19	6.44E-05	-0.04	5.98E-01	-0.23	9.84E-03
Slco1c1	0.19	5.98E-03	-0.15	1.82E-01	-0.35	3.43E-02
Dgkd	0.18	4.22E-09	0.02	8.16E-01	-0.17	5.44E-03
Timm9	0.18	3.41E-03	-0.13	1.70E-01	-0.31	1.15E-02
Plppr4	0.18	7.99E-04	-0.07	3.94E-01	-0.25	2.25E-02
Tmem167	0.18	5.54E-05	-0.01	8.88E-01	-0.19	3.14E-02
Chd4	0.18	2.27E-07	0.00	9.64E-01	-0.17	4.15E-02
Ints6	0.17	1.07E-02	-0.13	1.85E-01	-0.31	2.29E-02
Ralgds	0.17	1.27E-04	-0.08	3.86E-01	-0.26	2.49E-02
Eps8	0.17	9.82E-03	-0.13	2.17E-01	-0.31	2.85E-02
Tbc1d20	0.17	2.12E-04	-0.05	5.71E-01	-0.22	3.01E-02
Dag1	0.17	1.50E-05	-0.01	9.13E-01	-0.18	2.49E-02
Ip6k2	0.16	2.15E-04	-0.02	8.00E-01	-0.19	4.86E-02
Psmd13	0.16	8.48E-05	0.01	8.95E-01	-0.15	3.00E-02
Frmd4a	0.16	1.51E-03	-0.13	1.25E-01	-0.30	6.43E-03
Arhgef2	0.16	3.10E-07	0.02	7.66E-01	-0.14	1.93E-02
Zfp251	0.16	1.99E-04	-0.09	3.76E-01	-0.25	2.98E-02
Abhd17b	0.16	1.34E-03	-0.06	5.02E-01	-0.22	2.52E-02
Cdc27	0.16	9.34E-04	-0.06	5.14E-01	-0.22	2.95E-02
Npnt	0.16	4.21E-04	-0.16	7.53E-02	-0.32	3.89E-03
Tbc1d14	0.16	3.53E-05	-0.07	2.88E-01	-0.23	2.13E-03
Ccp110	0.16	2.32E-04	-0.10	1.81E-01	-0.26	5.13E-03
Ptprz1	0.15	4.88E-04	-0.07	4.23E-01	-0.23	3.13E-02
Slc1a3	0.15	4.01E-06	-0.07	2.55E-01	-0.23	1.40E-03
2610507B11Rik	0.15	1.86E-06	0.01	8.97E-01	-0.14	4.52E-02
Cask	0.15	8.35E-03	-0.08	2.68E-01	-0.23	2.63E-02
Slk	0.15	4.72E-03	-0.13	1.18E-01	-0.28	1.24E-02
Itgb1	0.14	3.90E-03	-0.09	1.90E-01	-0.23	7.74E-03
Foxn3	0.13	8.40E-03	-0.05	4.94E-01	-0.19	4.63E-02
Tmx1	0.13	1.25E-02	-0.07	4.26E-01	-0.20	4.29E-02
Mfsd14b	0.13	1.10E-02	-0.05	4.47E-01	-0.19	3.50E-02
Limch1	0.12	4.16E-03	-0.07	3.54E-01	-0.20	3.16E-02
Flna	0.12	1.44E-02	-0.17	7.50E-02	-0.30	2.47E-02
Ccny	0.12	2.68E-03	-0.09	2.55E-01	-0.21	2.77E-02
1110004F10Rik	0.11	1.31E-02	-0.07	3.33E-01	-0.18	4.58E-02
Mta1	0.11	1.57E-02	-0.07	3.39E-01	-0.18	4.97E-02
Zfp354c	0.11	3.67E-02	-0.18	5.51E-02	-0.30	1.96E-02
Rims3	0.08	3.93E-02	0.37	2.17E-07	0.30	4.31E-03
Tspyl4	-0.08	2.38E-02	0.09	9.85E-02	0.17	1.12E-02
Kcnc1	-0.09	6.08E-03	0.13	5.20E-02	0.23	5.22E-03
Rtn1	-0.09	1.79E-02	0.05	3.94E-01	0.14	4.23E-02
Fam234b	-0.10	1.43E-02	0.07	2.02E-01	0.17	1.40E-02

Table S3 (6/9)

Reep5	-0.11	1.57E-04	0.09	2.56E-01	0.20	1.78E-02
Zcchc18	-0.11	1.30E-03	0.01	9.35E-01	0.12	3.75E-02
Tmem130	-0.12	8.36E-03	0.12	1.08E-01	0.24	1.25E-02
Tecr	-0.12	5.48E-03	0.07	2.49E-01	0.19	1.26E-02
Glrb	-0.12	8.59E-04	0.08	3.54E-01	0.20	4.86E-02
Gabra3	-0.12	5.51E-03	0.08	1.82E-01	0.21	7.49E-03
B3gat3	-0.13	4.54E-03	0.06	4.69E-01	0.19	4.78E-02
Rhobtb2	-0.13	6.25E-05	0.06	4.94E-01	0.19	2.56E-02
Chmp3	-0.13	1.57E-03	0.09	1.35E-01	0.23	1.44E-03
Trim66	-0.14	1.45E-02	0.13	7.70E-02	0.27	7.49E-03
Gga1	-0.14	8.77E-04	0.04	5.98E-01	0.19	2.35E-02
1110051M20Rik	-0.15	7.40E-04	0.03	7.34E-01	0.18	2.00E-02
Mrps10	-0.15	2.38E-02	0.09	3.00E-01	0.25	2.43E-02
Pef1	-0.16	5.00E-04	0.06	4.86E-01	0.22	1.31E-02
Bnip3l	-0.16	4.56E-05	-0.02	7.59E-01	0.14	3.42E-02
Marcksl1	-0.16	4.63E-03	-0.47	1.62E-08	-0.34	2.36E-02
Vegfb	-0.17	1.59E-03	0.07	4.84E-01	0.25	4.01E-02
Bmerb1	-0.17	1.53E-07	-0.05	2.13E-01	0.12	2.02E-02
Aip	-0.19	5.73E-04	0.13	2.41E-01	0.33	2.24E-02
Smim10l1	-0.19	4.86E-07	0.07	5.07E-01	0.27	2.81E-02
Nat14	-0.19	1.75E-03	0.11	2.87E-01	0.32	2.46E-02
Scrn3	-0.20	2.44E-03	0.10	2.75E-01	0.31	8.02E-03
Atrnl1	-0.20	4.23E-05	0.01	9.18E-01	0.21	2.57E-02
Phyhip	-0.20	7.04E-08	-0.01	9.37E-01	0.19	9.15E-03
Plekho2	-0.20	5.21E-03	0.17	6.98E-02	0.38	1.61E-03
Lman2l	-0.20	2.03E-03	0.11	3.31E-01	0.33	3.43E-02
Ddx3x	-0.20	4.84E-08	0.18	7.37E-02	0.40	1.59E-03
Syt4	-0.21	6.34E-09	-0.02	8.74E-01	0.19	4.39E-02
Ccdc184	-0.21	6.40E-03	0.09	3.77E-01	0.31	3.49E-02
Cntnap1	-0.21	1.88E-07	-0.01	9.12E-01	0.20	3.00E-02
Itm2b	-0.21	6.61E-15	-0.05	4.63E-01	0.16	3.50E-02
Phyh	-0.22	3.13E-05	0.06	6.05E-01	0.28	2.58E-02
Rpusd1	-0.22	4.77E-06	0.03	7.92E-01	0.25	2.25E-02
Rnf122	-0.22	6.58E-03	-0.65	2.78E-14	-0.48	9.67E-04
Med9	-0.22	7.27E-05	0.02	8.35E-01	0.25	2.96E-02
Zbtb4	-0.22	2.48E-10	-0.02	7.23E-01	0.20	2.31E-03
Mllt6	-0.22	1.39E-11	-0.08	6.72E-02	0.14	7.82E-03
Anapc11	-0.22	3.52E-04	0.07	5.24E-01	0.31	2.63E-02
Smim12	-0.22	4.11E-04	0.05	6.69E-01	0.28	2.36E-02
Gaa	-0.22	2.69E-07	-0.02	7.51E-01	0.20	1.41E-02
Pdk1	-0.23	1.96E-06	0.02	8.50E-01	0.25	1.76E-02
Map1lc3b	-0.23	9.62E-09	-0.04	5.96E-01	0.19	4.03E-02
Stk32c	-0.24	2.42E-06	0.07	3.96E-01	0.32	2.27E-03
Necab1	-0.24	1.30E-07	0.09	4.36E-01	0.33	9.02E-03
Mlip	-0.24	2.28E-03	0.17	2.21E-01	0.43	3.71E-02
Nceh1	-0.24	1.61E-12	-0.07	2.97E-01	0.17	2.02E-02
Moxd1	-0.24	2.19E-02	0.13	2.67E-01	0.39	2.08E-02
Hdac11	-0.25	2.27E-11	-0.02	8.06E-01	0.23	1.81E-02
Abhd8	-0.25	5.98E-08	0.03	8.38E-01	0.29	3.57E-02
Scn2b	-0.25	2.81E-11	-0.01	8.96E-01	0.24	2.95E-03
Fam171a2	-0.25	2.40E-07	0.05	5.97E-01	0.31	4.31E-03
Panx2	-0.25	1.43E-08	0.03	8.17E-01	0.29	2.63E-02
Shisa5	-0.25	4.58E-05	0.02	8.87E-01	0.28	3.23E-02
Pcdhgb6	-0.26	4.62E-03	0.11	3.60E-01	0.39	1.48E-02
Megf8	-0.26	2.76E-09	-0.06	4.64E-01	0.20	4.86E-02
Meis2	-0.26	8.61E-07	0.02	8.56E-01	0.29	2.43E-02
Prxl2b	-0.26	1.24E-04	0.13	1.81E-01	0.41	3.12E-03
Lzts3	-0.26	2.24E-10	0.06	4.53E-01	0.33	3.01E-04
Fam102a	-0.26	1.85E-12	-0.02	8.55E-01	0.25	7.54E-03
Nrsn2	-0.27	1.12E-06	0.06	6.62E-01	0.34	2.47E-02
Mfge8	-0.27	9.47E-07	0.14	2.47E-01	0.44	8.02E-03
Lonrf1	-0.27	1.93E-04	0.05	5.94E-01	0.34	1.01E-02
Pde7b	-0.27	5.41E-05	-0.03	7.68E-01	0.25	4.31E-02
Coa6	-0.28	2.26E-03	0.09	5.55E-01	0.39	3.27E-02
Apln	-0.28	1.82E-04	0.18	2.15E-01	0.49	1.41E-02
Mmut	-0.28	5.33E-06	0.00	9.75E-01	0.29	3.06E-02
Lgi4	-0.28	3.43E-06	0.11	3.73E-01	0.42	1.06E-02
Sncb	-0.29	5.07E-11	-0.05	4.74E-01	0.24	6.28E-03
Ppp2r3d	-0.29	8.02E-07	0.07	6.22E-01	0.37	2.43E-02
Etfrf1	-0.29	5.09E-04	0.09	4.41E-01	0.40	8.88E-03
Pltp	-0.29	3.53E-04	0.05	6.79E-01	0.36	3.50E-02
Prr13	-0.29	2.99E-06	0.05	6.49E-01	0.36	6.70E-03
Lrrc24	-0.29	5.60E-06	0.05	7.04E-01	0.36	2.84E-02
Rit2	-0.29	9.35E-10	0.05	6.94E-01	0.35	8.65E-03
Nsg2	-0.29	7.39E-17	-0.13	3.06E-03	0.17	8.88E-03
Intu	-0.30	6.86E-05	-0.02	9.08E-01	0.29	4.88E-02
Sptbn4	-0.30	1.33E-08	-0.09	2.09E-01	0.21	4.45E-02
Tsen34	-0.30	7.32E-09	0.00	9.76E-01	0.31	2.42E-02
Tyw3	-0.30	5.92E-04	0.05	7.01E-01	0.37	1.82E-02
Cyb5d2	-0.31	1.11E-04	0.00	9.90E-01	0.32	4.03E-02
Anxa7	-0.31	7.69E-15	-0.10	4.83E-02	0.20	1.57E-03
Camkv	-0.31	1.47E-18	-0.11	1.09E-01	0.20	1.51E-02
Fads3	-0.31	7.41E-09	-0.09	3.00E-01	0.23	4.33E-02
Cmss1	-0.31	4.53E-03	0.06	7.20E-01	0.40	4.03E-02
Pnma8b	-0.31	1.07E-13	-0.09	2.03E-01	0.23	1.39E-02
Incenp	-0.31	5.43E-06	0.02	8.66E-01	0.35	8.07E-03
Tcaim	-0.32	3.14E-06	-0.08	4.06E-01	0.25	4.39E-02
Emc9	-0.32	8.66E-05	0.06	6.23E-01	0.40	1.01E-02
Usp11	-0.32	1.08E-18	-0.15	1.85E-03	0.17	1.37E-02
Sema4f	-0.32	3.32E-13	-0.13	1.52E-02	0.19	1.69E-02
Nelfcd	-0.33	7.86E-12	-0.12	8.19E-02	0.21	2.94E-02
Tmsb10	-0.33	1.14E-10	-0.03	8.04E-01	0.30	2.98E-02
Ppm1m	-0.33	2.90E-08	-0.11	1.91E-01	0.23	4.93E-02
Isyna1	-0.34	1.07E-07	0.06	6.82E-01	0.41	1.30E-02
Stmn1	-0.34	1.13E-13	-0.05	6.69E-01	0.29	2.97E-02
Eif2s3x	-0.34	3.97E-06	0.27	8.22E-02	0.67	3.99E-03
Cep63	-0.34	1.25E-09	-0.04	7.45E-01	0.31	6.03E-03
Ptprk	-0.35	8.06E-17	-0.15	1.14E-02	0.20	1.59E-02
Nicn1	-0.35	1.41E-20	-0.17	2.76E-03	0.18	3.21E-02
Ankrd35	-0.35	1.81E-04	0.05	7.65E-01	0.43	4.70E-02

Table S3 (7/9)

Kcnj9	-0.35	3.79E-16	-0.14	2.92E-02	0.21	3.00E-02
Ppcdc	-0.35	1.03E-05	-0.05	7.15E-01	0.32	3.00E-02
Cd302	-0.35	5.69E-05	0.05	7.69E-01	0.42	2.28E-02
Extl2	-0.36	2.03E-17	-0.14	1.87E-02	0.21	1.25E-02
Rab10os	-0.36	1.08E-11	0.05	7.06E-01	0.42	5.30E-03
Bcas3	-0.36	9.48E-16	-0.15	2.60E-02	0.21	2.00E-02
Capn1	-0.36	4.73E-07	0.00	9.79E-01	0.38	4.95E-03
Serpinb9	-0.37	1.01E-04	0.04	7.93E-01	0.43	1.06E-02
Nelfb	-0.37	3.71E-16	-0.14	3.81E-02	0.23	1.71E-02
Gnb4	-0.37	2.13E-11	-0.64	1.21E-20	-0.29	1.97E-02
Slc9a8	-0.38	8.49E-16	-0.17	2.04E-02	0.21	4.95E-02
Ptpn21	-0.38	2.97E-06	-0.06	6.03E-01	0.32	2.94E-02
Aldh2	-0.38	1.71E-13	0.08	5.66E-01	0.48	2.59E-03
Il17d	-0.38	2.65E-04	0.08	6.33E-01	0.50	2.45E-02
Calhm5	-0.38	2.66E-04	-0.01	9.50E-01	0.39	4.52E-02
Khdrbs2	-0.38	2.91E-05	0.03	8.56E-01	0.44	1.74E-02
Tmem132a	-0.39	7.30E-13	-0.12	1.08E-01	0.27	2.46E-02
Ldhd	-0.39	1.65E-05	-0.01	9.59E-01	0.40	3.65E-02
Glt8d2	-0.39	8.13E-08	-0.06	6.19E-01	0.33	4.11E-02
Smim45	-0.39	6.51E-20	-0.18	1.95E-03	0.21	1.11E-02
Nr2f1	-0.39	8.60E-25	-0.20	1.22E-04	0.19	9.39E-03
Parm1	-0.39	3.16E-15	-0.12	1.48E-01	0.28	1.09E-02
Mansc1	-0.39	1.72E-05	-0.04	7.87E-01	0.37	4.54E-02
Cbx7	-0.39	3.90E-15	-0.12	2.60E-01	0.27	4.97E-02
Pcdh10	-0.39	1.26E-22	-0.16	3.34E-02	0.23	3.37E-02
Fn3k	-0.39	2.93E-10	-0.06	5.47E-01	0.34	4.31E-03
Prelp	-0.39	3.01E-07	0.18	3.99E-01	0.67	4.97E-02
Glb1	-0.40	4.30E-10	-0.09	3.59E-01	0.31	9.39E-03
Fam241b	-0.40	3.17E-09	-0.09	4.40E-01	0.31	3.65E-02
Tnip1	-0.40	2.16E-11	-0.09	3.21E-01	0.31	7.35E-03
Ring1	-0.40	2.77E-13	-0.07	5.67E-01	0.33	2.34E-02
Tle2	-0.40	1.11E-10	-0.06	6.19E-01	0.34	2.02E-02
Tbr1	-0.40	1.13E-17	-0.11	1.55E-01	0.29	5.55E-03
Faim2	-0.40	1.24E-26	-0.01	9.06E-01	0.40	2.25E-09
Eepd1	-0.41	1.41E-07	-0.04	7.70E-01	0.37	3.63E-02
Flot1	-0.41	5.86E-20	-0.21	3.97E-04	0.20	3.10E-02
Bbs9	-0.42	3.15E-09	-0.15	1.23E-01	0.27	4.86E-02
Phf1	-0.42	2.27E-15	-0.15	6.19E-02	0.27	1.39E-02
Efemp1	-0.42	1.39E-04	0.14	3.82E-01	0.61	1.06E-02
Cmbl	-0.42	1.62E-04	0.06	7.66E-01	0.53	4.76E-02
Aifm3	-0.42	1.68E-18	-0.02	9.18E-01	0.41	1.15E-02
Cideb	-0.43	9.95E-03	0.31	6.87E-02	0.90	2.78E-03
Klc4	-0.43	2.21E-10	-0.12	1.47E-01	0.32	6.51E-03
Nat8f4	-0.43	2.20E-08	-0.04	8.36E-01	0.41	3.07E-02
Akap12	-0.43	5.79E-14	-0.09	3.73E-01	0.34	9.02E-03
Al854703	-0.43	5.04E-15	-0.18	1.71E-02	0.26	2.23E-02
Rnf144b	-0.44	1.20E-14	-0.03	8.13E-01	0.41	3.73E-03
Mxra7	-0.44	5.42E-07	0.00	9.98E-01	0.46	1.06E-02
Ly6h	-0.44	1.69E-22	-0.09	3.63E-01	0.36	1.14E-03
Pcdhb17	-0.44	4.47E-09	-0.03	8.01E-01	0.42	5.68E-04
Lamc2	-0.44	2.73E-11	-0.02	8.97E-01	0.43	1.27E-02
Gm47863	-0.44	2.71E-02	0.19	4.08E-01	0.88	4.90E-02
Ccdc65	-0.45	2.22E-05	-0.03	8.69E-01	0.44	4.48E-02
Hps6	-0.45	2.93E-05	0.15	2.51E-01	0.64	2.77E-04
Smoc2	-0.45	2.60E-07	0.05	7.77E-01	0.53	1.03E-02
Pknox2	-0.45	3.60E-24	-0.21	3.29E-03	0.24	2.36E-02
G6pc3	-0.45	3.79E-15	-0.05	6.59E-01	0.41	9.34E-04
Smarca2	-0.45	5.44E-22	-0.11	5.45E-02	0.35	1.71E-05
Caly	-0.45	2.04E-24	-0.09	3.68E-01	0.36	1.12E-03
Klhdc1	-0.45	3.77E-11	-0.08	4.37E-01	0.38	1.42E-03
Slc4a3	-0.45	1.32E-24	-0.24	5.46E-08	0.21	1.06E-02
Ankrd24	-0.46	7.93E-18	-0.12	2.95E-01	0.34	1.38E-02
3830406C13Rik	-0.46	5.35E-11	-0.18	2.18E-02	0.29	2.04E-02
Sgpp2	-0.46	6.01E-09	0.07	6.62E-01	0.55	1.14E-03
Gm49937	-0.46	3.68E-03	0.18	3.95E-01	0.78	2.38E-02
Pgghg	-0.46	1.38E-05	0.04	8.56E-01	0.54	1.82E-02
Pcdhga9	-0.46	5.73E-05	0.16	2.29E-01	0.69	4.39E-04
Tmem106c	-0.47	1.32E-12	0.02	8.70E-01	0.51	4.11E-05
Grhpr	-0.47	1.23E-08	-0.11	3.40E-01	0.37	2.41E-02
H1f10	-0.47	2.67E-08	0.01	9.77E-01	0.50	3.20E-02
Hlf	-0.47	3.10E-34	-0.20	8.75E-03	0.27	1.02E-02
Car11	-0.47	1.59E-24	-0.04	7.60E-01	0.43	8.28E-04
Kiz	-0.47	4.84E-07	-0.03	8.94E-01	0.47	2.60E-02
Gsta4	-0.47	1.03E-13	-0.08	5.67E-01	0.40	2.59E-02
Gm30371	-0.47	2.80E-04	0.25	2.20E-01	0.87	7.00E-03
Prune2	-0.48	3.06E-28	-0.26	3.39E-06	0.21	1.96E-02
Tmem191c	-0.48	2.83E-22	-0.17	3.33E-02	0.31	7.49E-03
Rlbp1	-0.48	2.17E-13	-0.08	5.89E-01	0.42	9.39E-03
Them4	-0.48	1.60E-12	-0.19	1.39E-02	0.29	1.94E-02
Nudt2	-0.48	7.14E-08	-0.04	8.36E-01	0.46	2.78E-02
Pcdha10	-0.49	9.34E-04	0.30	7.15E-02	0.93	1.12E-03
Islr	-0.49	9.17E-09	0.10	5.65E-01	0.63	3.99E-03
Dguok	-0.50	1.66E-10	-0.20	2.18E-02	0.30	4.45E-02
L1cam	-0.50	4.33E-50	-0.26	9.45E-06	0.23	7.68E-03
Pck2	-0.50	2.61E-14	-0.21	6.13E-03	0.29	2.24E-02
Cdh7	-0.50	9.49E-11	-0.08	5.90E-01	0.43	1.87E-02
Ctxn2	-0.50	2.05E-05	0.00	9.99E-01	0.54	1.60E-02
Wdr19	-0.50	2.74E-18	-0.28	1.34E-05	0.23	4.25E-02
Cul9	-0.51	1.27E-37	-0.18	1.30E-03	0.32	1.77E-05
Trpm2	-0.51	4.85E-23	-0.19	4.02E-03	0.33	3.30E-04
Asah2	-0.51	2.14E-09	-0.14	1.82E-01	0.39	1.37E-02
Bmp3	-0.51	1.47E-14	0.00	9.94E-01	0.52	6.36E-03
4921531C22Rik	-0.52	2.15E-03	0.08	7.16E-01	0.73	3.50E-02
Slc13a4	-0.52	8.16E-08	0.03	9.03E-01	0.58	1.63E-02
Pcdhga12	-0.52	5.33E-14	-0.20	3.16E-02	0.33	1.94E-02
Cfap46	-0.52	3.19E-04	0.09	6.11E-01	0.70	1.11E-02
D130017N08Rik	-0.53	1.02E-12	-0.08	5.05E-01	0.46	2.32E-03
Tspo	-0.53	6.68E-04	0.20	3.13E-01	0.89	6.51E-03
Hemk1	-0.53	5.07E-13	-0.11	2.95E-01	0.44	8.73E-04
Acads	-0.53	2.13E-06	-0.08	6.18E-01	0.48	3.62E-02

Table S3 (8/9)

Eps8l2	-0.53	5.79E-04	0.17	4.31E-01	0.88	2.25E-02
Fuz	-0.53	7.14E-14	-0.08	6.40E-01	0.46	3.85E-02
Dnah1	-0.54	5.46E-10	-0.02	9.38E-01	0.55	8.19E-03
Cdkl4	-0.54	9.34E-14	-0.23	7.75E-03	0.31	4.52E-02
Vars2	-0.54	2.19E-15	-0.26	4.33E-05	0.29	2.55E-02
Klhdc7b	-0.55	9.69E-03	0.29	1.60E-01	1.22	8.88E-03
Ccdc136	-0.55	3.73E-37	-0.31	2.27E-05	0.24	4.11E-02
Mapk3	-0.56	6.71E-41	-0.26	5.95E-05	0.30	1.65E-03
Trim45	-0.56	2.45E-09	-0.19	1.00E-01	0.38	4.86E-02
Gm5069	-0.56	3.33E-04	0.17	4.14E-01	0.88	7.28E-03
P2rx3	-0.56	9.53E-03	0.21	3.38E-01	1.10	2.12E-02
5530601H04Rik	-0.56	1.11E-19	0.07	6.83E-01	0.65	2.07E-04
Cracr2a	-0.56	1.41E-04	0.09	6.56E-01	0.75	9.15E-03
Cd6	-0.56	3.18E-04	0.27	1.12E-01	0.99	7.29E-04
Cpne4	-0.57	5.88E-36	-0.25	2.02E-05	0.32	1.30E-04
Ntn4	-0.57	6.66E-13	-0.07	6.00E-01	0.52	3.63E-04
Plppr3	-0.57	2.59E-23	-0.18	4.39E-02	0.40	1.74E-03
Crispld1	-0.58	3.79E-08	-0.08	6.90E-01	0.52	3.43E-02
Rhov	-0.58	4.56E-07	-0.04	8.71E-01	0.58	3.20E-02
Gemin8	-0.58	1.82E-08	-0.14	3.40E-01	0.46	2.86E-02
Aldh1a2	-0.58	1.20E-09	0.00	9.88E-01	0.61	2.44E-02
Dlec1	-0.58	6.84E-05	0.00	1.00E+00	0.66	4.98E-02
Eps8l1	-0.58	1.15E-02	0.15	5.38E-01	1.87	3.84E-02
Kdm6a	-0.59	3.38E-15	0.02	9.21E-01	0.63	1.54E-03
Cib2	-0.59	7.53E-17	-0.10	4.28E-01	0.50	4.95E-04
Atp10d	-0.59	4.10E-08	-0.17	1.97E-01	0.45	3.00E-02
Aph1c	-0.59	1.70E-09	-0.23	3.17E-02	0.38	4.51E-02
Ypel4	-0.59	8.65E-53	-0.26	6.47E-04	0.33	1.44E-03
Jpx	-0.60	5.41E-11	-0.04	8.48E-01	0.58	1.16E-02
Mycbpap	-0.60	1.99E-03	0.27	2.01E-01	1.19	8.48E-03
C030014I23Rik	-0.60	1.44E-07	-0.13	4.64E-01	0.50	4.18E-02
Tmem255a	-0.60	8.38E-12	-0.17	1.15E-01	0.45	1.10E-02
Pik3ip1	-0.61	2.29E-21	-0.30	9.55E-05	0.30	2.69E-02
Mrgpre	-0.61	3.25E-11	-0.25	2.40E-02	0.37	4.61E-02
Igsf8	-0.61	7.02E-36	-0.24	5.14E-03	0.36	7.30E-03
B230303O12Rik	-0.61	4.22E-03	0.31	1.40E-01	1.43	6.70E-03
Ccn3	-0.61	1.74E-34	-0.33	2.95E-05	0.28	3.99E-02
Echdc2	-0.61	2.77E-12	-0.09	5.70E-01	0.54	1.02E-02
Gucy2e	-0.63	2.30E-05	0.14	4.17E-01	0.89	1.60E-03
Tcf19	-0.63	8.51E-09	-0.11	4.96E-01	0.55	1.76E-02
Nol3	-0.63	2.49E-19	-0.13	2.83E-01	0.51	2.91E-04
Pcdhb12	-0.63	6.92E-13	-0.11	3.33E-01	0.54	3.01E-04
Gstt1	-0.63	4.56E-10	-0.14	3.04E-01	0.52	4.65E-03
Igfbp5	-0.63	9.09E-64	-0.20	6.08E-02	0.42	3.12E-03
Aloxe3	-0.64	5.69E-11	-0.22	5.59E-02	0.44	2.63E-02
Idua	-0.64	2.72E-21	-0.14	3.25E-01	0.51	5.83E-03
Tspan17	-0.64	7.84E-26	-0.11	3.83E-01	0.54	1.07E-04
Cc2d2a	-0.65	7.56E-23	-0.33	5.43E-06	0.32	2.07E-02
Mgat5b	-0.66	2.59E-34	-0.30	2.42E-09	0.36	1.36E-04
Prr16	-0.66	1.54E-17	-0.14	3.83E-01	0.51	1.93E-02
Ptger3	-0.66	1.22E-06	-0.02	9.49E-01	0.72	2.25E-02
Cd83	-0.67	8.11E-15	-0.14	2.62E-01	0.56	4.29E-04
Asb16	-0.67	5.23E-04	0.18	4.26E-01	1.18	9.84E-03
Itgbl1	-0.68	7.70E-08	-0.04	8.80E-01	0.69	2.30E-02
Gm20628	-0.68	2.37E-04	0.04	8.79E-01	0.91	1.43E-02
Col8a2	-0.69	2.02E-07	0.16	4.69E-01	1.00	9.27E-03
Slc47a1	-0.69	5.12E-09	-0.03	8.90E-01	0.71	2.91E-02
Rnf207	-0.70	3.49E-12	-0.23	1.11E-01	0.47	4.40E-02
Timeless	-0.70	2.96E-11	-0.21	8.70E-02	0.51	1.06E-02
Cst6	-0.72	2.13E-08	-0.08	7.52E-01	0.70	3.44E-02
Rgsl1	-0.72	3.28E-08	-0.12	5.15E-01	0.66	1.70E-02
Plxnd1	-0.72	4.54E-41	-0.37	1.34E-07	0.35	4.09E-03
Rorb	-0.73	8.50E-36	-0.28	1.74E-02	0.43	1.76E-02
Vill	-0.73	3.91E-17	-0.10	5.69E-01	0.66	1.02E-03
Kitl	-0.73	9.70E-27	-0.26	8.51E-05	0.49	5.64E-05
Gpr88	-0.74	2.38E-66	-0.15	2.77E-01	0.59	3.53E-04
Slc16a11	-0.76	5.19E-26	-0.36	2.28E-04	0.39	2.66E-02
Crocc	-0.76	1.19E-27	-0.32	4.35E-03	0.43	2.95E-02
AW495222	-0.77	8.44E-08	-0.24	1.35E-01	0.59	4.43E-02
Ccdc171	-0.78	1.58E-09	0.02	9.45E-01	0.88	2.56E-04
Gm26653	-0.79	1.97E-05	0.00	9.91E-01	1.01	2.40E-02
Lama4	-0.79	7.86E-30	-0.18	2.00E-01	0.61	1.08E-03
6430571L13Rik	-0.79	5.76E-09	-0.18	3.31E-01	0.67	2.07E-02
Ccdc14	-0.81	1.07E-08	-0.25	1.18E-01	0.61	3.81E-02
Evc2	-0.81	5.73E-27	-0.15	1.63E-01	0.67	4.91E-06
Nme4	-0.82	6.05E-08	-0.23	1.80E-01	0.67	2.96E-02
Sytl2	-0.82	2.92E-56	-0.53	2.01E-13	0.29	3.15E-02
Gucy1a1	-0.82	1.82E-51	-0.36	2.79E-05	0.45	1.08E-03
Rwdd3	-0.83	2.28E-10	-0.29	3.94E-02	0.59	2.45E-02
Slc9b2	-0.83	4.59E-11	-0.18	2.70E-01	0.71	3.08E-03
Itga11	-0.84	2.21E-08	0.09	6.69E-01	1.09	4.11E-04
Tle6	-0.84	4.17E-10	0.05	8.40E-01	1.01	2.10E-03
Ngb	-0.86	1.02E-15	-0.37	1.12E-03	0.51	1.24E-02
Glra3	-0.86	7.68E-14	-0.25	9.81E-02	0.62	2.01E-02
Shisa3	-0.86	9.84E-11	-0.16	4.64E-01	0.74	4.65E-02
4933406C10Rik	-0.86	6.16E-11	-0.27	1.26E-01	0.63	4.50E-02
Cchcr1	-0.88	1.19E-17	-0.34	5.80E-03	0.56	4.54E-03
Acat3	-0.89	5.96E-10	-0.10	6.34E-01	0.89	3.03E-03
Brca2	-0.91	6.51E-14	-0.37	7.14E-03	0.56	4.51E-02
Gm45470	-0.93	2.36E-11	-0.15	4.73E-01	0.87	4.52E-03
Ntn5	-0.93	5.18E-42	0.12	4.49E-01	1.11	4.55E-11
Mettl27	-0.93	9.20E-15	-0.47	3.83E-06	0.50	2.30E-02
Mme	-0.95	8.04E-22	-0.43	3.76E-04	0.50	2.59E-02
Gmnc	-0.95	2.69E-07	-0.18	4.15E-01	0.96	4.03E-02
Mdfic2	-0.96	2.87E-08	0.34	9.96E-02	1.93	5.76E-04
1700001L05Rik	-0.97	5.33E-31	-0.39	9.72E-03	0.54	4.11E-02
Cdkl1	-0.97	3.28E-24	-0.41	8.91E-08	0.60	1.02E-04
Otof	-1.00	1.30E-66	-0.40	1.45E-05	0.60	1.60E-05
Sec1	-1.00	2.44E-16	-0.30	9.38E-02	0.70	3.33E-02
Cdsn	-1.02	3.52E-09	-0.04	8.87E-01	1.21	9.56E-04

Table S3 (9/9)

Gbp9	-1.04	9.46E-19	-0.50	1.74E-04	0.55	4.11E-02
Gm5148	-1.05	5.72E-20	-0.34	2.15E-02	0.72	4.92E-03
Bnip5	-1.06	1.08E-25	-0.38	8.21E-04	0.70	8.48E-04
Gm29674	-1.06	3.86E-17	-0.22	2.42E-01	0.90	3.70E-03
Col8a1	-1.10	1.07E-23	-0.49	6.84E-05	0.62	7.62E-03
Qrfpr	-1.19	3.74E-21	-0.26	1.09E-01	0.99	5.64E-05
Plk5	-1.19	1.40E-45	-0.10	4.15E-01	1.14	1.09E-17
Rprm	-1.25	2.51E-87	-0.74	1.41E-32	0.52	9.96E-06
Spag5	-1.33	2.17E-66	-0.49	2.92E-08	0.86	5.26E-09
Gm12371	-1.51	3.64E-34	-0.63	4.47E-05	0.84	9.39E-03
Rskr	-1.52	2.69E-69	-0.42	1.88E-04	1.12	1.14E-09
Gpr6	-1.74	3.02E-27	-0.67	1.63E-05	1.23	2.91E-04
Samd3	-2.16	4.93E-32	-0.73	3.00E-05	1.76	3.37E-04

Table S4– Gene set A (1/9)

gene_name	chromosome	gene_type	WT_light_vs_dark.l2fc	WT_light_vs_dark.padj	WT_hr12_vs_dark.l2fc	WT_hr12_vs_dark.padj	SWAP_light_vs_dark.l2fc	SWAP_light_vs_dark.padj	SWAP_hr12_vs_dark.l2fc	SWAP_hr12_vs_dark.padj
Igfn1	1	protein_coding	0.83	2.06E-32	0.45	2.04E-08	0.58	4.24E-10	0.75	8.55E-12
Asap1	15	protein_coding	0.35	1.58E-27	0.44	4.32E-38	0.20	3.89E-04	0.31	4.75E-08
Kcnv1	15	protein_coding	0.45	2.41E-25	0.48	5.22E-30	0.25	1.95E-04	0.35	2.30E-06
Pmepa1	2	protein_coding	0.52	2.43E-23	1.72	1.13E-142	0.27	6.22E-06	1.12	8.65E-95
Tamalin	15	protein_coding	0.60	1.68E-21	1.58	1.51E-97	0.19	3.56E-02	1.13	2.86E-37
Lingo1	9	protein_coding	0.46	5.93E-21	1.00	7.83E-101	0.27	3.77E-07	0.76	1.04E-43
Slc6a17	3	protein_coding	0.26	3.65E-18	0.72	7.31E-109	0.07	4.28E-01	0.39	7.45E-08
Rgs4	1	protein_coding	0.40	4.16E-18	0.08	7.64E-03	0.14	9.33E-02	0.03	7.88E-01
Scube1	15	protein_coding	0.44	6.65E-18	1.55	7.33E-175	0.07	5.36E-01	0.89	7.14E-38
Lancl2	6	protein_coding	0.30	2.00E-17	0.14	1.71E-03	0.14	4.36E-03	0.09	2.23E-01
Gdpd5	7	protein_coding	0.42	2.91E-16	0.67	2.35E-38	0.23	2.19E-04	0.62	2.34E-21
Arhgap10	8	protein_coding	0.48	1.29E-15	0.33	3.43E-06	0.25	1.41E-03	0.35	3.27E-07
St8sia5	18	protein_coding	0.37	1.65E-15	0.75	3.66E-106	0.12	5.34E-02	0.48	1.43E-13
Nptxr	15	protein_coding	0.27	3.68E-15	0.60	2.60E-44	0.08	3.59E-01	0.35	3.05E-06
Strip2	6	protein_coding	0.55	3.80E-15	0.33	9.29E-06	0.21	4.17E-02	0.24	1.05E-01
Gcnt4	13	protein_coding	0.57	6.64E-15	1.24	2.96E-111	0.23	8.33E-03	0.77	5.60E-19
Car10	11	protein_coding	0.32	7.40E-15	0.42	1.15E-22	0.15	3.39E-02	0.39	3.99E-08
Fosb	7	protein_coding	0.86	8.60E-15	2.62	2.74E-136	0.18	2.48E-01	1.61	4.60E-24
Mthfd1l	10	protein_coding	0.53	1.35E-14	0.25	1.07E-02	0.17	2.05E-01	0.10	5.94E-01
Cacng3	7	protein_coding	0.35	1.69E-14	0.25	6.73E-08	0.15	1.88E-02	0.25	1.44E-04
Lipg	18	protein_coding	0.78	3.64E-14	1.81	1.22E-45	0.65	1.01E-11	1.64	1.68E-48
Hkdc1	10	protein_coding	0.54	3.76E-14	0.93	8.13E-33	0.29	8.05E-06	0.44	4.39E-11
Fbxw7	3	protein_coding	0.29	3.76E-14	0.10	7.43E-03	0.07	3.65E-01	0.12	1.42E-01
Stard8	X	protein_coding	0.52	9.68E-14	1.23	2.68E-73	0.14	2.28E-01	0.79	1.03E-24
Ndrg3	2	protein_coding	0.24	3.78E-13	0.09	1.61E-02	-0.02	7.57E-01	0.03	7.66E-01
Nlk	11	protein_coding	0.30	6.00E-13	0.44	1.29E-38	0.06	4.59E-01	0.36	4.62E-08
Dnajb5	4	protein_coding	0.37	8.53E-13	1.34	1.80E-94	0.25	6.22E-06	0.99	3.22E-46
Rgs7	1	protein_coding	0.36	1.23E-12	0.31	1.24E-08	0.11	5.31E-02	0.18	3.63E-03
Prmt8	6	protein_coding	0.50	5.36E-12	0.69	8.78E-32	0.16	5.64E-04	0.47	6.10E-17
Diras2	13	protein_coding	0.40	7.74E-12	0.44	1.89E-24	0.19	1.04E-02	0.37	2.61E-06
Pak6	2	protein_coding	0.37	1.38E-11	0.61	2.14E-27	0.10	1.03E-01	0.29	2.13E-07
Snap25	2	protein_coding	0.28	3.15E-11	0.16	7.94E-06	0.08	7.97E-02	0.27	9.77E-08
Ttl	2	protein_coding	0.30	3.93E-11	0.34	1.02E-16	0.21	4.60E-03	0.30	2.26E-05
Net1	13	protein_coding	0.49	7.79E-11	0.45	1.37E-10	0.00	9.83E-01	0.48	2.32E-05
Mpp3	11	protein_coding	0.34	9.85E-11	0.55	4.85E-29	0.12	1.06E-01	0.34	4.89E-08
Nptx2	5	protein_coding	0.73	1.02E-10	2.50	9.00E-137	0.54	1.65E-06	2.12	6.73E-98
Dusp14	11	protein_coding	0.40	1.10E-10	0.90	8.95E-44	0.16	5.37E-03	0.72	5.71E-24
Scg3	9	protein_coding	0.29	1.28E-10	0.33	6.78E-24	0.07	1.53E-01	0.15	3.23E-03
Plcl2	17	protein_coding	0.33	1.42E-10	0.57	1.19E-41	0.02	7.45E-01	0.28	1.35E-08
Rgs8	1	protein_coding	0.24	1.42E-10	0.58	8.48E-44	0.10	1.53E-01	0.37	3.96E-08
Pdp1	4	protein_coding	0.35	1.94E-10	1.14	5.66E-105	0.10	3.30E-01	0.78	5.08E-23
Stx1b	7	protein_coding	0.24	2.39E-10	0.52	2.70E-72	0.02	8.13E-01	0.34	6.23E-17
Camkk2	5	protein_coding	0.22	3.88E-10	0.26	1.38E-13	0.14	9.05E-02	0.23	3.71E-03
Map3k5	10	protein_coding	0.39	4.83E-10	0.40	7.46E-09	0.25	3.20E-04	0.35	1.48E-06
Car7	8	protein_coding	0.40	6.94E-10	0.28	1.93E-05	0.21	2.57E-03	0.25	5.96E-03
Coq10b	1	protein_coding	0.46	7.72E-10	0.52	2.22E-10	0.31	2.42E-06	0.44	4.35E-09
Serpinb8	1	protein_coding	0.63	7.72E-10	2.07	4.71E-124	0.03	8.75E-01	0.91	2.62E-11
Rgs2	1	protein_coding	0.36	7.95E-10	0.24	1.31E-04	0.07	3.21E-01	0.32	8.68E-08
Gm29695	1	protein_coding	0.56	8.30E-10	0.82	6.50E-32	0.31	2.01E-03	0.47	3.33E-04
Lgi2	5	protein_coding	0.35	9.21E-10	0.19	8.18E-04	0.23	3.35E-03	0.16	1.15E-01
Cacng2	15	protein_coding	0.23	9.48E-10	0.54	4.98E-39	0.05	5.65E-01	0.35	1.28E-07
Pi4ka	16	protein_coding	0.18	1.47E-09	0.40	4.74E-48	-0.01	9.06E-01	0.21	3.97E-03
Inka2	3	protein_coding	0.33	1.54E-09	0.91	1.52E-89	0.14	2.96E-02	0.61	8.43E-29
Cdk5r2	1	protein_coding	0.21	1.64E-09	0.39	2.87E-22	0.19	2.27E-04	0.29	1.53E-06
Dusp3	11	protein_coding	0.24	2.81E-09	0.21	1.09E-11	0.19	3.32E-06	0.16	1.77E-03
Pspc1	14	protein_coding	0.33	2.81E-09	0.25	3.86E-05	0.05	5.57E-01	0.05	6.34E-01
Klf9	19	protein_coding	0.34	2.83E-09	0.79	5.69E-141	-0.03	7.85E-01	0.46	1.05E-09
Phf21b	15	protein_coding	0.54	3.14E-09	1.14	1.74E-57	0.20	7.52E-02	0.68	1.48E-08
Sst	16	protein_coding	0.31	3.77E-09	0.27	1.94E-10	0.24	3.73E-04	0.19	2.01E-02
Ptgs2	1	protein_coding	0.67	4.21E-09	2.01	3.63E-30	0.35	1.10E-03	1.59	3.05E-41
Arpp19	9	protein_coding	0.32	4.81E-09	0.21	1.44E-06	0.10	1.86E-01	0.27	1.69E-03
Hr	14	protein_coding	0.34	5.42E-09	0.33	2.40E-08	0.17	2.02E-02	0.24	5.61E-07
6430548M08Rik	8	protein_coding	0.21	8.09E-09	0.62	5.02E-60	0.13	9.79E-05	0.50	1.91E-41
Sulf2	2	protein_coding	0.24	8.76E-09	0.64	2.51E-50	0.00	9.69E-01	0.32	5.24E-09
Tmem132d	5	protein_coding	0.38	9.48E-09	0.48	9.08E-14	0.16	1.14E-01	0.21	5.59E-02
Grm4	17	protein_coding	0.31	1.12E-08	0.37	1.77E-12	0.19	4.30E-02	0.33	2.40E-03
Tfrc	16	protein_coding	0.29	1.27E-08	0.42	1.29E-23	0.13	1.29E-01	0.25	1.14E-02
Rnf115	3	protein_coding	0.28	2.05E-08	0.41	4.00E-18	0.04	6.84E-01	0.22	1.22E-03
Pim3	15	protein_coding	0.41	2.93E-08	0.47	1.86E-14	0.19	1.02E-01	0.55	4.90E-06
Gpr153	4	protein_coding	0.45	3.05E-08	0.95	6.23E-29	0.29	1.17E-02	0.73	1.26E-08
Il15ra	2	protein_coding	0.55	3.26E-08	1.16	3.44E-20	0.28	1.01E-02	0.72	3.85E-10
Mark1	1	protein_coding	0.25	3.33E-08	0.46	2.08E-41	0.09	1.35E-01	0.21	5.89E-05
Sun1	5	protein_coding	0.25	3.56E-08	0.39	3.55E-24	0.08	1.61E-01	0.24	2.97E-05
Lingo3	10	protein_coding	0.49	3.66E-08	1.26	1.54E-93	0.24	8.99E-03	0.95	9.85E-29
Plcb1	2	protein_coding	0.20	3.73E-08	0.14	3.08E-03	0.07	4.28E-01	0.11	1.64E-01
Mapk4	18	protein_coding	0.38	3.84E-08	0.98	2.54E-40	0.02	8.79E-01	0.61	4.79E-29
Gpr26	7	protein_coding	0.25	5.34E-08	0.45	4.45E-55	0.23	1.70E-03	0.31	1.24E-04
R3hdm2	10	protein_coding	0.21	5.49E-08	0.33	1.87E-21	0.01	9.46E-01	0.22	5.34E-04
Mllt11	3	protein_coding	0.24	6.01E-08	0.21	3.55E-08	0.03	6.96E-01	-0.02	8.68E-01
Rimbp2	5	protein_coding	0.30	6.63E-08	0.32	1.66E-14	0.02	8.87E-01	0.18	1.31E-01
Fst	13	protein_coding	0.58	6.97E-08	1.67	1.03E-39	0.20	1.41E-01	1.15	2.69E-21
Smim43	3	protein_coding	0.45	7.18E-08	0.97	5.52E-82	-0.01	9.43E-01	0.59	3.54E-12
Egr1	18	protein_coding	0.61	7.30E-08	1.73	3.79E-81	0.21	1.46E-01	1.04	1.81E-11
Brinp1	4	protein_coding	0.30	7.57E-08	0.29	8.68E-11	0.14	2.48E-02	0.30	4.85E-07
Fhl2	1	protein_coding	0.31	7.57E-08	0.40	5.25E-11	0.22	6.05E-03	0.42	1.63E-05
Slc9a5	8	protein_coding	0.46	7.71E-08	1.29	5.39E-101	0.04	7.68E-01	0.85	7.74E-47
Vgf	5	protein_coding	0.44	8.73E-08	1.36	3.18E-94	0.31	2.46E-05	1.04	4.69E-41
St3gal5	6	protein_coding	0.31	1.11E-07	0.52	8.73E-44	0.11	3.98E-02	0.41	2.02E-17
Npnt	3	protein_coding	0.27	1.17E-07	0.16	4.21E-04	-0.05	6.35E-01	-0.16	7.53E-02
Doc2a	7	protein_coding	0.37	1.23E-07	0.33	4.28E-05	0.35	4.55E-14	0.22	8.75E-04
Fam107a	14	protein_coding	0.30	1.35E-07	0.70	3.17E-40	-0.14	2.28E-01	0.39	5.34E-04
Sel1l3	5	protein_coding	0.22	1.40E-07	0.30	8.40E-13	0.07	4.13E-01	0.18	6.98E-03
Ttc39b	4	protein_coding	0.25	1.46E-07	0.57	1.23E-36	0.17	2.55E-02	0.37	8.40E-08
Lamp5	2	protein_coding	0.38	1.46E-07	0.27	1.01E-06	0.21	6.86E-03	0.28	2.78E-03
Rnd1	15	protein_coding	0.46	1.64E-07	0.42	2.27E-06	-0.02	9.05E-01	0.15	1.35E-01
Pcsk1	13	protein_coding	0.42	1.77E-07	0.90	8.77E-31	0.23	5.33E-03	0.74	4.80E-13
Myl4	11	protein_coding	0.50	1.90E-07	0.47	5.11E-07	0.46	2.99E-07	0.30	1.62E-02
Mfsd2a	4	protein_coding	0.39	2.21E-07	1.28	6.07E-81	-0.16	2.96E-01	0.31	1.08E-01
Sorbs2	8	protein_coding	0.31	2.30E-07	0.44	1.40E-17	0.16	6.94E-02	0.22	4.26E-03
Actn4	7	protein_coding	0.22	2.51E-07	0.62	2.31E-57	0.01	9.30E-01	0.41	4.68E-18
Rph3a	5	protein_coding	0.22	2.59E-07	0.87	1.82E-124	0.15	1.81E-04	0.52	2.84E-43
Sema3a	5	protein_coding	0.32	2.81E-07	0.16	4.26E-02	0.17	4.09E-02	0.21	1.33E-02
Hrh2	13	protein_coding	0.35	3.11E-07	0.49	7.34E-14	0.16	5.44E-02	0.41	4.30E-07
Hmgcr	13	protein_coding	0.28	3.14E-07	0.78	1.12E-65	0.28	5.29E-04	0.49	7.73E-08

Table S4 (2/9)

Smap1	1	protein_coding	0.22	3.41E-07	0.27	2.66E-13	0.01	9.44E-01	0.08	1.40E-01
Septin6	X	protein_coding	0.22	3.55E-07	0.34	6.07E-17	0.12	3.98E-02	0.19	6.44E-03
Adam19	11	protein_coding	0.27	4.41E-07	0.72	1.72E-49	0.10	1.80E-01	0.34	9.15E-05
Ugcg	4	protein_coding	0.21	4.49E-07	0.19	1.35E-05	0.05	6.13E-01	0.14	3.77E-02
Mamld1	X	protein_coding	0.31	4.90E-07	0.98	3.63E-47	-0.20	8.41E-02	0.38	3.41E-03
Mfap3l	8	protein_coding	0.27	4.93E-07	0.16	1.66E-03	0.10	6.84E-02	0.04	6.69E-01
Mapk9	11	protein_coding	0.15	6.09E-07	0.12	3.74E-05	0.06	3.26E-01	0.09	1.10E-01
Plcxd2	16	protein_coding	0.22	6.52E-07	0.39	2.64E-26	0.17	4.58E-02	0.39	1.20E-06
Ackr1	1	protein_coding	0.24	7.50E-07	0.22	1.62E-04	0.05	6.47E-01	-0.04	7.78E-01
Sema7a	9	protein_coding	0.25	1.00E-06	0.83	1.64E-95	0.16	7.86E-03	0.58	3.09E-25
Denr	5	protein_coding	0.26	1.02E-06	0.19	4.40E-04	0.03	7.96E-01	0.11	1.90E-01
Inhba	13	protein_coding	0.56	1.04E-06	2.74	2.50E-59	0.30	1.44E-02	1.52	3.23E-21
Ergic1	17	protein_coding	0.18	1.08E-06	0.23	2.87E-12	0.06	2.65E-01	0.14	2.12E-03
Atp2a2	5	protein_coding	0.18	1.09E-06	0.40	4.06E-36	0.04	6.19E-01	0.24	1.67E-05
Dclk1	3	protein_coding	0.21	1.10E-06	0.61	1.36E-69	0.00	9.89E-01	0.18	2.60E-02
Camk1g	1	protein_coding	0.42	1.11E-06	1.43	7.38E-124	0.07	5.90E-01	0.78	1.24E-22
Etl4	2	protein_coding	0.23	1.11E-06	0.16	3.18E-05	0.06	5.57E-01	0.11	2.20E-01
Actr3b	5	protein_coding	0.21	1.11E-06	0.24	4.79E-09	-0.01	9.62E-01	-0.01	9.35E-01
Egr3	14	protein_coding	0.56	1.12E-06	2.14	1.33E-112	0.09	4.98E-01	1.66	1.88E-54
Smarcd1	15	protein_coding	0.17	1.24E-06	0.27	2.55E-11	0.03	6.90E-01	0.12	3.29E-02
Igsf9	1	protein_coding	0.45	1.26E-06	0.41	5.44E-06	0.21	1.07E-01	0.40	3.71E-03
Nrn1	13	protein_coding	0.39	1.26E-06	1.10	5.25E-132	0.12	9.43E-02	0.78	1.33E-46
Smyd2	1	protein_coding	0.28	1.45E-06	0.35	1.57E-13	0.04	6.55E-01	0.20	3.06E-03
Fdft1	14	protein_coding	0.27	1.47E-06	0.28	4.47E-09	0.13	8.13E-02	0.23	3.71E-03
Pparg	6	protein_coding	0.48	1.58E-06	0.43	1.45E-03	0.13	3.48E-01	0.17	3.75E-01
Syndig1	2	protein_coding	0.31	1.65E-06	0.49	2.09E-16	0.14	1.07E-01	0.39	3.15E-06
Ift57	16	protein_coding	0.26	2.01E-06	0.17	2.18E-03	0.02	7.96E-01	0.08	2.81E-01
Klhl40	9	protein_coding	0.46	2.01E-06	1.69	3.89E-79	0.10	5.09E-01	0.72	3.83E-07
Mapk6	9	protein_coding	0.34	2.36E-06	0.61	5.55E-30	0.06	3.96E-01	0.44	4.47E-10
Fgf12	16	protein_coding	0.20	2.47E-06	0.11	2.63E-02	0.13	5.32E-02	0.09	2.40E-01
Fmnl1	11	protein_coding	0.29	2.62E-06	1.14	1.05E-181	0.05	6.34E-01	0.79	1.97E-18
Pcp4l1	1	protein_coding	0.25	2.65E-06	0.15	1.80E-02	0.19	1.36E-03	0.13	1.28E-01
Rnd3	2	protein_coding	0.39	2.72E-06	1.29	1.14E-59	0.04	7.50E-01	0.74	5.18E-20
Cap2	13	protein_coding	0.19	2.78E-06	0.42	5.49E-37	0.04	4.52E-01	0.35	3.83E-20
Itgav	2	protein_coding	0.24	2.78E-06	0.53	4.48E-28	0.18	3.45E-03	0.34	2.76E-08
Ntm	9	protein_coding	0.21	3.06E-06	0.11	1.69E-02	0.09	9.17E-02	0.04	5.47E-01
Dok5	2	protein_coding	0.34	3.17E-06	0.53	1.22E-14	0.23	3.79E-02	0.29	1.95E-02
Jcad	18	protein_coding	0.20	3.19E-06	0.68	9.63E-107	0.08	3.93E-01	0.52	1.11E-14
Lsm11	11	protein_coding	0.40	3.21E-06	1.21	3.91E-93	0.13	1.38E-01	0.64	8.38E-19
Tle3	9	protein_coding	0.26	3.48E-06	0.56	1.29E-24	0.04	7.83E-01	0.25	1.62E-02
Pcdh7	5	protein_coding	0.21	3.74E-06	0.26	6.48E-07	0.20	5.07E-04	0.16	2.93E-02
Rtn4rl2	2	protein_coding	0.31	3.78E-06	0.95	1.54E-41	0.22	1.21E-02	0.75	3.03E-21
Sorcs1	19	protein_coding	0.20	4.15E-06	0.27	3.04E-09	-0.01	9.31E-01	0.09	4.65E-01
Tnfrsf12a	17	protein_coding	0.51	4.18E-06	1.62	1.11E-35	0.04	8.27E-01	1.02	1.31E-15
Uvrag	7	protein_coding	0.22	4.21E-06	0.51	3.17E-24	0.00	9.69E-01	0.23	1.52E-04
Atf2	2	protein_coding	0.17	4.41E-06	0.20	2.75E-05	-0.04	7.12E-01	0.07	4.81E-01
Ptprj	2	protein_coding	0.25	4.41E-06	0.44	5.84E-23	-0.07	2.38E-01	0.17	1.63E-02
Ptprn	1	protein_coding	0.22	4.71E-06	0.55	5.04E-48	0.07	2.32E-01	0.31	1.73E-11
Larp1b	3	protein_coding	0.31	4.86E-06	0.33	1.56E-05	0.22	5.87E-03	0.19	4.30E-02
Ppm1h	10	protein_coding	0.34	5.02E-06	0.64	2.68E-49	0.03	7.42E-01	0.46	3.88E-12
Asb11	X	protein_coding	0.48	5.64E-06	1.02	4.42E-16	0.03	8.81E-01	0.53	8.40E-05
Nrep	18	protein_coding	0.32	5.85E-06	0.39	4.37E-17	0.18	1.04E-01	0.13	3.69E-01
Sertad1	7	protein_coding	0.47	5.87E-06	1.47	1.39E-40	0.35	4.92E-05	1.15	1.44E-33
Mxi1	19	protein_coding	0.22	5.87E-06	0.20	7.69E-05	-0.11	2.34E-01	0.02	9.15E-01
Znfx1	2	protein_coding	0.25	7.24E-06	0.37	6.29E-17	0.12	9.88E-02	0.35	1.11E-08
Lrrc8b	5	protein_coding	0.18	7.33E-06	0.14	8.18E-04	0.11	4.86E-02	0.08	2.79E-01
Grsf1	5	protein_coding	0.23	8.10E-06	0.22	3.38E-08	-0.02	8.29E-01	0.14	6.67E-02
Fam219a	4	protein_coding	0.16	9.13E-06	0.25	6.57E-13	0.08	4.67E-02	0.14	3.37E-04
Hmgb3	X	protein_coding	0.37	9.56E-06	0.42	9.09E-06	0.09	3.68E-01	0.03	8.37E-01
Midn	10	protein_coding	0.33	1.06E-05	1.15	4.41E-67	0.38	1.11E-06	0.87	9.65E-21
Kif5c	2	protein_coding	0.19	1.11E-05	0.20	3.24E-12	0.07	1.58E-01	0.06	2.08E-01
Cpne9	6	protein_coding	0.37	1.21E-05	0.30	2.97E-05	0.37	2.98E-05	0.48	2.62E-05
Tmod1	4	protein_coding	0.28	1.34E-05	0.32	4.84E-12	0.10	2.09E-01	0.23	6.43E-03
Ism1	2	protein_coding	0.45	1.36E-05	0.72	1.55E-08	0.03	8.63E-01	0.41	1.18E-03
Rab6b	9	protein_coding	0.13	1.37E-05	0.14	9.76E-06	0.05	2.38E-01	0.10	3.76E-02
Scrn1	6	protein_coding	0.18	1.38E-05	0.12	3.91E-03	0.12	4.71E-04	0.07	2.01E-01
Ogdh	11	protein_coding	0.15	1.41E-05	0.23	3.80E-12	0.04	4.78E-01	0.17	2.44E-04
Apcdd1	18	protein_coding	0.31	1.47E-05	0.24	8.19E-05	0.07	4.98E-01	-0.18	4.29E-02
Tmem267	13	protein_coding	0.43	1.52E-05	0.27	3.91E-02	0.00	9.82E-01	0.17	3.02E-01
Ache	5	protein_coding	0.27	1.53E-05	0.18	2.94E-03	0.16	1.66E-02	-0.05	6.88E-01
Pitpna	11	protein_coding	0.16	1.65E-05	0.29	8.07E-19	-0.01	8.77E-01	0.14	1.08E-03
Elmo1	13	protein_coding	0.18	1.71E-05	0.10	8.94E-03	0.00	9.99E-01	0.16	2.39E-04
Metrnl	11	protein_coding	0.46	1.80E-05	1.01	6.05E-17	0.23	6.56E-02	0.79	3.04E-13
Plpbp	8	protein_coding	0.20	1.89E-05	0.46	1.90E-25	0.02	7.58E-01	0.31	5.35E-11
Penk	4	protein_coding	0.39	2.00E-05	1.00	1.19E-41	0.24	3.26E-04	0.77	1.23E-30
Ywhah	5	protein_coding	0.17	2.00E-05	0.13	1.71E-04	0.06	1.09E-01	0.16	1.27E-04
Pip4k2c	10	protein_coding	0.24	2.35E-05	0.73	8.18E-77	0.07	3.37E-01	0.59	2.86E-28
Osbp2	11	protein_coding	0.23	2.46E-05	0.12	2.02E-03	0.07	2.55E-01	0.01	9.57E-01
Numb	12	protein_coding	0.23	2.53E-05	0.35	7.99E-12	0.09	2.03E-01	0.24	2.87E-05
Bdnf	2	protein_coding	0.49	2.60E-05	1.85	1.39E-108	0.29	5.12E-04	1.29	4.93E-37
Slc7a5	8	protein_coding	0.27	2.80E-05	0.72	4.07E-44	0.12	3.46E-02	0.42	7.25E-21
Slc6a8	X	protein_coding	0.18	2.80E-05	0.46	1.67E-28	0.05	4.43E-01	0.24	6.21E-06
Foxk2	11	protein_coding	0.19	2.80E-05	0.43	1.89E-28	0.05	4.56E-01	0.23	5.80E-05
Dusp6	10	protein_coding	0.50	2.80E-05	1.56	2.33E-104	0.31	1.45E-02	0.93	5.24E-11
Rasl11b	5	protein_coding	0.28	2.83E-05	0.45	1.14E-18	0.23	5.03E-04	0.26	1.29E-03
Cabp1	5	protein_coding	0.23	2.96E-05	0.43	1.82E-23	0.03	7.81E-01	0.32	7.23E-05
Scg2	1	protein_coding	0.36	3.01E-05	1.05	2.39E-83	0.01	8.96E-01	0.62	3.71E-34
Map9	3	protein_coding	0.23	3.07E-05	0.11	4.73E-02	-0.01	8.99E-01	0.02	8.25E-01
Prkg2	5	protein_coding	0.42	3.07E-05	0.73	9.88E-15	0.17	1.21E-01	0.58	3.29E-07
Kcns1	2	protein_coding	0.33	3.13E-05	0.39	2.20E-08	0.21	2.87E-02	0.39	2.20E-06
Brsk2	7	protein_coding	0.14	3.14E-05	0.43	1.70E-49	-0.01	9.28E-01	0.18	8.36E-03
Vamp2	11	protein_coding	0.14	3.63E-05	0.17	1.96E-06	-0.01	9.10E-01	0.08	1.63E-01
Trp53inp2	2	protein_coding	0.18	3.75E-05	0.23	1.59E-11	0.11	1.06E-01	0.07	4.45E-01
Chgb	2	protein_coding	0.29	4.05E-05	0.14	1.01E-02	0.07	3.32E-01	0.28	4.97E-07
Rgs20	1	protein_coding	0.28	4.05E-05	0.33	8.25E-09	0.17	3.62E-02	0.18	3.59E-02
Bdh1	16	protein_coding	0.23	4.18E-05	0.15	2.77E-02	0.13	3.66E-02	-0.04	7.24E-01
Herc6	6	protein_coding	0.36	4.36E-05	0.33	2.66E-03	0.23	2.27E-02	0.50	1.07E-05
Gbe1	16	protein_coding	0.33	4.36E-05	0.33	9.02E-05	0.04	7.63E-01	0.07	6.36E-01
Kcnh1	1	protein_coding	0.21	4.36E-05	0.19	8.20E-05	0.15	9.77E-02	0.18	1.82E-02
Atp1b1	1	protein_coding	0.20	4.40E-05	0.32	3.43E-20	0.05	3.05E-01	0.18	2.26E-05
Tbc1d9	8	protein_coding	0.17	4.55E-05	0.10	1.34E-02	0.13	1.94E-02	0.07	2.94E-01
Stac2	11	protein_coding	0.25	4.56E-05	0.30	5.22E-13	0.29	2.70E-03	0.42	5.10E-05
Nrsn1	13	protein_coding	0.18	4.70E-05	0.20	3.27E-05	0.04	6.85E-01	0.23	2.46E-03
Ttyh3	5	protein_coding	0.16	5.03E-05	0.47	1.58E-34	-0.01	9.57E-01	0.23	1.03E-03
Rasgrp1	2	protein_coding	0.23	5.32E-05	0.45	1.66E-19	0.00	9.99E-01	0.26	4.92E-04

Table S4 (3/9)

Kcnip3	2	protein_coding	0.22	5.81E-05	0.96	8.11E-89	0.12	3.64E-02	0.63	4.12E-25
Arhgef2	3	protein_coding	0.14	5.95E-05	0.16	3.10E-07	0.03	7.13E-01	0.02	7.66E-01
Bbln	2	protein_coding	0.33	5.96E-05	0.72	1.19E-44	0.32	1.81E-04	0.68	7.42E-14
Dusp7	9	protein_coding	0.18	6.03E-05	0.51	1.27E-23	0.12	5.99E-02	0.45	5.56E-21
Ppm1l	3	protein_coding	0.19	6.13E-05	0.24	7.99E-11	0.16	4.86E-02	0.15	3.44E-02
Prkar1b	5	protein_coding	0.22	6.44E-05	0.22	7.66E-11	0.22	1.03E-10	0.28	9.19E-11
Plcxd1	5	protein_coding	0.30	6.54E-05	0.36	1.13E-04	0.29	1.39E-04	0.35	2.43E-04
Ppp1r1a	15	protein_coding	0.25	6.66E-05	0.60	5.55E-24	0.14	9.11E-02	0.44	2.19E-10
Gadd45g	13	protein_coding	0.45	8.29E-05	0.51	1.03E-06	0.08	6.86E-01	0.60	5.09E-05
Syt12	19	protein_coding	0.33	8.93E-05	1.15	1.56E-84	0.14	9.21E-02	0.73	2.51E-29
Rps6ka3	X	protein_coding	0.24	8.93E-05	0.44	5.30E-15	0.05	6.22E-01	0.29	1.84E-04
Trhde	10	protein_coding	0.29	9.20E-05	0.35	2.39E-05	0.19	1.44E-02	0.12	1.97E-01
Ppargc1a	5	protein_coding	0.26	9.34E-05	0.40	1.08E-12	0.03	8.50E-01	0.23	4.67E-03
Ifrd1	12	protein_coding	0.30	9.45E-05	1.03	5.07E-69	0.04	7.16E-01	0.74	8.66E-35
Phyhipl	10	protein_coding	0.22	9.52E-05	0.34	2.43E-24	0.04	4.96E-01	0.20	1.10E-04
Bcor	X	protein_coding	0.31	9.52E-05	0.84	2.76E-40	0.14	1.43E-01	0.61	1.99E-20
Actn1	12	protein_coding	0.19	9.68E-05	0.59	3.47E-53	-0.11	3.54E-01	0.30	4.33E-03
Ptpn3	4	protein_coding	0.21	9.90E-05	0.50	1.29E-23	-0.13	8.59E-02	0.20	3.08E-03
Elovl4	9	protein_coding	0.22	1.03E-04	0.45	3.61E-16	-0.02	8.06E-01	0.17	3.75E-02
Egr2	10	protein_coding	0.35	1.05E-04	2.73	8.25E-50	0.16	7.33E-02	0.67	5.50E-06
Reep2	18	protein_coding	0.20	1.09E-04	0.15	3.35E-03	0.12	1.06E-01	0.06	4.92E-01
Jdp2	12	protein_coding	0.28	1.09E-04	0.77	7.24E-55	0.03	8.33E-01	0.51	7.49E-09
Bzw1	1	protein_coding	0.20	1.15E-04	0.40	5.98E-23	0.04	4.74E-01	0.20	1.48E-04
Zfand5	19	protein_coding	0.18	1.16E-04	0.14	2.82E-04	0.06	3.05E-01	0.03	6.74E-01
Nop56	2	protein_coding	0.17	1.31E-04	0.21	2.30E-07	0.01	9.26E-01	0.15	1.65E-03
Ttc19	11	protein_coding	0.19	1.33E-04	0.40	3.51E-17	0.05	5.60E-01	0.21	4.64E-03
Gm42517	5	protein_coding	0.30	1.36E-04	0.58	5.36E-23	0.26	2.03E-03	0.43	1.46E-06
Fosl2	5	protein_coding	0.36	1.40E-04	1.42	4.07E-110	0.10	3.76E-01	1.00	1.20E-18
Cs	10	protein_coding	0.13	1.47E-04	0.12	8.37E-04	0.09	1.44E-02	0.10	3.21E-02
Ext1	15	protein_coding	0.20	1.49E-04	0.19	8.08E-05	0.07	4.93E-01	0.10	2.41E-01
Osbpl3	6	protein_coding	0.30	1.62E-04	1.08	2.14E-51	0.10	2.21E-01	0.68	1.61E-22
Ppme1	7	protein_coding	0.31	1.69E-04	0.60	2.25E-58	0.10	1.65E-01	0.59	4.90E-26
Ndufs1	1	protein_coding	0.20	1.71E-04	0.16	1.42E-05	0.04	4.16E-01	0.10	3.87E-02
Adgrd1	5	protein_coding	0.39	1.76E-04	0.92	2.48E-24	0.24	3.56E-02	0.88	1.51E-16
Asic2	11	protein_coding	0.18	2.02E-04	0.40	1.27E-18	-0.01	9.25E-01	0.33	1.67E-08
Hsd17b12	2	protein_coding	0.20	2.25E-04	0.38	3.41E-17	0.07	3.38E-01	0.26	1.02E-04
Nudt4	10	protein_coding	0.17	2.40E-04	0.16	3.18E-04	0.00	9.82E-01	0.02	8.15E-01
Ttyh1	7	protein_coding	0.14	2.40E-04	0.17	2.35E-06	0.03	6.76E-01	0.03	6.14E-01
Pdlim1	19	protein_coding	0.42	2.75E-04	0.56	1.78E-08	0.22	4.02E-02	0.44	1.84E-05
Lhx6	2	protein_coding	0.23	2.75E-04	0.42	7.21E-11	-0.09	4.76E-01	0.09	5.29E-01
Magi2	5	protein_coding	0.21	2.75E-04	0.44	3.82E-48	-0.01	9.42E-01	0.19	7.70E-02
Cdk5r1	11	protein_coding	0.20	2.91E-04	0.34	4.17E-17	0.15	5.92E-05	0.30	1.03E-11
Cd7	11	protein_coding	0.45	3.02E-04	1.06	3.11E-10	0.20	1.78E-01	0.75	2.23E-06
Hepacam	9	protein_coding	0.17	3.03E-04	0.19	2.79E-04	-0.02	7.81E-01	-0.01	9.34E-01
Kcnk1	8	protein_coding	0.24	3.05E-04	0.76	5.39E-81	-0.01	9.53E-01	0.43	4.07E-12
Abhd2	7	protein_coding	0.21	3.10E-04	0.32	1.47E-20	0.24	1.39E-04	0.29	5.66E-06
Idh3a	9	protein_coding	0.16	3.14E-04	0.20	2.22E-11	0.04	4.56E-01	0.09	4.80E-02
Adcyap1	17	protein_coding	0.27	3.16E-04	0.62	4.62E-23	0.21	9.95E-02	0.39	4.75E-03
Kcns2	15	protein_coding	0.35	3.16E-04	0.43	2.11E-09	0.09	3.28E-01	0.36	8.65E-05
Dlst	12	protein_coding	0.15	3.20E-04	0.27	6.95E-15	0.03	5.55E-01	0.14	2.62E-04
Nmnat2	1	protein_coding	0.14	3.25E-04	0.23	1.24E-10	0.04	4.93E-01	0.20	4.58E-06
Akirin1	4	protein_coding	0.19	3.27E-04	0.48	1.94E-24	0.05	5.13E-01	0.27	1.16E-04
Tmem229b	12	protein_coding	0.22	3.49E-04	0.34	4.48E-10	0.07	2.25E-01	0.03	7.54E-01
Cox5b	1	protein_coding	0.18	3.58E-04	0.11	4.68E-02	0.09	3.69E-01	0.18	6.32E-02
Homer1	13	protein_coding	0.40	3.64E-04	1.71	1.99E-53	-0.02	9.14E-01	0.87	2.39E-07
Dnajc2	5	protein_coding	0.27	3.65E-04	0.52	8.91E-17	0.07	3.86E-01	0.33	6.83E-08
Gfra2	14	protein_coding	0.27	3.66E-04	1.02	1.84E-100	0.12	4.49E-02	0.77	8.61E-53
Rtl5	X	protein_coding	0.25	3.66E-04	0.65	7.87E-19	0.12	8.71E-02	0.51	2.18E-17
Sec14l1	11	protein_coding	0.13	3.76E-04	0.22	2.17E-11	0.02	7.63E-01	0.21	2.09E-04
Nkiras1	14	protein_coding	0.20	3.76E-04	0.22	2.94E-08	0.07	1.73E-01	0.16	2.36E-04
Kcnk3	5	protein_coding	0.23	3.76E-04	0.47	4.19E-12	0.09	3.45E-01	0.25	6.32E-04
Cdc42se2	11	protein_coding	0.15	3.83E-04	0.24	1.41E-14	-0.02	8.54E-01	-0.04	6.21E-01
Gad2	2	protein_coding	0.19	3.86E-04	0.44	3.16E-35	0.03	7.43E-01	0.18	4.88E-03
Fbxo9	9	protein_coding	0.18	3.97E-04	0.16	7.53E-04	0.09	2.86E-01	0.15	7.41E-02
Srebf2	15	protein_coding	0.13	4.05E-04	0.19	2.92E-07	0.21	1.03E-03	0.25	6.34E-04
Unc5d	8	protein_coding	0.29	4.05E-04	0.35	1.76E-08	0.25	1.35E-03	0.18	7.51E-02
Rnf39	17	protein_coding	0.38	4.20E-04	1.06	1.08E-26	0.41	1.55E-05	0.81	1.89E-13
Zfpm1	8	protein_coding	0.26	4.28E-04	0.79	1.13E-32	0.05	7.31E-01	0.67	4.95E-15
R3hdm1	1	protein_coding	0.24	4.32E-04	0.27	1.83E-06	0.07	5.10E-01	0.12	1.81E-01
Dclk3	9	protein_coding	0.27	4.38E-04	0.45	5.58E-09	0.01	9.37E-01	0.25	1.25E-03
Atf6	1	protein_coding	0.23	4.39E-04	0.52	9.34E-42	-0.03	8.34E-01	0.33	8.23E-07
Fzd4	7	protein_coding	0.29	4.42E-04	0.68	6.92E-17	0.03	8.13E-01	0.38	3.81E-05
Cry1	10	protein_coding	0.28	4.42E-04	1.09	2.21E-50	-0.03	8.89E-01	0.54	9.65E-05
Tnnc1	14	protein_coding	0.42	4.48E-04	0.59	8.75E-07	0.43	2.12E-04	0.28	1.10E-01
Ppp5c	7	protein_coding	0.17	4.57E-04	0.16	1.85E-04	0.03	6.45E-01	0.12	2.62E-02
Trpc3	3	protein_coding	0.23	4.68E-04	0.55	6.80E-19	-0.02	9.04E-01	0.42	7.95E-08
Cul3	1	protein_coding	0.20	4.73E-04	0.34	2.83E-16	-0.02	8.10E-01	0.17	6.09E-03
Slc25a37	14	protein_coding	0.21	4.91E-04	0.54	5.61E-29	0.11	1.58E-01	0.44	6.26E-13
Heg1	16	protein_coding	0.24	4.91E-04	0.18	4.20E-03	0.14	1.40E-01	0.05	6.60E-01
Igfbp7	5	protein_coding	0.28	4.97E-04	0.36	1.45E-04	0.27	1.68E-03	0.27	2.72E-03
Neu2	1	protein_coding	0.39	4.97E-04	0.96	2.27E-15	0.28	1.16E-02	0.62	3.12E-07
Trib1	15	protein_coding	0.43	4.97E-04	1.51	9.86E-23	0.31	1.65E-02	1.15	3.54E-14
Hnrnph2	X	protein_coding	0.17	5.00E-04	0.13	2.61E-03	-0.01	9.22E-01	0.10	3.56E-02
Itpk1	12	protein_coding	0.17	5.00E-04	0.51	3.01E-29	-0.12	2.12E-01	0.23	9.11E-03
Skil	3	protein_coding	0.22	5.15E-04	1.13	8.91E-85	0.05	6.78E-01	0.59	1.55E-10
Gadd45b	10	protein_coding	0.44	5.15E-04	1.29	8.57E-15	0.27	7.09E-03	1.29	6.54E-39
Pld3	7	protein_coding	0.19	5.20E-04	0.10	4.15E-02	0.10	3.21E-02	0.04	4.50E-01
Ddx1	12	protein_coding	0.20	5.20E-04	0.24	4.48E-11	-0.02	8.10E-01	0.11	8.43E-02
Mboat2	12	protein_coding	0.18	5.32E-04	0.21	4.14E-07	0.00	9.71E-01	-0.03	7.05E-01
Ube2ql1	13	protein_coding	0.19	5.65E-04	0.31	9.61E-14	0.10	4.35E-02	0.31	5.01E-11
Fos	12	protein_coding	0.33	5.69E-04	1.75	3.57E-23	0.07	6.67E-01	0.70	7.53E-05
Grm8	6	protein_coding	0.28	5.73E-04	0.40	8.70E-08	-0.02	9.35E-01	0.21	9.90E-02
Npy	6	protein_coding	0.29	5.81E-04	0.42	2.43E-10	0.21	2.19E-04	0.18	1.24E-02
Slc35f3	8	protein_coding	0.27	5.83E-04	0.75	9.67E-47	-0.08	4.94E-01	0.42	2.13E-07
Kcnma1	14	protein_coding	0.24	5.84E-04	0.47	4.01E-24	0.01	9.58E-01	0.17	1.59E-01
Frmd5	2	protein_coding	0.20	5.94E-04	0.22	1.88E-06	0.02	8.59E-01	0.02	8.49E-01
Cacna2d3	14	protein_coding	0.15	6.13E-04	0.33	3.46E-13	0.08	2.28E-01	0.22	5.09E-05
Plaa	4	protein_coding	0.20	6.21E-04	0.39	2.40E-15	0.00	9.76E-01	0.07	5.13E-01
Tpgs2	18	protein_coding	0.16	6.21E-04	0.11	2.03E-02	0.00	9.95E-01	0.07	2.33E-01
Nr4a1	15	protein_coding	0.39	6.21E-04	1.35	1.72E-18	0.33	9.48E-03	1.04	1.73E-11
Sgms1	19	protein_coding	0.23	6.37E-04	0.60	2.38E-20	-0.05	7.34E-01	0.26	9.34E-03
Tgfb1i1	7	protein_coding	0.25	6.64E-04	1.04	6.59E-38	0.21	3.55E-02	0.75	7.99E-18
Cds1	5	protein_coding	0.18	6.65E-04	0.18	1.04E-07	0.16	8.59E-04	0.22	2.12E-05
Htr2a	14	protein_coding	0.25	6.84E-04	1.31	3.23E-99	0.13	1.16E-01	0.71	4.90E-26
AI593442	9	protein_coding	0.17	7.26E-04	0.14	4.45E-03	-0.03	7.26E-01	0.05	6.01E-01

Table S4 (4/9)

Dtna	18	protein_coding	0.15	7.49E-04	0.09	2.46E-02	0.05	5.41E-01	0.10	1.25E-01
Nrxn3	12	protein_coding	0.15	7.85E-04	0.45	1.05E-42	0.10	1.66E-01	0.21	2.25E-03
Rnf4	5	protein_coding	0.15	8.09E-04	0.39	6.69E-20	-0.02	8.11E-01	0.23	5.89E-05
Csrnp1	9	protein_coding	0.37	8.25E-04	1.40	6.40E-16	0.42	1.64E-04	1.04	3.79E-11
Pitpnm3	11	protein_coding	0.18	8.34E-04	0.62	2.11E-52	0.06	5.68E-01	0.27	2.90E-03
Epha10	4	protein_coding	0.27	8.39E-04	0.65	7.29E-32	-0.11	2.80E-01	0.37	1.16E-05
Chrm2	6	protein_coding	0.28	8.50E-04	0.34	3.27E-04	-0.16	1.21E-01	0.07	6.20E-01
Etv5	16	protein_coding	0.22	8.74E-04	0.87	4.31E-144	-0.02	8.71E-01	0.55	3.96E-14
Ctla2a	13	protein_coding	0.41	8.90E-04	1.29	2.13E-15	0.15	3.60E-01	0.27	1.24E-01
Atp1a1	3	protein_coding	0.18	9.00E-04	0.24	7.13E-10	0.00	9.99E-01	0.08	2.53E-01
Dennd5b	6	protein_coding	0.18	9.16E-04	0.30	4.84E-12	0.01	9.40E-01	0.18	7.03E-02
1810055G02Rik	19	protein_coding	0.22	9.42E-04	0.36	1.72E-11	0.07	3.83E-01	0.11	1.75E-01
Luzp2	7	protein_coding	0.15	9.51E-04	0.11	3.00E-02	0.16	4.14E-02	0.10	2.60E-01
Fam81a	9	protein_coding	0.16	9.79E-04	0.48	2.60E-24	-0.02	8.20E-01	0.21	1.78E-05
Cx3cl1	8	protein_coding	0.17	9.84E-04	0.60	4.47E-52	0.08	1.74E-01	0.41	3.19E-14
Zmiz1	14	protein_coding	0.22	9.89E-04	0.86	1.24E-82	-0.05	6.68E-01	0.53	1.14E-08
Daglb	5	protein_coding	0.24	1.01E-03	0.13	3.98E-02	0.19	1.25E-02	0.32	2.52E-05
Hmgb1	5	protein_coding	0.20	1.02E-03	0.35	1.99E-16	0.04	5.50E-01	0.20	5.53E-05
Nol4	18	protein_coding	0.17	1.02E-03	0.56	1.82E-49	0.07	3.64E-01	0.40	1.29E-09
Cd164l2	4	protein_coding	0.40	1.04E-03	0.75	3.19E-08	0.26	2.86E-02	0.39	4.00E-03
Dab2ip	2	protein_coding	0.18	1.11E-03	0.36	1.17E-16	-0.01	9.40E-01	0.14	1.82E-01
Kcnn2	18	protein_coding	0.21	1.11E-03	0.32	4.86E-07	-0.12	6.50E-02	0.10	1.53E-01
Ipo5	14	protein_coding	0.19	1.12E-03	0.43	1.43E-36	0.06	1.79E-01	0.34	2.01E-16
Chfr	5	protein_coding	0.17	1.12E-03	0.35	6.44E-15	-0.16	1.68E-01	-0.12	3.83E-01
Lclat1	17	protein_coding	0.16	1.13E-03	0.11	3.22E-02	0.09	1.14E-01	0.17	8.17E-03
Spry2	14	protein_coding	0.24	1.13E-03	0.79	2.28E-38	0.09	2.86E-01	0.54	2.41E-13
Mchr1	15	protein_coding	0.26	1.13E-03	0.52	2.02E-17	0.02	8.56E-01	0.34	7.09E-07
Med10	13	protein_coding	0.21	1.16E-03	0.27	9.46E-05	0.06	4.22E-01	0.18	6.83E-03
Plxna2	1	protein_coding	0.20	1.16E-03	0.43	1.84E-29	-0.01	9.48E-01	0.19	7.51E-02
Sstr2	11	protein_coding	0.29	1.16E-03	1.33	2.73E-58	0.06	7.18E-01	0.64	3.34E-08
Golm2	2	protein_coding	0.20	1.21E-03	0.22	1.17E-06	0.03	7.48E-01	0.13	3.02E-02
Rhbdl3	11	protein_coding	0.26	1.22E-03	1.12	1.87E-72	-0.25	4.46E-02	0.23	1.72E-01
Atxn2	5	protein_coding	0.18	1.30E-03	0.41	2.58E-26	-0.03	8.20E-01	0.11	2.42E-01
Ubr3	2	protein_coding	0.15	1.30E-03	0.15	8.14E-04	-0.05	6.62E-01	-0.07	5.31E-01
Srm	4	protein_coding	0.23	1.37E-03	0.47	2.52E-19	0.20	7.57E-03	0.43	3.49E-09
Csnk2b	17	protein_coding	0.17	1.39E-03	0.24	8.22E-07	-0.05	4.44E-01	0.14	7.93E-03
Rcan2	17	protein_coding	0.20	1.39E-03	0.37	2.48E-27	0.03	8.00E-01	0.44	2.06E-09
Tsnax	8	protein_coding	0.28	1.43E-03	1.01	5.77E-134	0.01	8.71E-01	0.77	3.28E-69
Dock3	9	protein_coding	0.17	1.50E-03	0.26	7.92E-12	0.07	3.93E-01	0.08	3.67E-01
Egr4	6	protein_coding	0.38	1.51E-03	1.25	1.86E-20	0.31	1.55E-02	0.87	1.76E-07
Ppp2ca	11	protein_coding	0.17	1.51E-03	0.30	1.24E-19	0.04	3.38E-01	0.18	2.21E-08
Fam78b	1	protein_coding	0.19	1.53E-03	0.48	6.45E-27	0.02	8.73E-01	0.24	1.74E-03
Crhbp	13	protein_coding	0.26	1.55E-03	0.84	2.29E-30	0.20	1.01E-02	0.57	1.90E-18
Cltb	13	protein_coding	0.14	1.56E-03	0.32	3.51E-17	0.08	8.25E-02	0.20	1.09E-05
Ubtf	11	protein_coding	0.18	1.58E-03	0.43	1.66E-25	0.06	2.49E-01	0.34	3.04E-16
Slco1a4	6	protein_coding	0.24	1.60E-03	0.26	1.72E-04	0.03	8.37E-01	0.05	6.96E-01
Mgat5	1	protein_coding	0.14	1.63E-03	0.08	3.71E-02	0.14	1.20E-03	0.08	1.58E-01
Atmin	8	protein_coding	0.15	1.65E-03	0.44	6.85E-22	0.02	8.96E-01	0.35	6.21E-06
Ppp2r2d	7	protein_coding	0.17	1.66E-03	0.33	9.43E-14	-0.01	9.31E-01	0.11	2.80E-01
Ube2g1	11	protein_coding	0.17	1.66E-03	0.37	4.03E-17	-0.07	2.65E-01	0.06	4.91E-01
Tmem128	5	protein_coding	0.23	1.67E-03	0.38	8.96E-10	0.05	5.08E-01	0.16	4.61E-02
Slc31a1	4	protein_coding	0.23	1.70E-03	0.25	1.65E-04	0.03	7.26E-01	0.04	7.27E-01
Phtf2	5	protein_coding	0.23	1.71E-03	0.49	1.19E-15	-0.06	6.28E-01	0.16	1.63E-01
Gnl2	4	protein_coding	0.19	1.73E-03	0.21	9.05E-06	-0.03	7.24E-01	-0.02	8.62E-01
Psmd12	11	protein_coding	0.19	1.74E-03	0.42	1.25E-20	-0.08	2.34E-01	0.18	4.55E-03
Tpm1	9	protein_coding	0.15	1.77E-03	0.42	9.43E-27	0.07	2.00E-01	0.30	3.76E-12
Chn2	6	protein_coding	0.22	1.80E-03	0.22	2.50E-05	0.03	8.27E-01	0.02	8.79E-01
Gga2	7	protein_coding	0.22	1.80E-03	0.28	1.20E-05	0.03	7.35E-01	0.21	9.03E-03
Vopp1	6	protein_coding	0.16	1.80E-03	0.12	1.22E-03	0.08	2.63E-01	0.12	1.25E-01
Hivep2	10	protein_coding	0.21	1.82E-03	0.35	9.77E-17	-0.02	8.99E-01	0.06	6.28E-01
Lhfp	3	protein_coding	0.22	1.83E-03	0.92	3.16E-42	-0.07	4.93E-01	0.50	1.40E-09
Vapa	17	protein_coding	0.15	1.86E-03	0.27	5.09E-15	-0.01	8.91E-01	0.14	1.70E-02
Ubtd2	11	protein_coding	0.25	1.87E-03	0.71	8.57E-27	-0.03	8.34E-01	0.24	6.14E-03
Tbc1d24	17	protein_coding	0.20	1.88E-03	0.34	8.41E-20	0.07	5.56E-01	0.10	4.51E-01
Kif2a	13	protein_coding	0.15	1.88E-03	0.24	1.09E-08	-0.01	9.61E-01	0.07	4.96E-01
Josd1	15	protein_coding	0.19	1.89E-03	0.47	4.85E-23	0.00	9.81E-01	0.25	1.18E-03
Hs3st2	7	protein_coding	0.26	1.90E-03	0.83	5.36E-45	0.27	2.02E-04	0.67	8.04E-13
Zrsr2	X	protein_coding	0.20	1.90E-03	0.39	9.10E-13	0.07	3.83E-01	0.27	2.54E-06
Unc13a	8	protein_coding	0.14	1.92E-03	0.41	3.73E-51	0.11	1.67E-01	0.29	1.54E-04
Cdkn1a	17	protein_coding	0.39	1.92E-03	2.72	7.65E-110	0.35	1.39E-04	2.02	4.42E-79
Dusp5	19	protein_coding	0.39	1.92E-03	1.28	3.03E-16	0.38	1.68E-04	1.16	4.50E-24
Sigmar1	4	protein_coding	0.19	1.94E-03	0.34	3.43E-10	0.15	4.56E-02	0.30	1.03E-05
Kpna3	14	protein_coding	0.14	1.99E-03	0.16	1.60E-04	-0.01	8.50E-01	0.05	5.47E-01
Tcf25	8	protein_coding	0.10	2.00E-03	0.07	1.59E-02	0.07	3.17E-02	0.07	7.10E-02
Cend1	7	protein_coding	0.17	2.03E-03	0.13	3.67E-04	0.09	5.95E-02	0.09	1.13E-01
Pim1	17	protein_coding	0.35	2.07E-03	1.83	1.15E-44	0.06	7.53E-01	1.46	2.48E-33
Acsl5	19	protein_coding	0.19	2.08E-03	0.45	1.03E-17	0.07	2.18E-01	0.35	7.97E-13
Baalc	15	protein_coding	0.14	2.11E-03	0.28	2.45E-13	0.02	8.15E-01	0.25	1.70E-05
Spock1	13	protein_coding	0.14	2.16E-03	0.13	6.04E-05	0.08	3.42E-01	0.10	2.38E-01
Hras	7	protein_coding	0.19	2.19E-03	0.34	2.98E-15	0.11	1.18E-01	0.27	7.54E-06
Nptn	9	protein_coding	0.12	2.21E-03	0.08	7.92E-03	0.03	5.47E-01	0.06	3.00E-01
Ece1	4	protein_coding	0.24	2.23E-03	0.73	5.24E-39	0.14	1.96E-02	0.50	3.98E-17
Rad23b	4	protein_coding	0.14	2.26E-03	0.27	5.22E-13	0.00	9.66E-01	0.15	6.85E-03
Rap1gds1	3	protein_coding	0.15	2.34E-03	0.08	3.99E-02	0.06	2.36E-01	0.07	2.60E-01
Ina	19	protein_coding	0.19	2.38E-03	0.25	3.96E-07	0.06	3.00E-01	0.35	6.43E-13
Tdg	10	protein_coding	0.25	2.40E-03	0.55	8.95E-16	0.06	5.30E-01	0.29	8.46E-06
Map4k3	17	protein_coding	0.14	2.45E-03	0.36	4.09E-17	-0.14	8.65E-02	0.10	3.72E-01
Rbm3	X	protein_coding	0.18	2.54E-03	0.31	3.03E-08	-0.09	4.54E-01	-0.30	6.05E-03
Ranbp9	13	protein_coding	0.14	2.54E-03	0.19	2.67E-05	-0.13	1.64E-01	0.04	7.78E-01
Mtmr2	9	protein_coding	0.14	2.61E-03	0.33	5.38E-15	-0.09	1.43E-01	0.05	6.02E-01
Ccdc25	14	protein_coding	0.26	2.61E-03	0.37	3.46E-11	0.05	6.00E-01	0.21	2.91E-03
Mrps2	2	protein_coding	0.18	2.62E-03	0.25	5.77E-05	0.05	5.69E-01	0.26	2.81E-05
Cbarp	10	protein_coding	0.16	2.63E-03	0.22	1.06E-07	0.14	3.64E-02	0.13	6.47E-02
Cck	9	protein_coding	0.22	2.64E-03	0.24	3.89E-07	0.25	5.45E-03	0.39	2.36E-04
Hspa9	18	protein_coding	0.17	2.65E-03	0.32	3.57E-24	0.03	4.78E-01	0.25	5.20E-11
Cox10	11	protein_coding	0.18	2.70E-03	0.28	1.40E-06	-0.02	8.34E-01	0.10	1.91E-01
Sstr3	15	protein_coding	0.20	2.74E-03	0.60	3.72E-23	0.16	9.46E-02	0.27	5.38E-03
Tyro3	2	protein_coding	0.21	2.76E-03	0.45	1.20E-32	0.25	2.38E-07	0.45	1.90E-18
Max	12	protein_coding	0.16	2.77E-03	0.36	8.93E-16	-0.04	5.49E-01	0.14	2.69E-02
Arhgap31	16	protein_coding	0.24	2.78E-03	0.69	6.04E-09	-0.02	8.66E-01	0.42	6.49E-05
Adam23	1	protein_coding	0.19	2.79E-03	0.16	6.90E-03	0.08	3.55E-01	0.03	7.63E-01
Dnmt3a	12	protein_coding	0.19	2.80E-03	0.44	2.97E-26	0.01	9.43E-01	-0.09	3.81E-01
Ddah1	3	protein_coding	0.18	2.83E-03	0.42	3.23E-30	0.17	1.75E-02	0.25	3.71E-03
Sh3rf3	10	protein_coding	0.21	2.84E-03	0.43	4.23E-14	-0.11	4.09E-01	0.01	9.62E-01
Slc2a1	4	protein_coding	0.24	2.98E-03	1.02	3.41E-95	-0.15	3.19E-01	0.35	3.46E-02

Table S4 (5/9)

Ccn1	3	protein_coding	0.27	2.99E-03	0.91	1.83E-13	0.12	2.96E-01	0.51	7.72E-03
Hs2st1	3	protein_coding	0.13	3.05E-03	0.24	3.06E-09	0.05	3.98E-01	0.09	2.00E-01
Zbtb16	9	protein_coding	0.28	3.05E-03	0.99	4.41E-61	-0.13	4.28E-01	0.35	4.54E-02
Ahcyl1	3	protein_coding	0.11	3.12E-03	0.27	1.86E-24	-0.01	8.78E-01	0.14	1.51E-03
Chga	12	protein_coding	0.17	3.15E-03	1.05	3.40E-82	0.19	3.86E-03	0.58	1.40E-18
Cinp	12	protein_coding	0.22	3.22E-03	0.57	2.70E-34	0.03	7.10E-01	0.32	1.20E-10
Uck2	1	protein_coding	0.18	3.25E-03	0.75	2.02E-49	0.12	5.28E-02	0.24	6.00E-04
Slc2a13	15	protein_coding	0.17	3.33E-03	0.33	1.76E-17	-0.01	8.54E-01	0.15	2.76E-03
Fam43a	16	protein_coding	0.29	3.47E-03	0.80	5.62E-27	0.31	1.57E-03	0.73	2.25E-11
Pdha1	X	protein_coding	0.12	3.50E-03	0.08	2.26E-02	0.04	2.93E-01	0.02	7.79E-01
Pank1	19	protein_coding	0.21	3.51E-03	0.23	1.62E-04	0.12	1.48E-01	0.25	1.59E-03
Dbndd2	2	protein_coding	0.19	3.56E-03	0.33	2.90E-10	-0.11	2.86E-01	0.01	9.38E-01
Fndc3b	3	protein_coding	0.22	3.57E-03	0.62	3.49E-25	-0.05	6.27E-01	0.34	6.60E-05
Adipor2	6	protein_coding	0.22	3.58E-03	0.73	2.51E-50	-0.14	1.76E-01	0.29	3.77E-03
Tacc1	8	protein_coding	0.16	3.60E-03	0.38	2.88E-28	0.03	7.97E-01	0.21	7.12E-04
Mapk8	14	protein_coding	0.13	3.62E-03	0.16	2.02E-04	0.00	9.70E-01	0.05	5.17E-01
Tbc1d4	14	protein_coding	0.29	3.66E-03	0.65	6.98E-15	-0.19	1.76E-01	0.17	3.75E-01
Fscn1	5	protein_coding	0.17	3.78E-03	0.60	4.14E-36	0.11	1.20E-01	0.41	3.44E-13
Man1c1	4	protein_coding	0.18	3.85E-03	0.18	5.30E-04	0.11	1.42E-01	0.24	1.41E-03
Tob2	15	protein_coding	0.24	3.96E-03	0.35	1.01E-09	-0.03	8.59E-01	0.24	1.32E-02
Mtarc2	1	protein_coding	0.19	3.97E-03	0.25	3.87E-06	0.19	7.41E-03	0.27	1.22E-03
Fam216a	5	protein_coding	0.18	4.00E-03	0.37	9.51E-15	-0.01	8.91E-01	0.28	4.77E-08
Hey1	3	protein_coding	0.17	4.01E-03	0.47	2.35E-18	0.06	4.13E-01	0.24	1.64E-05
Tspan5	3	protein_coding	0.14	4.09E-03	0.59	1.13E-66	0.05	4.69E-01	0.34	3.54E-12
Trp53bp1	2	protein_coding	0.16	4.10E-03	0.29	2.59E-12	0.03	6.23E-01	0.14	1.19E-02
Btbd10	7	protein_coding	0.22	4.21E-03	0.33	1.09E-19	0.02	8.68E-01	0.25	5.10E-05
Galnt1	18	protein_coding	0.19	4.31E-03	0.18	1.62E-03	0.02	7.85E-01	0.01	9.15E-01
Myo1e	9	protein_coding	0.20	4.33E-03	0.48	3.91E-13	-0.02	8.45E-01	0.13	9.72E-02
Vip	10	protein_coding	0.23	4.35E-03	0.35	1.87E-07	-0.02	8.79E-01	0.21	6.76E-03
Clec18a	8	protein_coding	0.35	4.36E-03	1.02	2.10E-25	0.60	5.70E-11	0.79	6.39E-11
Hs6st1	1	protein_coding	0.13	4.39E-03	0.28	5.35E-11	-0.02	7.87E-01	0.14	9.19E-03
Sc5d	9	protein_coding	0.15	4.43E-03	0.16	1.93E-03	0.14	3.17E-02	0.00	9.77E-01
Pacsin1	17	protein_coding	0.12	4.47E-03	0.42	9.13E-30	0.02	8.25E-01	0.33	3.74E-09
Ctps	4	protein_coding	0.17	4.52E-03	0.29	1.44E-09	0.12	6.92E-02	0.15	2.69E-02
Lrrfip1	1	protein_coding	0.15	4.53E-03	0.32	7.74E-13	-0.05	6.24E-01	0.12	2.69E-01
Herc3	6	protein_coding	0.11	4.57E-03	0.24	1.58E-10	-0.01	8.96E-01	0.16	1.38E-02
Ttc9b	7	protein_coding	0.22	4.58E-03	0.22	2.07E-04	0.28	5.84E-05	0.28	5.52E-03
Hip1	5	protein_coding	0.19	4.65E-03	0.49	9.24E-34	-0.10	3.43E-01	0.12	2.88E-01
Gimap6	6	protein_coding	0.35	4.69E-03	0.85	2.29E-10	-0.11	4.92E-01	0.00	9.90E-01
Kcnip1	11	protein_coding	0.19	4.71E-03	0.32	4.58E-08	0.03	7.90E-01	0.08	4.46E-01
Osbpl10	9	protein_coding	0.17	4.74E-03	0.31	8.46E-09	-0.01	9.62E-01	0.15	9.27E-02
Gphn	12	protein_coding	0.19	4.81E-03	0.34	6.41E-16	-0.08	2.24E-01	0.15	8.53E-03
Kcnab3	11	protein_coding	0.20	4.84E-03	0.13	1.92E-02	0.00	9.84E-01	0.08	4.95E-01
Hccs	X	protein_coding	0.19	4.85E-03	0.17	8.59E-03	0.03	8.07E-01	0.09	2.93E-01
Cox6b1	7	protein_coding	0.16	4.91E-03	0.14	7.87E-03	0.08	3.50E-01	0.06	4.42E-01
Vcan	13	protein_coding	0.22	4.92E-03	0.26	5.63E-05	-0.05	7.23E-01	-0.24	1.47E-02
Zbtb1	12	protein_coding	0.29	4.92E-03	0.62	1.31E-10	-0.03	8.46E-01	0.45	7.00E-10
Ttll11	2	protein_coding	0.24	4.92E-03	0.46	4.03E-17	0.12	1.61E-01	0.51	2.93E-13
Ezr	17	protein_coding	0.20	5.07E-03	0.73	2.34E-57	-0.07	5.99E-01	0.35	2.08E-03
Mcl1	3	protein_coding	0.18	5.08E-03	0.62	9.27E-27	0.00	9.81E-01	0.32	9.83E-08
Aldh1a1	19	protein_coding	0.21	5.08E-03	0.14	4.16E-03	-0.04	8.06E-01	0.04	8.83E-01
Zfr	15	protein_coding	0.13	5.23E-03	0.19	1.23E-08	-0.04	3.99E-01	0.13	2.76E-03
Gramd1b	9	protein_coding	0.14	5.26E-03	0.62	1.94E-56	-0.01	9.62E-01	0.31	6.47E-05
Rell2	18	protein_coding	0.19	5.32E-03	0.15	1.51E-03	0.17	6.03E-03	0.16	1.61E-02
Tbk1	10	protein_coding	0.15	5.33E-03	0.27	4.05E-09	-0.06	3.24E-01	0.08	1.61E-01
Rala	13	protein_coding	0.14	5.48E-03	0.15	6.02E-04	0.01	9.44E-01	0.04	6.14E-01
Dlg1	16	protein_coding	0.15	5.50E-03	0.33	1.60E-18	0.04	6.94E-01	0.24	7.78E-05
Anp32e	3	protein_coding	0.18	5.50E-03	0.52	2.59E-41	0.06	3.59E-01	0.35	1.11E-10
Map7d2	X	protein_coding	0.16	5.51E-03	0.33	3.48E-13	-0.02	8.12E-01	0.27	6.37E-10
Tfg	16	protein_coding	0.16	5.56E-03	0.37	3.74E-16	-0.06	4.61E-01	0.16	7.50E-02
Zc3h15	2	protein_coding	0.19	5.60E-03	0.28	1.64E-11	0.01	9.21E-01	0.25	5.13E-06
Npas4	19	protein_coding	0.26	5.65E-03	1.17	3.84E-15	-0.08	5.44E-01	0.52	6.04E-03
Ablim1	19	protein_coding	0.15	5.69E-03	0.25	1.53E-06	0.03	7.16E-01	0.18	2.65E-03
Stx3	19	protein_coding	0.18	5.73E-03	0.17	4.06E-03	-0.08	4.73E-01	-0.11	3.24E-01
Fndc9	11	protein_coding	0.36	5.80E-03	2.44	2.34E-64	0.18	2.53E-01	1.58	8.43E-29
Csnk2a2	8	protein_coding	0.14	5.83E-03	0.31	1.48E-10	0.02	8.24E-01	0.12	4.77E-02
Ccnf	17	protein_coding	0.28	5.95E-03	1.07	7.01E-28	0.09	5.49E-01	0.71	4.94E-10
Pde4dip	3	protein_coding	0.12	5.96E-03	0.35	9.50E-31	-0.05	6.06E-01	0.13	1.47E-01
Cort	4	protein_coding	0.30	5.98E-03	0.78	5.99E-18	0.19	5.22E-02	0.25	1.30E-02
Eng	2	protein_coding	0.24	6.04E-03	0.34	6.50E-06	0.08	5.70E-01	0.17	1.34E-01
Ppif	14	protein_coding	0.17	6.06E-03	0.33	1.27E-08	0.04	6.55E-01	0.22	1.07E-03
Gpr3	4	protein_coding	0.29	6.06E-03	1.58	3.78E-53	0.59	4.03E-11	1.35	6.67E-29
Pou2f2	7	protein_coding	0.27	6.11E-03	0.22	2.37E-02	0.17	5.92E-02	0.11	3.23E-01
Psme3	11	protein_coding	0.14	6.29E-03	0.33	2.62E-17	-0.03	6.61E-01	0.19	6.93E-04
Tmem248	5	protein_coding	0.15	6.34E-03	0.23	1.88E-06	0.02	8.24E-01	0.17	1.38E-02
Lrrc8c	5	protein_coding	0.16	6.36E-03	0.78	6.68E-54	-0.15	2.54E-01	0.31	2.45E-02
Uxs1	1	protein_coding	0.20	6.36E-03	0.33	2.04E-08	0.02	8.31E-01	0.20	2.74E-03
Ppfibp1	6	protein_coding	0.22	6.37E-03	0.42	1.08E-11	0.06	5.46E-01	0.01	9.52E-01
Fbxo45	16	protein_coding	0.15	6.38E-03	0.32	2.58E-14	-0.03	7.23E-01	0.16	1.34E-02
Shisa4	1	protein_coding	0.16	6.54E-03	0.27	7.26E-08	0.24	1.78E-02	0.25	4.63E-02
Cdc27	11	protein_coding	0.14	6.63E-03	0.16	9.34E-04	-0.09	1.83E-01	-0.06	5.14E-01
Sanbr	11	protein_coding	0.14	6.64E-03	0.12	1.29E-02	-0.03	8.06E-01	-0.08	5.03E-01
Dlgap4	2	protein_coding	0.11	6.67E-03	0.44	2.56E-29	-0.02	7.09E-01	0.30	1.27E-10
Slc25a46	18	protein_coding	0.17	6.68E-03	0.22	9.31E-08	0.02	8.21E-01	0.18	3.92E-04
Notch4	17	protein_coding	0.29	6.70E-03	1.03	1.57E-24	-0.06	7.24E-01	0.35	4.00E-03
Pde4a	9	protein_coding	0.14	7.08E-03	0.76	1.89E-91	0.02	8.13E-01	0.46	8.39E-12
Fut8	12	protein_coding	0.14	7.09E-03	0.10	2.28E-02	0.05	5.13E-01	0.11	1.61E-01
Adam9	8	protein_coding	0.13	7.10E-03	0.13	1.97E-03	-0.07	3.63E-01	-0.03	7.64E-01
Bex3	X	protein_coding	0.16	7.14E-03	0.25	8.96E-09	0.04	6.62E-01	0.10	1.77E-01
Slc24a2	4	protein_coding	0.19	7.20E-03	0.16	3.67E-02	-0.01	9.49E-01	0.03	8.48E-01
Oprd1	4	protein_coding	0.21	7.25E-03	0.54	7.88E-18	0.17	1.18E-01	0.48	5.09E-07
Rasa3	8	protein_coding	0.12	7.26E-03	0.27	1.30E-10	0.06	4.01E-01	0.19	3.14E-04
Cacnb1	11	protein_coding	0.13	7.27E-03	0.49	2.38E-49	-0.02	8.49E-01	0.28	4.48E-04
Egln1	8	protein_coding	0.18	7.37E-03	0.54	7.99E-37	0.06	4.49E-01	0.37	8.82E-12
Zfp36	7	protein_coding	0.33	7.42E-03	0.39	4.82E-03	-0.07	6.92E-01	0.16	3.54E-01
Olfm1	2	protein_coding	0.11	7.44E-03	0.12	3.46E-04	0.05	3.56E-01	0.14	1.61E-03
Tspan31	10	protein_coding	0.18	7.44E-03	0.49	3.08E-20	0.07	3.70E-01	0.42	2.83E-10
Tafa1	6	protein_coding	0.28	7.51E-03	0.61	3.98E-30	0.05	5.37E-01	0.12	1.23E-01
Eif5b	1	protein_coding	0.17	7.52E-03	0.27	2.14E-09	-0.07	1.86E-01	0.14	1.82E-02
Adgrl4	3	protein_coding	0.29	7.65E-03	0.58	9.34E-10	0.15	1.95E-01	0.23	3.59E-02
Usp13	3	protein_coding	0.15	7.70E-03	0.22	1.05E-06	0.07	3.73E-01	0.08	4.05E-01
Eogt	6	protein_coding	0.25	7.94E-03	0.36	8.34E-10	-0.01	9.73E-01	0.05	7.59E-01
Picalm	7	protein_coding	0.12	7.94E-03	0.29	5.22E-14	-0.10	1.61E-01	0.04	6.87E-01
Arc	15	protein_coding	0.27	8.06E-03	2.36	9.70E-36	0.19	1.64E-01	1.34	3.50E-16
Adam33	2	protein_coding	0.33	8.10E-03	0.64	4.51E-09	0.38	1.45E-03	0.72	4.05E-06

Table S4 (6/9)

Tmem240	4	protein_coding	0.17	8.13E-03	0.32	2.74E-10	0.24	3.05E-04	0.29	3.27E-04
Nme1	11	protein_coding	0.21	8.18E-03	0.51	7.27E-27	0.13	9.20E-02	0.36	2.17E-08
Etf1	18	protein_coding	0.13	8.43E-03	0.49	7.49E-42	-0.01	9.29E-01	0.19	2.25E-04
Ica1	6	protein_coding	0.16	8.44E-03	0.12	1.35E-02	0.05	4.80E-01	0.06	4.25E-01
Exosc9	3	protein_coding	0.20	8.44E-03	0.23	1.61E-04	-0.03	7.14E-01	0.15	5.00E-02
Abcg2	6	protein_coding	0.18	8.44E-03	0.38	2.97E-09	-0.05	5.76E-01	0.07	5.15E-01
Pptc7	5	protein_coding	0.15	8.50E-03	0.48	4.25E-22	-0.02	8.49E-01	0.29	6.70E-05
Nefm	14	protein_coding	0.30	8.60E-03	0.78	5.54E-29	0.15	1.44E-01	0.50	6.08E-06
Zfp385b	2	protein_coding	0.18	8.79E-03	0.13	2.98E-02	0.13	3.56E-02	0.18	1.06E-02
Asap2	12	protein_coding	0.16	8.84E-03	0.27	2.60E-05	-0.22	1.68E-02	-0.05	7.72E-01
Usp32	11	protein_coding	0.14	8.85E-03	0.35	3.41E-15	-0.06	5.68E-01	0.15	6.71E-02
Foxj3	4	protein_coding	0.14	8.89E-03	0.19	3.82E-05	-0.02	8.36E-01	0.03	7.24E-01
Mark3	12	protein_coding	0.13	9.01E-03	0.44	1.38E-28	-0.07	3.65E-01	0.11	2.04E-01
Pou6f1	15	protein_coding	0.14	9.06E-03	0.22	2.29E-12	0.01	8.86E-01	0.08	3.41E-01
Rgs10	7	protein_coding	0.19	9.15E-03	0.33	7.02E-07	0.05	6.93E-01	0.18	9.48E-02
Cdk17	10	protein_coding	0.11	9.21E-03	0.09	3.94E-02	-0.03	6.47E-01	0.04	5.93E-01
Prkar2a	9	protein_coding	0.13	9.22E-03	0.53	1.33E-24	-0.03	7.26E-01	0.30	5.43E-04
Sult2b1	7	protein_coding	0.27	9.39E-03	0.56	1.22E-11	0.27	4.38E-03	0.55	1.33E-07
Sowahb	5	protein_coding	0.26	9.44E-03	0.93	8.26E-37	0.28	1.03E-03	0.84	1.29E-21
Rbpj	5	protein_coding	0.19	9.50E-03	0.66	2.81E-32	0.00	9.80E-01	0.38	4.40E-05
Ppil4	10	protein_coding	0.15	9.54E-03	0.21	5.60E-05	-0.15	1.58E-01	0.05	7.15E-01
Ppp1r15a	7	protein_coding	0.26	9.54E-03	0.23	8.03E-03	-0.11	2.50E-01	0.07	5.57E-01
Sema4a	3	protein_coding	0.16	9.58E-03	0.52	7.05E-23	0.17	4.48E-02	0.50	1.70E-14
B4galt5	2	protein_coding	0.12	9.64E-03	0.39	6.87E-22	-0.03	7.23E-01	0.14	9.56E-02
Erc1	6	protein_coding	0.16	9.71E-03	0.30	2.98E-11	0.00	9.96E-01	0.02	8.46E-01
Wac	18	protein_coding	0.13	9.73E-03	0.26	2.59E-09	-0.14	2.98E-02	0.09	2.78E-01
Slc9a9	9	protein_coding	0.24	9.77E-03	0.25	6.41E-03	0.23	2.07E-03	0.18	1.09E-01
Carm1	9	protein_coding	0.11	9.79E-03	0.22	3.33E-09	-0.07	4.80E-01	0.08	4.41E-01
Pou3f1	4	protein_coding	0.19	9.81E-03	0.52	7.05E-14	0.04	7.09E-01	0.27	2.69E-03
Mas1	17	protein_coding	0.34	9.81E-03	0.99	2.62E-41	0.09	4.97E-01	0.71	8.04E-13
Nkrf	X	protein_coding	0.18	9.93E-03	0.47	2.84E-16	-0.06	5.98E-01	0.24	5.85E-04
Sh3kbp1	X	protein_coding	0.18	9.95E-03	0.22	8.01E-05	0.04	5.70E-01	0.03	7.65E-01
Vmp1	11	protein_coding	0.18	1.02E-02	0.17	9.37E-05	0.08	1.82E-01	0.11	1.71E-01
Psmb10	8	protein_coding	0.24	1.02E-02	0.57	8.65E-28	0.07	5.34E-01	0.46	3.56E-09
Inpp5f	7	protein_coding	0.14	1.03E-02	0.26	1.37E-11	0.08	9.19E-02	0.11	5.20E-02
Crh	3	protein_coding	0.31	1.05E-02	0.93	3.03E-16	0.30	9.17E-03	0.67	1.31E-07
Cdr2	7	protein_coding	0.28	1.05E-02	0.88	1.61E-20	-0.04	8.31E-01	0.39	3.06E-03
Gria3	X	protein_coding	0.15	1.06E-02	0.18	1.30E-03	0.03	7.83E-01	0.07	3.77E-01
Ube2f	1	protein_coding	0.13	1.06E-02	0.27	4.47E-08	-0.01	9.14E-01	0.10	2.30E-01
Vipr1	9	protein_coding	0.21	1.06E-02	0.73	1.69E-31	0.18	7.95E-03	0.54	4.44E-23
Gng4	13	protein_coding	0.19	1.07E-02	0.44	2.08E-12	0.04	7.32E-01	0.20	2.12E-02
Hnrnpa1	15	protein_coding	0.16	1.11E-02	0.31	6.51E-12	0.09	2.97E-01	0.28	4.47E-04
Trim33	3	protein_coding	0.15	1.12E-02	0.23	6.46E-06	-0.04	7.24E-01	0.05	6.81E-01
Rnf126	10	protein_coding	0.14	1.14E-02	0.23	3.08E-06	0.04	7.14E-01	0.21	9.61E-03
Actb	5	protein_coding	0.14	1.16E-02	0.17	2.39E-08	0.05	4.74E-01	0.10	1.30E-01
Nrg3	14	protein_coding	0.19	1.16E-02	0.17	7.26E-03	-0.07	4.86E-01	0.11	3.08E-01
Mak16	8	protein_coding	0.18	1.16E-02	0.38	3.65E-10	-0.02	8.18E-01	0.17	2.87E-02
Cdk11b	4	protein_coding	0.16	1.18E-02	0.31	3.55E-13	0.01	9.39E-01	0.15	4.09E-03
Ndufv2	17	protein_coding	0.17	1.20E-02	0.23	7.80E-08	-0.01	9.37E-01	0.15	2.96E-03
Mta1	12	protein_coding	0.12	1.23E-02	0.11	1.57E-02	-0.04	6.19E-01	-0.07	3.39E-01
Atp10a	7	protein_coding	0.28	1.25E-02	0.93	2.12E-26	-0.29	2.00E-02	0.34	2.06E-02
Hars	18	protein_coding	0.14	1.25E-02	0.28	3.46E-12	-0.04	6.11E-01	0.11	1.22E-01
Smim3	18	protein_coding	0.31	1.25E-02	1.31	2.54E-62	-0.31	1.38E-02	0.31	7.05E-02
Dapk2	9	protein_coding	0.32	1.26E-02	0.40	1.77E-02	0.15	3.42E-01	0.18	4.04E-01
Clmp	9	protein_coding	0.21	1.26E-02	0.63	9.69E-13	0.06	4.92E-01	0.37	2.43E-06
Nostrin	2	protein_coding	0.31	1.27E-02	1.00	6.10E-14	0.01	9.63E-01	0.23	2.32E-01
Gnb1	4	protein_coding	0.08	1.27E-02	0.08	1.51E-02	0.02	7.12E-01	0.01	9.46E-01
Myl6	10	protein_coding	0.15	1.27E-02	0.10	4.77E-02	0.08	3.32E-01	0.13	8.31E-02
Scrt2	2	protein_coding	0.23	1.28E-02	0.74	9.95E-19	-0.07	5.34E-01	0.51	6.71E-09
Ell2	13	protein_coding	0.17	1.28E-02	0.23	3.06E-04	0.13	1.18E-01	0.11	2.98E-01
Tcerg1	18	protein_coding	0.13	1.29E-02	0.16	1.42E-03	0.07	2.70E-01	0.08	2.36E-01
Ccdc6	10	protein_coding	0.16	1.33E-02	0.82	5.53E-53	-0.10	3.86E-01	0.33	9.39E-04
Zmat4	8	protein_coding	0.17	1.33E-02	0.16	5.63E-03	0.05	7.01E-01	0.05	7.24E-01
Ppp2r5c	12	protein_coding	0.11	1.35E-02	0.14	1.86E-05	-0.03	5.20E-01	0.08	1.09E-01
4930453N24Rik	16	protein_coding	0.18	1.37E-02	0.40	1.79E-10	-0.01	9.32E-01	0.26	3.80E-04
Zfp330	8	protein_coding	0.17	1.38E-02	0.18	9.45E-03	0.05	6.36E-01	0.05	6.38E-01
Trhr2	8	protein_coding	0.33	1.39E-02	0.56	1.83E-03	0.32	1.21E-02	0.49	1.45E-03
Habp4	13	protein_coding	0.12	1.39E-02	0.19	9.50E-09	0.05	2.35E-01	0.13	6.98E-03
Eif3a	19	protein_coding	0.13	1.42E-02	0.26	1.56E-12	-0.05	3.30E-01	0.08	1.51E-01
Zfp617	8	protein_coding	0.21	1.44E-02	0.17	3.45E-02	-0.12	2.21E-01	0.06	5.67E-01
Cep83	10	protein_coding	0.17	1.44E-02	0.38	1.68E-11	-0.02	9.00E-01	0.24	1.85E-03
Mt2	8	protein_coding	0.29	1.44E-02	0.68	7.92E-20	0.08	6.85E-01	0.30	1.63E-01
Sik3	9	protein_coding	0.11	1.44E-02	0.33	7.84E-12	-0.11	1.12E-01	0.11	2.28E-01
Gadd45a	6	protein_coding	0.31	1.45E-02	1.34	3.07E-24	0.36	2.60E-03	0.94	1.22E-13
Ptp4a3	15	protein_coding	0.15	1.48E-02	0.55	5.36E-23	0.20	3.26E-05	0.44	9.75E-15
Phospho2	2	protein_coding	0.17	1.48E-02	0.47	1.09E-15	-0.14	2.20E-01	0.20	9.49E-02
Ppp2r2a	14	protein_coding	0.13	1.49E-02	0.27	6.62E-11	0.02	8.20E-01	0.18	9.03E-04
Ncl	1	protein_coding	0.17	1.50E-02	0.18	3.23E-07	0.01	8.61E-01	0.14	3.07E-03
Aco2	15	protein_coding	0.10	1.53E-02	0.07	2.34E-02	0.03	6.30E-01	0.05	4.06E-01
Cox5a	9	protein_coding	0.21	1.54E-02	0.33	1.27E-14	0.15	2.93E-02	0.29	1.97E-04
Yaf2	15	protein_coding	0.13	1.57E-02	0.13	5.49E-03	0.07	2.03E-01	0.08	2.14E-01
Hprt	X	protein_coding	0.16	1.58E-02	0.20	3.14E-05	0.04	6.75E-01	0.14	1.93E-02
Vma21	X	protein_coding	0.17	1.59E-02	0.19	2.25E-03	0.09	2.49E-01	0.08	3.52E-01
Jade3	X	protein_coding	0.21	1.59E-02	0.31	1.41E-04	0.08	5.40E-01	0.03	8.67E-01
Med15	16	protein_coding	0.14	1.59E-02	0.23	3.76E-08	-0.04	6.74E-01	0.13	1.26E-01
Neto2	8	protein_coding	0.12	1.59E-02	0.33	2.81E-09	0.03	7.67E-01	0.16	4.27E-02
Ivns1abp	1	protein_coding	0.13	1.59E-02	0.44	1.46E-25	-0.06	4.29E-01	0.21	5.96E-03
Cipc	12	protein_coding	0.13	1.60E-02	0.15	3.76E-03	0.03	7.78E-01	0.05	5.28E-01
Map4	9	protein_coding	0.10	1.60E-02	0.12	2.38E-04	0.04	4.27E-01	0.02	7.43E-01
Ap2b1	11	protein_coding	0.11	1.61E-02	0.29	3.21E-16	-0.02	8.45E-01	0.16	9.87E-03
Utp4	8	protein_coding	0.16	1.61E-02	0.48	5.17E-21	-0.10	3.04E-01	0.22	1.09E-02
Ntng2	2	protein_coding	0.19	1.62E-02	0.21	5.27E-03	0.20	1.84E-02	0.13	2.31E-01
Plk2	13	protein_coding	0.18	1.65E-02	0.38	3.14E-18	0.02	8.33E-01	0.24	2.00E-03
Slc25a44	3	protein_coding	0.11	1.65E-02	0.22	7.82E-09	-0.05	5.80E-01	0.09	3.51E-01
2510009E07Rik	16	protein_coding	0.15	1.69E-02	0.36	1.16E-13	0.00	9.99E-01	0.13	1.59E-01
Pde4c	8	protein_coding	0.30	1.69E-02	0.45	2.01E-03	0.17	2.17E-01	0.31	3.25E-02
Orai1	5	protein_coding	0.26	1.70E-02	0.28	2.28E-02	0.02	9.21E-01	0.02	9.05E-01
Stam	2	protein_coding	0.11	1.71E-02	0.16	1.88E-04	0.02	8.35E-01	0.08	3.07E-01
Myo19	11	protein_coding	0.21	1.73E-02	0.67	4.57E-22	0.11	3.13E-01	0.39	3.92E-05
Wee1	7	protein_coding	0.19	1.75E-02	0.19	7.64E-03	0.01	9.50E-01	0.30	6.55E-04
Ncbp1	4	protein_coding	0.15	1.75E-02	0.47	8.55E-27	-0.16	2.33E-02	0.17	3.82E-02
Tmem204	17	protein_coding	0.24	1.76E-02	0.50	9.89E-08	0.15	2.86E-01	0.26	6.06E-02
Gak	5	protein_coding	0.10	1.76E-02	0.22	1.09E-09	0.00	9.99E-01	0.10	1.13E-01
Sec13	6	protein_coding	0.15	1.76E-02	0.33	5.14E-14	-0.04	5.97E-01	0.13	2.85E-02
Zfp821	8	protein_coding	0.17	1.77E-02	0.21	3.52E-04	0.01	9.31E-01	0.04	5.96E-01

Table S4 (7/9)

Higd1a	9	protein_coding	0.17	1.78E-02	0.23	3.76E-07	0.08	2.13E-01	0.20	5.61E-04
Calm2	17	protein_coding	0.14	1.79E-02	0.24	1.69E-10	-0.01	8.59E-01	0.13	9.80E-03
Nek7	1	protein_coding	0.15	1.80E-02	0.26	7.00E-08	0.08	2.86E-01	0.23	4.70E-03
Dstn	2	protein_coding	0.14	1.81E-02	0.09	3.69E-02	0.04	5.71E-01	0.04	5.67E-01
Dusp1	17	protein_coding	0.27	1.81E-02	0.66	1.64E-04	0.22	1.32E-01	0.60	4.88E-04
Tbpl1	10	protein_coding	0.14	1.81E-02	0.12	9.21E-03	0.02	8.22E-01	0.07	3.18E-01
Clip1	5	protein_coding	0.10	1.83E-02	0.27	5.35E-12	-0.08	3.16E-01	0.14	8.46E-02
Crip2	12	protein_coding	0.16	1.88E-02	0.22	7.93E-05	0.16	1.12E-03	0.21	1.76E-04
Smc3	19	protein_coding	0.14	1.89E-02	0.23	1.47E-05	-0.09	2.62E-01	0.06	5.49E-01
Ddx50	10	protein_coding	0.14	1.89E-02	0.36	2.04E-11	-0.03	6.94E-01	0.09	2.48E-01
Psma1	7	protein_coding	0.14	1.90E-02	0.19	2.27E-05	-0.06	3.84E-01	0.05	4.52E-01
Uhrf1bp1l	10	protein_coding	0.15	1.92E-02	0.31	1.24E-12	-0.03	8.39E-01	0.06	5.90E-01
Insyn2a	7	protein_coding	0.21	1.95E-02	0.42	1.01E-06	0.16	1.27E-01	0.22	8.93E-02
Dip2c	13	protein_coding	0.18	1.97E-02	0.36	1.01E-19	-0.04	7.14E-01	0.19	1.50E-02
Rab6a	7	protein_coding	0.11	1.97E-02	0.32	1.54E-18	0.03	6.80E-01	0.21	9.69E-06
Ipo11	13	protein_coding	0.14	1.99E-02	0.18	4.42E-05	0.04	6.44E-01	0.16	1.52E-02
Ier5	1	protein_coding	0.24	2.03E-02	1.03	3.27E-17	0.47	6.14E-14	0.98	1.35E-44
Pnpla2	7	protein_coding	0.18	2.04E-02	0.22	4.27E-03	-0.11	2.80E-01	0.14	3.22E-01
Ccnd3	17	protein_coding	0.16	2.04E-02	0.52	1.18E-17	0.00	9.88E-01	0.39	1.97E-07
Emcn	3	protein_coding	0.27	2.04E-02	0.44	7.02E-04	0.01	9.64E-01	0.10	6.32E-01
Gclc	9	protein_coding	0.13	2.05E-02	0.30	3.08E-12	-0.08	3.52E-01	0.11	2.20E-01
Hif1a	12	protein_coding	0.14	2.06E-02	0.12	3.19E-02	-0.01	8.99E-01	0.02	8.12E-01
Rab1a	11	protein_coding	0.11	2.07E-02	0.13	3.99E-04	0.04	5.48E-01	0.12	7.24E-02
Slc7a4	16	protein_coding	0.15	2.07E-02	0.40	3.30E-15	0.15	4.51E-03	0.43	7.69E-12
Abce1	8	protein_coding	0.14	2.08E-02	0.35	7.83E-16	-0.01	9.38E-01	0.21	7.44E-04
2210408I21Rik	13	protein_coding	0.25	2.08E-02	0.23	3.34E-02	0.09	4.95E-01	-0.08	5.74E-01
Azin1	15	protein_coding	0.15	2.08E-02	0.44	1.46E-39	0.02	8.09E-01	0.23	1.88E-05
Cask	X	protein_coding	0.14	2.09E-02	0.15	8.35E-03	0.10	1.45E-01	-0.08	2.68E-01
Ccl27a	4	protein_coding	0.16	2.09E-02	0.25	5.15E-04	0.08	4.66E-01	0.18	7.29E-02
Ccdc141	2	protein_coding	0.23	2.10E-02	0.44	3.97E-08	-0.16	1.90E-01	-0.08	6.49E-01
Rnf19b	4	protein_coding	0.16	2.11E-02	0.61	1.86E-29	0.06	3.88E-01	0.42	1.07E-11
Cap1	4	protein_coding	0.18	2.11E-02	0.52	1.75E-44	0.06	2.17E-01	0.44	7.52E-16
Necab3	2	protein_coding	0.15	2.19E-02	0.25	7.86E-07	0.09	8.41E-02	0.23	6.55E-04
Ndufaf4	4	protein_coding	0.21	2.19E-02	0.58	2.83E-19	-0.02	8.26E-01	0.38	1.65E-08
Tax1bp1	6	protein_coding	0.13	2.22E-02	0.23	3.87E-11	-0.06	3.15E-01	0.18	2.82E-04
Pde5a	3	protein_coding	0.21	2.23E-02	0.27	7.87E-03	0.00	9.97E-01	0.09	4.54E-01
Rnf157	11	protein_coding	0.09	2.25E-02	0.12	1.12E-03	0.04	5.91E-01	0.04	5.64E-01
Shoc2	19	protein_coding	0.13	2.26E-02	0.17	3.72E-04	0.01	9.51E-01	0.07	3.77E-01
Samd10	2	protein_coding	0.16	2.28E-02	0.28	1.24E-05	0.03	7.41E-01	0.21	1.15E-03
Nemf	12	protein_coding	0.15	2.31E-02	0.14	2.09E-02	-0.04	7.07E-01	0.10	2.48E-01
D5Ertd579e	5	protein_coding	0.10	2.32E-02	0.33	1.38E-18	0.00	9.96E-01	0.15	3.37E-03
Ss18l2	9	protein_coding	0.15	2.32E-02	0.27	2.07E-05	0.08	2.62E-01	0.17	1.30E-02
Smap2	4	protein_coding	0.13	2.34E-02	0.30	1.12E-18	0.00	9.71E-01	0.30	2.14E-17
Bbip1	19	protein_coding	0.13	2.34E-02	0.15	4.12E-03	0.05	5.47E-01	0.07	3.78E-01
Rbp4	19	protein_coding	0.25	2.36E-02	0.64	5.85E-17	0.24	2.03E-02	0.44	6.60E-05
Zdhhc23	16	protein_coding	0.16	2.41E-02	0.23	2.31E-04	0.10	1.29E-01	0.10	1.54E-01
Kcnf1	12	protein_coding	0.11	2.47E-02	0.25	1.14E-10	0.12	3.12E-02	0.19	8.03E-03
Rab11fip3	17	protein_coding	0.09	2.48E-02	0.25	4.19E-12	-0.02	8.13E-01	0.14	5.74E-02
Rheb	5	protein_coding	0.22	2.50E-02	0.79	9.00E-71	0.11	6.30E-02	0.58	7.35E-18
Ptgfrn	3	protein_coding	0.17	2.51E-02	0.66	1.39E-29	0.17	4.87E-03	0.45	2.93E-13
Dnm1l	16	protein_coding	0.10	2.53E-02	0.11	4.48E-03	-0.05	5.05E-01	0.04	6.42E-01
Naa25	5	protein_coding	0.11	2.55E-02	0.43	4.10E-27	-0.02	8.58E-01	0.22	3.81E-04
Ccne1	7	protein_coding	0.21	2.59E-02	0.43	6.71E-08	0.08	4.14E-01	0.18	5.26E-02
Ubap2l	3	protein_coding	0.11	2.59E-02	0.11	3.11E-03	-0.08	3.81E-01	0.03	8.35E-01
Wdr26	1	protein_coding	0.15	2.63E-02	0.32	9.31E-12	-0.03	7.08E-01	0.03	7.28E-01
Psme4	11	protein_coding	0.17	2.63E-02	0.28	1.35E-07	-0.02	8.78E-01	0.03	7.36E-01
Dcaf10	4	protein_coding	0.17	2.66E-02	0.40	1.71E-10	-0.04	7.41E-01	0.07	6.23E-01
Prrt3	6	protein_coding	0.15	2.73E-02	0.52	4.15E-25	0.10	1.48E-01	0.43	8.23E-15
Ptprt	2	protein_coding	0.15	2.74E-02	0.21	3.42E-12	0.09	3.81E-01	0.04	7.14E-01
Jazf1	6	protein_coding	0.18	2.74E-02	0.23	2.66E-04	0.00	9.79E-01	0.09	2.35E-01
Atp2b1	10	protein_coding	0.16	2.75E-02	0.30	3.24E-07	-0.08	3.76E-01	0.05	6.49E-01
Sergef	7	protein_coding	0.17	2.75E-02	0.34	3.73E-08	-0.01	9.42E-01	0.11	2.34E-01
Foxo3	10	protein_coding	0.12	2.75E-02	0.15	6.81E-03	0.01	9.55E-01	0.06	5.85E-01
Afap1l1	18	protein_coding	0.16	2.75E-02	0.33	3.54E-08	0.12	1.81E-01	0.19	3.52E-03
Smc6	12	protein_coding	0.16	2.76E-02	0.35	4.82E-11	-0.03	7.96E-01	0.11	3.38E-01
Lurap1	4	protein_coding	0.15	2.76E-02	0.40	1.07E-12	0.03	8.15E-01	0.29	1.29E-05
Arhgef9	X	protein_coding	0.11	2.79E-02	0.18	3.03E-07	-0.02	8.22E-01	0.11	5.26E-02
Ildr2	1	protein_coding	0.15	2.83E-02	0.34	3.02E-19	0.01	9.30E-01	0.10	2.77E-01
Sptlc2	12	protein_coding	0.13	2.83E-02	0.34	7.42E-11	0.06	4.56E-01	0.11	1.49E-01
Rrp1	10	protein_coding	0.11	2.83E-02	0.28	1.05E-17	-0.02	8.31E-01	0.15	2.04E-03
Tac1	6	protein_coding	0.25	2.85E-02	0.66	1.90E-09	0.05	7.46E-01	0.20	8.29E-02
Atp5g1	11	protein_coding	0.17	2.85E-02	0.36	7.78E-11	-0.05	6.20E-01	0.17	2.50E-02
Cacna1a	8	protein_coding	0.14	2.88E-02	0.36	7.72E-27	0.05	6.31E-01	0.20	9.71E-03
Slc25a25	2	protein_coding	0.11	2.91E-02	0.61	1.63E-52	0.12	3.98E-02	0.45	7.60E-17
Utp15	13	protein_coding	0.15	2.93E-02	0.23	2.18E-04	-0.04	6.09E-01	0.10	2.18E-01
Dcun1d4	5	protein_coding	0.10	2.93E-02	0.14	3.18E-04	-0.01	8.90E-01	0.04	5.86E-01
Etv6	6	protein_coding	0.18	2.94E-02	0.23	9.99E-05	-0.07	4.86E-01	0.01	9.67E-01
Msantd3	4	protein_coding	0.19	2.94E-02	0.31	7.77E-05	-0.01	9.54E-01	0.12	2.35E-01
Hnrnpu	1	protein_coding	0.14	2.97E-02	0.24	5.14E-08	-0.04	5.36E-01	0.12	6.40E-02
Naa50	16	protein_coding	0.17	2.98E-02	0.54	1.74E-34	0.06	3.13E-01	0.40	5.51E-15
Nrd1	4	protein_coding	0.15	3.01E-02	0.27	1.74E-14	0.02	7.57E-01	0.13	2.76E-02
Spire1	18	protein_coding	0.11	3.03E-02	0.24	6.30E-10	-0.12	6.17E-02	0.10	1.86E-01
Mia3	1	protein_coding	0.11	3.03E-02	0.24	1.45E-09	-0.03	6.42E-01	0.09	1.60E-01
Noct	3	protein_coding	0.18	3.10E-02	0.60	1.35E-29	-0.01	9.51E-01	0.31	7.95E-08
Pthlh	6	protein_coding	0.27	3.11E-02	0.41	4.15E-03	0.05	7.94E-01	0.40	1.11E-02
Raly	2	protein_coding	0.15	3.12E-02	0.37	2.59E-17	0.08	2.39E-01	0.25	5.94E-05
Psmc1	12	protein_coding	0.14	3.12E-02	0.38	2.67E-16	-0.09	9.55E-02	0.20	5.58E-04
Pdcd6	13	protein_coding	0.15	3.12E-02	0.29	7.24E-06	0.02	8.36E-01	0.21	1.93E-03
Spats2	15	protein_coding	0.14	3.15E-02	0.22	1.16E-04	-0.04	7.18E-01	-0.01	9.64E-01
Robo4	9	protein_coding	0.23	3.18E-02	0.37	3.34E-04	0.07	6.35E-01	0.00	1.00E+00
Eif4a1	11	protein_coding	0.14	3.18E-02	0.33	4.12E-15	-0.02	8.11E-01	0.18	9.41E-04
Asic1	15	protein_coding	0.15	3.18E-02	0.25	2.50E-06	0.09	2.07E-01	0.28	1.86E-05
Agpat5	8	protein_coding	0.12	3.20E-02	0.13	4.77E-03	0.09	2.31E-01	0.09	3.07E-01
Kcnj4	15	protein_coding	0.15	3.20E-02	0.23	3.44E-05	0.15	4.86E-02	0.22	8.66E-03
Lactb	9	protein_coding	0.20	3.28E-02	0.34	1.25E-05	0.04	7.17E-01	0.25	6.01E-03
Ephx4	5	protein_coding	0.15	3.28E-02	0.15	1.90E-03	0.05	4.85E-01	0.16	5.03E-03
Pik3ca	3	protein_coding	0.11	3.29E-02	0.29	1.62E-09	-0.07	4.23E-01	0.15	5.70E-02
Eif1ad	19	protein_coding	0.16	3.33E-02	0.25	7.60E-05	-0.02	8.58E-01	0.06	4.80E-01
Mt1	8	protein_coding	0.20	3.33E-02	0.57	8.86E-19	0.01	9.80E-01	0.38	1.82E-02
Lmtk2	5	protein_coding	0.13	3.36E-02	0.22	3.40E-13	0.09	1.86E-01	0.12	9.12E-02
Efhd2	4	protein_coding	0.16	3.36E-02	0.38	2.38E-18	0.18	1.74E-03	0.44	1.11E-18
Ppm1e	11	protein_coding	0.16	3.37E-02	0.44	1.16E-17	-0.08	4.78E-01	0.17	9.02E-02
Mtmr4	11	protein_coding	0.11	3.39E-02	0.45	4.88E-29	-0.03	7.77E-01	0.14	1.34E-01
Slc35e2	4	protein_coding	0.12	3.39E-02	0.44	1.27E-20	-0.03	7.80E-01	0.06	5.98E-01
Stac3	10	protein_coding	0.27	3.40E-02	0.94	1.74E-09	0.24	3.79E-02	0.44	4.30E-03

Table S4 (8/9)

Lin54	5	protein_coding	0.18	3.42E-02	0.49	1.96E-11	-0.08	6.19E-01	0.11	4.86E-01
Zfp703	8	protein_coding	0.15	3.42E-02	0.34	2.66E-10	0.14	7.61E-02	0.33	2.41E-04
Csde1	3	protein_coding	0.10	3.42E-02	0.16	1.19E-05	-0.04	5.22E-01	0.05	4.07E-01
Pip4k2a	2	protein_coding	0.14	3.42E-02	0.35	5.03E-18	0.04	5.49E-01	0.32	7.00E-10
Nucb2	7	protein_coding	0.20	3.42E-02	0.28	2.31E-03	-0.05	7.40E-01	0.18	1.12E-01
Top2b	14	protein_coding	0.14	3.42E-02	0.15	6.98E-04	-0.04	6.18E-01	-0.03	7.95E-01
Nacc1	8	protein_coding	0.09	3.44E-02	0.26	4.82E-14	-0.01	9.09E-01	0.14	1.67E-02
Mrpl32	13	protein_coding	0.17	3.46E-02	0.31	3.23E-05	-0.04	6.87E-01	0.17	2.65E-02
Acta1	8	protein_coding	0.21	3.46E-02	0.33	7.28E-05	0.28	1.46E-02	0.37	6.00E-03
Nifk	1	protein_coding	0.16	3.49E-02	0.36	2.06E-07	0.00	9.76E-01	0.16	3.55E-02
Lpgat1	1	protein_coding	0.10	3.51E-02	0.25	3.15E-10	0.09	2.95E-01	0.28	7.68E-05
Wsb2	5	protein_coding	0.10	3.51E-02	0.14	8.25E-05	-0.01	9.57E-01	0.03	8.01E-01
Il17ra	6	protein_coding	0.19	3.55E-02	0.94	2.27E-41	0.19	3.72E-02	0.69	9.35E-17
Camsap1	2	protein_coding	0.09	3.55E-02	0.24	2.46E-13	-0.04	6.56E-01	0.12	1.91E-01
Lig3	11	protein_coding	0.13	3.55E-02	0.30	1.23E-09	0.00	9.88E-01	0.10	1.27E-01
Pdzd8	19	protein_coding	0.13	3.55E-02	0.32	5.70E-09	-0.03	7.66E-01	0.17	4.67E-03
Gm20604	12	protein_coding	0.19	3.56E-02	0.20	1.27E-02	0.02	8.84E-01	0.15	1.43E-01
Sumo3	10	protein_coding	0.11	3.57E-02	0.10	4.65E-02	-0.08	3.38E-01	0.01	9.53E-01
Slc17a7	7	protein_coding	0.11	3.58E-02	0.14	5.61E-04	0.09	2.24E-01	0.00	9.91E-01
Ssb	2	protein_coding	0.13	3.58E-02	0.16	2.63E-03	-0.03	7.54E-01	0.05	5.61E-01
Ube2e1	14	protein_coding	0.13	3.59E-02	0.18	1.31E-04	0.04	5.63E-01	0.12	7.86E-02
Ppp1r16b	2	protein_coding	0.11	3.60E-02	0.45	1.06E-30	-0.04	6.88E-01	0.25	8.54E-04
Zmym2	14	protein_coding	0.12	3.62E-02	0.18	1.29E-03	-0.06	3.74E-01	0.02	8.65E-01
Slco1c1	6	protein_coding	0.14	3.62E-02	0.19	5.98E-03	0.04	7.10E-01	-0.15	1.82E-01
Atp2b2	6	protein_coding	0.14	3.62E-02	0.12	2.88E-03	0.08	3.74E-01	0.12	1.15E-01
Synpo	18	protein_coding	0.12	3.64E-02	0.52	7.92E-29	-0.04	6.94E-01	0.39	3.16E-11
Cdk13	13	protein_coding	0.13	3.65E-02	0.42	5.81E-18	-0.01	9.53E-01	0.23	3.32E-03
Cfap36	11	protein_coding	0.14	3.67E-02	0.15	2.06E-03	-0.06	2.77E-01	0.02	7.34E-01
Wdr1	5	protein_coding	0.14	3.68E-02	0.35	5.91E-16	0.03	7.74E-01	0.16	2.61E-02
Sptan1	2	protein_coding	0.07	3.69E-02	0.09	1.52E-03	-0.02	7.55E-01	0.00	9.89E-01
Gspt1	16	protein_coding	0.12	3.69E-02	0.33	7.01E-12	0.02	8.19E-01	0.21	4.92E-04
Arl4d	11	protein_coding	0.29	3.71E-02	1.05	3.79E-27	0.37	5.03E-04	1.18	2.32E-24
Acsl3	1	protein_coding	0.12	3.71E-02	0.15	5.03E-04	-0.07	3.60E-01	0.13	1.20E-01
Cdh22	2	protein_coding	0.19	3.71E-02	0.57	6.29E-13	0.12	1.42E-01	0.69	9.30E-32
Cycs	6	protein_coding	0.20	3.71E-02	0.40	1.63E-08	0.20	1.71E-02	0.31	7.57E-04
Top1	2	protein_coding	0.14	3.71E-02	0.48	2.90E-24	-0.11	3.23E-01	0.20	4.80E-02
Sec62	3	protein_coding	0.12	3.72E-02	0.19	8.96E-09	0.02	8.00E-01	0.20	2.65E-03
Pdgfb	15	protein_coding	0.22	3.73E-02	0.97	6.97E-14	0.15	1.81E-01	0.58	5.32E-11
Copb2	9	protein_coding	0.13	3.73E-02	0.13	2.10E-03	-0.03	7.55E-01	0.10	1.46E-01
Klhl3	13	protein_coding	0.13	3.73E-02	0.61	1.05E-55	-0.09	3.91E-01	0.30	2.19E-03
Tmem132b	5	protein_coding	0.10	3.75E-02	0.13	5.58E-03	0.03	7.30E-01	-0.01	9.34E-01
Ntrk2	13	protein_coding	0.14	3.76E-02	0.34	4.25E-15	-0.05	4.70E-01	0.17	3.47E-03
Cxxc5	18	protein_coding	0.14	3.77E-02	0.64	8.19E-46	0.11	1.67E-01	0.52	1.92E-15
Gdi2	13	protein_coding	0.13	3.81E-02	0.24	1.41E-10	-0.02	8.00E-01	0.12	2.42E-02
Zfp770	2	protein_coding	0.14	3.84E-02	0.15	2.32E-02	-0.01	9.51E-01	0.07	4.85E-01
Ccdc134	15	protein_coding	0.23	3.85E-02	0.90	1.01E-26	-0.05	7.55E-01	0.46	1.26E-04
Pias2	18	protein_coding	0.15	3.94E-02	0.34	2.02E-13	-0.11	2.83E-01	0.11	3.47E-01
Fem1b	9	protein_coding	0.11	3.95E-02	0.41	2.46E-25	0.02	8.67E-01	0.23	2.07E-04
Timm9	12	protein_coding	0.14	3.96E-02	0.18	3.41E-03	-0.11	1.22E-01	-0.13	1.70E-01
Rars	11	protein_coding	0.13	3.96E-02	0.33	4.85E-10	-0.07	3.97E-01	0.12	1.10E-01
Slc35f6	5	protein_coding	0.12	4.00E-02	0.28	4.08E-09	-0.01	9.38E-01	0.17	2.61E-03
Golga7b	19	protein_coding	0.13	4.05E-02	0.21	1.15E-05	0.18	9.26E-04	0.13	7.70E-02
Gad1	2	protein_coding	0.10	4.06E-02	0.30	1.13E-17	0.06	3.38E-01	0.19	6.58E-04
Ppard	17	protein_coding	0.16	4.06E-02	0.42	2.99E-14	0.06	5.13E-01	0.18	8.83E-02
Cltc	11	protein_coding	0.12	4.06E-02	0.25	1.58E-11	0.02	8.23E-01	0.13	3.24E-02
Zmynd8	2	protein_coding	0.09	4.07E-02	0.44	5.33E-37	-0.12	2.57E-01	0.16	1.47E-01
Rubcn	16	protein_coding	0.10	4.10E-02	0.29	6.76E-15	-0.02	8.42E-01	0.14	4.73E-02
Zdbf2	1	protein_coding	0.23	4.13E-02	0.59	6.40E-11	0.00	9.89E-01	0.34	1.95E-02
Ankrd13b	11	protein_coding	0.12	4.13E-02	0.39	2.27E-17	0.03	7.39E-01	0.14	5.37E-02
Rtca	3	protein_coding	0.14	4.13E-02	0.19	4.57E-04	-0.04	7.70E-01	0.05	6.67E-01
Sult1a1	7	protein_coding	0.26	4.14E-02	1.10	8.44E-23	-0.35	5.26E-03	0.31	1.47E-01
Entpd7	19	protein_coding	0.17	4.14E-02	0.49	3.24E-11	0.09	3.23E-01	0.15	1.92E-01
Hif3a	7	protein_coding	0.26	4.16E-02	1.71	3.32E-53	-0.25	4.32E-02	0.27	2.17E-01
Gm14295	2	protein_coding	0.22	4.16E-02	0.48	9.46E-05	0.01	9.53E-01	0.10	4.48E-01
Cnksr2	X	protein_coding	0.13	4.17E-02	0.12	2.96E-02	0.06	5.35E-01	0.03	8.13E-01
Med8	4	protein_coding	0.17	4.17E-02	0.32	1.28E-07	-0.14	1.30E-01	0.06	7.20E-01
Gars	6	protein_coding	0.14	4.17E-02	0.23	1.25E-08	0.06	3.65E-01	0.24	2.83E-05
Tubb4b	2	protein_coding	0.12	4.17E-02	0.20	2.06E-06	0.11	5.44E-02	0.16	1.02E-02
Arhgap1	2	protein_coding	0.10	4.18E-02	0.11	8.68E-03	-0.04	6.38E-01	0.06	5.24E-01
Dek	13	protein_coding	0.15	4.25E-02	0.21	4.73E-04	-0.04	6.85E-01	0.13	1.05E-01
Kctd15	7	protein_coding	0.18	4.25E-02	0.24	1.78E-03	0.22	1.24E-02	0.23	3.66E-02
Bend5	4	protein_coding	0.20	4.25E-02	0.19	4.55E-02	0.08	4.18E-01	0.12	2.86E-01
Samd4	14	protein_coding	0.16	4.25E-02	0.31	8.14E-10	0.11	1.65E-01	0.20	2.01E-02
B230219D22Rik	13	protein_coding	0.09	4.25E-02	0.13	1.86E-03	-0.02	8.33E-01	0.03	6.62E-01
Tpp2	1	protein_coding	0.14	4.25E-02	0.23	1.07E-05	-0.05	5.96E-01	0.05	5.81E-01
Lhfpl3	5	protein_coding	0.17	4.26E-02	0.15	3.49E-02	0.05	5.20E-01	-0.07	4.77E-01
Paqr8	1	protein_coding	0.16	4.26E-02	0.66	7.81E-60	-0.17	5.56E-02	0.33	9.39E-04
Abi3bp	16	protein_coding	0.28	4.26E-02	0.71	1.90E-16	0.54	9.03E-08	0.32	4.28E-02
Herpud1	8	protein_coding	0.13	4.26E-02	0.53	4.20E-20	-0.11	2.31E-01	0.38	3.61E-06
Sra1	18	protein_coding	0.16	4.29E-02	0.20	2.01E-03	-0.05	5.64E-01	0.06	5.22E-01
Serpine2	1	protein_coding	0.11	4.33E-02	0.17	3.92E-05	0.05	5.30E-01	0.09	1.73E-01
Ube2r2	4	protein_coding	0.11	4.35E-02	0.10	3.09E-02	-0.02	8.50E-01	-0.01	9.46E-01
Otud1	2	protein_coding	0.18	4.36E-02	0.24	4.07E-04	0.13	2.17E-01	0.12	3.75E-01
Blzf1	1	protein_coding	0.13	4.42E-02	0.25	7.61E-04	0.01	8.85E-01	0.02	8.16E-01
Nfkbia	12	protein_coding	0.22	4.49E-02	0.67	9.62E-13	-0.08	5.20E-01	0.46	3.62E-06
Trmt6	2	protein_coding	0.15	4.49E-02	0.15	1.43E-02	0.06	5.54E-01	0.11	2.81E-01
Insyn1	9	protein_coding	0.12	4.49E-02	0.53	5.07E-28	0.05	5.57E-01	0.27	6.49E-06
Inf2	12	protein_coding	0.14	4.52E-02	1.10	7.06E-92	0.13	1.45E-01	0.69	3.60E-26
Eprs	1	protein_coding	0.15	4.52E-02	0.32	9.44E-18	0.01	9.18E-01	0.16	3.14E-04
Sik1	17	protein_coding	0.28	4.52E-02	1.15	9.76E-09	0.39	6.62E-04	0.76	8.33E-06
Mob4	1	protein_coding	0.13	4.54E-02	0.29	2.17E-11	-0.02	8.03E-01	0.16	1.58E-02
Otulinl	15	protein_coding	0.15	4.58E-02	0.22	1.84E-03	-0.12	2.49E-01	-0.03	8.71E-01
Pabpc1	15	protein_coding	0.12	4.59E-02	0.29	6.60E-12	-0.07	2.12E-01	0.06	3.85E-01
Zfp651	9	protein_coding	0.10	4.62E-02	0.50	2.74E-35	-0.02	8.39E-01	0.26	3.09E-05
Psmc6	14	protein_coding	0.12	4.62E-02	0.22	3.71E-08	-0.01	9.44E-01	0.13	5.76E-02
Rnf168	16	protein_coding	0.13	4.71E-02	0.30	3.39E-08	-0.04	6.72E-01	0.06	5.18E-01
Rai2	X	protein_coding	0.19	4.72E-02	0.26	3.23E-03	0.03	8.37E-01	0.37	4.89E-05
1700025G04Rik	1	protein_coding	0.12	4.72E-02	0.31	1.34E-12	0.03	7.18E-01	0.09	2.79E-01
Alpk1	3	protein_coding	0.21	4.73E-02	0.33	1.18E-03	0.16	2.70E-01	0.14	4.57E-01
Exoc5	14	protein_coding	0.12	4.77E-02	0.39	2.83E-13	-0.02	8.84E-01	0.15	5.89E-02
Mat2a	6	protein_coding	0.13	4.80E-02	0.79	5.32E-68	-0.15	8.32E-02	0.34	4.22E-05
Epb41l1	2	protein_coding	0.09	4.80E-02	0.40	3.03E-39	0.04	5.65E-01	0.30	5.81E-13
Chst8	7	protein_coding	0.19	4.80E-02	0.30	1.21E-04	-0.04	7.78E-01	0.23	4.71E-03
Atf4	15	protein_coding	0.15	4.82E-02	0.56	4.51E-23	0.07	3.41E-01	0.57	3.09E-20
Slc7a1	5	protein_coding	0.16	4.84E-02	0.61	1.08E-37	0.15	1.20E-02	0.41	9.96E-12

Table S4 (9/9)

Sgk1	10	protein_coding	0.17	4.84E-02	0.43	6.13E-25	-0.18	1.87E-02	0.69	4.53E-09
Arhgef3	14	protein_coding	0.13	4.87E-02	0.63	3.57E-38	-0.04	6.96E-01	0.36	1.30E-06
Rundc3b	5	protein_coding	0.14	4.88E-02	0.14	9.82E-03	0.05	4.41E-01	0.13	3.56E-02
Pfkp	13	protein_coding	0.09	4.88E-02	0.24	2.38E-11	0.09	1.07E-01	0.17	2.65E-03
Ccn4	15	protein_coding	0.28	4.89E-02	2.77	2.97E-120	0.42	3.08E-04	1.97	6.77E-76
Fth1	19	protein_coding	0.14	4.91E-02	0.12	1.83E-03	0.04	6.24E-01	0.27	5.12E-03
Nell1	7	protein_coding	0.18	4.91E-02	0.40	4.94E-09	0.09	4.83E-01	0.34	8.12E-04
Usp42	5	protein_coding	0.12	4.91E-02	0.26	8.18E-07	0.05	5.58E-01	0.16	3.64E-02
Zdhhc13	7	protein_coding	0.17	4.91E-02	0.20	5.69E-03	-0.03	7.58E-01	0.07	4.99E-01
Dlat	9	protein_coding	0.12	4.91E-02	0.24	5.18E-09	0.02	8.42E-01	0.06	4.43E-01
Zfp267	3	protein_coding	0.14	4.97E-02	0.18	2.69E-03	-0.01	9.54E-01	0.06	5.30E-01
Sorcs3	19	protein_coding	0.25	5.22E-02	0.88	6.21E-77	0.23	1.37E-02	0.79	8.51E-31
Ngef	1	protein_coding	0.14	6.49E-02	0.18	9.06E-04	0.14	3.79E-02	0.21	2.13E-03
Foxred2	15	protein_coding	0.16	6.68E-02	0.17	8.73E-03	0.26	3.32E-05	0.19	7.94E-03
Mei1	15	protein_coding	0.21	7.21E-02	0.00	9.92E-01	0.41	3.62E-06	0.39	1.10E-02
Ndfip2	14	protein_coding	0.11	7.27E-02	0.13	4.53E-03	0.14	2.07E-03	0.13	3.36E-02
Ldha	7	protein_coding	0.14	7.51E-02	0.35	4.10E-17	0.15	1.85E-03	0.33	2.48E-09
Dlk2	17	protein_coding	0.15	8.03E-02	0.21	1.68E-03	0.23	4.96E-03	0.44	4.12E-07
Ephb3	16	protein_coding	0.15	8.56E-02	0.50	8.89E-14	0.24	3.86E-03	0.38	1.37E-07
Rasgrp2	19	protein_coding	0.15	8.75E-02	0.06	4.90E-01	0.15	3.41E-02	0.16	3.13E-02
Ptpn5	7	protein_coding	0.12	9.04E-02	0.09	6.90E-02	0.18	6.35E-03	0.28	1.45E-05
Ankrd34a	3	protein_coding	0.11	9.88E-02	0.09	1.42E-01	0.13	2.45E-02	0.17	4.65E-03
Tuba4a	1	protein_coding	0.10	1.03E-01	0.20	6.02E-08	0.15	1.25E-02	0.23	1.73E-04
Kcnk12	17	protein_coding	0.20	1.04E-01	0.47	5.62E-05	0.29	7.34E-03	0.54	2.48E-05
Ank1	8	protein_coding	0.11	1.13E-01	0.17	1.33E-03	0.14	1.68E-02	0.23	1.23E-04
Hpcal1	12	protein_coding	0.16	1.15E-01	0.23	1.19E-03	0.25	4.28E-03	0.29	6.14E-03
Gucy2g	19	protein_coding	0.17	1.44E-01	0.12	3.26E-01	0.27	1.91E-02	0.34	2.46E-02
Sult4a1	15	protein_coding	0.09	1.47E-01	0.36	6.01E-22	0.11	8.22E-03	0.21	4.58E-06
Tmem151a	19	protein_coding	0.10	1.57E-01	0.14	1.15E-03	0.17	9.67E-03	0.16	3.35E-02
Irf2bp2	8	protein_coding	0.13	1.59E-01	0.26	3.43E-05	0.21	1.31E-03	0.33	2.04E-06
Jsrp1	10	protein_coding	0.22	1.59E-01	0.59	5.75E-04	0.29	2.82E-02	0.71	4.58E-06
Ntf3	6	protein_coding	-0.22	1.60E-01	-0.29	1.73E-01	-0.36	4.34E-03	-0.42	1.38E-02
Hs6st2	X	protein_coding	0.13	1.62E-01	0.34	2.87E-08	0.18	1.95E-02	0.31	2.73E-04
Stard10	7	protein_coding	0.14	1.62E-01	0.64	4.21E-27	0.19	3.97E-02	0.57	6.58E-09
Ttpal	2	protein_coding	0.08	1.75E-01	0.14	6.76E-04	0.15	2.03E-03	0.20	1.44E-04
Il33	19	protein_coding	0.15	1.78E-01	0.15	8.64E-02	0.34	7.57E-04	0.55	4.82E-06
Wnt10a	1	protein_coding	0.19	1.78E-01	0.38	1.82E-03	0.29	1.54E-02	0.63	1.46E-06
Klf10	15	protein_coding	0.21	1.80E-01	1.19	4.84E-10	0.37	3.65E-03	1.08	2.14E-12
Tpm2	4	protein_coding	0.17	1.89E-01	0.08	6.54E-01	0.22	4.40E-02	0.28	3.83E-02
Per1	11	protein_coding	0.14	1.96E-01	0.71	7.21E-08	0.23	1.10E-02	0.54	8.73E-09
Mtcl1	17	protein_coding	0.13	1.98E-01	0.25	4.00E-12	0.20	1.81E-04	0.26	2.11E-07
Tmem121b	6	protein_coding	0.10	1.99E-01	0.24	6.50E-05	0.21	3.41E-05	0.17	1.22E-02
Zfp574	7	protein_coding	0.10	2.07E-01	0.29	2.03E-05	0.16	1.58E-02	0.21	2.60E-03
Fkbp5	17	protein_coding	0.20	2.12E-01	1.73	6.45E-227	-0.39	1.85E-03	0.42	2.85E-02
Sccpdh	1	protein_coding	0.10	2.20E-01	0.40	5.62E-16	0.13	1.75E-02	0.17	7.71E-03
Bub1b	2	protein_coding	-0.16	2.24E-01	-0.39	1.17E-01	-0.55	3.54E-07	-0.53	1.22E-04
Chchd10	10	protein_coding	0.11	2.54E-01	0.09	1.51E-01	0.21	2.69E-02	0.36	9.23E-04
Rangap1	15	protein_coding	0.09	2.56E-01	0.26	1.29E-19	0.13	1.99E-02	0.32	3.74E-09
Dynll2	11	protein_coding	0.07	2.68E-01	0.20	2.68E-08	0.11	1.82E-02	0.19	1.12E-03
Irf2bpl	12	protein_coding	-0.10	2.99E-01	0.18	1.27E-02	0.25	1.41E-03	0.33	3.57E-04
Igfbp6	15	protein_coding	0.15	3.36E-01	0.08	3.79E-01	0.31	7.05E-03	0.56	1.20E-05
Fem1a	17	protein_coding	0.06	3.40E-01	0.17	5.68E-04	0.14	1.19E-02	0.15	1.44E-02
Vstm2l	2	protein_coding	0.10	3.57E-01	0.25	4.26E-05	0.26	2.86E-03	0.26	3.34E-02
Amy1	3	protein_coding	-0.09	3.73E-01	-0.17	4.79E-02	-0.35	2.95E-04	-0.34	3.35E-03
Phlda1	10	protein_coding	0.09	3.78E-01	0.55	8.40E-18	0.17	3.84E-02	0.48	3.85E-10
Mboat7	7	protein_coding	0.06	3.94E-01	0.17	7.58E-07	0.13	1.55E-02	0.28	3.29E-07
Nat8l	5	protein_coding	0.06	4.04E-01	0.04	3.39E-01	0.13	2.28E-02	0.15	4.38E-02
Scrt1	15	protein_coding	0.08	4.20E-01	-0.04	4.11E-01	0.16	1.96E-02	0.15	2.88E-02
Plk3	4	protein_coding	0.10	4.72E-01	0.98	1.43E-40	0.32	1.88E-06	0.77	1.36E-25
Lbh	17	protein_coding	0.05	4.73E-01	0.28	8.17E-08	0.12	4.59E-02	0.27	8.98E-04
Stk40	4	protein_coding	0.08	4.76E-01	1.25	7.18E-26	0.26	3.85E-06	0.90	2.86E-28
Socs3	11	protein_coding	0.12	4.87E-01	0.39	1.08E-02	0.32	2.86E-03	0.47	8.21E-04
Riox1	12	protein_coding	0.09	4.89E-01	0.47	2.78E-08	0.25	3.48E-03	0.41	4.69E-05
Hcn2	10	protein_coding	0.06	5.17E-01	0.03	6.11E-01	0.17	1.78E-02	0.21	1.60E-02
Lmna	3	protein_coding	0.07	5.42E-01	0.43	5.85E-10	0.20	4.51E-03	0.41	4.96E-08
Mn1	5	protein_coding	0.09	5.54E-01	0.48	5.25E-13	0.20	1.38E-02	0.30	2.78E-05
Prr7	13	protein_coding	0.08	5.58E-01	0.34	1.10E-04	0.31	4.38E-03	0.40	4.14E-03
Ephb6	6	protein_coding	0.06	5.62E-01	0.22	6.48E-06	0.16	1.14E-03	0.18	1.48E-02
Arid3b	9	protein_coding	0.07	5.91E-01	1.14	4.23E-44	0.24	9.67E-03	0.73	8.36E-09
Slc20a1	2	protein_coding	0.03	6.00E-01	-0.03	5.43E-01	0.14	1.37E-03	0.12	2.32E-02
Klhl21	4	protein_coding	0.06	6.06E-01	0.04	7.14E-01	0.17	3.75E-02	0.22	1.27E-02
Mnt	11	protein_coding	-0.06	6.20E-01	0.04	5.38E-01	0.15	1.41E-02	0.15	4.26E-02
Alox12b	11	protein_coding	-0.08	6.21E-01	0.47	2.18E-05	-0.37	3.24E-03	0.35	4.30E-02
Hapln4	8	protein_coding	0.06	6.36E-01	0.04	4.53E-01	0.31	3.71E-05	0.42	2.52E-06
Dhrs13	11	protein_coding	0.08	6.53E-01	0.14	4.12E-01	0.25	4.51E-02	0.32	4.13E-02
Serinc2	4	protein_coding	0.07	6.60E-01	1.47	5.51E-56	0.28	1.40E-02	1.14	4.76E-21
Etnk2	1	protein_coding	-0.07	6.60E-01	0.00	9.86E-01	0.25	2.88E-02	0.43	6.30E-04
Jund	8	protein_coding	0.05	6.72E-01	0.04	7.08E-01	0.28	9.48E-03	0.29	3.63E-02
Tmem184b	15	protein_coding	0.04	7.02E-01	0.03	6.15E-01	0.17	3.98E-03	0.13	4.33E-02
Sox8	17	protein_coding	0.04	7.13E-01	0.16	2.56E-02	0.26	7.55E-03	0.30	1.15E-02
Scn4b	9	protein_coding	0.06	7.21E-01	-0.11	2.46E-01	0.26	3.15E-03	0.29	1.94E-02
Smad7	18	protein_coding	-0.04	7.21E-01	0.65	1.81E-20	0.19	1.44E-02	0.52	5.80E-11
Rps6ka4	19	protein_coding	0.03	7.82E-01	0.32	1.02E-04	0.19	1.46E-03	0.26	1.21E-03
Kcna6	6	protein_coding	0.03	7.85E-01	0.17	1.32E-04	0.18	6.88E-04	0.16	1.88E-02
Lrfn1	7	protein_coding	0.02	8.10E-01	0.27	9.46E-09	0.19	7.57E-03	0.37	1.04E-07
Adcy5	16	protein_coding	-0.02	8.39E-01	0.27	1.16E-10	0.16	2.83E-03	0.17	7.03E-03
Hcn3	3	protein_coding	-0.03	8.62E-01	0.11	1.84E-01	0.24	1.81E-04	0.17	4.46E-02
Phf13	4	protein_coding	0.03	8.79E-01	0.34	1.42E-03	0.20	3.52E-02	0.32	2.76E-03
Usp36	11	protein_coding	-0.02	8.89E-01	0.15	6.66E-03	0.12	6.94E-03	0.18	7.60E-04
Mrm1	11	protein_coding	0.02	8.89E-01	0.14	1.87E-01	0.19	2.52E-02	0.21	4.07E-02
Mrps18a	17	protein_coding	0.02	8.98E-01	0.07	3.20E-01	0.14	1.55E-02	0.22	2.41E-04
Rgcc	14	protein_coding	-0.02	9.09E-01	0.18	3.15E-02	0.26	1.11E-02	0.41	8.11E-05
Ovgp1	3	protein_coding	-0.02	9.10E-01	-0.01	9.70E-01	-0.35	6.03E-03	-0.43	1.97E-02
Vegfa	17	protein_coding	0.01	9.11E-01	0.45	3.39E-11	0.23	1.49E-03	0.25	9.38E-03
Ier5l	2	protein_coding	-0.03	9.13E-01	0.22	3.93E-01	0.37	2.52E-04	0.55	6.56E-06
Rpl22l1	3	protein_coding	-0.01	9.33E-01	0.32	1.03E-05	0.17	3.62E-02	0.33	1.06E-05
Fam43b	4	protein_coding	0.01	9.44E-01	0.87	2.43E-24	0.23	4.75E-03	0.62	5.58E-13
Vwa1	4	protein_coding	0.01	9.46E-01	0.71	1.27E-21	0.20	4.83E-02	0.46	1.53E-05
Dkkl1	7	protein_coding	0.01	9.53E-01	0.02	8.95E-01	0.29	8.55E-04	0.41	2.90E-05
Tex264	9	protein_coding	0.00	9.72E-01	-0.01	8.55E-01	0.14	4.96E-03	0.14	2.72E-02
N4bp3	11	protein_coding	0.00	9.88E-01	0.84	1.53E-16	0.22	1.38E-02	0.65	2.45E-19
Prag1	8	protein_coding	0.00	9.91E-01	0.48	1.86E-20	0.19	1.54E-02	0.38	9.17E-05
Nab2	10	protein_coding	0.00	9.92E-01	0.68	4.08E-06	0.21	1.50E-02	0.63	1.25E-16

Table S5 - Gene set B (1/5)

gene_name	gene_type	WT_light_vs_dark.l2fc	WT_light_vs_dark.padj	WT_hr12_vs_dark.l2fc	WT_hr12_vs_dark.padj	SWAP_light_vs_dark.l2fc	SWAP_light_vs_dark.padj	SWAP_hr12_vs_dark.l2fc	SWAP_hr12_vs_dark.padj
Plk5	protein_coding	-1.04	1.34E-36	-1.19	1.40E-45	-0.29	2.04E-03	-0.10	4.15E-01
Otof	protein_coding	-0.72	1.32E-22	-1.00	1.30E-66	-0.37	4.20E-06	-0.40	1.45E-05
Hap1	protein_coding	-0.44	2.27E-22	-0.26	4.75E-06	-0.19	2.27E-02	-0.13	2.25E-01
Evc2	protein_coding	-0.58	1.66E-18	-0.81	5.73E-27	-0.24	7.56E-03	-0.15	1.63E-01
Nos1	protein_coding	-0.57	2.83E-14	-0.41	1.04E-07	-0.14	4.17E-02	-0.15	1.50E-01
Matn2	protein_coding	-0.64	4.74E-14	-0.84	7.02E-26	-0.58	2.33E-09	-0.72	4.19E-09
Mapk3	protein_coding	-0.32	2.50E-13	-0.56	6.71E-41	-0.22	5.92E-05	-0.26	5.95E-05
Nnat	protein_coding	-0.44	1.82E-12	-0.25	4.38E-02	0.05	7.91E-01	0.01	9.73E-01
Syt17	protein_coding	-0.53	3.12E-12	-0.89	7.92E-48	-0.33	1.87E-05	-0.54	1.29E-08
Pcdh19	protein_coding	-0.54	9.91E-12	-0.66	2.11E-18	-0.14	1.58E-01	-0.46	1.04E-05
Pcdh8	protein_coding	-0.41	1.06E-11	-0.64	1.85E-28	-0.25	2.40E-03	-0.39	1.13E-05
Spag5	protein_coding	-0.50	1.40E-11	-1.33	2.17E-66	-0.19	5.44E-02	-0.49	2.92E-08
Gm35339	protein_coding	-0.41	2.15E-10	-0.51	2.01E-14	-0.23	1.55E-02	-0.27	2.89E-02
Pnma8b	protein_coding	-0.26	4.84E-10	-0.31	1.07E-13	-0.09	1.60E-01	-0.09	2.03E-01
Rprm	protein_coding	-0.44	6.57E-10	-1.25	2.51E-87	-0.09	2.77E-01	-0.74	1.41E-32
Rps6ka5	protein_coding	-0.33	1.47E-09	-0.57	5.72E-18	-0.23	2.52E-05	-0.42	2.93E-11
Wnt5a	protein_coding	-0.46	3.15E-09	-0.57	5.87E-11	-0.13	1.84E-01	-0.27	1.11E-02
Apaf1	protein_coding	-0.39	4.86E-09	-0.24	7.83E-04	-0.27	3.97E-03	-0.31	3.71E-03
Psrc1	protein_coding	-0.40	6.06E-09	-0.36	5.73E-06	-0.20	7.31E-02	-0.10	4.80E-01
Samd14	protein_coding	-0.28	1.38E-08	-0.17	9.65E-04	-0.30	7.52E-05	-0.30	8.75E-04
Thra	protein_coding	-0.16	1.39E-08	-0.15	5.24E-07	-0.11	2.00E-01	-0.14	1.30E-01
Cpne4	protein_coding	-0.28	1.61E-08	-0.57	5.88E-36	-0.08	2.29E-01	-0.25	2.02E-05
Cpne6	protein_coding	-0.38	2.18E-08	-0.22	1.45E-03	-0.23	1.75E-02	-0.17	2.08E-01
Srebf1	protein_coding	-0.31	2.43E-08	-0.15	2.09E-03	-0.17	9.99E-02	-0.03	8.37E-01
Timeless	protein_coding	-0.49	3.56E-08	-0.70	2.96E-11	-0.07	6.40E-01	-0.21	8.70E-02
Gpr88	protein_coding	-0.32	1.06E-07	-0.74	2.38E-66	-0.09	3.57E-01	-0.15	2.77E-01
Echdc2	protein_coding	-0.40	1.33E-07	-0.61	2.77E-12	-0.13	2.99E-01	-0.09	5.70E-01
Rasl10a	protein_coding	-0.41	1.64E-07	-0.42	5.73E-09	-0.16	1.63E-01	-0.12	3.78E-01
Rnf112	protein_coding	-0.23	1.75E-07	-0.40	9.71E-28	-0.10	1.07E-01	-0.25	3.10E-04
Tmem255a	protein_coding	-0.42	3.41E-07	-0.60	8.38E-12	-0.21	4.99E-02	-0.17	1.15E-01
Prcd	protein_coding	-0.55	4.02E-07	-0.80	2.93E-07	-0.19	1.89E-01	-0.25	1.73E-01
Adamts17	protein_coding	-0.49	4.49E-07	-0.35	3.62E-03	-0.47	6.22E-06	-0.15	4.12E-01
Grm1	protein_coding	-0.39	4.98E-07	-0.66	2.53E-15	-0.23	2.74E-05	-0.33	1.28E-05
Lzts3	protein_coding	-0.25	5.83E-07	-0.26	2.24E-10	-0.08	3.03E-01	0.06	4.53E-01
Glt8d2	protein_coding	-0.38	6.09E-07	-0.39	8.13E-08	-0.12	1.55E-01	-0.06	6.19E-01
Mmp14	protein_coding	-0.42	6.20E-07	-0.60	2.89E-15	0.04	8.20E-01	-0.32	2.79E-02
Evc	protein_coding	-0.35	7.50E-07	-0.49	3.21E-10	-0.23	1.10E-02	-0.25	1.24E-02
Kcnip2	protein_coding	-0.25	8.25E-07	-0.23	1.29E-06	-0.25	1.84E-04	-0.05	6.17E-01
Ypel4	protein_coding	-0.26	1.04E-06	-0.59	8.65E-53	-0.17	1.94E-02	-0.26	6.47E-04
Thbd	protein_coding	-0.38	1.24E-06	-0.17	3.80E-02	-0.02	9.15E-01	0.13	4.39E-01
Mgat5b	protein_coding	-0.35	1.85E-06	-0.66	2.59E-34	-0.11	1.76E-02	-0.30	2.42E-09
Diaph1	protein_coding	-0.23	1.94E-06	-0.12	3.54E-02	-0.28	7.76E-04	-0.23	2.60E-02
Fgf10	protein_coding	-0.46	2.65E-06	-0.94	1.25E-15	-0.26	2.76E-02	-0.45	7.44E-04
Pck2	protein_coding	-0.29	2.65E-06	-0.50	2.61E-14	-0.03	7.33E-01	-0.21	6.13E-03
Sec1	protein_coding	-0.48	2.71E-06	-1.00	2.44E-16	-0.01	9.52E-01	-0.30	9.38E-02
Slc18b1	protein_coding	-0.29	2.82E-06	-0.43	4.22E-11	-0.13	8.23E-02	-0.22	9.70E-03
Plppr3	protein_coding	-0.28	2.92E-06	-0.57	2.59E-23	0.08	4.32E-01	-0.18	4.39E-02
Tmcc2	protein_coding	-0.23	3.21E-06	-0.22	6.67E-06	-0.11	1.16E-01	-0.10	1.96E-01
Cbx7	protein_coding	-0.22	3.48E-06	-0.39	3.90E-15	-0.13	7.75E-02	-0.12	2.60E-01
Camkv	protein_coding	-0.19	3.74E-06	-0.31	1.47E-18	-0.07	2.84E-01	-0.11	1.09E-01
Ptpn14	protein_coding	-0.40	4.72E-06	-0.35	2.21E-06	-0.11	3.91E-01	-0.09	5.02E-01
Adamts2	protein_coding	-0.45	4.72E-06	-0.36	2.41E-02	-0.37	3.11E-04	-0.28	3.88E-02
Arhgef19	protein_coding	-0.31	5.61E-06	-0.20	4.76E-03	0.04	7.85E-01	-0.09	5.84E-01
Bhlhe22	protein_coding	-0.32	6.64E-06	-0.30	1.20E-06	-0.23	9.16E-04	-0.18	1.93E-02
Slc1a6	protein_coding	-0.40	6.67E-06	-0.52	3.23E-07	-0.15	1.65E-01	-0.20	1.29E-01
Cul9	protein_coding	-0.25	7.04E-06	-0.51	1.27E-37	0.02	8.18E-01	-0.18	1.30E-03
Tmem80	protein_coding	-0.24	1.11E-05	-0.33	7.07E-07	0.03	7.72E-01	-0.16	9.23E-02
Islr	protein_coding	-0.29	1.49E-05	-0.49	9.17E-09	0.04	8.20E-01	0.10	5.65E-01
Vstm4	protein_coding	-0.46	1.80E-05	-0.68	1.27E-08	0.00	9.95E-01	-0.34	5.38E-02
Kirrel3	protein_coding	-0.27	1.85E-05	-0.23	2.85E-05	0.02	8.88E-01	-0.18	2.56E-02
Rskr	protein_coding	-0.41	2.23E-05	-1.52	2.69E-69	0.04	8.12E-01	-0.42	1.88E-04
Mttp	protein_coding	-0.33	2.84E-05	-0.31	4.65E-04	-0.06	5.92E-01	-0.09	4.84E-01
Lman2l	protein_coding	-0.27	2.96E-05	-0.20	2.03E-03	-0.07	4.54E-01	0.11	3.31E-01
Jph4	protein_coding	-0.24	3.03E-05	-0.42	1.72E-28	-0.05	5.43E-01	-0.26	9.89E-06
Smoc2	protein_coding	-0.40	3.11E-05	-0.45	2.60E-07	-0.27	7.71E-03	0.05	7.77E-01
Smarca2	protein_coding	-0.21	3.39E-05	-0.45	5.44E-22	-0.11	1.99E-02	-0.11	5.45E-02
Lypd1	protein_coding	-0.24	3.81E-05	-0.13	3.00E-02	-0.10	1.53E-01	-0.02	8.16E-01
Pdgfrb	protein_coding	-0.26	3.81E-05	-0.44	2.10E-16	0.06	5.64E-01	-0.17	1.14E-01
Crocc	protein_coding	-0.37	4.21E-05	-0.76	1.19E-27	0.01	9.35E-01	-0.32	4.35E-03
Baiap3	protein_coding	-0.39	4.24E-05	-0.37	1.08E-03	-0.19	1.91E-01	-0.32	7.45E-02
Col23a1	protein_coding	-0.33	4.48E-05	-0.52	4.86E-14	-0.18	4.55E-02	-0.42	4.94E-06
Ncdn	protein_coding	-0.22	4.90E-05	-0.14	1.36E-02	-0.14	9.21E-02	-0.05	6.47E-01
Celsr1	protein_coding	-0.36	4.91E-05	-0.39	6.95E-06	0.18	1.17E-01	-0.12	4.19E-01
Gm1043	protein_coding	-0.41	5.36E-05	-0.32	2.69E-04	-0.13	3.54E-01	0.00	9.98E-01
Ift122	protein_coding	-0.21	5.82E-05	-0.26	4.44E-07	-0.10	6.90E-02	-0.16	9.18E-03
Pde1b	protein_coding	-0.17	6.68E-05	-0.10	8.73E-03	-0.06	5.19E-01	0.02	8.97E-01
Ngb	protein_coding	-0.38	6.74E-05	-0.86	1.02E-15	-0.20	5.63E-02	-0.37	1.12E-03
Egfem1	protein_coding	-0.33	7.32E-05	-0.41	8.95E-06	-0.22	1.41E-02	-0.34	6.81E-04
Col8a1	protein_coding	-0.45	9.34E-05	-1.10	1.07E-23	-0.04	8.13E-01	-0.49	6.84E-05
Pkia	protein_coding	-0.17	1.05E-04	-0.17	4.69E-05	-0.12	9.43E-02	-0.27	5.66E-05
Slc29a1	protein_coding	-0.27	1.33E-04	-0.39	4.75E-08	-0.03	8.51E-01	-0.11	3.45E-01
Pnck	protein_coding	-0.19	1.39E-04	-0.54	7.21E-32	-0.13	3.10E-02	-0.39	2.32E-09
Ly6h	protein_coding	-0.26	1.52E-04	-0.44	1.69E-22	0.04	7.29E-01	-0.09	3.63E-01
Mxra7	protein_coding	-0.34	1.72E-04	-0.44	5.42E-07	-0.05	7.28E-01	0.00	9.98E-01
Dixdc1	protein_coding	-0.18	1.84E-04	-0.16	4.05E-03	-0.21	5.32E-04	-0.12	1.97E-01
Azin2	protein_coding	-0.25	1.87E-04	-0.53	4.57E-16	0.03	8.33E-01	-0.31	1.18E-03
Crispld1	protein_coding	-0.43	2.22E-04	-0.58	3.79E-08	-0.18	1.63E-01	-0.08	6.90E-01
Tcerg1l	protein_coding	-0.35	2.29E-04	-0.39	1.96E-04	-0.32	6.05E-05	-0.18	9.85E-02
Mturn	protein_coding	-0.18	2.34E-04	-0.30	3.34E-17	-0.07	1.43E-01	-0.17	2.34E-03
Arid5b	protein_coding	-0.27	2.40E-04	-0.17	6.39E-03	-0.19	3.79E-02	0.01	9.53E-01
Pold1	protein_coding	-0.33	2.64E-04	-0.33	5.98E-04	-0.03	8.65E-01	-0.04	8.19E-01
Napepld	protein_coding	-0.23	2.68E-04	-0.22	1.79E-03	-0.31	1.27E-05	-0.15	1.80E-01
Nbeal2	protein_coding	-0.31	2.81E-04	-0.17	2.80E-02	-0.13	2.62E-01	-0.19	1.37E-01
Ifi27	protein_coding	-0.26	3.07E-04	-0.22	2.72E-03	-0.13	2.46E-01	-0.09	5.71E-01
Aldh1a2	protein_coding	-0.36	3.14E-04	-0.58	1.20E-09	0.12	4.47E-01	0.00	9.88E-01
Pigv	protein_coding	-0.30	3.35E-04	-0.55	1.43E-09	0.01	9.65E-01	-0.28	1.57E-02
Fxyd6	protein_coding	-0.18	3.37E-04	-0.45	4.66E-18	-0.03	7.43E-01	-0.26	3.97E-05
Nelfb	protein_coding	-0.21	3.62E-04	-0.37	3.71E-16	0.00	9.99E-01	-0.14	3.81E-02
Slc13a4	protein_coding	-0.33	3.86E-04	-0.52	8.16E-08	0.08	6.13E-01	0.03	9.03E-01
Ankrd46	protein_coding	-0.15	3.93E-04	-0.23	3.81E-10	-0.07	1.40E-01	-0.12	1.66E-02
Itga8	protein_coding	-0.37	4.32E-04	-0.36	1.16E-04	-0.36	2.95E-04	-0.38	2.31E-03

Table S5 (2/5)

Col5a1	protein_coding	-0.29	4.39E-04	-0.39	4.14E-14	-0.10	1.82E-01	-0.26	2.03E-04
Cc2d2a	protein_coding	-0.27	4.86E-04	-0.65	7.56E-23	-0.04	5.90E-01	-0.33	5.43E-06
Iqcc	protein_coding	-0.25	5.15E-04	-0.37	3.69E-08	-0.15	3.53E-02	-0.37	6.64E-06
Mroh7	protein_coding	-0.36	5.32E-04	-0.43	5.27E-04	-0.05	7.82E-01	-0.01	9.56E-01
Adat1	protein_coding	-0.29	5.43E-04	-0.29	1.85E-03	-0.07	5.22E-01	-0.12	3.59E-01
Pik3ip1	protein_coding	-0.21	5.87E-04	-0.61	2.29E-21	0.01	9.08E-01	-0.30	9.55E-05
Bbs12	protein_coding	-0.37	5.94E-04	-0.42	1.33E-03	-0.07	6.72E-01	-0.20	2.50E-01
Bmp6	protein_coding	-0.35	6.37E-04	-0.41	8.75E-07	0.10	5.35E-01	0.01	9.63E-01
Marcks	protein_coding	-0.15	6.84E-04	-0.41	2.60E-40	0.02	8.67E-01	-0.35	1.39E-06
Tprkb	protein_coding	-0.23	6.88E-04	-0.47	4.12E-25	0.00	9.99E-01	-0.23	4.04E-03
Erich3	protein_coding	-0.25	6.92E-04	-0.60	9.44E-16	0.00	9.99E-01	-0.36	1.04E-05
St6galnac6	protein_coding	-0.17	7.09E-04	-0.37	1.97E-25	-0.07	2.80E-01	-0.23	2.25E-04
Oplah	protein_coding	-0.24	7.17E-04	-0.24	2.63E-04	-0.05	7.24E-01	-0.01	9.42E-01
Exosc5	protein_coding	-0.27	7.45E-04	-0.16	4.93E-02	0.00	9.99E-01	-0.09	4.49E-01
Cldn5	protein_coding	-0.33	8.02E-04	-0.65	1.26E-26	0.16	2.55E-01	-0.30	3.51E-02
Zfp358	protein_coding	-0.20	8.07E-04	-0.26	1.19E-05	0.05	6.57E-01	-0.08	4.18E-01
Cep63	protein_coding	-0.19	8.34E-04	-0.34	1.25E-09	0.02	8.91E-01	-0.04	7.45E-01
Efcab12	protein_coding	-0.28	8.34E-04	-0.51	7.78E-09	-0.19	7.40E-02	-0.28	2.49E-02
Tmtc4	protein_coding	-0.26	8.57E-04	-0.49	1.13E-09	-0.13	1.62E-01	-0.20	4.26E-02
Ring1	protein_coding	-0.20	8.64E-04	-0.40	2.77E-13	0.03	8.07E-01	-0.07	5.67E-01
Cchcr1	protein_coding	-0.35	8.74E-04	-0.88	1.19E-17	0.11	3.59E-01	-0.34	5.80E-03
Elk1	protein_coding	-0.24	8.74E-04	-0.23	1.48E-04	-0.11	1.13E-01	-0.06	5.26E-01
Ctxn2	protein_coding	-0.33	9.00E-04	-0.50	2.05E-05	-0.03	8.54E-01	0.00	9.99E-01
Thap3	protein_coding	-0.28	9.99E-04	-0.64	1.19E-13	-0.12	2.13E-01	-0.39	1.56E-04
Tmem260	protein_coding	-0.22	1.00E-03	-0.29	8.72E-06	-0.06	5.65E-01	-0.09	3.36E-01
Vtn	protein_coding	-0.22	1.01E-03	-0.34	1.26E-10	0.14	2.36E-01	0.01	9.74E-01
Bnip5	protein_coding	-0.31	1.09E-03	-1.06	1.08E-25	0.10	3.79E-01	-0.38	8.21E-04
Prelp	protein_coding	-0.28	1.12E-03	-0.39	3.01E-07	0.08	6.54E-01	0.18	3.99E-01
Sfi1	protein_coding	-0.26	1.13E-03	-0.42	1.29E-12	-0.01	9.31E-01	-0.25	9.56E-03
Hlf	protein_coding	-0.16	1.14E-03	-0.47	3.10E-34	-0.15	3.37E-02	-0.20	8.75E-03
Cib2	protein_coding	-0.25	1.18E-03	-0.59	7.53E-17	-0.01	9.69E-01	-0.10	4.28E-01
Aldh2	protein_coding	-0.20	1.19E-03	-0.38	1.71E-13	0.03	8.71E-01	0.08	5.66E-01
Slc6a20a	protein_coding	-0.32	1.21E-03	-0.35	8.55E-05	0.05	7.71E-01	-0.23	4.96E-02
Asgr1	protein_coding	-0.41	1.22E-03	-0.70	3.06E-05	0.10	5.41E-01	-0.22	3.38E-01
Rnf32	protein_coding	-0.25	1.39E-03	-0.31	1.06E-04	-0.24	7.14E-03	-0.15	2.30E-01
Arhgap4	protein_coding	-0.33	1.39E-03	-0.30	1.44E-02	-0.08	5.70E-01	0.04	8.28E-01
Cdkl4	protein_coding	-0.26	1.39E-03	-0.54	9.34E-14	-0.10	3.10E-01	-0.23	7.75E-03
Car11	protein_coding	-0.17	1.45E-03	-0.47	1.59E-24	0.03	8.03E-01	-0.04	7.60E-01
Tpd52l1	protein_coding	-0.29	1.50E-03	-0.21	2.74E-02	0.00	9.96E-01	-0.01	9.59E-01
Igfbp5	protein_coding	-0.28	1.52E-03	-0.63	9.09E-64	0.06	5.51E-01	-0.20	6.08E-02
Tapbp	protein_coding	-0.26	1.65E-03	-0.30	3.05E-05	0.04	7.26E-01	-0.12	1.59E-01
Wdr6	protein_coding	-0.21	1.74E-03	-0.56	6.75E-35	-0.03	7.80E-01	-0.46	8.87E-10
Rnf207	protein_coding	-0.30	1.77E-03	-0.70	3.49E-12	-0.11	4.01E-01	-0.23	1.11E-01
Dcn	protein_coding	-0.25	1.82E-03	-0.33	2.79E-04	0.05	7.96E-01	-0.19	2.31E-01
Sema4f	protein_coding	-0.18	1.83E-03	-0.32	3.32E-13	0.01	8.79E-01	-0.13	1.52E-02
Samm50	protein_coding	-0.15	1.87E-03	-0.09	2.95E-02	-0.06	2.07E-01	-0.01	8.46E-01
Ccdc159	protein_coding	-0.28	1.90E-03	-0.43	4.91E-09	0.07	5.76E-01	-0.19	1.07E-01
Pygb	protein_coding	-0.12	2.05E-03	-0.18	3.78E-07	0.00	9.95E-01	-0.10	1.47E-01
Ar	protein_coding	-0.27	2.10E-03	-0.33	2.94E-04	-0.25	1.11E-03	-0.17	1.09E-01
Pot1a	protein_coding	-0.21	2.18E-03	-0.26	1.01E-04	-0.05	6.16E-01	-0.15	6.34E-02
Mme	protein_coding	-0.33	2.29E-03	-0.95	8.04E-22	-0.16	1.83E-01	-0.43	3.76E-04
Isyna1	protein_coding	-0.26	2.38E-03	-0.34	1.07E-07	0.08	5.06E-01	0.06	6.82E-01
Trim45	protein_coding	-0.26	2.40E-03	-0.56	2.45E-09	0.05	6.87E-01	-0.19	1.00E-01
Anxa6	protein_coding	-0.16	2.51E-03	-0.28	4.32E-12	-0.02	8.48E-01	-0.15	6.48E-02
Cdkn1c	protein_coding	-0.33	2.71E-03	-0.63	5.38E-08	0.15	3.38E-01	-0.10	6.50E-01
Vwa3a	protein_coding	-0.32	2.74E-03	-1.06	4.94E-25	-0.06	6.28E-01	-0.72	4.14E-15
Sft2d2	protein_coding	-0.16	2.78E-03	-0.11	4.23E-02	-0.04	5.77E-01	0.00	9.69E-01
Itm2c	protein_coding	-0.17	2.95E-03	-0.25	6.12E-13	-0.06	4.86E-01	-0.08	3.24E-01
Tle6	protein_coding	-0.33	3.07E-03	-0.84	4.17E-10	0.08	6.39E-01	0.05	8.40E-01
Pomt1	protein_coding	-0.21	3.11E-03	-0.29	1.68E-06	-0.13	9.93E-02	-0.19	6.62E-02
Cage1	protein_coding	-0.35	3.11E-03	-0.59	1.76E-05	-0.17	1.81E-01	-0.30	4.19E-02
Calhm5	protein_coding	-0.28	3.14E-03	-0.38	2.66E-04	-0.20	4.98E-02	-0.01	9.50E-01
Smc2	protein_coding	-0.26	3.16E-03	-0.38	4.29E-05	-0.19	2.85E-02	-0.24	1.31E-02
Rasd2	protein_coding	-0.25	3.30E-03	-0.22	1.01E-02	-0.15	1.08E-01	0.08	5.33E-01
Bad	protein_coding	-0.23	3.33E-03	-0.22	7.13E-04	-0.04	7.57E-01	-0.19	3.60E-02
Abcd4	protein_coding	-0.22	3.39E-03	-0.28	1.16E-04	-0.05	6.53E-01	-0.16	1.66E-01
Katnal2	protein_coding	-0.33	3.47E-03	-0.40	2.95E-03	-0.13	4.06E-01	-0.11	5.76E-01
Cpt1c	protein_coding	-0.12	3.58E-03	-0.28	5.62E-17	-0.05	3.78E-01	-0.16	1.16E-02
Pcdhb12	protein_coding	-0.26	3.60E-03	-0.63	6.92E-13	-0.03	8.33E-01	-0.11	3.33E-01
Fuz	protein_coding	-0.20	3.73E-03	-0.53	7.14E-14	0.09	5.27E-01	-0.08	6.40E-01
Cygb	protein_coding	-0.16	3.83E-03	-0.18	4.57E-04	-0.21	6.02E-03	-0.09	4.50E-01
Magee2	protein_coding	-0.29	4.00E-03	-0.65	2.08E-10	-0.12	3.79E-01	-0.43	1.36E-03
Tap2	protein_coding	-0.27	4.01E-03	-0.43	4.31E-05	0.08	5.17E-01	-0.08	6.07E-01
Rreb1	protein_coding	-0.34	4.05E-03	-0.15	3.65E-02	-0.39	3.47E-07	-0.04	8.26E-01
Plxna3	protein_coding	-0.23	4.31E-03	-0.47	4.12E-21	-0.02	8.67E-01	-0.22	1.20E-02
Atp2b4	protein_coding	-0.18	4.52E-03	-0.18	1.87E-06	0.01	9.65E-01	-0.06	5.88E-01
Tmem43	protein_coding	-0.16	4.57E-03	-0.22	1.16E-04	-0.10	1.60E-01	-0.17	3.94E-03
Gstm7	protein_coding	-0.25	4.58E-03	-0.19	3.94E-02	-0.08	5.73E-01	0.11	5.26E-01
Specc1	protein_coding	-0.15	4.59E-03	-0.16	2.23E-03	-0.11	1.32E-01	-0.05	6.32E-01
Synpr	protein_coding	-0.21	4.60E-03	-0.16	1.62E-02	-0.09	2.48E-01	-0.16	5.90E-02
Myt1	protein_coding	-0.29	4.62E-03	-0.56	1.68E-11	-0.09	3.35E-01	-0.50	1.22E-11
Dync2h1	protein_coding	-0.24	4.81E-03	-0.23	1.34E-03	-0.18	2.96E-02	-0.15	1.27E-01
Tradd	protein_coding	-0.34	5.11E-03	-0.51	1.43E-04	0.02	9.02E-01	-0.22	1.93E-01
Sord	protein_coding	-0.23	5.11E-03	-0.47	2.51E-09	-0.07	4.61E-01	-0.20	5.16E-02
Cnnm3	protein_coding	-0.14	5.33E-03	-0.26	1.73E-08	-0.08	3.21E-01	-0.24	2.69E-03
Mccc2	protein_coding	-0.20	5.35E-03	-0.53	1.22E-13	0.04	6.96E-01	-0.23	2.04E-02
Nat14	protein_coding	-0.19	5.38E-03	-0.19	1.75E-03	0.08	4.32E-01	0.11	2.87E-01
Hdac10	protein_coding	-0.22	5.50E-03	-0.41	6.83E-09	-0.02	8.93E-01	-0.27	1.20E-03
Pcdhb11	protein_coding	-0.31	5.50E-03	-0.32	1.03E-02	-0.07	6.85E-01	-0.19	2.36E-01
Tnip2	protein_coding	-0.20	5.54E-03	-0.31	3.81E-06	-0.04	7.35E-01	-0.17	5.51E-02
Abcc5	protein_coding	-0.17	5.56E-03	-0.20	1.69E-04	-0.08	2.05E-01	-0.10	1.63E-01
Myoc	protein_coding	-0.21	5.60E-03	-0.45	8.05E-11	0.12	4.86E-01	0.19	4.07E-01
Wdr41	protein_coding	-0.16	5.65E-03	-0.26	5.59E-06	0.00	9.91E-01	-0.15	3.82E-02
Cd83	protein_coding	-0.25	5.67E-03	-0.67	8.11E-15	-0.03	8.63E-01	-0.14	2.62E-01
Cyth1	protein_coding	-0.12	5.94E-03	-0.21	2.04E-06	-0.13	5.76E-02	-0.29	2.04E-05
Chst12	protein_coding	-0.19	6.23E-03	-0.50	4.20E-12	-0.16	4.47E-02	-0.32	1.04E-04
Icam5	protein_coding	-0.15	6.27E-03	-0.27	7.67E-09	-0.01	9.65E-01	-0.12	1.58E-01
Rlbp1	protein_coding	-0.19	6.41E-03	-0.48	2.17E-13	0.02	9.02E-01	-0.08	5.89E-01
Amz1	protein_coding	-0.27	6.54E-03	-0.40	8.49E-05	0.00	9.84E-01	-0.35	6.69E-03
AW549877	protein_coding	-0.15	6.64E-03	-0.28	1.27E-10	-0.07	1.41E-01	-0.28	5.62E-12

Table S5 (3/5)

Mllt6	protein_coding	-0.18	6.65E-03	-0.22	1.39E-11	-0.03	5.85E-01	-0.08	6.72E-02
2810459M11	protein_coding	-0.22	6.68E-03	-0.46	6.43E-09	0.16	2.65E-01	-0.24	1.27E-01
Smo	protein_coding	-0.22	7.11E-03	-0.20	5.32E-03	0.06	5.73E-01	-0.01	9.46E-01
Crebrf	protein_coding	-0.18	7.44E-03	-0.30	5.46E-06	-0.21	8.99E-03	-0.22	2.02E-02
Jrk	protein_coding	-0.24	7.56E-03	-0.33	5.78E-04	0.14	2.81E-01	-0.04	8.51E-01
Zscan18	protein_coding	-0.18	7.58E-03	-0.31	8.55E-07	-0.03	7.56E-01	-0.22	1.10E-02
Fam126a	protein_coding	-0.19	7.59E-03	-0.15	2.29E-02	-0.11	2.96E-01	-0.27	1.70E-02
Pcdhga12	protein_coding	-0.23	7.66E-03	-0.52	5.33E-14	0.04	7.81E-01	-0.20	3.16E-02
Uvssa	protein_coding	-0.24	7.69E-03	-0.51	2.76E-10	-0.11	2.99E-01	-0.46	1.51E-05
Wdr66	protein_coding	-0.28	8.06E-03	-0.56	3.50E-08	-0.07	6.09E-01	-0.24	5.96E-02
Tbata	protein_coding	-0.29	8.17E-03	-0.51	1.82E-04	-0.24	4.32E-02	-0.46	1.88E-04
Zkscan16	protein_coding	-0.26	8.20E-03	-0.62	2.18E-13	-0.16	1.93E-01	-0.38	3.71E-03
Abhd8	protein_coding	-0.21	8.26E-03	-0.25	5.98E-08	0.06	6.05E-01	0.03	8.38E-01
Rgl1	protein_coding	-0.14	8.28E-03	-0.14	2.19E-03	-0.13	1.28E-02	-0.04	5.74E-01
Gprin1	protein_coding	-0.14	8.29E-03	-0.10	2.61E-02	-0.07	3.81E-01	-0.16	4.26E-02
Brd9	protein_coding	-0.12	8.32E-03	-0.24	2.07E-09	-0.03	8.12E-01	-0.07	4.76E-01
Nicn1	protein_coding	-0.15	8.33E-03	-0.35	1.41E-20	-0.06	4.12E-01	-0.17	2.76E-03
Tbc1d32	protein_coding	-0.20	8.36E-03	-0.27	1.29E-02	-0.18	5.26E-02	-0.30	2.62E-03
Zfp512	protein_coding	-0.14	8.41E-03	-0.25	2.49E-08	0.00	9.80E-01	-0.18	1.15E-03
Jph1	protein_coding	-0.26	8.48E-03	-0.35	3.67E-05	-0.14	1.08E-01	-0.13	2.25E-01
Rftn1	protein_coding	-0.29	8.50E-03	-0.30	6.16E-03	-0.01	9.76E-01	0.00	9.88E-01
Col12a1	protein_coding	-0.28	8.72E-03	-0.55	9.16E-18	0.03	8.95E-01	-0.25	1.10E-01
Zfp395	protein_coding	-0.25	8.89E-03	-0.57	6.05E-11	0.03	8.79E-01	-0.33	8.26E-03
Met	protein_coding	-0.26	9.11E-03	-0.92	2.31E-45	-0.04	7.68E-01	-0.79	3.76E-25
Slc35c2	protein_coding	-0.16	9.27E-03	-0.15	2.69E-03	-0.05	6.46E-01	-0.12	1.65E-01
Kctd8	protein_coding	-0.25	9.28E-03	-0.46	2.06E-05	-0.16	1.33E-01	-0.22	8.93E-02
Cc2d1a	protein_coding	-0.13	9.57E-03	-0.14	6.33E-03	-0.10	1.16E-01	-0.14	5.76E-02
Ascc1	protein_coding	-0.22	9.64E-03	-0.27	1.54E-03	-0.10	3.98E-01	-0.14	2.31E-01
Tbc1d16	protein_coding	-0.17	9.84E-03	-0.17	4.14E-03	-0.15	4.29E-02	-0.30	1.76E-03
Dguok	protein_coding	-0.19	9.84E-03	-0.50	1.66E-10	-0.05	6.07E-01	-0.20	2.18E-02
Gm5148	protein_coding	-0.29	9.93E-03	-1.05	5.72E-20	-0.05	7.60E-01	-0.34	2.15E-02
Mapk7	protein_coding	-0.18	9.95E-03	-0.32	7.68E-09	0.05	6.18E-01	-0.20	5.20E-02
Extl2	protein_coding	-0.15	9.97E-03	-0.36	2.03E-17	-0.02	8.31E-01	-0.14	1.87E-02
Lepr	protein_coding	-0.31	9.97E-03	-0.61	3.65E-08	0.10	4.94E-01	-0.39	1.01E-02
Prkdc	protein_coding	-0.22	1.04E-02	-0.49	1.02E-11	-0.02	8.42E-01	-0.36	8.36E-08
Man2c1	protein_coding	-0.15	1.04E-02	-0.23	1.77E-07	-0.03	7.88E-01	-0.12	6.42E-02
Mpdz	protein_coding	-0.17	1.07E-02	-0.14	3.02E-02	-0.10	2.00E-01	0.09	3.87E-01
Orai3	protein_coding	-0.21	1.10E-02	-0.24	4.26E-03	-0.01	9.48E-01	-0.04	8.10E-01
Phyhip	protein_coding	-0.11	1.14E-02	-0.20	7.04E-08	-0.09	4.14E-02	-0.01	9.37E-01
Tef	protein_coding	-0.13	1.16E-02	-0.29	3.31E-18	-0.10	3.06E-01	-0.14	1.88E-01
Crebl2	protein_coding	-0.15	1.16E-02	-0.13	2.13E-02	-0.12	1.15E-01	-0.03	7.75E-01
Ppcdc	protein_coding	-0.21	1.18E-02	-0.35	1.03E-05	0.06	5.34E-01	-0.05	7.15E-01
Fhl1	protein_coding	-0.13	1.18E-02	-0.33	3.69E-12	-0.07	2.14E-01	-0.26	1.89E-07
Gucy1a1	protein_coding	-0.13	1.22E-02	-0.82	1.82E-51	0.00	9.86E-01	-0.36	2.79E-05
Hebp1	protein_coding	-0.21	1.24E-02	-0.35	7.38E-07	0.09	5.22E-01	-0.07	6.41E-01
Atp2a3	protein_coding	-0.29	1.25E-02	-0.65	9.11E-11	0.13	3.26E-01	-0.22	1.46E-01
Nlrx1	protein_coding	-0.23	1.26E-02	-0.77	1.99E-18	0.02	9.06E-01	-0.48	2.95E-05
Bbs2	protein_coding	-0.17	1.27E-02	-0.47	6.06E-15	0.00	9.72E-01	-0.27	1.02E-03
Htra3	protein_coding	-0.29	1.28E-02	-0.88	2.47E-19	0.15	2.90E-01	-0.28	9.85E-02
Ccdc61	protein_coding	-0.27	1.30E-02	-0.33	9.54E-04	0.11	3.49E-01	0.00	9.86E-01
Sh3bp4	protein_coding	-0.18	1.30E-02	-0.24	1.01E-03	-0.09	2.84E-01	-0.36	6.22E-07
H1f2	protein_coding	-0.26	1.31E-02	-1.04	1.39E-38	0.19	1.81E-01	-0.12	6.42E-01
Trpm2	protein_coding	-0.20	1.32E-02	-0.51	4.85E-23	0.07	2.88E-01	-0.19	4.02E-03
Cln3	protein_coding	-0.18	1.33E-02	-0.28	1.82E-04	-0.04	7.21E-01	-0.12	1.92E-01
Pcdhb17	protein_coding	-0.19	1.33E-02	-0.44	4.47E-09	0.04	7.42E-01	-0.03	8.01E-01
Tspo	protein_coding	-0.32	1.33E-02	-0.53	6.68E-04	0.06	7.42E-01	0.20	3.13E-01
Lta4h	protein_coding	-0.14	1.33E-02	-0.20	9.11E-05	-0.05	5.10E-01	-0.13	9.63E-02
Vstm2a	protein_coding	-0.16	1.33E-02	-0.43	1.45E-22	-0.09	9.83E-02	-0.28	1.02E-08
Ap1g2	protein_coding	-0.23	1.35E-02	-0.54	1.54E-09	-0.30	1.43E-02	-0.72	5.94E-07
Nelfcd	protein_coding	-0.15	1.36E-02	-0.33	7.86E-12	0.02	8.58E-01	-0.12	8.19E-02
Bcat2	protein_coding	-0.20	1.38E-02	-0.18	2.61E-02	-0.09	3.99E-01	-0.01	9.65E-01
Vps51	protein_coding	-0.17	1.38E-02	-0.22	3.63E-05	0.07	4.01E-01	-0.05	5.90E-01
H3f3a	protein_coding	-0.16	1.38E-02	-0.19	1.88E-04	0.01	9.06E-01	-0.15	6.02E-02
Pwwp3a	protein_coding	-0.14	1.39E-02	-0.43	1.81E-16	0.07	3.57E-01	-0.24	5.46E-04
Slc12a9	protein_coding	-0.17	1.40E-02	-0.26	1.14E-06	-0.01	9.46E-01	-0.27	2.15E-04
Nfatc2	protein_coding	-0.20	1.41E-02	-0.19	3.10E-02	0.03	7.85E-01	-0.04	7.63E-01
Aasdh	protein_coding	-0.19	1.44E-02	-0.33	4.74E-05	-0.04	7.74E-01	-0.10	3.37E-01
Pofut1	protein_coding	-0.16	1.45E-02	-0.43	8.76E-15	0.01	9.03E-01	-0.37	9.78E-09
Cars2	protein_coding	-0.19	1.45E-02	-0.25	1.51E-03	-0.20	4.61E-03	-0.17	4.04E-02
Npy2r	protein_coding	-0.33	1.47E-02	-0.37	4.88E-02	-0.51	2.71E-06	-0.33	1.10E-01
Arhgap17	protein_coding	-0.19	1.47E-02	-0.22	5.90E-03	-0.14	1.37E-01	-0.27	7.46E-03
Ccn3	protein_coding	-0.17	1.47E-02	-0.61	1.74E-34	0.05	6.53E-01	-0.33	2.95E-05
Tspan17	protein_coding	-0.20	1.50E-02	-0.64	7.84E-26	0.11	2.81E-01	-0.11	3.83E-01
Id2	protein_coding	-0.12	1.51E-02	-0.24	2.29E-12	-0.12	1.49E-01	-0.14	1.05E-01
Cdk5rap1	protein_coding	-0.26	1.53E-02	-0.28	1.70E-02	-0.26	1.27E-02	-0.23	7.34E-02
Caly	protein_coding	-0.14	1.54E-02	-0.45	2.04E-24	0.02	8.91E-01	-0.09	3.68E-01
Fmod	protein_coding	-0.24	1.57E-02	-0.25	5.70E-04	-0.09	5.55E-01	0.04	8.48E-01
Unc93b1	protein_coding	-0.19	1.57E-02	-0.31	8.25E-05	0.05	6.97E-01	-0.22	4.88E-02
Aldh4a1	protein_coding	-0.22	1.59E-02	-0.28	5.96E-04	0.01	9.16E-01	-0.12	2.15E-01
Slc6a13	protein_coding	-0.33	1.59E-02	-0.59	4.30E-09	0.11	5.18E-01	-0.04	8.80E-01
Padi2	protein_coding	-0.21	1.60E-02	-0.25	1.67E-04	0.10	4.90E-01	-0.09	6.06E-01
Sox2	protein_coding	-0.19	1.65E-02	-0.24	8.53E-05	0.06	5.80E-01	-0.12	3.09E-01
Ntn5	protein_coding	-0.26	1.69E-02	-0.93	5.18E-42	0.08	6.27E-01	0.12	4.49E-01
Hmg20a	protein_coding	-0.11	1.69E-02	-0.21	4.61E-07	-0.09	2.10E-01	-0.10	2.05E-01
Rad9b	protein_coding	-0.26	1.70E-02	-0.41	4.19E-04	-0.11	4.19E-01	-0.39	1.63E-03
Adck2	protein_coding	-0.18	1.70E-02	-0.44	2.13E-08	0.05	5.23E-01	-0.23	4.71E-03
Cerkl	protein_coding	-0.31	1.72E-02	-0.67	1.54E-05	-0.11	5.01E-01	-0.17	3.50E-01
Dus3l	protein_coding	-0.14	1.75E-02	-0.19	3.56E-04	-0.04	6.25E-01	-0.10	1.46E-01
Crtc1	protein_coding	-0.16	1.77E-02	-0.12	2.41E-03	-0.16	2.92E-02	-0.10	2.93E-01
Gsta4	protein_coding	-0.16	1.77E-02	-0.47	1.03E-13	-0.01	9.59E-01	-0.08	5.67E-01
Bbs9	protein_coding	-0.17	1.77E-02	-0.42	3.15E-09	-0.13	9.43E-02	-0.15	1.23E-01
Cmtm6	protein_coding	-0.17	1.80E-02	-0.26	9.63E-05	0.10	2.97E-01	-0.18	4.33E-02
Atg13	protein_coding	-0.11	1.81E-02	-0.21	6.41E-08	-0.08	2.88E-01	-0.14	7.00E-02
Aifm3	protein_coding	-0.21	1.82E-02	-0.42	1.68E-18	-0.02	9.03E-01	-0.02	9.18E-01
Prnp	protein_coding	-0.13	1.83E-02	-0.22	2.85E-10	-0.09	1.33E-01	-0.12	6.71E-02
Sash1	protein_coding	-0.20	1.83E-02	-0.33	1.73E-11	0.01	9.16E-01	-0.31	1.35E-04
Rpusd1	protein_coding	-0.15	1.83E-02	-0.22	4.77E-06	-0.04	7.23E-01	0.03	7.92E-01
Pdzrn4	protein_coding	-0.30	1.86E-02	-0.99	8.01E-15	-0.08	5.40E-01	-0.65	5.68E-10
Obsl1	protein_coding	-0.17	1.97E-02	-0.20	9.33E-04	0.00	9.76E-01	-0.15	9.09E-02
Phf20	protein_coding	-0.13	1.97E-02	-0.19	3.94E-04	-0.10	5.93E-02	-0.14	1.99E-02

Table S5 (4/5)

Nfs1	protein_coding	-0.14	1.97E-02	-0.21	6.15E-05	-0.02	8.41E-01	-0.09	2.97E-01
Gpr6	protein_coding	-0.31	2.01E-02	-1.74	3.02E-27	-0.02	9.42E-01	-0.67	1.63E-05
Faim2	protein_coding	-0.15	2.03E-02	-0.40	1.24E-26	0.00	9.75E-01	-0.01	9.06E-01
Phf1	protein_coding	-0.19	2.04E-02	-0.42	2.27E-15	-0.01	9.43E-01	-0.15	6.19E-02
Pgghg	protein_coding	-0.25	2.07E-02	-0.46	1.38E-05	0.07	6.82E-01	0.04	8.56E-01
Thbs2	protein_coding	-0.26	2.07E-02	-0.54	9.25E-14	-0.07	4.87E-01	-0.40	4.98E-05
Ebf4	protein_coding	-0.21	2.07E-02	-0.43	8.29E-07	-0.11	1.83E-01	-0.40	5.20E-07
Rcn1	protein_coding	-0.18	2.09E-02	-0.58	1.24E-14	0.01	9.51E-01	-0.22	9.18E-02
Akap12	protein_coding	-0.19	2.09E-02	-0.43	5.79E-14	0.03	8.29E-01	-0.09	3.73E-01
Slc27a1	protein_coding	-0.16	2.10E-02	-0.15	2.17E-03	0.07	5.46E-01	0.04	7.75E-01
H2bc21	protein_coding	-0.22	2.10E-02	-0.33	4.05E-04	-0.09	5.05E-01	-0.06	6.97E-01
Lhfpl2	protein_coding	-0.21	2.10E-02	-0.27	4.51E-04	-0.15	1.43E-01	-0.26	3.55E-02
Dcaf6	protein_coding	-0.09	2.11E-02	-0.23	1.34E-09	-0.15	3.03E-03	-0.16	8.99E-03
Cdkl1	protein_coding	-0.25	2.11E-02	-0.97	3.28E-24	0.05	6.23E-01	-0.41	8.91E-08
Sptbn4	protein_coding	-0.17	2.11E-02	-0.30	1.33E-08	0.02	8.13E-01	-0.09	2.09E-01
Trim17	protein_coding	-0.25	2.11E-02	-0.32	4.35E-03	-0.08	5.40E-01	0.01	9.71E-01
Igsf8	protein_coding	-0.20	2.14E-02	-0.61	7.02E-36	0.08	4.46E-01	-0.24	5.14E-03
Slc16a11	protein_coding	-0.21	2.22E-02	-0.76	5.19E-26	0.00	9.85E-01	-0.36	2.28E-04
Wdr24	protein_coding	-0.15	2.25E-02	-0.21	5.59E-04	-0.09	2.38E-01	-0.20	4.61E-03
Dhtkd1	protein_coding	-0.23	2.26E-02	-0.57	5.23E-13	0.08	4.20E-01	-0.27	1.07E-02
Pcdhga6	protein_coding	-0.23	2.29E-02	-0.28	1.23E-02	-0.03	8.38E-01	-0.04	8.13E-01
Prr13	protein_coding	-0.17	2.29E-02	-0.29	2.99E-06	0.00	9.99E-01	0.05	6.49E-01
Klc4	protein_coding	-0.21	2.30E-02	-0.43	2.21E-10	-0.03	7.84E-01	-0.12	1.47E-01
Wwox	protein_coding	-0.19	2.30E-02	-0.29	5.12E-04	0.05	7.41E-01	-0.05	7.56E-01
Abhd14b	protein_coding	-0.19	2.32E-02	-0.59	2.21E-15	-0.12	1.81E-01	-0.36	2.58E-04
Adamts16	protein_coding	-0.19	2.32E-02	-0.71	8.51E-17	0.03	8.23E-01	-0.41	1.27E-04
Mical1	protein_coding	-0.20	2.34E-02	-0.37	5.56E-06	0.05	7.63E-01	-0.18	2.41E-01
Hsf4	protein_coding	-0.26	2.35E-02	-0.45	3.43E-06	0.18	1.14E-01	0.44	1.10E-04
Nr3c2	protein_coding	-0.30	2.43E-02	-0.31	3.74E-02	-0.24	1.38E-02	-0.43	3.44E-05
Hps1	protein_coding	-0.16	2.46E-02	-0.51	2.15E-16	0.23	3.39E-02	-0.10	5.49E-01
Zfp316	protein_coding	-0.14	2.47E-02	-0.50	4.21E-15	0.08	3.56E-01	-0.28	3.23E-03
Gaa	protein_coding	-0.12	2.47E-02	-0.22	2.69E-07	-0.03	6.33E-01	-0.02	7.51E-01
Thbs3	protein_coding	-0.19	2.47E-02	-0.33	7.90E-07	-0.25	5.25E-05	-0.50	1.89E-08
Gga1	protein_coding	-0.13	2.49E-02	-0.14	8.77E-04	0.06	4.70E-01	0.04	5.98E-01
Gjb2	protein_coding	-0.23	2.49E-02	-0.52	8.06E-11	0.12	4.62E-01	-0.06	7.81E-01
Aldh3a2	protein_coding	-0.13	2.54E-02	-0.23	7.95E-07	-0.02	8.47E-01	-0.09	1.29E-01
Immp2l	protein_coding	-0.29	2.61E-02	-0.40	1.32E-02	0.01	9.82E-01	0.05	8.40E-01
Zic4	protein_coding	-0.25	2.61E-02	-0.36	4.74E-03	0.12	4.02E-01	-0.07	7.11E-01
Cep164	protein_coding	-0.17	2.62E-02	-0.33	2.44E-07	0.08	3.03E-01	-0.22	5.04E-03
Rnasel	protein_coding	-0.19	2.62E-02	-0.64	3.48E-17	-0.09	3.95E-01	-0.38	1.54E-05
Tmem209	protein_coding	-0.14	2.63E-02	-0.36	1.75E-08	0.03	7.44E-01	-0.14	9.90E-02
Cacna1c	protein_coding	-0.21	2.64E-02	-0.20	7.31E-03	-0.22	1.09E-02	-0.20	7.46E-02
Elac1	protein_coding	-0.15	2.66E-02	-0.42	2.11E-13	-0.09	2.60E-01	-0.23	6.82E-03
Sh2d3c	protein_coding	-0.21	2.72E-02	-0.74	2.95E-16	0.16	1.42E-01	-0.33	1.07E-02
Ezh1	protein_coding	-0.13	2.72E-02	-0.26	6.54E-11	-0.14	4.45E-02	-0.17	4.46E-02
Ptgds	protein_coding	-0.27	2.73E-02	-0.24	4.41E-02	0.00	9.82E-01	0.20	1.07E-01
Epor	protein_coding	-0.27	2.74E-02	-0.44	9.98E-04	0.04	8.31E-01	0.32	1.07E-02
Gid4	protein_coding	-0.11	2.75E-02	-0.17	3.58E-04	-0.07	1.92E-01	-0.03	6.79E-01
Slitrk5	protein_coding	-0.16	2.76E-02	-0.31	5.64E-07	-0.09	1.38E-01	-0.14	2.76E-02
Sdr42e1	protein_coding	-0.24	2.76E-02	-0.43	5.60E-05	0.04	7.83E-01	-0.03	8.66E-01
Rbm11	protein_coding	-0.25	2.79E-02	-0.77	5.07E-11	0.10	5.04E-01	-0.36	2.71E-02
Dmrtc1a	protein_coding	-0.28	2.81E-02	-0.65	1.99E-06	-0.01	9.64E-01	-0.26	1.11E-01
Smim17	protein_coding	-0.19	2.83E-02	-0.47	4.24E-08	-0.06	6.52E-01	-0.29	1.28E-03
Mindy4	protein_coding	-0.23	2.83E-02	-0.37	2.98E-05	-0.07	5.49E-01	-0.29	2.58E-03
Grid1	protein_coding	-0.11	2.84E-02	-0.10	3.42E-02	-0.07	3.50E-01	-0.04	6.86E-01
Pcmtd2	protein_coding	-0.10	2.89E-02	-0.15	1.74E-04	-0.08	2.99E-01	-0.08	3.57E-01
Rgs14	protein_coding	-0.18	2.91E-02	-0.12	2.41E-02	0.01	9.06E-01	-0.11	2.39E-01
Pcdhga3	protein_coding	-0.20	2.94E-02	-0.20	1.25E-02	-0.25	3.37E-02	-0.37	6.32E-04
Hjurp	protein_coding	-0.12	3.02E-02	-0.15	1.20E-03	0.05	7.21E-01	-0.20	3.50E-01
Qrfpr	protein_coding	-0.27	3.12E-02	-1.19	3.74E-21	0.14	3.52E-01	-0.26	1.09E-01
Aph1c	protein_coding	-0.23	3.12E-02	-0.59	1.70E-09	-0.05	7.18E-01	-0.23	3.17E-02
Gm10037	protein_coding	-0.23	3.12E-02	-0.37	1.42E-03	-0.07	6.41E-01	-0.16	2.84E-01
Hes6	protein_coding	-0.21	3.12E-02	-0.57	1.61E-09	0.11	4.43E-01	-0.29	4.80E-02
Ddr1	protein_coding	-0.20	3.18E-02	-0.32	4.28E-07	0.11	3.38E-01	-0.30	3.08E-03
Pea15a	protein_coding	-0.11	3.18E-02	-0.17	1.90E-07	0.00	9.89E-01	-0.05	4.29E-01
Foxp2	protein_coding	-0.20	3.18E-02	-0.40	4.99E-07	-0.03	8.46E-01	-0.09	5.91E-01
Tbc1d9b	protein_coding	-0.10	3.20E-02	-0.12	1.43E-02	0.00	9.70E-01	-0.04	4.84E-01
Kank2	protein_coding	-0.21	3.20E-02	-0.31	3.06E-04	0.10	3.76E-01	0.03	8.69E-01
Cdh1	protein_coding	-0.28	3.23E-02	-0.67	2.51E-10	0.01	9.59E-01	-0.16	4.20E-01
Ptchd1	protein_coding	-0.25	3.24E-02	-0.27	6.19E-03	0.03	8.79E-01	-0.07	6.82E-01
Carmil3	protein_coding	-0.15	3.26E-02	-0.22	4.48E-06	-0.07	2.92E-01	-0.23	8.94E-03
Nyap1	protein_coding	-0.15	3.30E-02	-0.16	4.24E-04	-0.01	8.76E-01	-0.14	1.98E-02
Cep250	protein_coding	-0.14	3.32E-02	-0.19	1.55E-04	-0.04	7.01E-01	-0.15	9.23E-02
Coq8a	protein_coding	-0.20	3.34E-02	-0.46	1.80E-12	-0.13	1.63E-01	-0.31	1.65E-03
Polm	protein_coding	-0.21	3.38E-02	-0.46	7.60E-07	-0.01	9.26E-01	-0.28	6.00E-03
Dcdc2b	protein_coding	-0.22	3.42E-02	-0.34	6.68E-04	-0.28	3.27E-02	-0.23	3.07E-01
Lor	protein_coding	-0.28	3.43E-02	-0.41	8.65E-03	0.05	8.18E-01	-0.17	4.37E-01
Dtx3	protein_coding	-0.11	3.43E-02	-0.12	4.16E-03	0.00	9.97E-01	-0.03	7.01E-01
Pcolce	protein_coding	-0.24	3.46E-02	-0.37	1.30E-03	0.12	4.23E-01	-0.06	7.84E-01
Ehbp1l1	protein_coding	-0.18	3.51E-02	-0.34	1.12E-07	0.01	9.22E-01	-0.27	9.17E-04
Macrod1	protein_coding	-0.23	3.53E-02	-0.23	4.97E-02	0.02	9.22E-01	0.06	7.53E-01
Ap5z1	protein_coding	-0.18	3.54E-02	-0.16	4.84E-03	0.06	5.27E-01	-0.10	3.09E-01
Lrrc61	protein_coding	-0.16	3.56E-02	-0.46	1.16E-14	0.02	8.98E-01	-0.23	2.48E-02
Oat	protein_coding	-0.12	3.56E-02	-0.11	2.20E-02	0.03	7.44E-01	0.02	8.27E-01
Rasal1	protein_coding	-0.18	3.59E-02	-0.51	1.94E-20	-0.03	6.14E-01	-0.31	1.73E-07
Nedd4	protein_coding	-0.10	3.60E-02	-0.11	2.35E-03	-0.08	6.50E-02	-0.07	2.03E-01
Vwc2l	protein_coding	-0.22	3.62E-02	-0.38	2.39E-05	-0.03	8.41E-01	0.01	9.58E-01
Heyl	protein_coding	-0.24	3.62E-02	-0.39	3.24E-04	-0.01	9.72E-01	-0.24	1.86E-01
Cbx1	protein_coding	-0.13	3.62E-02	-0.12	3.31E-02	-0.05	5.60E-01	0.01	8.87E-01
Slc8b1	protein_coding	-0.20	3.64E-02	-0.43	1.52E-05	0.04	8.33E-01	-0.22	1.38E-01
Tatdn3	protein_coding	-0.15	3.64E-02	-0.28	3.98E-06	-0.03	8.15E-01	-0.21	2.63E-02
Smoc1	protein_coding	-0.18	3.69E-02	-0.19	2.96E-02	0.01	9.33E-01	-0.01	9.77E-01
Jun	protein_coding	-0.26	3.70E-02	-0.27	4.48E-02	-0.09	4.40E-01	-0.10	2.82E-01
Mtfp1	protein_coding	-0.11	3.70E-02	-0.14	9.05E-03	-0.06	3.60E-01	-0.10	8.63E-02
Cacna1e	protein_coding	-0.21	3.71E-02	-0.27	7.73E-03	-0.09	4.11E-01	-0.16	1.63E-01
Col6a2	protein_coding	-0.23	3.73E-02	-0.40	7.65E-06	-0.22	4.53E-02	-0.38	1.37E-03
Kitl	protein_coding	-0.19	3.78E-02	-0.73	9.70E-27	-0.10	1.92E-01	-0.26	8.51E-05
Col11a2	protein_coding	-0.15	3.82E-02	-0.17	1.08E-03	0.14	2.70E-01	-0.28	7.44E-03
Med16	protein_coding	-0.14	3.83E-02	-0.27	1.85E-07	-0.01	9.34E-01	-0.09	2.89E-01
Ypel1	protein_coding	-0.19	3.84E-02	-0.82	3.42E-41	-0.11	1.13E-01	-0.60	2.13E-22

Table S5 (5/5)

Atp10d	protein_coding	-0.22	3.94E-02	-0.59	4.10E-08	0.01	9.65E-01	-0.17	1.97E-01
Trappc6a	protein_coding	-0.26	3.94E-02	-0.57	2.10E-06	0.09	5.05E-01	-0.17	2.81E-01
Epop	protein_coding	-0.22	4.02E-02	-0.15	1.57E-02	0.06	5.86E-01	0.24	2.97E-02
Rtel1	protein_coding	-0.14	4.03E-02	-0.37	3.18E-08	0.06	5.72E-01	-0.19	8.03E-02
Samhd1	protein_coding	-0.16	4.04E-02	-0.22	2.21E-03	-0.17	3.67E-02	-0.24	3.29E-03
Bbc3	protein_coding	-0.26	4.04E-02	-0.80	2.04E-08	0.13	3.56E-01	-0.52	6.30E-05
Dvl2	protein_coding	-0.14	4.07E-02	-0.23	5.18E-04	0.01	9.15E-01	-0.23	1.12E-03
2700049A03R	protein_coding	-0.19	4.13E-02	-0.59	7.69E-13	-0.09	4.10E-01	-0.28	7.65E-03
Dnal4	protein_coding	-0.13	4.17E-02	-0.16	4.82E-03	-0.04	6.21E-01	-0.09	2.47E-01
Nudt2	protein_coding	-0.20	4.24E-02	-0.48	7.14E-08	0.08	5.57E-01	-0.04	8.36E-01
Brme1	protein_coding	-0.27	4.28E-02	-0.76	5.10E-06	0.07	6.88E-01	-0.31	6.94E-02
Tmem9	protein_coding	-0.13	4.31E-02	-0.21	2.80E-04	-0.06	5.33E-01	-0.17	4.95E-02
Apeh	protein_coding	-0.16	4.35E-02	-0.33	1.57E-05	-0.04	7.46E-01	-0.06	6.23E-01
Mxra8	protein_coding	-0.21	4.43E-02	-0.44	2.50E-06	0.10	5.22E-01	-0.15	3.93E-01
Pan2	protein_coding	-0.13	4.43E-02	-0.29	1.49E-07	-0.04	6.16E-01	-0.19	4.23E-03
Acat3	protein_coding	-0.26	4.44E-02	-0.89	5.96E-10	0.15	3.11E-01	-0.10	6.34E-01
Vps39	protein_coding	-0.10	4.45E-02	-0.21	1.07E-08	-0.10	1.54E-02	-0.12	1.90E-02
Rwdd3	protein_coding	-0.27	4.49E-02	-0.83	2.28E-10	-0.10	4.47E-01	-0.29	3.94E-02
Atp6v0e	protein_coding	-0.14	4.49E-02	-0.16	1.97E-02	0.08	4.85E-01	-0.08	5.69E-01
Stk32c	protein_coding	-0.15	4.50E-02	-0.24	2.42E-06	-0.01	8.93E-01	0.07	3.96E-01
Emilin1	protein_coding	-0.27	4.50E-02	-0.69	7.35E-08	0.16	2.79E-01	-0.23	2.37E-01
Notch2	protein_coding	-0.22	4.52E-02	-0.15	8.94E-03	-0.02	8.86E-01	-0.17	5.94E-02
Gabpb2	protein_coding	-0.16	4.54E-02	-0.23	5.26E-05	-0.04	7.12E-01	-0.05	6.94E-01
Rhpn1	protein_coding	-0.17	4.56E-02	-0.25	1.27E-03	-0.07	5.36E-01	-0.03	8.18E-01
Abcc10	protein_coding	-0.19	4.57E-02	-0.24	1.92E-03	0.00	9.82E-01	-0.16	1.53E-01
Gm266	protein_coding	-0.27	4.58E-02	-0.82	1.40E-07	0.04	8.47E-01	-0.29	1.47E-01
Bicral	protein_coding	-0.13	4.67E-02	-0.11	1.53E-02	-0.08	3.29E-01	-0.06	5.26E-01
Coa6	protein_coding	-0.20	4.72E-02	-0.28	2.26E-03	0.18	9.46E-02	0.09	5.55E-01
Rpap1	protein_coding	-0.13	4.72E-02	-0.25	1.57E-05	-0.02	8.06E-01	-0.18	6.39E-03
Dcaf17	protein_coding	-0.16	4.72E-02	-0.38	3.60E-07	0.02	8.69E-01	-0.31	2.57E-04
Castor2	protein_coding	-0.12	4.77E-02	-0.20	7.94E-05	-0.20	4.98E-02	-0.22	8.24E-02
Abcb8	protein_coding	-0.13	4.77E-02	-0.21	1.37E-04	0.06	5.34E-01	-0.10	2.86E-01
Cfap65	protein_coding	-0.21	4.80E-02	-0.56	9.44E-09	0.06	7.21E-01	-0.15	3.23E-01
Vps72	protein_coding	-0.15	4.81E-02	-0.21	9.16E-04	-0.03	7.70E-01	-0.03	7.81E-01
Slc39a3	protein_coding	-0.11	4.81E-02	-0.10	4.87E-02	0.03	6.40E-01	-0.03	6.64E-01
Mlh3	protein_coding	-0.16	4.82E-02	-0.26	2.74E-04	-0.01	9.46E-01	-0.09	2.67E-01
Prr16	protein_coding	-0.18	4.85E-02	-0.66	1.54E-17	-0.01	9.76E-01	-0.14	3.83E-01
Map2k6	protein_coding	-0.24	4.87E-02	-0.37	2.61E-03	-0.22	3.97E-02	-0.21	1.12E-01
Egflam	protein_coding	-0.21	4.87E-02	-0.48	6.26E-05	0.07	6.25E-01	-0.16	3.14E-01
Cgn	protein_coding	-0.23	4.96E-02	-0.39	1.03E-03	0.07	6.51E-01	-0.36	1.21E-02
Ptov1	protein_coding	-0.13	4.96E-02	-0.18	1.12E-05	0.04	6.72E-01	-0.06	5.79E-01
Syt4	protein_coding	-0.11	4.98E-02	-0.21	6.34E-09	-0.05	5.84E-01	-0.02	8.74E-01
Bmp1	protein_coding	-0.11	5.93E-02	0.06	2.02E-01	-0.21	1.30E-02	-0.21	4.24E-02
Rapgef6	protein_coding	-0.18	6.63E-02	-0.03	7.46E-01	-0.19	1.68E-03	-0.18	2.38E-02
Fyco1	protein_coding	-0.16	7.13E-02	-0.21	1.39E-04	-0.18	4.04E-02	-0.20	3.51E-02
Slc4a7	protein_coding	-0.18	7.56E-02	-0.03	8.25E-01	-0.22	5.16E-03	-0.23	3.78E-02
Inpp5k	protein_coding	-0.12	7.69E-02	-0.26	1.05E-08	-0.20	2.77E-02	-0.30	3.08E-03
Ccdc85a	protein_coding	-0.16	7.74E-02	-0.10	2.51E-01	-0.20	4.83E-03	-0.22	1.16E-02
Stxbp4	protein_coding	-0.14	7.96E-02	-0.31	7.70E-07	-0.14	4.42E-02	-0.16	3.35E-02
Gng7	protein_coding	-0.13	9.62E-02	0.07	2.52E-01	-0.16	1.44E-02	-0.16	4.57E-02
Metap1d	protein_coding	-0.12	1.04E-01	-0.15	1.48E-02	-0.15	4.45E-03	-0.19	7.91E-03
Asic4	protein_coding	-0.15	1.06E-01	-0.15	1.11E-01	-0.22	3.86E-03	-0.20	2.97E-02
Htr1a	protein_coding	-0.14	1.07E-01	-0.50	6.10E-11	-0.23	1.06E-02	-0.42	1.76E-07
Neurod1	protein_coding	-0.18	1.13E-01	-0.31	3.55E-05	-0.30	2.03E-05	-0.31	1.21E-04
Armt1	protein_coding	-0.13	1.18E-01	-0.22	1.61E-03	-0.15	3.52E-02	-0.16	4.84E-02
N4bp2	protein_coding	-0.19	1.23E-01	-0.08	4.76E-01	-0.24	2.23E-02	-0.35	3.73E-03
Calcoco1	protein_coding	-0.10	1.36E-01	-0.37	3.57E-17	-0.20	1.75E-02	-0.35	1.36E-04
Scn3a	protein_coding	-0.15	1.42E-01	-0.20	1.96E-03	-0.23	4.82E-03	-0.27	2.76E-03
Dnajc10	protein_coding	-0.08	1.49E-01	-0.15	9.58E-05	-0.10	2.13E-02	-0.14	6.40E-03
Hdac1	protein_coding	-0.10	1.77E-01	-0.14	3.80E-02	-0.27	1.80E-03	-0.31	1.67E-03
Nudt13	protein_coding	-0.13	1.80E-01	-0.44	9.44E-09	-0.17	1.98E-02	-0.37	7.60E-07
Rapgefl1	protein_coding	-0.08	2.01E-01	-0.13	2.16E-03	-0.13	1.38E-02	-0.13	3.52E-02
Ablim3	protein_coding	-0.13	2.09E-01	-0.17	1.78E-03	-0.32	1.75E-06	-0.33	3.08E-05
Ndst3	protein_coding	-0.12	2.30E-01	-0.09	2.93E-01	-0.22	3.57E-03	-0.19	4.24E-02
1500011B03R	protein_coding	-0.07	2.91E-01	-0.20	2.78E-05	-0.10	3.64E-02	-0.13	9.26E-03
Rfx3	protein_coding	-0.16	3.21E-01	-0.05	6.56E-01	-0.28	2.11E-04	-0.19	4.89E-02
Nfib	protein_coding	-0.10	3.45E-01	-0.16	3.37E-02	-0.19	3.56E-03	-0.33	1.27E-05
Msh3	protein_coding	-0.09	3.47E-01	-0.11	1.59E-01	-0.18	1.54E-02	-0.21	1.23E-02
Grhl1	protein_coding	-0.10	4.03E-01	-0.24	3.86E-03	-0.22	6.16E-03	-0.29	4.88E-03
Sema5a	protein_coding	-0.12	4.91E-01	0.08	7.10E-01	-0.25	3.00E-03	-0.31	1.01E-02
Klf6	protein_coding	0.08	4.91E-01	-0.30	1.46E-04	-0.20	7.82E-03	-0.28	6.94E-04
Lrrn3	protein_coding	-0.06	5.26E-01	-0.18	5.76E-03	-0.15	1.61E-02	-0.12	3.18E-02
Usp40	protein_coding	-0.06	5.55E-01	-0.17	1.80E-02	-0.17	8.78E-03	-0.16	4.40E-02
Ddc	protein_coding	-0.08	5.93E-01	0.00	9.80E-01	-0.31	6.57E-04	-0.33	6.72E-03
Cacnb2	protein_coding	-0.05	6.18E-01	-0.33	1.65E-06	-0.18	1.27E-03	-0.21	3.72E-03
Eml6	protein_coding	-0.05	6.26E-01	-0.13	3.74E-02	-0.18	3.72E-02	-0.22	1.85E-02
Sphkap	protein_coding	-0.05	6.67E-01	-0.14	2.49E-02	-0.22	2.89E-04	-0.28	1.65E-04
Plekhg1	protein_coding	0.05	6.82E-01	0.13	3.65E-02	-0.18	5.26E-03	-0.31	2.77E-02
Rnpc3	protein_coding	-0.05	7.16E-01	-0.14	5.55E-02	-0.28	4.31E-04	-0.26	1.04E-02
Mcm7	protein_coding	-0.05	7.28E-01	-0.09	4.13E-01	-0.18	2.17E-02	-0.19	4.00E-02
B3galt2	protein_coding	-0.03	8.18E-01	-0.51	1.22E-05	-0.22	7.41E-03	-0.40	9.35E-09
Ilk	protein_coding	0.02	8.39E-01	-0.09	4.49E-02	-0.11	2.27E-02	-0.15	2.10E-02
Glrx	protein_coding	-0.03	8.59E-01	-0.22	7.08E-03	-0.22	4.84E-03	-0.25	4.75E-03
Flrt3	protein_coding	0.02	9.12E-01	-0.29	1.76E-03	-0.26	2.07E-05	-0.22	6.63E-04
Stag2	protein_coding	0.01	9.54E-01	0.00	9.72E-01	-0.21	1.16E-04	-0.15	1.84E-02
Pdcd4	protein_coding	0.00	9.66E-01	-0.27	1.08E-06	-0.16	4.17E-02	-0.29	5.11E-04
Ppp1r14c	protein_coding	-0.01	9.69E-01	-0.10	2.30E-01	-0.17	2.24E-02	-0.25	6.00E-03
Sparc	protein_coding	0.00	9.76E-01	0.12	1.33E-01	-0.21	2.24E-02	-0.25	1.23E-02
Krt9	protein_coding	0.00	9.93E-01	-0.14	3.63E-01	-0.27	1.74E-02	-0.34	2.70E-02

Table S6 – Genes from Gene set A that are differentially expressed under standard light in Swap

gene_name	WT_light_avg_fpkm	SWAP_light_avg_fpkm	light_SWAP_vs_WT.l2fc	light_SWAP_vs_WT.padj
Pim1	1.50	0.96	-0.35	5.97E-05
Scube1	11.91	9.07	-0.33	5.09E-07
Homer1	39.82	27.54	-0.28	3.75E-03
Egr3	54.18	35.35	-0.26	7.08E-03
Sult1a1	5.16	3.73	-0.25	1.13E-02
Rnd1	17.56	14.03	-0.25	2.17E-03
Tnfrsf12a	3.37	2.36	-0.25	1.35E-02
Npnt	17.89	14.83	-0.24	1.12E-04
Dapk2	1.70	1.23	-0.23	3.54E-02
Mamld1	10.24	8.62	-0.22	6.15E-04
Fosb	4.81	2.78	-0.22	1.55E-02
Epha10	15.06	12.38	-0.22	1.64E-02
Med8	12.76	10.70	-0.21	9.73E-03
Tamalin	20.65	17.69	-0.21	1.17E-03
Slc9a5	12.56	10.33	-0.20	4.34E-02
Asap2	10.40	8.96	-0.20	1.62E-03
AI593442	43.84	38.25	-0.20	1.04E-06
Inhba	2.47	1.27	-0.20	1.81E-02
Zfpm1	8.72	7.42	-0.20	2.12E-02
Adam19	5.52	4.80	-0.20	6.15E-04
Chrm2	2.91	2.49	-0.19	2.61E-02
Fbxw7	61.48	54.06	-0.19	5.69E-06
Arhgap31	5.99	5.13	-0.19	3.12E-02
Fmnl1	41.72	36.15	-0.19	1.11E-02
St8sia5	16.62	14.56	-0.18	2.44E-03
Neto2	14.27	12.50	-0.18	8.73E-03
R3hdm1	64.91	56.85	-0.17	2.87E-02
Actn4	46.19	41.02	-0.17	2.98E-04
Lhfp	8.13	7.18	-0.17	1.91E-02
Fscn1	96.08	85.51	-0.16	1.63E-02
Vip	18.66	16.57	-0.16	2.87E-02
Wee1	7.16	6.35	-0.16	4.59E-02
Ina	68.59	61.28	-0.16	1.42E-02
Actn1	28.63	25.61	-0.16	1.05E-02
Sulf2	34.38	31.06	-0.15	1.85E-04
Mapk4	18.72	16.79	-0.15	4.46E-02
Osbpl10	16.51	14.88	-0.15	1.15E-02
Rnf126	36.57	32.98	-0.15	7.22E-03
Lingo1	125.79	112.86	-0.15	4.34E-02
Med15	22.63	20.47	-0.14	2.67E-02
Ccl27a	59.35	53.79	-0.14	1.65E-02
Cacng3	53.50	48.53	-0.14	8.67E-03
Sel1l3	23.14	21.01	-0.14	8.43E-03
Sik3	29.17	26.64	-0.14	2.05E-04
Cacng2	19.05	17.37	-0.14	9.91E-03
Stx1b	166.54	152.15	-0.13	8.50E-03
Plcl2	18.92	17.30	-0.13	3.66E-02
Nlk	33.87	31.03	-0.13	4.95E-02
Zmynd8	27.69	25.40	-0.13	1.89E-02
Itpk1	19.37	17.76	-0.13	4.92E-02
Dlgap4	65.89	60.73	-0.12	6.40E-03
Cdk5r2	121.30	111.80	-0.12	1.94E-02
Map4k3	21.11	19.52	-0.12	1.85E-02
Wac	19.85	18.38	-0.12	1.07E-02
Asic2	20.66	19.28	-0.11	3.47E-02
Ndrg3	147.47	138.65	-0.10	5.10E-03
Smarcd1	55.62	52.26	-0.10	2.40E-02
Slc25a25	15.42	17.09	0.12	5.00E-02
Ache	17.03	19.24	0.14	4.95E-02
Doc2a	22.09	25.13	0.15	3.30E-02
Mthfd1l	5.24	6.03	0.16	4.44E-02
Rbm3	19.55	22.59	0.17	9.86E-03
Irf2bpl	14.61	17.23	0.18	2.18E-02
Nab2	13.50	16.08	0.20	8.73E-03
Crhbp	11.13	13.56	0.21	1.19E-02
Ier5	21.87	27.02	0.21	2.86E-02
Serinc2	2.64	3.46	0.22	3.56E-02
Il33	5.14	6.48	0.22	1.55E-02
Phf13	5.57	6.86	0.24	1.15E-03
Sik1	2.88	3.83	0.24	1.72E-02
Stk40	9.12	11.30	0.26	1.44E-06
Gpr3	2.80	3.69	0.28	5.27E-04
Per1	27.00	36.01	0.32	1.04E-06

Table S7 (1/2) – Genes from Gene set A that are differentially expressed under dark in Swap

gene_name	WT_dark_avg_fpkm	SWAP_dark_avg_fpkm	dark_SWAP_vs_WT.l2fc	dark_SWAP_vs_WT.padj
Ccn1	1.91	4.31	0.70	1.25E-11
Asb11	1.60	2.48	0.47	1.49E-05
Serpinb8	1.21	2.05	0.46	1.26E-04
Npas4	5.41	16.29	0.44	6.30E-05
Smim3	1.29	2.02	0.41	9.07E-04
Rbm3	17.41	24.26	0.41	7.00E-06
Fkbp5	6.95	13.40	0.41	1.18E-03
Atp10a	2.11	3.20	0.40	7.88E-04
Cort	8.85	11.90	0.38	2.90E-05
Camk1g	12.52	16.79	0.37	3.47E-05
Bdnf	4.69	6.35	0.36	1.75E-04
Dusp1	9.18	14.77	0.36	5.74E-03
Mthfd1l	3.55	5.09	0.36	2.73E-03
Rhbdl3	4.18	5.96	0.36	3.30E-03
Klhl40	1.98	2.87	0.35	4.81E-03
Net1	6.37	8.29	0.34	8.99E-05
Hif3a	0.77	1.89	0.34	3.33E-03
Adipor2	12.20	15.79	0.33	2.05E-04
Gimap6	0.74	1.05	0.33	1.04E-02
Gbe1	2.31	2.99	0.33	2.01E-04
Gm14295	2.24	2.92	0.32	7.52E-04
Phf21b	3.84	5.01	0.32	2.72E-03
Igfn1	2.57	3.29	0.31	2.14E-03
Ptgs2	1.67	2.36	0.31	2.02E-02
Ism1	1.29	1.76	0.31	1.58E-02
Zbtb1	1.27	1.62	0.31	8.37E-04
Fam107a	106.37	133.99	0.30	1.46E-03
Fzd4	1.89	2.38	0.30	2.26E-03
Fos	6.58	16.55	0.30	8.25E-03
Crhbp	9.28	11.58	0.29	1.80E-04
Pdlim1	2.02	2.57	0.29	4.29E-03
Ptpn3	8.23	10.12	0.29	1.33E-05
Zbtb16	9.04	12.82	0.29	3.63E-02
Scg2	63.43	77.41	0.29	3.25E-08
Nptx2	9.47	11.85	0.29	2.60E-03
Slc2a1	22.64	30.46	0.28	3.64E-02
Mfsd2a	8.58	12.07	0.28	4.51E-02
Ccdc6	7.98	9.90	0.28	4.81E-03
Fst	0.74	1.03	0.27	4.95E-02
Notch4	0.87	1.11	0.27	2.37E-02
Cry1	4.37	5.74	0.27	4.23E-02
Sult1a1	4.09	6.77	0.27	4.51E-02
Hmgb3	6.63	8.20	0.27	3.47E-03
Ppp1r15a	4.33	5.29	0.27	2.85E-03
Mpp3	9.95	11.97	0.27	1.59E-05
Mxi1	15.34	18.62	0.26	1.65E-03
Rgs2	11.92	14.39	0.26	2.09E-04
Coq10b	8.34	10.15	0.26	3.30E-03
Paqr8	25.02	30.31	0.26	2.73E-03
Dbndd2	12.90	15.74	0.26	7.87E-03
Strip2	3.30	4.03	0.26	1.07E-02
Klf9	50.26	60.46	0.26	7.23E-04
Arc	35.02	62.87	0.26	4.69E-02
Prmt8	22.83	27.39	0.26	3.95E-04
Ache	14.22	17.03	0.25	6.44E-04
Mamld1	8.28	10.22	0.25	3.39E-02
Arhgef3	21.18	25.25	0.25	9.57E-04
Smim43	12.69	15.27	0.25	9.65E-03
Tac1	3.81	4.71	0.25	4.23E-02
Utp4	7.83	9.32	0.25	2.26E-03
Slc35f3	7.90	9.43	0.24	5.00E-03
Chfr	14.36	17.45	0.24	2.91E-02
Sgms1	6.74	8.08	0.24	1.09E-02
2210408I21Rik	1.90	2.32	0.24	3.95E-02
Nfkbia	9.20	11.17	0.24	3.77E-02
Tfrc	23.19	27.53	0.23	6.77E-03
Rimbp2	28.63	34.39	0.23	2.89E-02
Per1	24.59	29.69	0.23	3.99E-02
Amy1	9.25	11.17	0.23	4.48E-02
Ptprj	13.95	16.31	0.23	1.90E-04
Gng4	12.34	14.58	0.23	7.63E-03
Phospho2	5.88	7.01	0.23	3.31E-02
Scrt2	3.08	3.65	0.22	2.97E-02
Tob2	6.13	7.17	0.22	1.06E-02
Nell1	3.78	4.50	0.22	3.71E-02
Mtmr4	17.77	20.69	0.22	6.50E-03
Lsm11	5.39	6.30	0.22	1.21E-02
Abcg2	3.71	4.33	0.21	1.33E-02
Vgf	50.69	58.93	0.21	1.21E-02
Timm9	13.07	15.15	0.21	1.25E-02
Chrm2	2.40	2.81	0.21	5.00E-02
Plaa	10.53	12.22	0.21	1.33E-02
Mat2a	49.22	57.05	0.21	1.49E-02
Nkrf	7.56	8.73	0.21	2.95E-03
Mapk4	14.30	16.55	0.21	1.43E-02
Pptc7	10.27	11.87	0.21	9.83E-03
Grsf1	27.78	31.97	0.21	2.26E-03
Sgk1	17.79	20.47	0.20	7.06E-03
Ncbp1	16.95	19.49	0.20	7.06E-03
Hip1	9.85	11.41	0.20	3.31E-02
Slc24a2	59.47	68.91	0.20	3.19E-02
Stx3	10.61	12.27	0.20	2.30E-02
Actr3b	45.18	51.79	0.20	1.99E-03
Rnd3	4.08	4.73	0.20	2.08E-02
Slco1a4	13.25	15.32	0.20	3.36E-02
Ranbp9	23.99	27.67	0.20	2.74E-02
Smc3	9.70	11.13	0.20	1.25E-02
Gphn	19.23	21.87	0.20	2.81E-04
Map9	21.64	24.71	0.20	6.10E-03

Table S7 (2/2)

Magi2	17.69	20.36	0.19	4.43E-02
Bcor	5.22	6.00	0.19	3.01E-02
Ddx50	13.73	15.64	0.19	5.31E-03
Cdc42se2	59.03	66.92	0.19	3.68E-04
Ppm1e	42.88	49.24	0.19	4.81E-02
Fndc3b	2.79	3.18	0.19	1.70E-02
Kcnn2	11.72	13.33	0.19	5.04E-03
Doc2a	17.01	19.40	0.19	2.86E-02
Slc9a5	8.84	10.03	0.19	1.99E-02
Pdp1	25.18	28.73	0.19	3.64E-02
Rasgrp1	92.73	105.56	0.19	2.74E-02
Arhgap10	5.73	6.50	0.19	2.63E-02
Mrpl32	4.33	4.89	0.19	1.56E-02
Rnf168	7.27	8.25	0.18	1.10E-02
Herpud1	23.48	26.67	0.18	3.71E-02
Noct	4.87	5.51	0.18	4.81E-03
Ubtd2	14.90	16.99	0.18	4.66E-02
Slc25a44	30.63	34.68	0.18	2.75E-02
Mtmr2	13.76	15.46	0.18	4.01E-04
Rnf115	17.44	19.64	0.18	1.11E-02
Lancl2	37.06	41.58	0.18	2.16E-04
Etf1	19.46	21.79	0.18	2.43E-04
Psmc1	58.15	65.22	0.18	3.60E-03
Pspc1	8.52	9.64	0.17	3.71E-02
Mllt11	116.62	130.55	0.17	2.26E-03
Tpp2	11.69	13.11	0.17	1.43E-02
Diras2	61.72	69.57	0.17	4.99E-02
Sumo3	28.21	31.70	0.17	3.57E-02
Gad2	24.94	27.89	0.17	5.74E-03
Mcl1	18.99	21.24	0.17	1.33E-02
Map7d2	34.14	38.09	0.17	5.31E-03
Mchr1	7.45	8.37	0.17	3.08E-02
Ube2g1	14.74	16.46	0.17	9.71E-03
Gclc	15.86	17.77	0.17	4.54E-02
Plcl2	15.19	16.93	0.17	1.92E-03
Max	26.52	29.51	0.17	8.19E-03
Myo1e	4.06	4.53	0.17	1.99E-02
Rars	15.00	16.77	0.16	2.01E-02
Ppm1h	15.23	16.96	0.16	2.89E-02
Chgb	131.81	147.10	0.16	2.74E-02
Eif1ad	8.03	8.97	0.16	2.66E-02
Psmd12	25.89	28.82	0.16	1.06E-02
Denr	9.14	10.18	0.16	1.93E-02
Slc6a17	109.46	121.76	0.16	3.11E-02
Pi4ka	55.64	61.85	0.16	2.69E-02
Osbp2	28.37	31.37	0.16	2.26E-03
Hprt	65.96	73.17	0.16	1.04E-02
Ndrg3	126.96	140.50	0.16	3.60E-03
Psma1	50.70	56.07	0.16	1.48E-03
Rgs7	22.56	25.08	0.16	3.77E-02
Apcdd1	3.03	3.36	0.16	2.14E-02
Tsnax	57.76	63.76	0.16	1.57E-03
Foxo3	16.98	18.77	0.16	1.26E-02
Tbk1	14.91	16.42	0.15	3.30E-03
Hars	35.56	39.29	0.15	2.63E-02
Akirin1	13.70	15.11	0.15	6.67E-03
Uxs1	7.26	8.06	0.15	2.74E-02
Dnajc2	5.03	5.57	0.15	4.37E-02
B4galt5	13.26	14.61	0.15	3.57E-02
Gdi2	36.47	40.14	0.15	2.34E-03
Zmym2	13.91	15.33	0.15	2.36E-02
Rgs8	9.81	10.82	0.15	3.87E-02
Picalm	18.14	19.99	0.15	3.14E-02
Ddx1	21.11	23.20	0.15	9.63E-03
Kcnk1	34.51	38.02	0.15	3.84E-02
Smyd2	27.82	30.69	0.15	4.50E-02
Spire1	34.56	37.89	0.14	3.95E-02
Adam9	16.65	18.24	0.14	4.17E-02
Mboat2	7.29	7.95	0.14	6.26E-03
Uvrag	7.04	7.70	0.14	3.82E-02
Galnt1	11.78	12.94	0.14	4.54E-02
Smap1	39.53	43.13	0.14	6.38E-03
Cfap36	39.20	42.78	0.14	5.04E-03
Pak6	25.05	27.38	0.14	2.76E-02
Plpbp	13.21	14.37	0.14	1.83E-02
Scg3	107.27	116.69	0.14	3.62E-03
Cul3	24.72	26.97	0.14	4.35E-02
Trp53bp1	13.63	14.84	0.14	2.01E-02
Pitpna	82.84	89.93	0.14	3.95E-04
Snap25	347.87	377.51	0.14	4.01E-04
4930548M08Rik	53.64	58.13	0.13	2.09E-04
Ndufs1	44.66	48.46	0.13	1.17E-03
Zfand5	20.31	22.07	0.13	7.59E-03
Uck2	8.02	8.74	0.13	4.11E-02
Sec14l1	52.90	57.22	0.13	3.92E-03
Slc7a5	19.93	21.60	0.13	3.88E-02
Btbd10	24.66	26.67	0.13	2.58E-02
Kpna3	22.31	24.12	0.13	1.54E-02
Eif3a	27.75	29.97	0.13	1.81E-02
Rph3a	93.56	100.83	0.13	2.04E-03
Hnrnph2	23.18	25.03	0.13	5.71E-03
Eif5b	9.41	10.18	0.13	3.19E-02
Atp2a2	168.34	181.49	0.12	2.63E-02
Ipo5	33.29	35.86	0.12	9.63E-03
Gad1	87.40	94.29	0.12	4.76E-02
Rad23b	45.47	49.01	0.12	1.94E-02
Idh3a	71.98	77.16	0.12	2.20E-03
Cap1	75.67	81.17	0.12	4.98E-02
Ppp2ca	46.52	49.82	0.12	1.92E-03
Scrn1	55.60	59.35	0.11	2.43E-02
Hspa9	55.51	59.18	0.11	3.00E-03
Atp1b1	511.88	545.81	0.11	2.38E-02
Fam81a	58.38	62.23	0.11	4.50E-02
Tax1bp1	25.87	27.55	0.11	3.47E-02
Ncl	24.86	26.47	0.11	9.83E-03
St3gal5	42.15	44.86	0.11	1.51E-02
Nkiras1	15.01	15.93	0.10	2.31E-02
Elmo1	19.23	20.30	0.09	3.99E-02
Mapk9	50.30	53.04	0.09	4.38E-02
Pdha1	70.48	74.03	0.09	3.14E-02
Tex264	34.52	31.25	-0.12	4.81E-02
Vegfa	22.19	18.99	-0.19	1.45E-02
Dkkl1	11.12	8.97	-0.23	4.59E-02
Jund	48.67	38.87	-0.24	2.72E-02
Etnk2	3.70	2.82	-0.27	2.81E-02

Table S8 (1/2) - Genes from Gene set A that are differentially expressed under 12Hr in Swap

gene_name	WT_12hr_avg_fpkm	SWAP_12hr_avg_fpkm	hr12_SWAP_vs_WT.l2fc	hr12_SWAP_vs_WT.padj
Scube1	24.8	15.8	-0.6	1.11E-21
Ccn4	3.4	2.1	-0.5	4.94E-07
Htr2a	8.8	6.2	-0.5	1.29E-11
Ctla2a	3.3	1.7	-0.4	8.78E-05
Chga	133.3	96.0	-0.4	4.89E-11
Pmepa1	28.0	20.1	-0.4	4.70E-10
Tafa1	16.2	12.1	-0.4	6.96E-09
Fndc9	3.2	2.1	-0.4	2.25E-03
Dnmt3a	19.9	15.0	-0.4	2.94E-08
Il17ra	6.2	4.6	-0.4	1.16E-05
Adam19	7.3	5.6	-0.3	1.72E-05
Inf2	55.1	42.9	-0.3	2.36E-09
Sstr2	21.3	15.9	-0.3	9.74E-04
Uck2	12.9	10.1	-0.3	8.23E-06
Vegfa	28.8	22.2	-0.3	7.22E-04
Neu2	4.8	3.5	-0.3	8.32E-03
Pim1	4.4	3.1	-0.3	1.68E-02
Adgrl4	5.5	4.2	-0.3	2.37E-03
Rhbdl3	8.8	7.0	-0.3	9.93E-05
Vwa1	11.6	9.1	-0.3	3.01E-03
Cdkn1a	46.1	29.6	-0.3	3.00E-02
Fscn1	124.8	101.9	-0.3	3.00E-08
Hkdc1	8.1	6.5	-0.3	7.39E-04
Lsm11	12.0	9.8	-0.3	7.49E-05
Mfsd2a	20.2	16.0	-0.3	5.19E-03
Vcan	2.4	1.9	-0.3	1.82E-04
Dclk1	191.0	157.3	-0.3	3.70E-06
Gimap6	1.4	1.0	-0.3	4.78E-02
Hmgcr	47.0	38.8	-0.3	1.91E-04
Fam43b	14.8	12.0	-0.3	8.65E-03
Rnd3	9.8	8.0	-0.2	1.83E-02
Osbpl3	13.8	11.3	-0.2	7.33E-03
Pdgfb	16.8	13.9	-0.2	5.37E-03
Neto2	15.9	13.2	-0.2	1.13E-03
Syt12	17.4	14.5	-0.2	7.35E-04
Tgfb1i1	6.6	5.4	-0.2	1.16E-02
Lhfp	12.8	10.6	-0.2	9.51E-03
Robo4	1.8	1.4	-0.2	3.50E-02
Npnt	15.9	13.4	-0.2	1.58E-05
Skil	22.5	18.6	-0.2	5.39E-03
Notch4	1.8	1.4	-0.2	3.92E-02
Slco1c1	22.6	18.7	-0.2	1.29E-02
Ptgfrn	12.0	10.0	-0.2	1.36E-03
Rasl11b	41.8	35.2	-0.2	2.11E-04
Smim3	3.1	2.6	-0.2	3.22E-02
Apcdd1	3.4	2.9	-0.2	1.90E-02
Sema7a	82.0	70.0	-0.2	2.17E-05
Ubtd2	23.4	19.8	-0.2	1.14E-02
Gcnt4	7.6	6.4	-0.2	3.48E-03
Ppfibp1	11.1	9.5	-0.2	1.64E-03
Kcnip3	96.5	82.1	-0.2	3.14E-03
Myo19	5.0	4.2	-0.2	1.16E-02
Fmnl1	72.1	61.2	-0.2	3.04E-02
Cx3cl1	419.6	361.3	-0.2	4.62E-04
Sulf2	43.8	37.8	-0.2	3.65E-05
Smad7	7.2	6.1	-0.2	3.64E-02
Rph3a	163.0	140.9	-0.2	3.04E-05
Ankrd13b	40.5	35.1	-0.2	2.20E-04
Slc9a5	20.8	18.0	-0.2	6.39E-03
Pitpnm3	32.8	28.5	-0.2	4.41E-04
Itgav	16.8	14.6	-0.2	5.28E-04
Tmem229b	11.1	9.6	-0.2	4.76E-03
Ddah1	34.6	30.1	-0.2	4.20E-03
Etv5	43.9	38.3	-0.2	2.53E-03
Tspan5	36.8	32.2	-0.2	1.17E-04
Cdk5r2	132.7	115.9	-0.2	4.73E-03
Rgs20	12.9	11.2	-0.2	1.47E-02
Nrep	59.0	51.7	-0.2	1.82E-03
Lingo1	175.5	153.8	-0.2	1.41E-02
Fam78b	10.4	9.1	-0.2	4.21E-03
Mat2a	81.0	71.3	-0.2	1.10E-02
Sstr3	8.6	7.5	-0.2	2.76E-02
Chfr	17.5	15.4	-0.2	3.47E-03
Sccpdh	17.3	15.3	-0.2	1.11E-02
Cinp	32.2	28.5	-0.2	4.41E-03
Adcy5	21.9	19.4	-0.2	3.41E-03
Nrxn3	36.9	32.7	-0.2	2.16E-03
Trp53inp2	70.9	63.0	-0.2	3.17E-05
Cacna1a	32.6	29.0	-0.2	1.80E-03
St8sia5	20.6	18.3	-0.2	2.67E-02
Mark3	18.4	16.3	-0.2	1.10E-02
Ptprn	224.2	199.8	-0.2	3.54E-04
Ttyh3	91.0	81.0	-0.2	2.83E-03
Tmem121b	22.3	19.8	-0.2	1.63E-02
Hivep2	54.0	47.9	-0.2	2.52E-02
Camk1g	32.7	29.1	-0.2	1.19E-02
Slc35e2	9.6	8.6	-0.2	4.58E-02
Cask	10.8	9.7	-0.2	5.99E-03
Zmynd8	34.1	30.5	-0.2	1.10E-03
R3hdm1	63.8	57.0	-0.2	1.73E-02
Gramd1b	54.4	48.5	-0.2	4.00E-02
Actn4	58.8	52.8	-0.2	4.67E-03
Gfra2	42.4	38.0	-0.2	2.37E-02
Pde4a	43.3	39.0	-0.1	2.30E-02
Insyn1	91.1	82.0	-0.1	2.17E-02
Mark1	35.4	32.0	-0.1	1.69E-03
Slc7a5	31.3	28.2	-0.1	3.24E-02
Nrn1	194.5	175.7	-0.1	5.00E-03
Lig3	8.1	7.3	-0.1	3.78E-02

Table S8 (2/2)

Fam81a	77.4	69.9	-0.1	3.76E-02
Unc13a	62.6	56.7	-0.1	1.10E-02
Nptxr	238.3	215.6	-0.1	2.63E-02
Wdr26	20.9	18.9	-0.1	2.88E-02
Pabpc1	52.5	47.7	-0.1	1.73E-02
Kcnk1	55.5	50.4	-0.1	3.42E-02
Inka2	40.7	37.1	-0.1	1.62E-02
Hip1	13.2	12.1	-0.1	3.20E-02
Brsk2	67.5	62.5	-0.1	3.12E-02
Epb41l1	92.7	86.0	-0.1	2.57E-02
Ppme1	94.8	103.0	0.1	4.96E-02
Map7d2	40.9	44.6	0.1	2.14E-02
Brinp1	93.9	103.2	0.1	4.18E-02
Map9	22.2	24.3	0.1	3.54E-02
Ywhah	211.4	231.9	0.1	5.96E-03
Dtna	28.5	31.4	0.1	1.09E-02
Prkar1b	282.1	312.5	0.1	6.74E-03
Rcan2	68.4	75.9	0.1	3.17E-02
Grsf1	30.8	34.2	0.1	9.92E-03
Elmo1	19.6	22.0	0.1	3.85E-03
Ptpn5	58.9	66.1	0.2	2.61E-04
Arpp19	68.9	78.4	0.2	4.16E-02
Rimbp2	33.8	38.4	0.2	1.60E-03
Stac2	30.5	34.9	0.2	1.45E-03
Lgi2	19.6	22.7	0.2	4.17E-03
Coq10b	11.6	13.6	0.2	3.92E-02
Nell1	4.8	5.6	0.2	1.70E-02
Arhgap10	6.9	8.1	0.2	1.41E-02
Daglb	9.3	11.0	0.2	2.24E-03
Klhl21	4.6	5.7	0.2	2.95E-03
Snap25	368.7	444.3	0.2	1.53E-05
Ccn1	3.6	8.8	0.3	1.27E-02
Hapln4	24.8	30.3	0.3	4.38E-05
Wnt10a	2.5	3.2	0.3	2.21E-02
Jsrp1	1.8	2.6	0.3	4.48E-02
Gucy2g	2.6	3.3	0.3	1.27E-02
Igfbp6	24.9	31.2	0.3	1.48E-03
Gadd45g	10.0	12.8	0.3	1.14E-02
Dusp1	15.3	26.7	0.3	2.68E-02
Adam33	2.4	3.3	0.3	1.99E-02
Sgk1	22.8	34.4	0.3	1.35E-02
Mthfd1l	4.0	5.4	0.3	2.33E-03
Chgb	137.5	173.9	0.3	3.79E-16
Fos	29.5	50.0	0.3	6.74E-03
Rgs2	13.4	17.6	0.4	7.52E-11
Arl4d	15.3	21.0	0.4	6.90E-05
Herc6	2.6	3.6	0.4	2.52E-04
Net1	8.3	11.7	0.4	1.30E-04
Npas4	13.1	36.0	0.4	6.87E-05
Il33	4.9	7.2	0.4	2.58E-07
Igfn1	3.4	5.7	0.5	2.05E-05

Table S9 - Genes from Gene set B that are differentially expressed under standard light in Swap

gene_name	WT_light_avg_fpkm	SWAP_light_avg_fpkm	light_SWAP_vs_WT.l2fc	ight_SWAP_vs_WT.pad
Celsr1	0.91	1.18	0.24	1.04E-02
Nnat	67.56	82.58	0.21	1.37E-02
Tpd52l1	7.11	8.79	0.20	3.47E-02
Erich3	2.23	2.70	0.20	1.38E-02
Hebp1	6.02	7.32	0.20	3.38E-02
Azin2	14.48	16.96	0.19	3.77E-03
Crebl2	8.04	9.27	0.17	4.16E-03
Cep164	4.16	4.83	0.17	3.12E-02
Synpr	17.98	20.65	0.16	4.07E-02
Zfp316	4.79	5.44	0.15	2.90E-02
Pkia	46.73	51.74	0.12	1.11E-02
Mturn	28.23	31.11	0.12	3.03E-02
Id2	58.24	53.00	-0.14	2.61E-02
Kcnip2	32.99	29.93	-0.14	3.26E-02
B3galt2	7.22	6.14	-0.21	2.94E-03
Adamts17	1.21	0.99	-0.21	1.86E-02
Hdac1	10.18	8.48	-0.22	8.20E-03
Flrt3	8.57	7.13	-0.23	1.40E-03

Table S10 - Genes from Gene set B that are differentially expressed under dark in Swap

gene_name	WT_dark_avg_fpkm	SWAP_dark_avg_fpkm	dark_SWAP_vs_WT.l2fc	dark_SWAP_vs_WT.padj
Plk5	10.00	6.14	-0.58	2.91E-15
Otof	9.88	6.37	-0.52	4.22E-13
Rskr	16.92	11.47	-0.43	3.56E-06
Timeless	1.86	1.25	-0.43	4.22E-06
Mmp14	6.46	4.34	-0.43	1.78E-05
Col8a1	1.86	1.29	-0.41	1.10E-05
Htra3	4.32	2.82	-0.40	9.57E-04
Atp2a3	2.42	1.69	-0.39	1.24E-04
Cldn5	26.35	18.09	-0.39	3.74E-04
Crocc	21.66	15.14	-0.39	1.26E-04
Ntn5	10.60	7.49	-0.38	1.78E-04
Gpr6	2.08	1.40	-0.38	1.57E-03
Nos1	9.14	6.66	-0.37	1.78E-05
Vstm4	2.30	1.56	-0.35	4.72E-03
Epop	27.42	20.46	-0.35	9.40E-06
Spag5	10.47	7.66	-0.35	2.09E-04
Psrc1	8.38	6.18	-0.35	1.17E-04
Aldh1a2	5.69	4.05	-0.34	3.42E-03
Emilin1	1.85	1.26	-0.34	8.86E-03
Cdkn1c	3.80	2.66	-0.34	7.20E-03
Jrk	2.26	1.62	-0.34	4.25E-03
Evc2	9.53	7.07	-0.33	3.74E-04
Bnip5	3.46	2.56	-0.33	8.23E-04
Mxra7	5.50	4.16	-0.33	3.95E-04
Sec1	2.50	1.71	-0.32	1.51E-02
Tle6	2.21	1.51	-0.32	1.68E-02
Gpr88	21.08	16.33	-0.32	4.08E-07
Heyl	1.53	1.08	-0.31	1.79E-02
Tspo	3.45	2.37	-0.31	2.34E-02
Gm1043	3.76	2.75	-0.30	1.29E-02
Thbd	8.94	6.68	-0.30	1.10E-02
Arhgap4	1.30	0.96	-0.30	1.26E-02
Zic4	1.67	1.24	-0.29	1.69E-02
Cchcr1	2.62	2.03	-0.29	1.64E-03
Asgr1	1.80	1.03	-0.29	2.98E-02
Cdh1	1.66	1.26	-0.28	2.05E-02
Hps1	6.06	4.71	-0.28	8.82E-03
Mxra8	4.67	3.56	-0.28	2.01E-02
Pdgfrb	8.11	6.44	-0.28	1.00E-03
Nlrx1	3.87	3.01	-0.27	1.49E-02
Bmp6	3.43	2.56	-0.27	3.55E-02
Col12a1	2.60	1.98	-0.27	2.89E-02
Tap2	2.50	1.99	-0.27	6.73E-03
Arhgef19	7.12	5.51	-0.27	1.85E-02
Trim17	3.30	2.52	-0.27	2.69E-02
Qrfpr	2.91	2.24	-0.26	3.77E-02
Islr	13.99	11.00	-0.25	3.31E-02
Kank2	3.18	2.54	-0.25	1.58E-02
Cpne4	20.68	17.01	-0.25	1.45E-06
Padi2	10.32	8.11	-0.24	4.81E-02
Rprm	50.17	41.18	-0.24	2.81E-04
Mme	1.45	1.15	-0.24	3.50E-02
Plppr3	23.02	18.87	-0.24	1.47E-03
Wnt5a	2.29	1.85	-0.24	1.90E-02
Isyna1	17.95	14.46	-0.24	2.12E-02
Igfbp5	47.13	38.55	-0.24	4.64E-03
Ring1	15.54	12.68	-0.24	7.92E-03
Ccdc61	4.10	3.31	-0.24	2.64E-02
Ly6h	60.31	49.62	-0.24	1.62E-03
Celsr1	1.25	1.01	-0.24	2.86E-02
Sox2	14.90	12.24	-0.23	5.31E-03
Akap12	6.67	5.49	-0.23	5.99E-03
Mgat5b	27.59	22.90	-0.23	5.28E-05
Pcdh19	5.90	4.80	-0.23	2.60E-02
Lman2l	11.56	9.47	-0.23	1.70E-02
Ptchd1	3.70	3.00	-0.22	3.50E-02
Dguok	6.77	5.64	-0.22	3.30E-03
Rlbp1	11.73	9.66	-0.22	3.08E-02
Nat14	42.18	35.03	-0.22	1.25E-02
Adamts16	2.41	2.01	-0.21	3.29E-02
Gucy1a1	28.75	24.30	-0.21	2.38E-04
Pigv	2.42	2.02	-0.21	4.35E-02
Lypd1	15.56	13.20	-0.20	1.78E-04
Car11	108.14	90.96	-0.20	2.89E-02
Sptbn4	32.94	28.02	-0.20	2.28E-03
Slc27a1	38.58	32.39	-0.20	4.64E-02
Jph4	107.64	91.76	-0.20	1.03E-03
Lzts3	80.40	68.40	-0.19	6.36E-03
Obsl1	5.21	4.42	-0.19	1.12E-02
Tmem80	15.81	13.49	-0.19	1.11E-02
Abhd8	100.29	85.31	-0.19	3.64E-02
Prr13	20.86	17.80	-0.19	3.29E-02
Polm	3.29	2.80	-0.19	4.98E-02
Pck2	6.80	5.83	-0.19	9.71E-03
Rtel1	6.75	5.78	-0.18	3.71E-02
Smo	4.60	3.96	-0.18	2.72E-02
Col5a1	13.72	11.78	-0.18	2.34E-02
Mapk7	7.40	6.40	-0.18	1.76E-02
Mccc2	9.44	8.15	-0.18	2.86E-02
Met	4.04	3.47	-0.17	4.49E-02
Cep63	5.33	4.61	-0.17	3.00E-02
Smarca2	48.24	41.87	-0.17	8.31E-03
Dus3l	34.70	30.16	-0.17	1.58E-02
Zfp358	14.96	13.03	-0.17	3.08E-02
Iqcc	7.89	6.85	-0.16	3.62E-02
Tprkb	32.62	28.61	-0.16	3.84E-02
Dcaf17	3.07	2.70	-0.15	3.47E-02
Sash1	14.48	12.74	-0.15	4.44E-02
Mllt6	33.65	29.76	-0.15	7.62E-05
Gga1	26.88	23.73	-0.15	7.59E-03
Cul9	15.95	14.08	-0.15	6.38E-03
Tbc1d9b	50.22	44.78	-0.14	8.37E-04
Abcc5	59.90	53.25	-0.14	4.37E-02
Rnf112	155.12	138.21	-0.14	3.00E-02
Stag2	11.45	12.52	0.14	2.67E-02
Napepld	5.77	6.53	0.18	4.81E-02
Ablim3	8.11	9.38	0.21	6.25E-03
Krt9	1.60	2.04	0.26	3.98E-02

Table S11 - Genes from Gene set B that are differentially expressed under 12Hr in Swap

gene_name	WT_12hr_avg_fpkm	SWAP_12hr_avg_fpkm	hr12_SWAP_vs_WT.l2fc	hr12_SWAP_vs_WT.padj
Hsf4	3.54	5.88	0.55	4.90E-09
Ntn5	5.16	8.00	0.49	2.59E-08
Kitl	6.02	8.42	0.43	4.50E-12
Rskr	5.33	8.01	0.43	1.82E-05
Smoc2	2.66	3.95	0.41	5.90E-05
Spag5	3.80	5.15	0.38	1.29E-06
Plk5	4.00	5.53	0.37	9.93E-05
Cdkl1	4.95	7.06	0.36	1.10E-03
Prelp	4.80	6.44	0.35	2.93E-05
Epor	1.80	2.72	0.35	3.53E-03
Myoc	11.85	15.75	0.35	5.54E-06
Cd83	2.69	3.72	0.35	7.51E-04
Qrfpr	1.12	1.73	0.34	5.95E-03
Gm5148	1.15	1.61	0.29	2.43E-02
Hlf	34.71	43.01	0.29	1.50E-08
Tspan17	11.45	14.48	0.29	1.10E-03
Pcdhb12	2.18	2.82	0.29	7.52E-03
Ptgds	540.26	672.96	0.28	1.57E-04
Faim2	37.91	46.07	0.27	2.30E-12
Slc13a4	4.20	5.40	0.26	1.60E-02
Ypel4	29.64	36.24	0.26	1.39E-05
Tmem255a	2.97	3.75	0.26	1.09E-02
Tef	83.28	100.44	0.25	1.78E-09
Prr16	3.06	3.88	0.25	2.76E-02
Rnf207	1.26	1.62	0.25	4.59E-02
Aldh2	14.99	18.14	0.25	6.00E-05
Crebl2	7.95	9.61	0.25	6.87E-05
Cbx7	7.47	9.11	0.25	2.78E-03
Evc2	5.05	6.13	0.24	2.40E-03
Caly	70.00	83.99	0.24	2.63E-05
Pcdhb17	2.84	3.45	0.24	8.16E-03
Cib2	7.02	8.60	0.24	1.45E-02
Zkscan16	9.14	11.19	0.24	1.92E-02
Islr	9.27	11.49	0.24	3.04E-02
Stk32c	42.91	51.12	0.23	5.19E-04
Napepld	4.71	5.68	0.22	2.03E-02
Bbs9	3.79	4.60	0.22	3.02E-02
Rprm	19.51	23.42	0.22	1.46E-02
Aifm3	27.52	32.23	0.20	4.88E-03
Rasd2	17.22	20.03	0.20	1.38E-03
Arid5b	5.89	6.88	0.20	4.45E-03
Car11	73.61	85.50	0.19	3.09E-03
Phf1	9.28	10.81	0.19	6.45E-03
Fmod	8.84	10.35	0.19	1.99E-02
Rpusd1	25.72	29.80	0.19	1.64E-03
Rasal1	31.63	36.77	0.19	2.17E-02
Elac1	5.68	6.60	0.19	3.71E-02
Ezh1	15.09	17.38	0.19	2.39E-03
Gaa	80.96	92.82	0.18	2.18E-04
Crebrf	5.69	6.55	0.18	3.06E-02
Phyhip	169.66	194.22	0.18	5.04E-04
Mapk3	64.44	73.82	0.18	1.67E-03
Cygb	17.90	20.61	0.18	2.22E-02
Trpm2	4.05	4.63	0.18	1.07E-02
Mpdz	10.00	11.43	0.17	3.36E-02
Igsf8	57.38	65.19	0.17	6.23E-03
Smarca2	33.34	37.61	0.16	1.25E-03
Cul9	10.62	11.99	0.16	9.24E-03
Extl2	24.32	27.40	0.16	1.23E-02
St6galnac6	37.36	42.08	0.16	4.88E-03
Klf6	10.54	11.89	0.15	4.26E-02
Mturn	25.18	28.04	0.14	1.32E-02
Nicn1	32.18	35.83	0.14	1.02E-02
Prnp	248.05	272.58	0.13	1.24E-02
Pde1b	31.28	34.36	0.13	1.71E-02
Lzts3	63.41	69.47	0.12	1.10E-02
Pnma8b	73.95	80.94	0.12	3.91E-02
Camkv	139.31	152.18	0.12	2.98E-02
Ankrd46	40.17	43.52	0.11	3.20E-02
Arhgef19	5.81	5.00	-0.20	2.59E-02
Sparc	118.54	101.09	-0.20	2.36E-02
Hdac1	9.65	8.09	-0.21	4.18E-02
Ddr1	24.37	20.61	-0.22	3.17E-03
N4bp2	1.46	1.20	-0.22	4.28E-02
Col11a2	5.82	4.80	-0.25	4.64E-04

Figure S6 – Enrichment tables used for Fisher's exact test of Gene set A

Standard light

Differential expression in GluN2A$^{2B(CTR)/2B(CTR)}$

	Lower	not lower	Total
Gene set A	57	885	942
Not genes set A	73	11236	11309
Total	130	12121	12251

	Higher	not higher	Total
Gene set A	16	926	942
Not genes set A	60	11249	11309
Total	76	12175	12251

Dark

Differential expression in GluN2A$^{2B(CTR)/2B(CTR)}$

	Lower	not lower	Total
Gene set A	5	937	942
Not genes set A	244	11065	11309
Total	249	12002	12251

	Higher	not higher	Total
Gene set A	209	733	942
Not genes set A	241	11068	11309
Total	450	11801	12251

12Hr re-exposure

Differential expression in GluN2A$^{2B(CTR)/2B(CTR)}$

	Lower	not lower	Total
Gene set A	109	833	942
Not genes set A	508	10801	11309
Total	617	11634	12251

	Higher	not higher	Total
Gene set A	41	901	942
Not genes set A	459	10850	11309
Total	500	11751	12251

Figure S7 – Enrichment tables used for Fisher's exact test of Gene set B

Standard light

Differential expression in GluN2A$^{2B(CTR)/2B(CTR)}$

	Lower	not lower	Total
Gene set B	6	484	490
Not genes set B	124	11637	11761
Total	130	12121	12251

	Higher	not higher	Total
Gene set B	12	478	490
Not genes set B	64	11697	11761
Total	76	12175	12251

Dark

Differential expression in GluN2A$^{2B(CTR)/2B(CTR)}$

	Lower	not lower	Total
Gene set B	104	386	490
Not genes set B	145	11616	11761
Total	249	12002	12251

	Higher	not higher	Total
Gene set B	4	486	490
Not genes set B	446	11315	11761
Total	450	11801	12251

12Hr re-exposure

Differential expression in GluN2A$^{2B(CTR)/2B(CTR)}$

	Lower	not lower	Total
Gene set B	6	484	490
Not genes set B	611	11150	11761
Total	617	11634	12251

	Higher	not higher	Total
Gene set B	69	421	490
Not genes set B	431	11330	11761
Total	500	11751	12251

Addis, L., Virdee, J. K., Vidler, L. R., Collier, D. A., Pal, D. K. & Ursu, D. (2017) Epilepsy-associated GRIN2A mutations reduce NMDA receptor trafficking and agonist potency - molecular profiling and functional rescue. *Sci Rep*, 7(1), 66.
Ishchenko, Y., Carrizales, M. G. & Koleske, A. J. (2021) Regulation of the NMDA receptor by its cytoplasmic domains: (How) is the tail wagging the dog? *Neuropharmacology*, 195, 108634.
Lemke, J. R., Lal, D., Reinthaler, E. M., Steiner, I., Nothnagel, M., Alber, M., Geider, K., Laube, B., Schwake, M., Finsterwalder, K., Franke, A., Schilhabel, M., Jahn, J. A., Muhle, H., Boor, R., Van Paesschen, W., Caraballo, R., Fejerman, N., Weckhuysen, S., De Jonghe, P., Larsen, J., Moller, R. S., Hjalgrim, H., Addis, L., Tang, S., Hughes, E., Pal, D. K., Veri, K., Vaher, U., Talvik, T., Dimova, P., Guerrero Lopez, R., Serratosa, J. M., Linnankivi, T., Lehesjoki, A. E., Ruf, S., Wolff, M., Buerki, S., Wohlrab, G., Kroell, J., Datta, A. N., Fiedler, B., Kurlemann, G., Kluger, G., Hahn, A., Haberlandt, D. E., Kutzer, C., Sperner, J., Becker, F., Weber, Y. G., Feucht, M., Steinbock, H., Neophythou, B., Ronen, G. M., Gruber-Sedlmayr, U., Geldner, J., Harvey, R. J., Hoffmann, P., Herms, S., Altmuller, J., Toliat, M. R., Thiele, H., Nurnberg, P., Wilhelm, C., Stephani, U., Helbig, I., Lerche, H., Zimprich, F., Neubauer, B. A., Biskup, S. & von Spiczak, S. (2013) Mutations in GRIN2A cause idiopathic focal epilepsy with rolandic spikes. *Nat Genet*, 45(9), 1067-72.
Lesca, G., Rudolf, G., Bruneau, N., Lozovaya, N., Labalme, A., Boutry-Kryza, N., Salmi, M., Tsintsadze, T., Addis, L., Motte, J., Wright, S., Tsintsadze, V., Michel, A., Doummar, D., Lascelles, K., Strug, L., Waters, P., de Bellescize, J., Vrielynck, P., de Saint Martin, A., Ville, D., Ryvlin, P., Arzimanoglou, A., Hirsch, E., Vincent, A., Pal, D., Burnashev, N., Sanlaville, D. & Szepetowski, P. (2013) GRIN2A mutations in acquired epileptic aphasia and related childhood focal epilepsies and encephalopathies with speech and language dysfunction. *Nat Genet*, 45(9), 1061-6.
Liu, S., Zhou, L., Yuan, H., Vieira, M., Sanz-Clemente, A., Badger, J. D., 2nd, Lu, W., Traynelis, S. F. & Roche, K. W. (2017) A Rare Variant Identified Within the GluN2B C-Terminus in a Patient with Autism Affects NMDA Receptor Surface Expression and Spine Density. *J Neurosci*, 37(15), 4093-4102.
Mota Vieira, M., Nguyen, T. A., Wu, K., Badger, J. D., 2nd, Collins, B. M., Anggono, V., Lu, W. & Roche, K. W. (2020) An Epilepsy-Associated GRIN2A Rare Variant Disrupts CaMKIIalpha Phosphorylation of GluN2A and NMDA Receptor Trafficking. *Cell Rep*, 32(9), 108104.
Paoletti, P., Bellone, C. & Zhou, Q. (2013) NMDA receptor subunit diversity: impact on receptor properties, synaptic plasticity and disease. *Nat Rev Neurosci*, 14(6), 383-400.
Ryan, T. J., Kopanitsa, M. V., Indersmitten, T., Nithianantharajah, J., Afinowi, N. O., Pettit, C., Stanford, L. E., Sprengel, R., Saksida, L. M., Bussey, T. J., O'Dell, T. J., Grant, S. G. & Komiyama, N. H. (2013) Evolution of GluN2A/B cytoplasmic domains diversified vertebrate synaptic plasticity and behavior. *Nat Neurosci*, 16(1), 25-32.
Wyllie, D. J., Livesey, M. R. & Hardingham, G. E. (2013) Influence of GluN2 subunit identity on NMDA receptor function. *Neuropharmacology*, 74, 4-17.